NASA Contractor Report 3036

A Method for Predicting Full Scale Buffet Response With Rigid Wind Tunnel Model Fluctuating Pressure Data

Volume II: Power Spectral Densities for Method Assessment

Atlee M. Cunningham, Jr., David B. Benepe,
Darlene Watts, and Paul G. Waner

CONTRACT NAS2-7091
NOVEMBER 1978

NASA

NASA Contractor Report 3036

A Method for Predicting Full Scale Buffet Response With Rigid Wind Tunnel Model Fluctuating Pressure Data

Volume II: Power Spectral Densities for Method Assessment

Atlee M. Cunningham, Jr., David B. Benepe,
Darlene Watts, and Paul G. Waner
General Dynamics Corporation
Fort Worth, Texas

Prepared for
Ames Research Center
under Contract NAS2-7091

National Aeronautics
and Space Administration

Scientific and Technical
Information Office

1978

A METHOD FOR PREDICTING FULL SCALE BUFFET RESPONSE WITH RIGID WIND TUNNEL MODEL FLUCTUATING PRESSURE DATA

VOLUME II

POWER SPECTRAL DENSITIES FOR METHOD ASSESSMENT

By
Atlee M. Cunningham, Jr., David B. Benepe,
Darlene Watts, and Paul G. Waner
Fort Worth Division of General Dynamics

Abstract

This report documents the development and assessment of a method with which fluctuating pressure data obtained from rigid scaled wind-tunnel models can be used to predict flexible full-scale buffet response. The method requires unsteady aerodynamic forces, natural airplane modes, and the measured pressure data as input. A gust response computer program is used to calculate buffet response due to the forcing function posed by the measured pressure data. By calculating both symmetric and antisymmetric solutions, upper and lower bounds on full-scale buffet response are formed. Final results are given in the form of upper and lower bounds on the power spectral densities and the RMS values for angle of attack variation in maneuvers at several Mach-altitudes. Comparisons of predictions with flight test results are made and the effects of horizontal tail loads and static aeroelasticity are shown. Discussions are also presented on the effects of primary wing torsion modes, chordwise and span-wise phase angles, and altitude.

This second volume presents the predicted upper and lower bounds power spectra for all of the cases and response items given in Volume I. The flight test power spectra are shown on each prediction plot for the nominal value of angle of attack that most closely agrees with the flexible angle for the prediction. The flight test and prediction conditions are given in tabular form for all cases considered. The order in which the plots are given corresponds to that of the results given in Volume I.

CONTENTS

LIST OF TABLES

LIST OF FIGURES

A METHOD FOR PREDICTING FULL SCALE BUFFET RESPONSE WITH RIGID WIND TUNNEL MODEL FLUCTUATING PRESSURE DATA

VOLUME II

POWER SPECTRAL DENSITIES FOR METHOD ASSESSMENT

By
Atlee M. Cunningham, Jr., David B. Benepe,
Darlene Watts, and Paul G. Waner

SUMMARY

This volume presents the detailed power spectral density plots for the prediction method assessments presented in Volume I of this report. These plots show the comparison between flight test power spectra and the predicted upper and lower bounds spectra for all response items discussed in Volume I. The comparisons are made at nominal angles of attack and in some cases the exact angles of attack. The flight test and prediction conditions are given in tabular form for all cases considered. The order in which the plots are given corresponds to that of the results in Volume I. The figure numbers correspond to the case number.

INTRODUCTION

The first volume of this report presents a description of the method for predicting buffet intensity characteristics well beyond buffet onset and how the method evolved. Comparisons are made between predicted results and flight test data for a variety of cases in order to assess the capability of the method. These comparisons are made on the basis of RMS response and characteristic frequencies (frequency centroid of the power spectrum). The predictions are presented in the form of an upper and lower bounds for all response items except pilot seat and C.G. accelerometers. In addition, the calculated natural mode shapes of the airplane are given for all cases.

Comparison of integrated characteristics aids in rendering a complicated phenomena such as high intensity buffet into a comprehendible form. Thus, it is possible to evaluate the effect on buffet response of the gross parameters, wing sweep, altitude, Mach number, and angle of attack. In this case, it serves as a means of quickly establishing the validity of the upper and lower bounds concept, and provides insight as to how flight test data tends to be distributed within the bounds.

Many questions arise, however, that cannot be answered by the study of integrated characteristics alone. One example is what might cause one item to show excellent agreement with RMS values and poor agreement with characteristic frequencies or vice versa. Another example is anomalous degrees of agreement with flight test data for different response items. For these cases, comparison of flight test and predicted power spectra usually provide enough information to determine what the source of error might be. Such an increase in resolution, however, can lead to a third and disturbing example where integrated characteristics show excellent agreement but the power spectra are poor. This last example usually occurs in conjunction with the second example above.

This second volume presents the predicted upper and lower bounds power spectra for all of the cases and response items given in Volume I. The flight test power spectra are shown on each prediction plot for the nominal value of angle of attack that most closely agrees with the flexible angle for the prediction. The flight test and prediction conditions are given in tabular form for all cases considered. The order in which the plots are given corresponds to that of the results given in Volume I.

SYMBOLS

$\frac{C_{L\alpha\,FLEX}}{C_{L\alpha\,RIG}}$	ratio of the flexible to rigid lift coefficients for the F-111A
α	wing angle of attack
α_{FLT}	airplane angle of attack for flight test data
α_{FLEX}	angle of attack for a flexible airplane at equivalent flight conditions
α_{RIG}	angle of attack for a rigid airplane which corresponds to wind-tunnel test conditions
α_{MAX}	maximum value of α achieved during a maneuver
α_{NOM}	average value of α achieved during a time sample within a maneuver
α_1	value of α at the beginning of a time sample
α_2	value of α at the end of a time sample
ΔT	time sample length, sec
Λ	nominal wing sweep

PREDICTED BUFFET RESPONSE POWER SPECTRA

The plotted upper and lower bounds of the predicted buffet response power spectra are presented in this section. Tables are presented to describe the flight test and prediction conditions. The table and plot figure numbers correspond to the following case numbers:

Case 1: Wing alone prediction
$\Lambda = 26^{\circ}$, $M = 0.80$, Alt = 6035m

Case 2: Total airplane prediction (half horizontal tail, matched first wing torsion mode frequencies)
$\Lambda = 26^{\circ}$, $M = 0.80$, Alt = 6035m

Case 3: Total airplane prediction (final method)
$\Lambda = 26^{\circ}$, $M = 0.70$, Alt = 7559m

Case 4: Total airplane prediction (final method)
$\Lambda = 50^{\circ}$, $M = 0.85$, Alt = 8383m

Case 5: Total airplane prediction (final method)
$\Lambda = 72.5^{\circ}$, $M = 0.85$, Alt = 7285m

Case 6: Wing alone prediction (final method)
$\Lambda = 50^{\circ}$, $M = 1.20$, Alt = 9053m

Case 7: Wing alone prediction (final method)
$\Lambda = 72.5^{\circ}$, $M = 1.20$, Alt = 9083m

For clarification on the method used for each prediction, the reader is referred to the section "Capability Assessment of the Prediction Method" in Volume I.

The calculated mode shapes used in the predictions are given in Volume I as an aid to the reader in determining how various modes contribute to the overall response. Since the power spectra are in the form of upper and lower bounds and modal frequencies shift as a function of aerodynamic stiffness, it is sometimes difficult to separate closely spaced symmetric and antisymmetric modes. In such cases, however, the left and right hand wing-tip accelerometer flight test data tends to alternate between the upper and lower bounds as predicted.

Considerable discussion has been devoted to the prediction results in Volume I. Thus, only some general remarks will be made concerning the overall characteristics of the spectra. The wing tip accelerometer results usually show the best agreement with flight test where as the horizontal tail loads are usually the worst. Since the horizontal tail buffet pressures were estimated from wing loads, this is not surprising. The predicted wing bending moment and shear are also generally in agreement with flight test results. Due to the short moment arm, wing torsion is usually less in agreement with flight test.

An interesting observation can be made on the c.g. and pilot seat accelerometers. Since they are on the centerline, upper and lower bounds cannot be defined for these items as they are for the other response items. Hence, lateral accelerations are due to antisymmetric responses and vertical accelerations are due to symmetric responses. To the contrary, flight test results show that both vertical and lateral accelerometers each respond in both symmetric and antisymmetric modes. This is perhaps the strongest indication of the presence of asymmetric modes that has been observed.

The effect of using inaccurate unsteady aerodynamics was discussed in Volume I in relation to the predictions made for Case 7. The power spectra comparisons further illustrate the importance of accurate unsteady aerodynamics. The bounding of the flight test data is very poor for $\alpha = 8.4^{\circ}$ and 15.5° when compared with the other predictions for Cases 1-6.

CONCLUDING REMARKS

Detailed power spectral density plots have been presented in this volume as an aid to better understanding the integrated buffet response results given in Volume I of this report. Generally, the flight test power spectra are well bounded by the predicted upper and lower bounds power spectra. In many cases, where right and left hand data are available from the airplane, the flight test results verify the separation of the upper and lower bounds.

These results are presented also as a means of further verifying the prediction method as discussed in Volume I. Since high intensity buffet response of aircraft is highly dependent on type of maneuver, atmospheric conditions, pilot characteristics and other items, it was felt that a peak-by-peak discussion of each power spectrum was not warranted. What is more important is that the upper bound which represents the maximum possible response is rarely exceeded except in special cases or for certain items. Likewise, the lower bound which is the minimum possible response level rarely falls above flight test data. These were the desired results.

General Dynamics Corporation
P. O. Box 748
Fort Worth, Texas 76101, October 15, 1974

TABLE 1.- FLIGHT TEST AND PREDICTION CONDITIONS FOR CASE 1, WING ALONE, $\Lambda = 26^{o}$, M = 0.80, ALT = 6035m (19,800 ft)

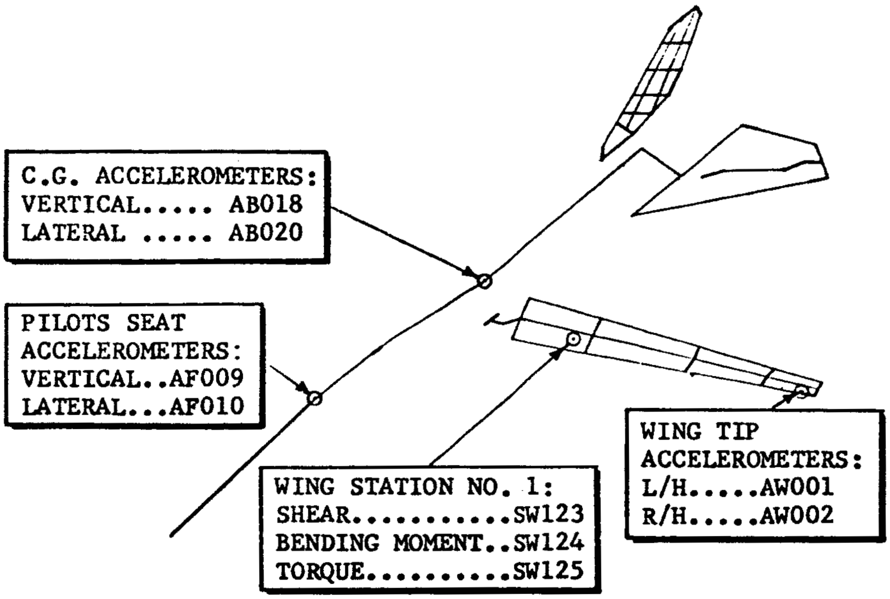

CASE 1 FLIGHT 77 RUN SC-R

	FLIGHT TEST CONDITIONS	PREDICTION CONDITIONS
Wing Sweep	25.6^{o}	26^{o}
Mach	0.80 - 0.78	0.80
Altitude	6035m (19,800 ft)	6035m (19,800 ft)
Gross Weight	266,004N (59,800 lb)	266,004N (59,800 lb)

POINTS ANALYSED

ΔT	α_1	α_2	α_{MAX}	α_{NOM}	α_{FLEX}*	α_{RIG}
2	4.22^{o}	5.98^{o}	-	5.1^{o}	-	-
2	6.80^{o}	7.12^{o}	-	6.9^{o}	6.6^{o}	6.1^{o}
2	8.15^{o}	9.35^{o}	-	8.9^{o}	-	-
2	10.35^{o}	12.90^{o}	-	11.7^{o}	11.1^{o}	10.18^{o}
2	12.70^{o}	14.65^{o}	14.95^{o}	14.1^{o}	14.4^{o}	13.26^{o}
3	11.05^{o}	14.95^{o}	14.95^{o}	13.0^{o}	-	-

* $\frac{C_{L\alpha_{FLEX}}}{C_{L\alpha_{RIG}}} = \frac{\alpha_{RIG}}{\alpha_{FLEX}} = 0.920$ as obtained from Figure 4, Vol. I

TABLE 2.- FLIGHT TEST AND PREDICTION CONDITIONS FOR CASE 2, TOTAL AIRPLANE (HALF HORIZONTAL TAIL), $\Lambda = 26^{\circ}$, M = 0.80, ALT = 6035m (19,800 ft)

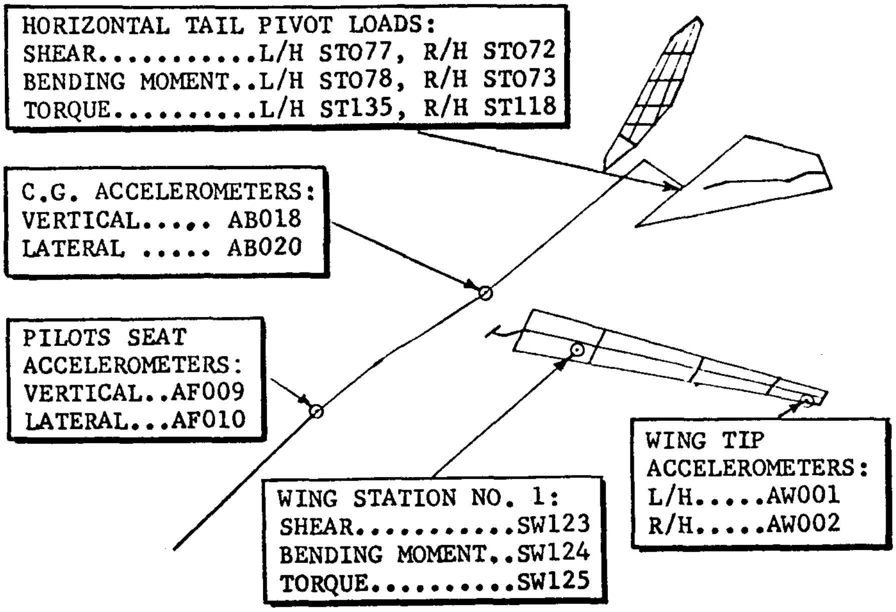

CASE 2 FLIGHT 77 RUN SC-R

	FLIGHT TEST CONDITIONS	PREDICTION CONDITIONS
Wing Sweep	25.6°	26°
Mach	0.80 - 0.78	0.80
Altitude	6035m (19,800 ft)	6035m (19,800 ft)
Gross Weight	266,004N (59,800 lb)	266,044N (59,800 lb)

POINTS ANALYSED

ΔT	α_1	α_2	α_{MAX}	α_{NOM}	α_{FLEX} *	α_{RIG}
2	4.22°	5.98°	-	5.1°	-	-
2	6.80°	7.12°	-	6.9°	6.6°	6.1°
2	8.15°	9.35°	-	8.9°	-	-
2	10.35°	12.90°	-	11.7°	11.1°	10.18°
2	12.70°	14.65°	14.95°	14.1°	14.4°	13.26°
3	11.05°	14.95°	14.95°	13.0°	-	-

* $\dfrac{C_{L\alpha_{FLEX}}}{C_{L\alpha_{RIG}}} = \dfrac{\alpha_{RIG}}{\alpha_{FLEX}} = 0.920$ as obtained from Figure 4, Vol. I

TABLE 3.- FLIGHT TEST AND PREDICTION CONDITIONS FOR CASE 3, TOTAL AIRPLANE (FINAL METHOD), $\Lambda = 26^{o}$, M = 0.70, ALT = 7559m (24,800 ft)

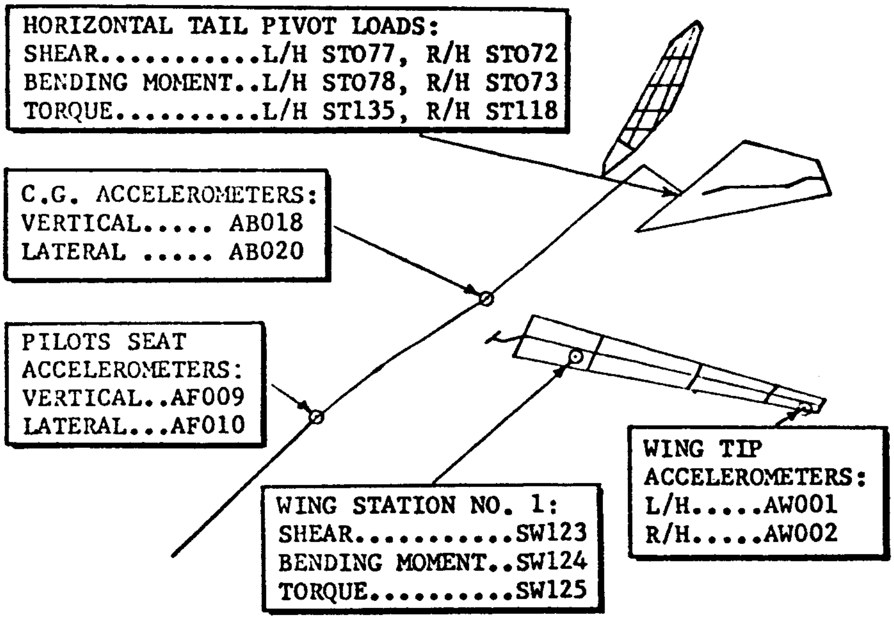

CASE 3 FLIGHT 48 RUN 6

	FLIGHT TEST CONDITIONS				PREDICTION CONDITIONS	
Wing Sweep	26.6^{o}				26^{o}	
Mach	0.70 - 0.68				0.70	
Altitude	7559m (24,800 ft)				7559m (24,800 ft)	
Gross Weight	294,472N (66,200 lb)				293,138N (65,900 lb)	
POINTS ANALYSED						
ΔT	α_1	α_2	α_{MAX}	α_{NOM}	α_{FLEX} *	α_{RIG}
1	8.72^{o}	9.55^{o}	-	8.8^{o}	9.6^{o}	9.2^{o}
1	9.70^{o}	10.75^{o}	-	9.8^{o}	10.7^{o}	10.2^{o}
1	10.30^{o}	11.75^{o}	-	10.7^{o}	11.8^{o}	11.2^{o}
1	11.15^{o}	13.55^{o}	-	11.8^{o}	12.8^{o}	12.2^{o}
1	14.25^{o}	16.60^{o}	-	14.6^{o}	17.1^{o}	16.3^{o}

* $\dfrac{C_{L\alpha_{FLEX}}}{C_{L\alpha_{RIG}}} = \dfrac{\alpha_{RIG}}{\alpha_{FLEX}} = 0.950$ as obtained from Figure 4, Vol. I

TABLE 4.- FLIGHT TEST AND PREDICTION CONDITIONS FOR CASE 4, TOTAL AIRPLANE (FINAL METHOD), $\Lambda = 50^{\circ}$, M = 0.85, ALT = 8382m (27,500 ft)

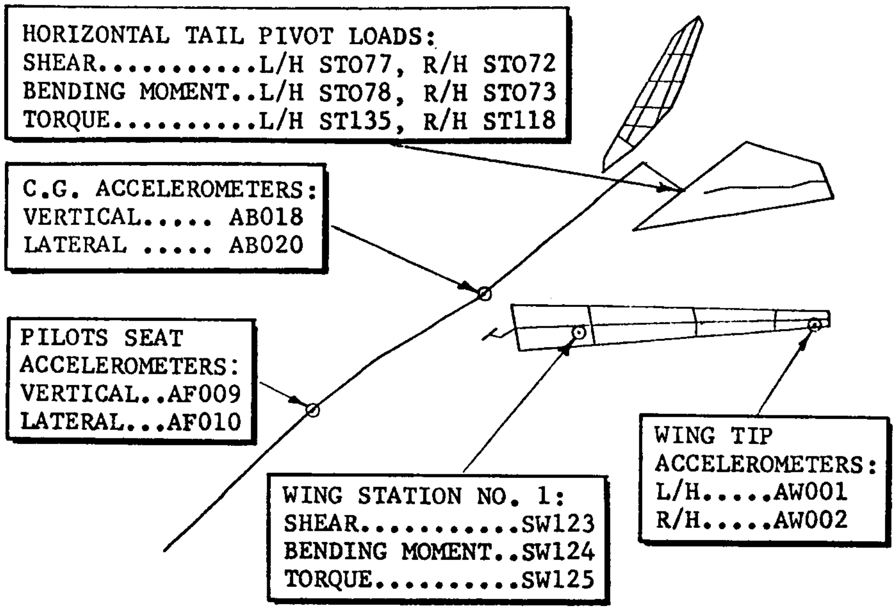

CASE 4 FLIGHT 61 RUN R227

	FLIGHT TEST CONDITIONS	PREDICTION CONDITIONS
Wing Sweep	49.1°	50°
Mach	0.82 - 0.79	0.85
Altitude	8382m (27,500 ft)	8382m (27,500 ft)
Gross Weight	330,948N (74,400 lb)	331,392N (74,515 lb)

POINTS ANALYSED

ΔT	α_1	α_2	α_{MAX}	α_{NOM}	α_{FLEX} *	α_{RIG}
1	7.10°	9.25°	-	7.9°	-	-
1	8.05°	10.10°	-	8.9°	8.9°	8.1°
1	10.10°	10.80°	-	10.0°	-	-
1	10.60°	12.70°	-	11.1°	11.1°	10.2°
1	12.90°	14.60°	14.60°	13.1°	14.4°	13.2°

* $\dfrac{C_{L\alpha_{FLEX}}}{C_{L\alpha_{RIG}}} = \dfrac{\alpha_{RIG}}{\alpha_{FLEX}} = 0.920$ as obtained from Figure 4, Vol. I

TABLE 5.- FLIGHT TEST AND PREDICTION CONDITIONS FOR CASE 5, TOTAL AIRPLANE (FINAL METHOD), $\Lambda = 72.5^{\circ}$, M = 0.85, ALT = 7285m (23,900 ft)

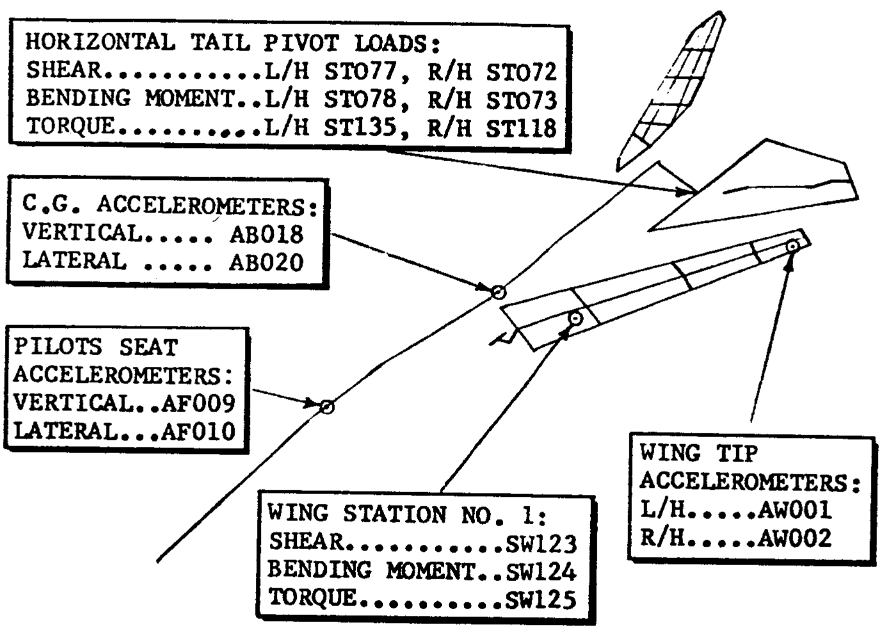

CASE 5 FLIGHT 48 RUN 7-R

		FLIGHT TEST CONDITIONS			PREDICTION CONDITIONS	
Wing Sweep		72.2°			72.5°	
Mach		0.89 - 0.84			0.85	
Altitude		7559m (24,800 ft)			7285m (23,900 ft)	
Gross Weight		265,559N (59,700 lb)			268,673N (60,500 lb)	
POINTS ANALYSED						
ΔT	α_1	α_2	α_{MAX}	α_{NOM}	α_{FLEX} *	α_{RIG}
1	7.15°	8.65°	-	7.8°	7.8°	7.1°
1	8.65°	10.00°	-	9.4°	-	-
1	10.75°	12.20°	-	11.1°	11.1°	10.2°
1	14.15°	16.15°	-	14.4°	14.4°	13.3°
1	17.90°	18.90°	19.35°	17.7°	-	-

* $\frac{C_{L\alpha_{FLEX}}}{C_{L\alpha_{RIG}}} = \frac{\alpha_{RIG}}{\alpha_{FLEX}} = 0.890$ as obtained from Figure 4, Vol. I

TABLE 6.- FLIGHT TEST AND PREDICTION CONDITIONS FOR CASE 6, WING ALONE (FINAL METHOD), $\Lambda = 50^{o}$, M = 1.20, ALT = 9053m (29,700 ft)

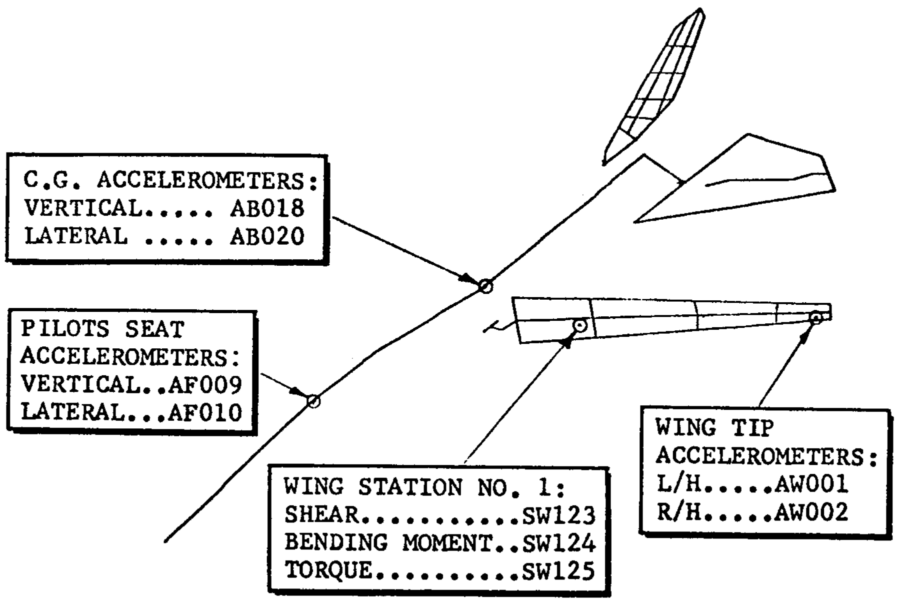

CASE 6 FLIGHT 48 RUN 4

	FLIGHT TEST CONDITIONS	PREDICTION CONDITIONS
Wing Sweep	49.8°	50°
Mach	1.20 - 1.15	1.20
Altitude	9053m (29,700 ft)	9053m (29,700 ft)
Gross Weight	261,111N (58,700 lb)	261,778N (58,900 lb)

POINTS ANALYSED

ΔT	α_1	α_2	α_{MAX}	α_{NOM}	α_{FLEX} *	α_{RIG}
1	4.70°	5.50°	-	4.9°	-	-
1	8.20°	9.80°	-	8.6°	-	-
1	12.10°	13.70°	-	12.4°	12.4°	10.2°
1	13.70°	13.90°	15.0°	13.7	16.1°	13.2°

* $\frac{C_{L\alpha_{FLEX}}}{C_{L\alpha_{RIG}}} = \frac{\alpha_{RIG}}{\alpha_{FLEX}} = 0.823$ as obtained from Figure 4, Vol. I

TABLE 7.- FLIGHT TEST AND PREDICTION CONDITIONS FOR CASE 7, WING ALONE (FINAL METHOD), $\Lambda = 72.5^{\circ}$, M = 1.20, ALT = 9083m (29,800 ft)

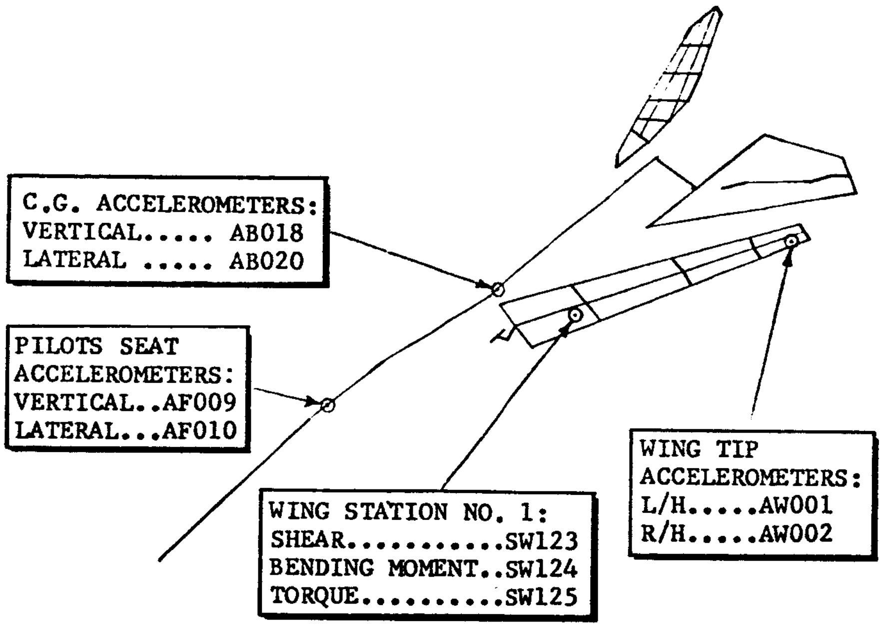

CASE 7 FLIGHT 48 RUN 5

	FLIGHT TEST CONDITIONS	PREDICTION CONDITIONS
Wing Sweep	72.2°	72.5°
Mach	1.20 - 1.16	1.20
Altitude	9083m (29,800 ft)	9083m (29,800 ft)
Gross Weight	274,455N (61,700 lb)	268,673N (60,500 lb)

POINTS ANALYSED

ΔT	α_1	α_2	α_{MAX}	α_{NOM}	* α_{FLEX}	α_{RIG}
1	4.80°	4.80°	-	4.8°	-	-
1	8.00°	8.80°	-	8.1°	8.1°	7.1°
1	11.30°	12.70°	-	11.6°	11.6°	10.2°
1	14.95°	16.75°	-	15.1°	15.1°	13.4°

* $\dfrac{C_{L\alpha_{FLEX}}}{C_{L\alpha_{RIG}}} = \dfrac{\alpha_{RIG}}{\alpha_{FLEX}} = 0.837$ as obtained from Figure 4, Vol. I

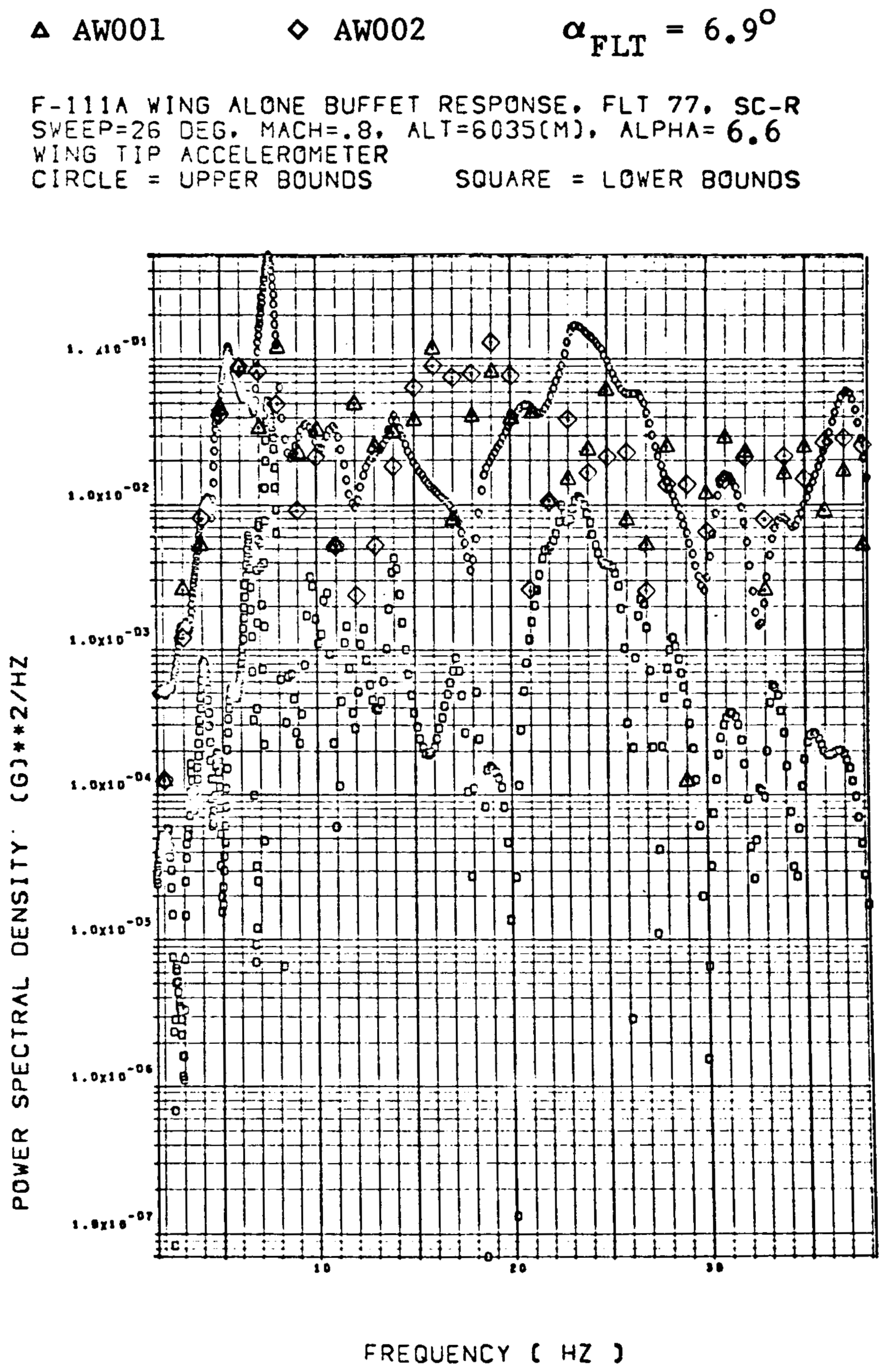

Figure 1.- Power spectra for
Case 1, wing alone, Λ =26°, M=0.80,
alt.=6035m (19,800 ft)
(a) wing tip accelerometer

△ AW001 ◇ AW002 $\alpha_{FLT} = 11.7^{\circ}$

F-111A WING ALONE BUFFET RESPONSE, FLT 77, SC-R
SWEEP=26 DEG, MACH=.8, ALT=6035(M), ALPHA= 11.1
WING TIP ACCELEROMETER
CIRCLE = UPPER BOUNDS SQUARE = LOWER BOUNDS

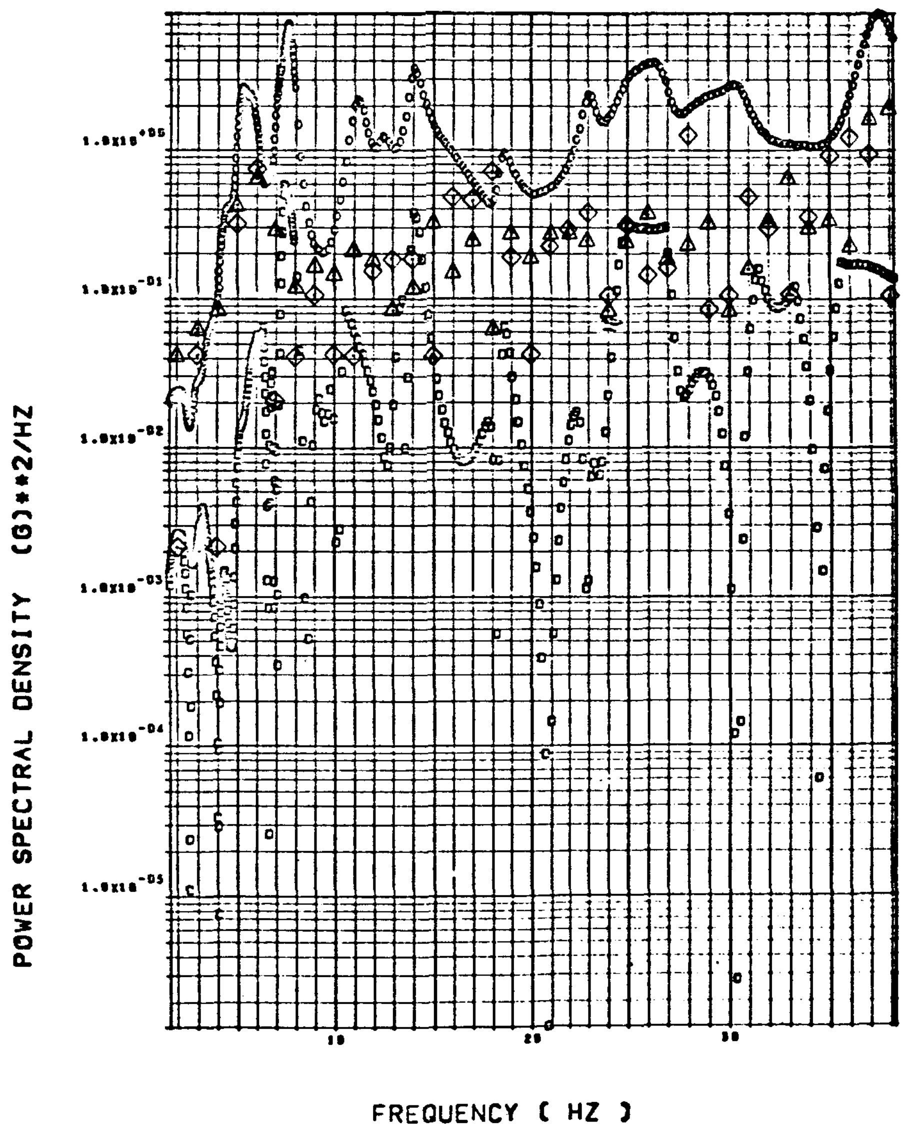

Figure 1.-(a) Wing tip accelerometer (continued)

Δ AW001 ◇ AW002 $\alpha_{FLT} = 14.1^{\circ}$

F-111A WING ALONE BUFFET RESPONSE, FLT 77, SC-R
SWEEP=26 DEG. MACH=.8, ALT=6035(M), ALPHA= 14.4
WING TIP ACCELEROMETER
CIRCLE = UPPER BOUNDS SQUARE = LOWER BOUNDS

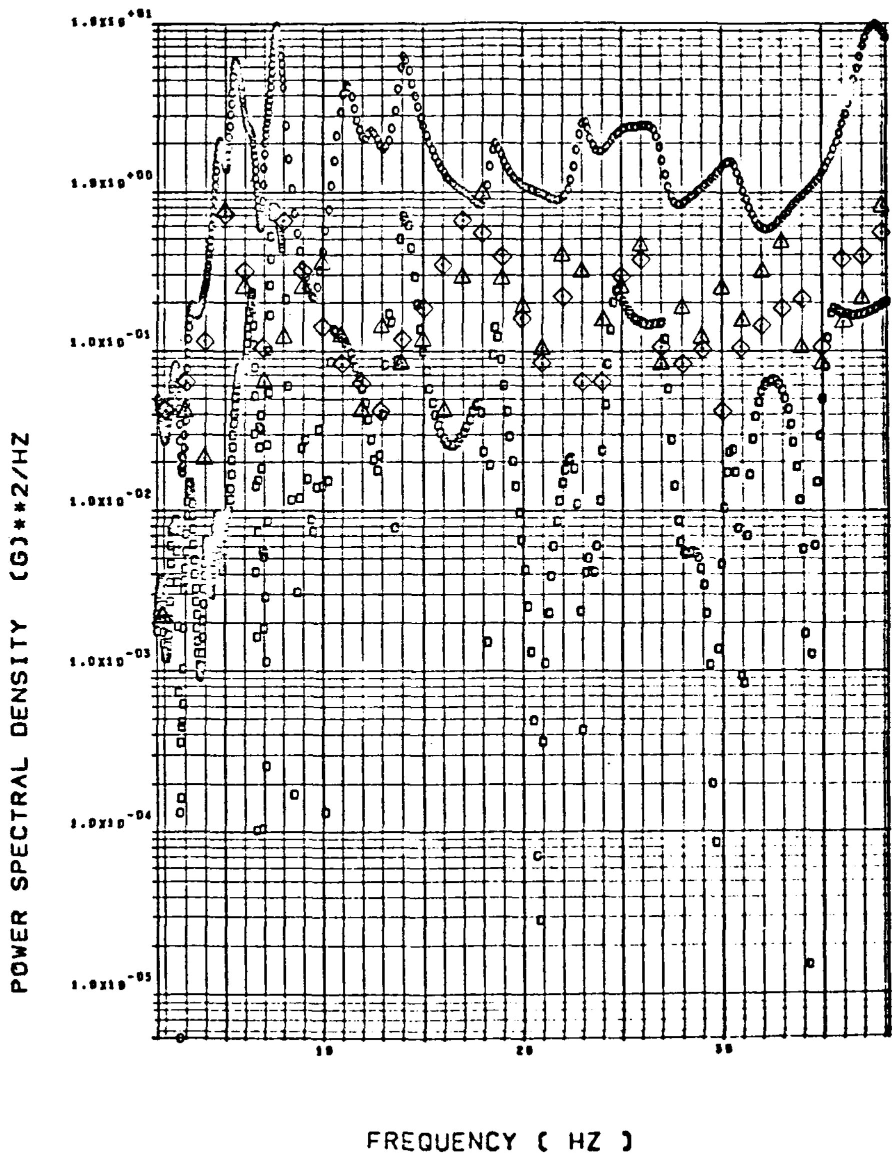

Figure 1.-(a) Wing tip accelerometer (continued)

◇ AB018 $\alpha_{FLT} = 6.9^{o}$

WING BUFFET RESPONSE. F-111A. CONTRACT NAS2 - 7091
SWEEP = 26 DEG. MACH = .8. ALT = 19.8K. ALPHA= 6.6
C.G. VERTICAL ACCELEROMETER. FS = 529
CIRCLE = 1 DOF PLUS = 2 DOF X = 9 DOF

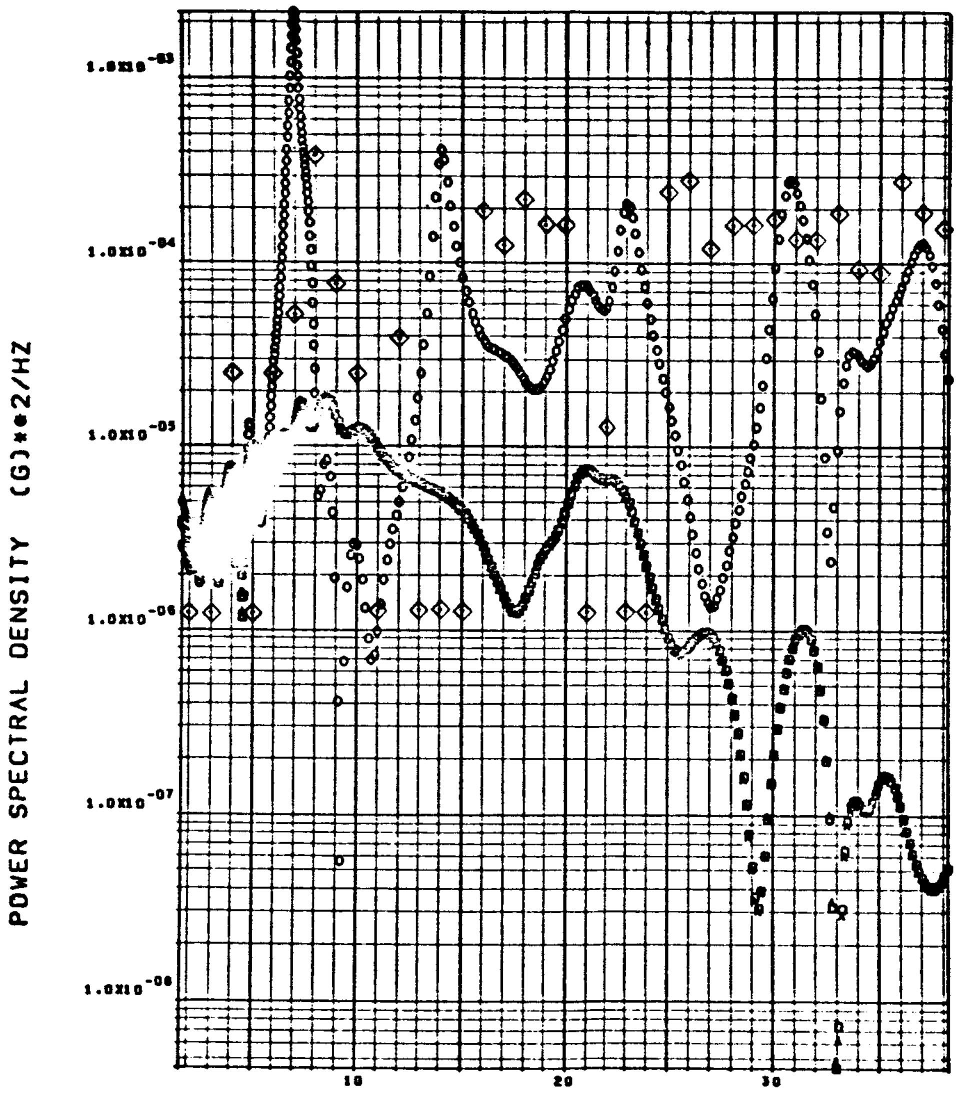

Figure 1.-(b) C.G. vertical accelerometer

◇ AB018 $\alpha_{FLT} = 11.7^{\circ}$

WING BUFFET RESPONSE. F-111A. CONTRACT NAS2 - 7091
SWEEP = 26 DEG. MACH= .8. ALT = 19.5K. ALPHA= 11.1
C.G. VERTICAL ACCELEROMETER. FS = 529
CIRCLE = 1 DOF PLUS = 2 DOF X = 9 DOF

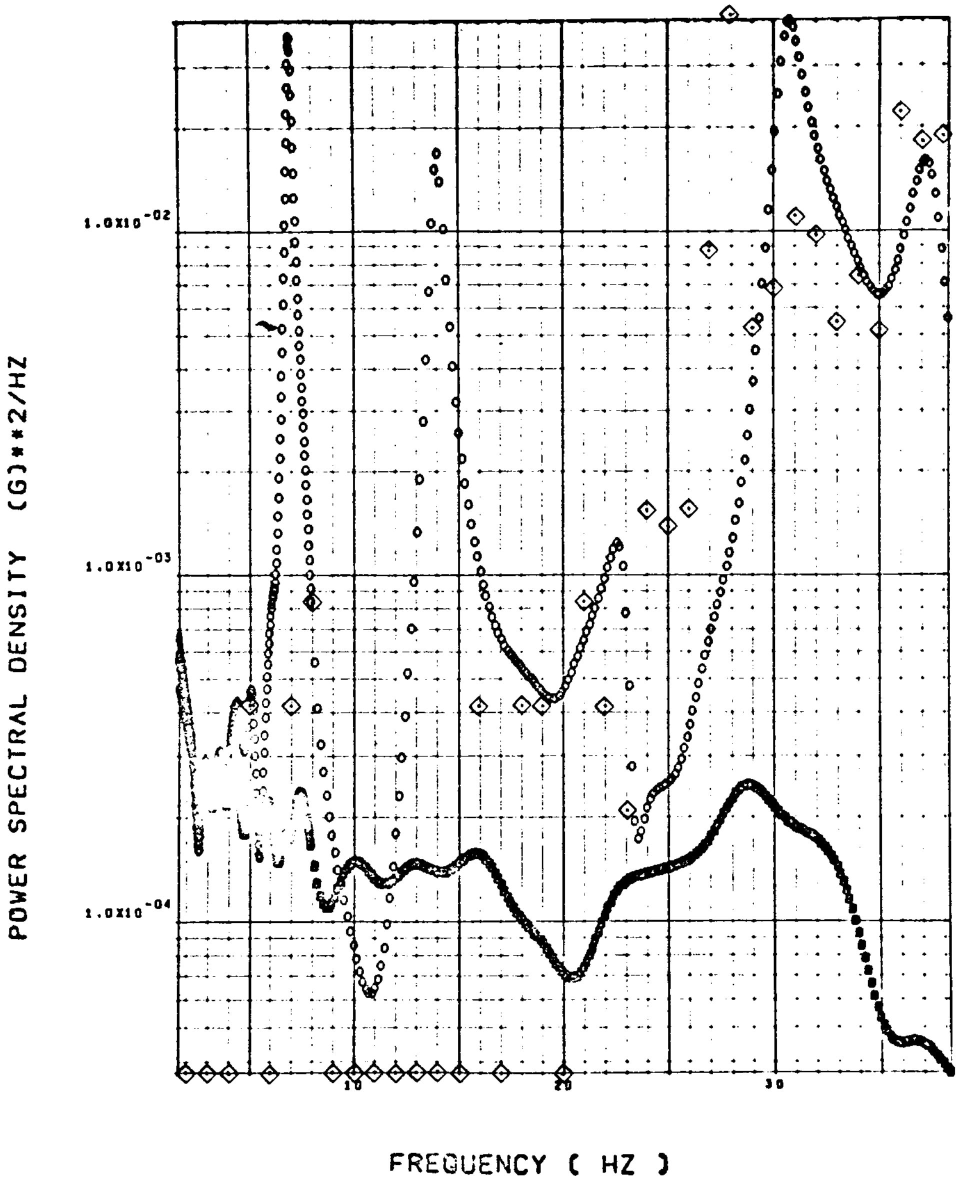

Figure 1.-(b) C.G. vertical accelerometer (continued)

◇ AB018 $\alpha_{FLT} = 14.1^{\circ}$

WING BUFFET RESPONSE. F-111A. CONTRACT NAS2 - 7091
SWEEP = 26 DEG. MACH= .8. ALT = 19.5K. ALPHA= 14.4
C.G. VERTICAL ACCELEROMETER. FS = 529
CIRCLE = 1 DOF PLUS = 2 DOF X = 9 DOF

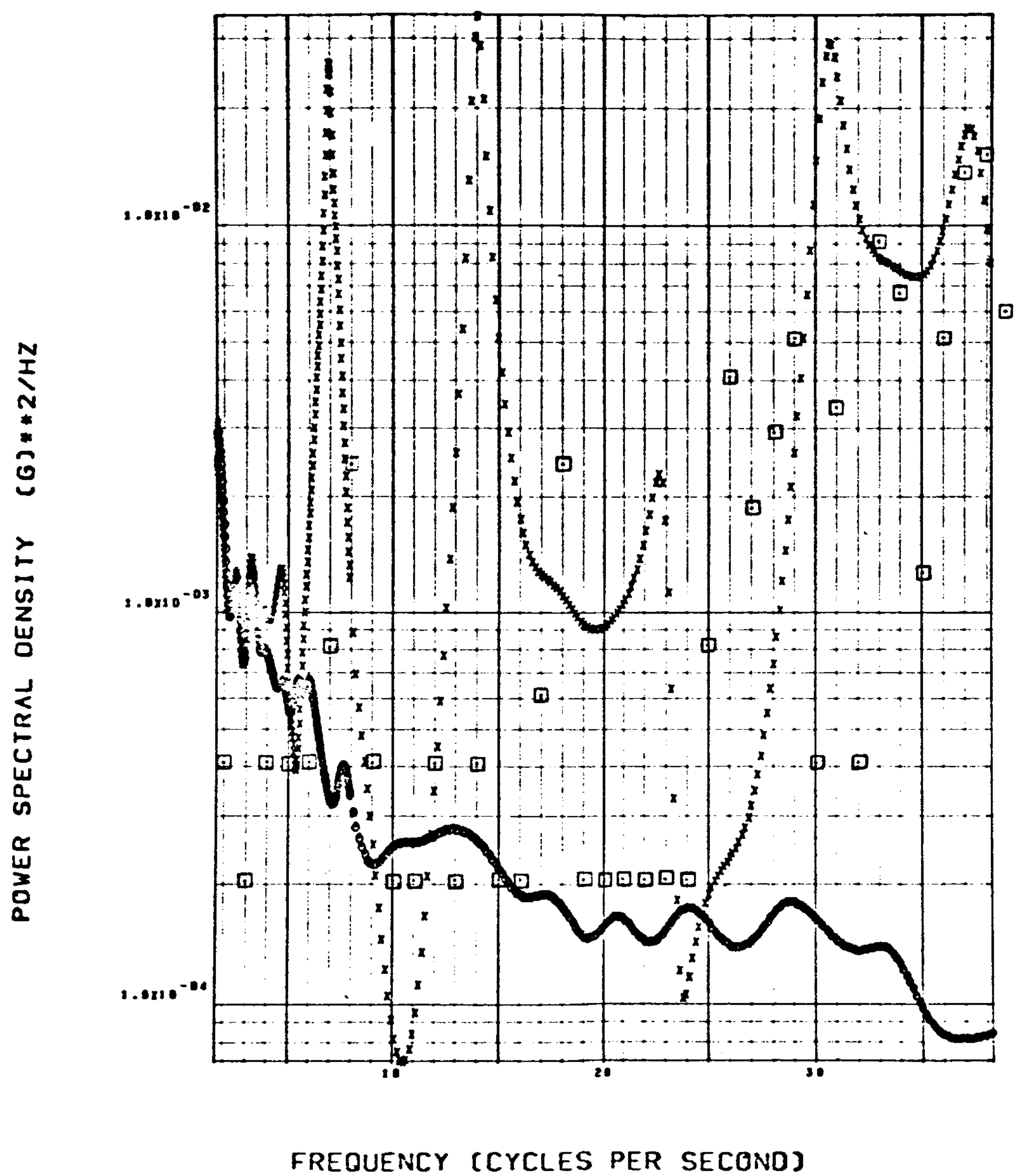

Figure 1.-(b) C.G. vertical accelerometer (continued)

◇ AF009 $\alpha_{FLT} = 6.9^{\circ}$

WING BUFFET RESPONSE. F-111A. CONTRACT NAS2 - 7091
SWEEP = 26 DEG. MACH = .8. ALT = 19.8K. ALPHA= 6.6
PILOT STATION VERTICAL ACCELEROMETER. FS = 255
CIRCLE = 1 DOF PLUS = 2 DOF X = 9 DOF

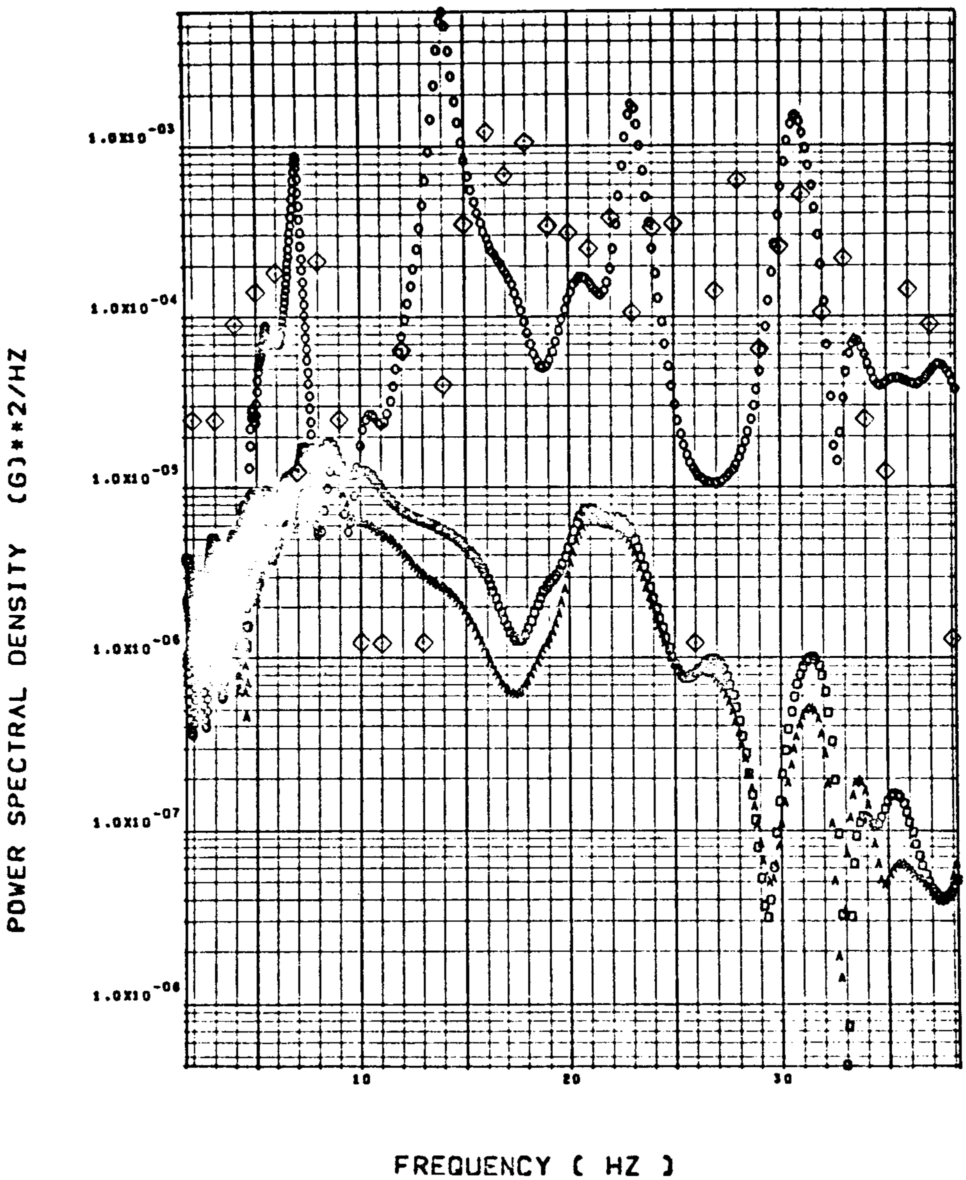

Figure 1.-(c) Pilot seat vertical accelerometer

◇ AF009 $\alpha_{FLT} = 11.7^{o}$

WING BUFFET RESPONSE. F-111A. CONTRACT NAS2 - 7091
SWEEP = 26 DEG. MACH= .8. ALT = 19.5K. ALPHA= 11.1
PILOT STATION VERTICAL ACCELEROMETER. FS = 255
CIRCLE = 1 DOF PLUS = 2 DOF X = 9 DOF

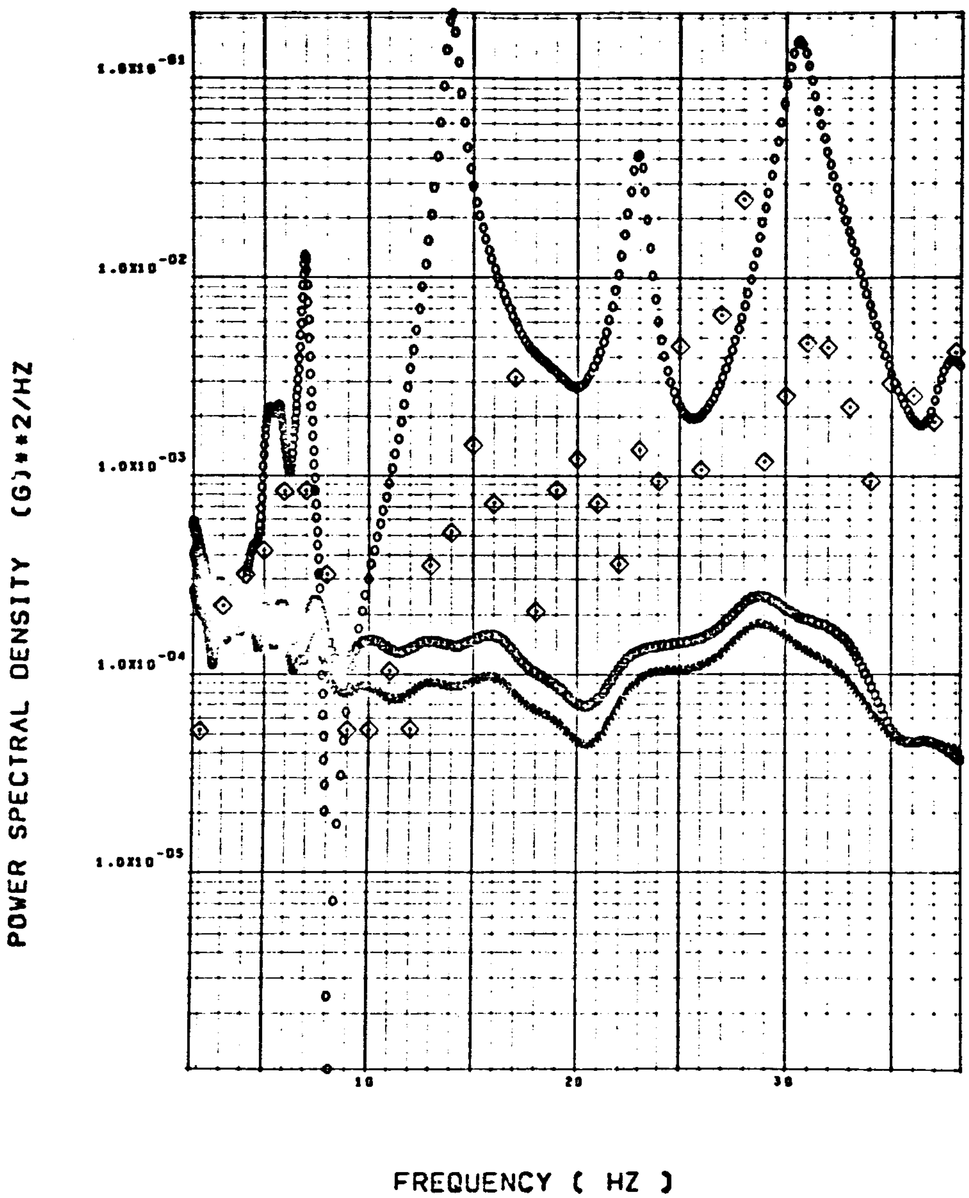

Figure 1.-(c) Pilot seat vertical accelerometer (continued)

◇ AF009 $\alpha_{FLT} = 14.1^{\circ}$

WING BUFFET RESPONSE. F-111A. CONTRACT NAS2 - 7091
SWEEP = 26 DEG. MACH= .8. ALT = 19.5K. ALPHA= 14.4
PILOT STATION VERTICAL ACCELEROMETER. FS = 255
CIRCLE = 1 DOF PLUS = 2 DOF X = 9 DOF

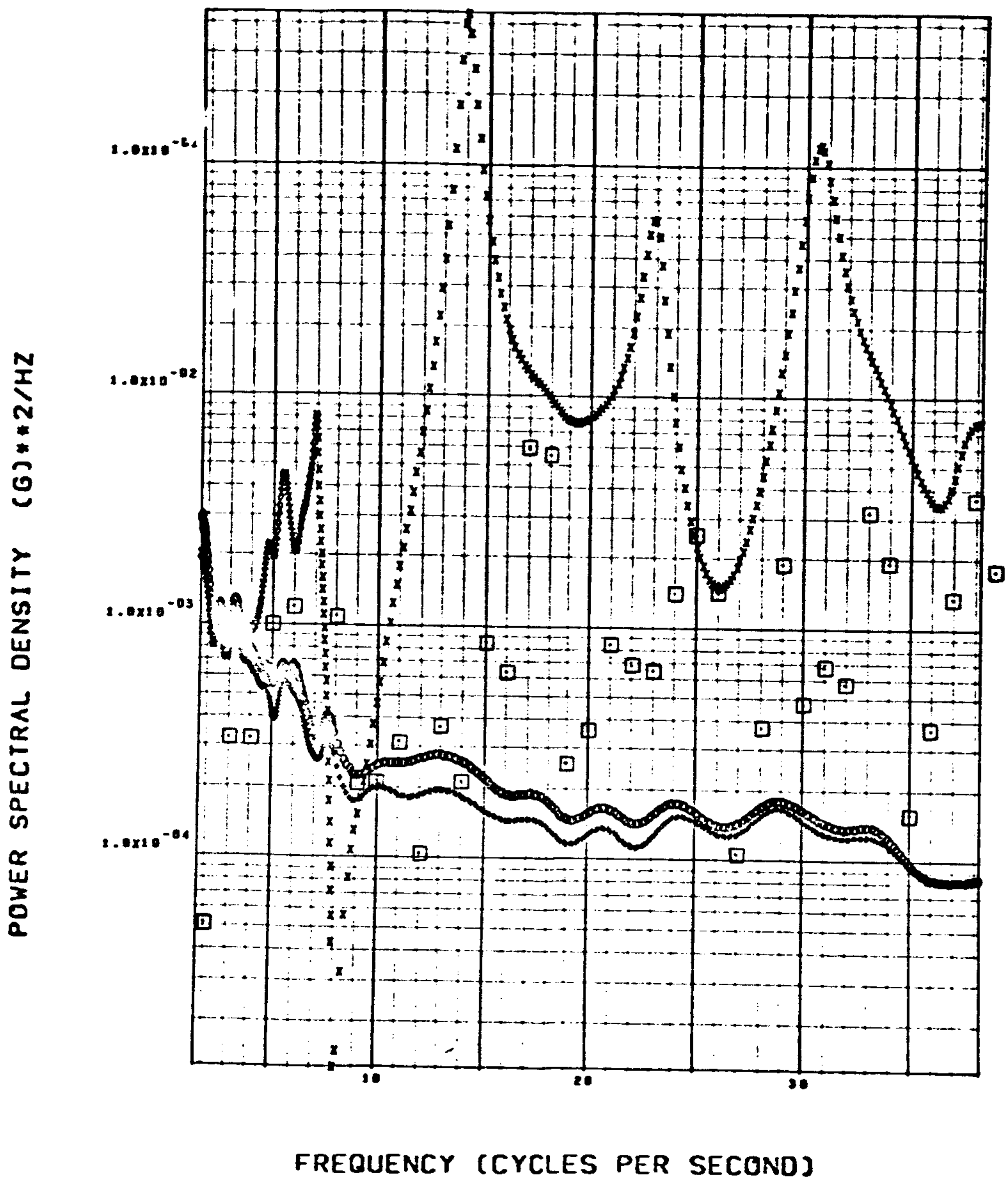

Figure 1.-(c) Pilot seat vertical accelerometer (continued)

◇ AB020 $\alpha_{FLT} = 6.9^{o}$

ANTI WING BUFFET RESPONSE. F-111A
SWEEP = 26 DEG. MACH= .8. ALT = 19.5K. ALPHA= 6.6
C.G. LATERAL ACCELEROMETER
SQUARE = 1 DOF A = 3 DOF CIRCLE = 10 DOF

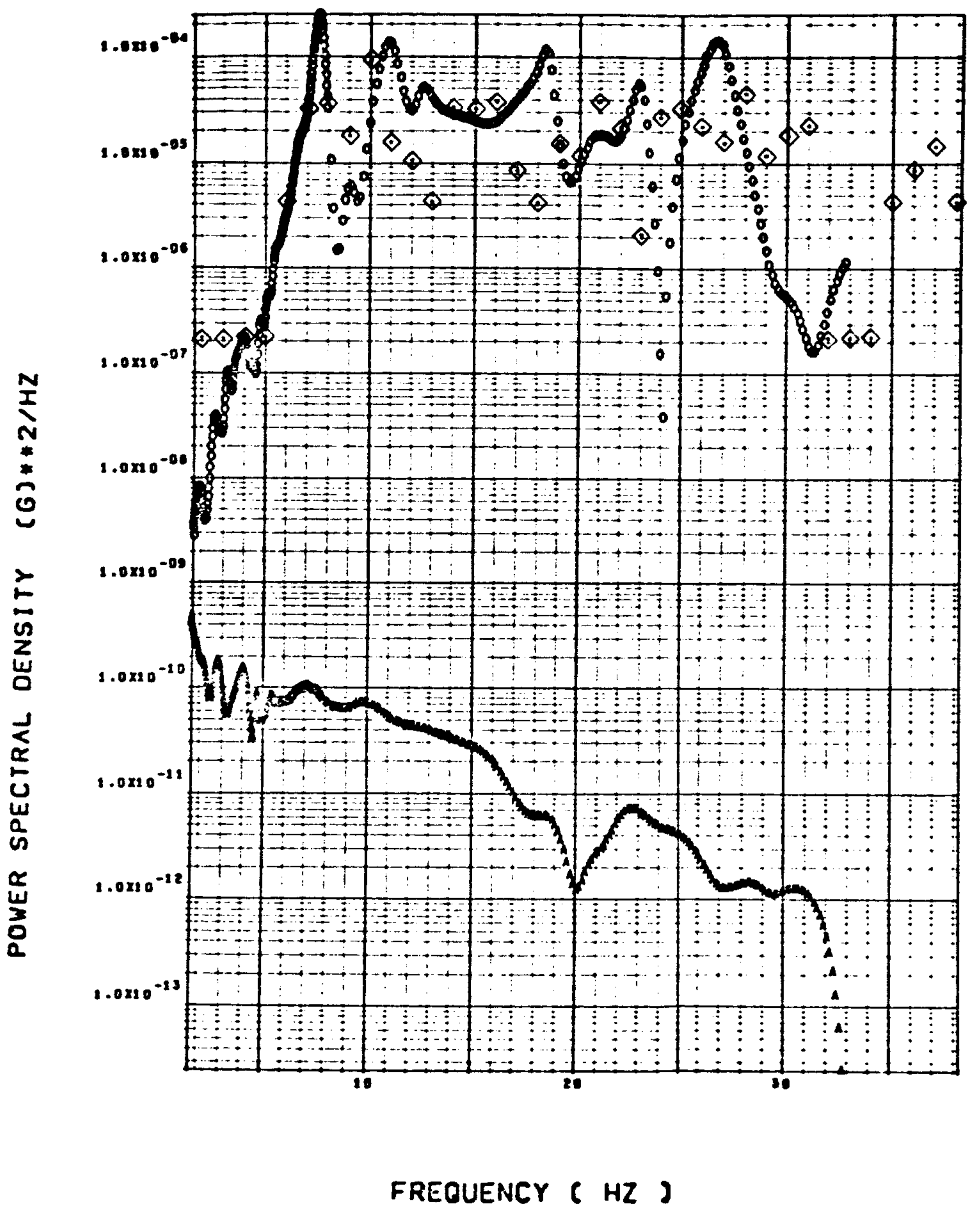

Figure 1.-(d) C.G. lateral accelerometer

◇ AB020 $\alpha_{FLT} = 11.7^{o}$

ANTI WING BUFFET RESPONSE, F-111A
SWEEP = 26 DEG, MACH= .8, ALT = 19.5K, ALPHA= 11.1
C.G. LATERAL ACCELEROMETER
SQUARE = 1 DOF A = 3 DOF CIRCLE = 10 DOF

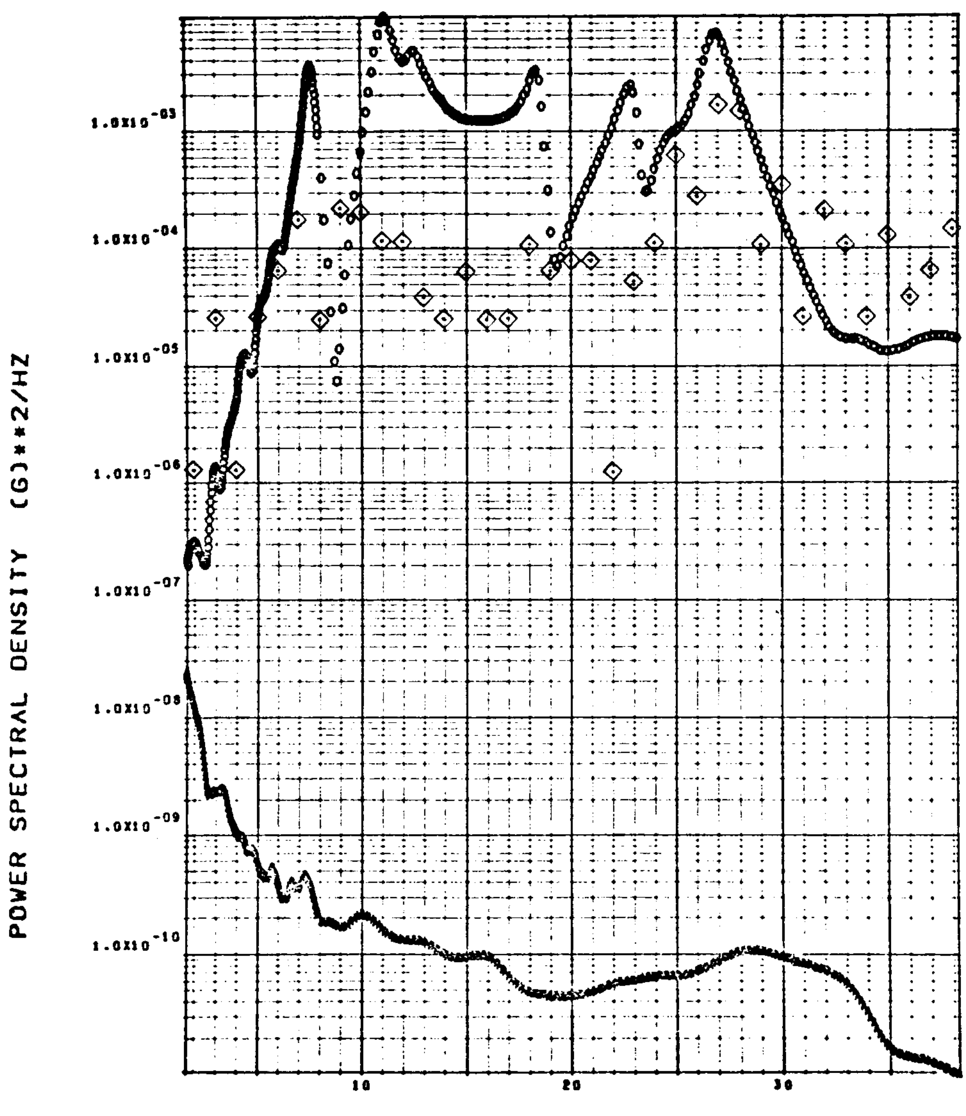

Figure 1.-(d) C.G. lateral accelerometer (continued)

◇ AB020 $\alpha_{FLT} = 14.1^{o}$

ANTI WING BUFFET RESPONSE. F-111A
SWEEP = 26 DEG. MACH= .8. ALT= 19.5K. ALPHA= 14.4
C.G. LATERAL ACCELEROMETER
SQUARE = 1 DOF A = 3 DOF CIRCLE = 10 DOF

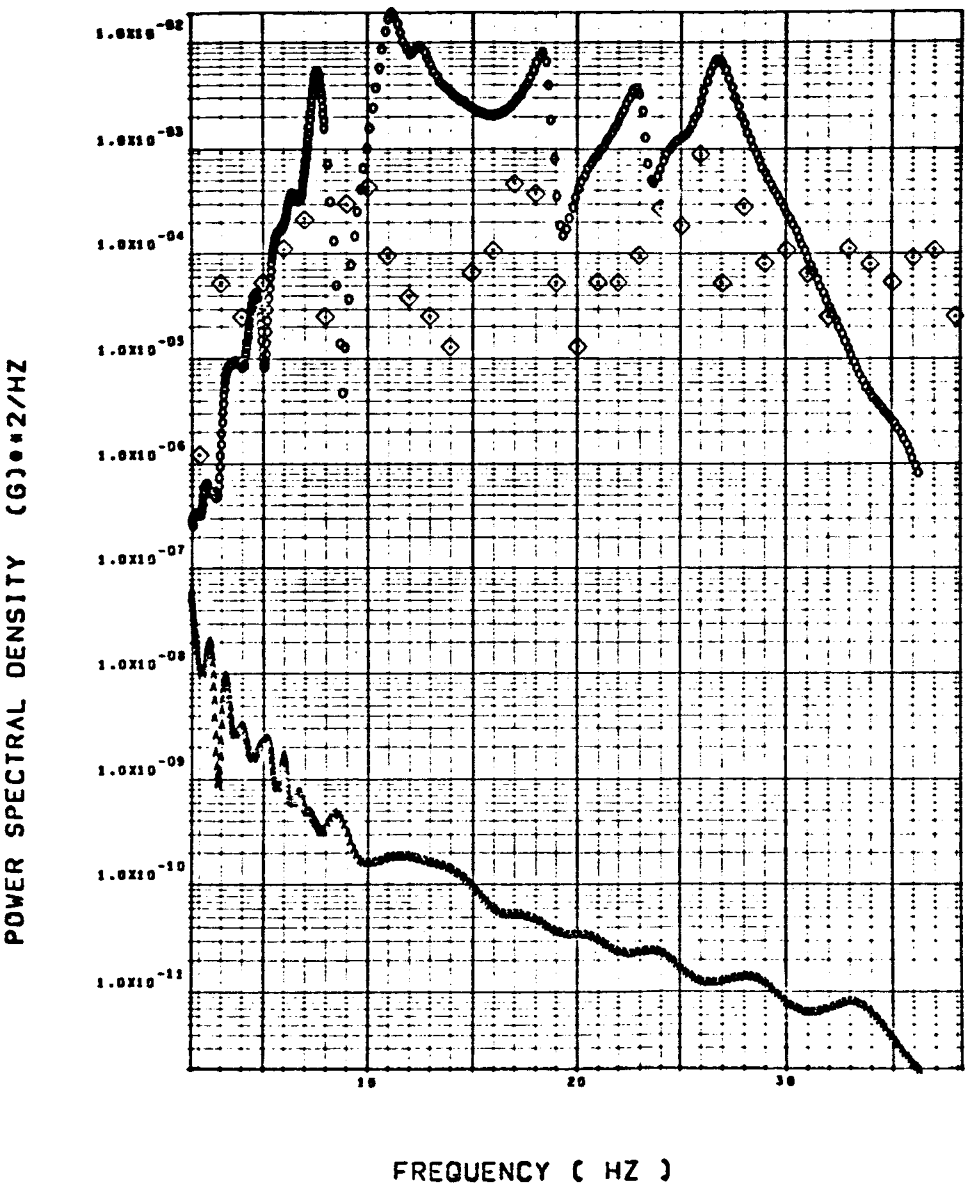

Figure 1.-(d) C.G. lateral accelerometer (continued)

◇ AF010 $\alpha_{FLT} = 6.9^{o}$

ANTI WING BUFFET RESPONSE. F-111A
SWEEP = 26 DEG. MACH= .8. ALT = 19.5K. ALPHA= 6.6
PILOT STATION LATERAL ACCELEROMETER. FS = 529
SQUARE = 1 DOF A = 3 DOF CIRCLE = 10 DOF

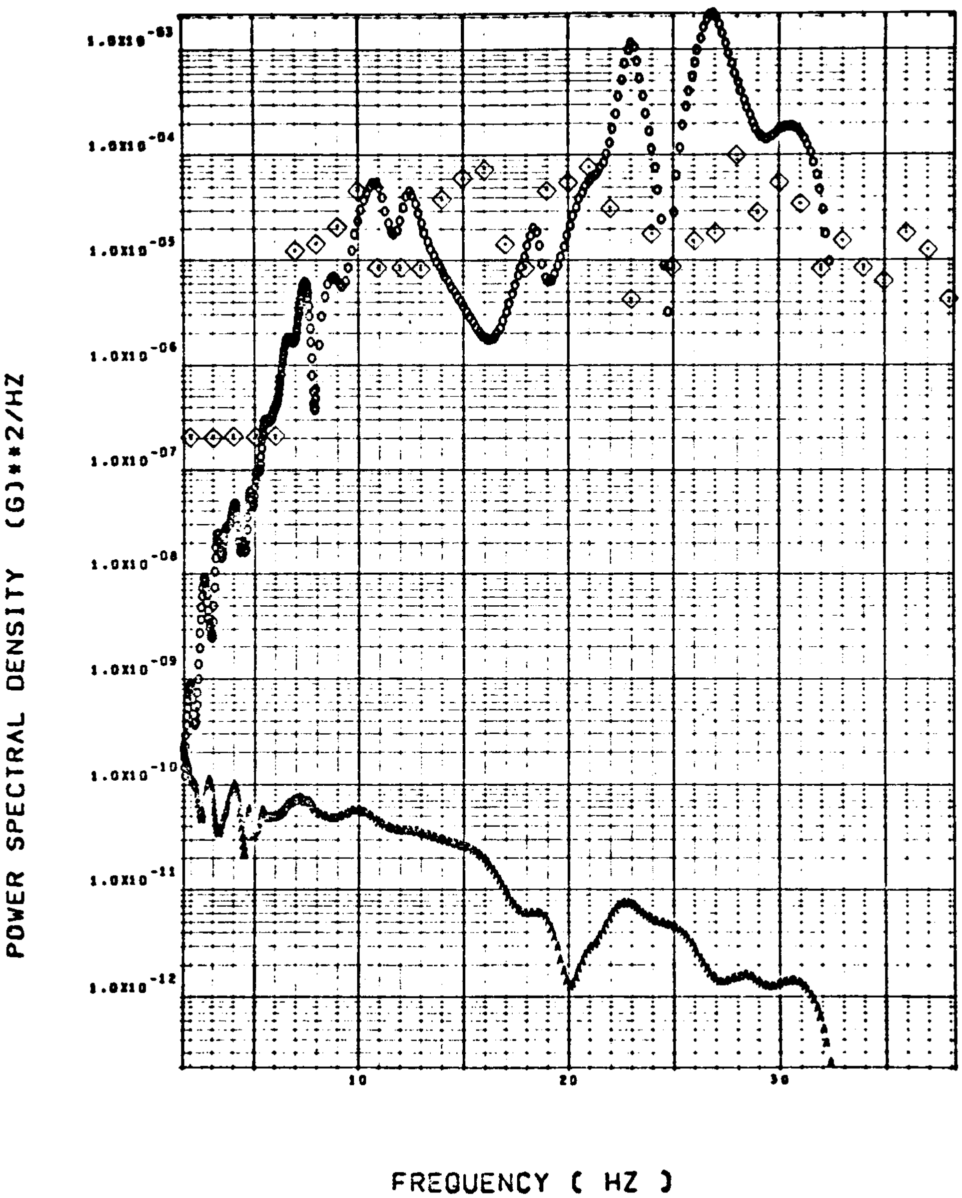

Figure 1.-(e) Pilot seat lateral accelerometer

◇ AF010 $\alpha_{FLT} = 11.7^{o}$

ANTI WING BUFFET RESPONSE. F-111A
SWEEP = 26 DEG. MACH= .8. ALT = 19.5K. ALPHA= 11.1
PILOT STATION LATERAL ACCELEROMETER. FS = 529
SQUARE = 1 DOF A = 3 DOF CIRCLE = 10 DOF

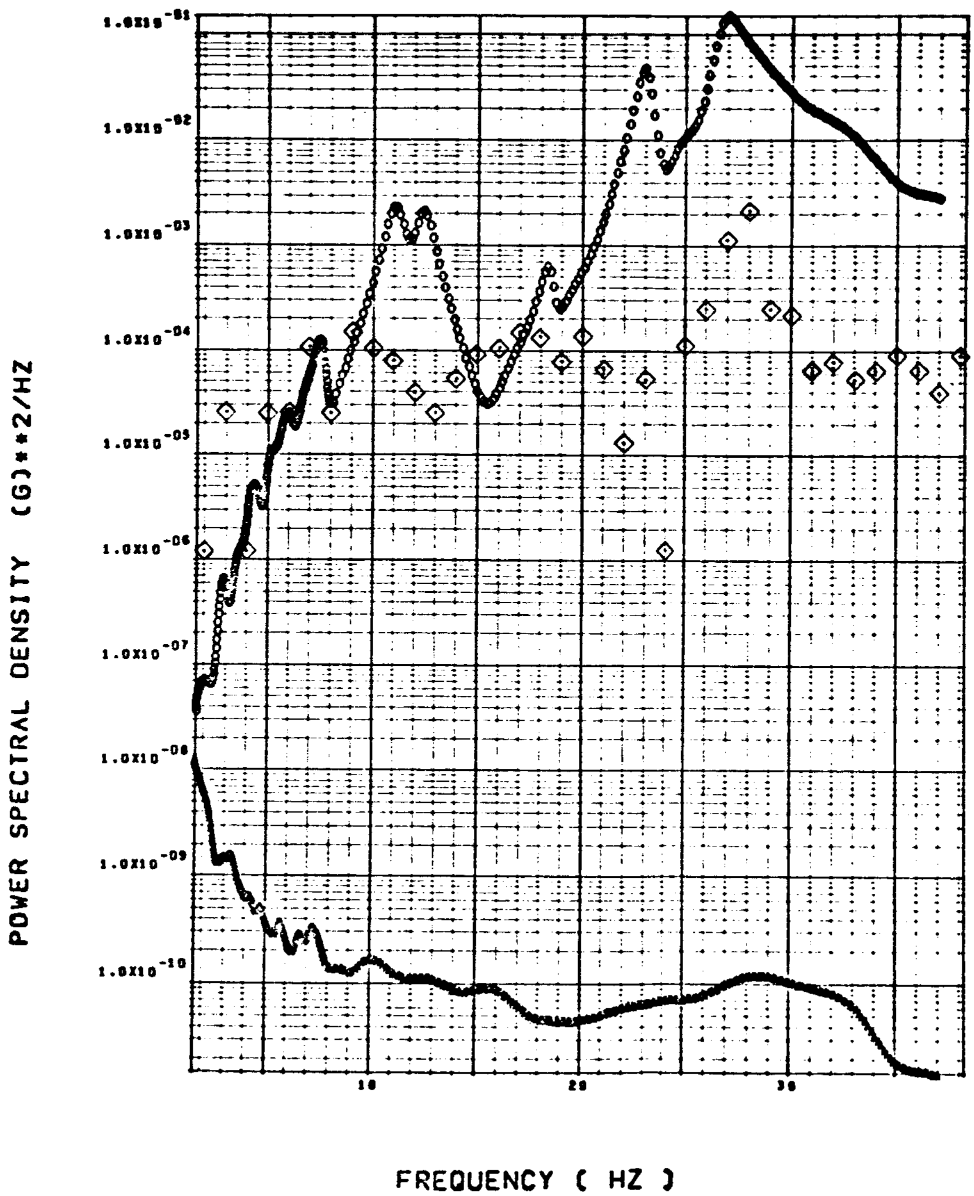

Figure 1.-(e) Pilot seat lateral accelerometer (continued)

◇ AF010 $\alpha_{FLT} = 14.1^{\circ}$

ANTI WING BUFFET RESPONSE. F-111A
SWEEP = 26 DEG. MACH= .8. ALT= 19.5K. ALPHA= 14.4
PILOT STATION LATERAL ACCELEROMETER. FS = 529
SQUARE = 1 DOF A = 3 DOF CIRCLE = 10 DOF

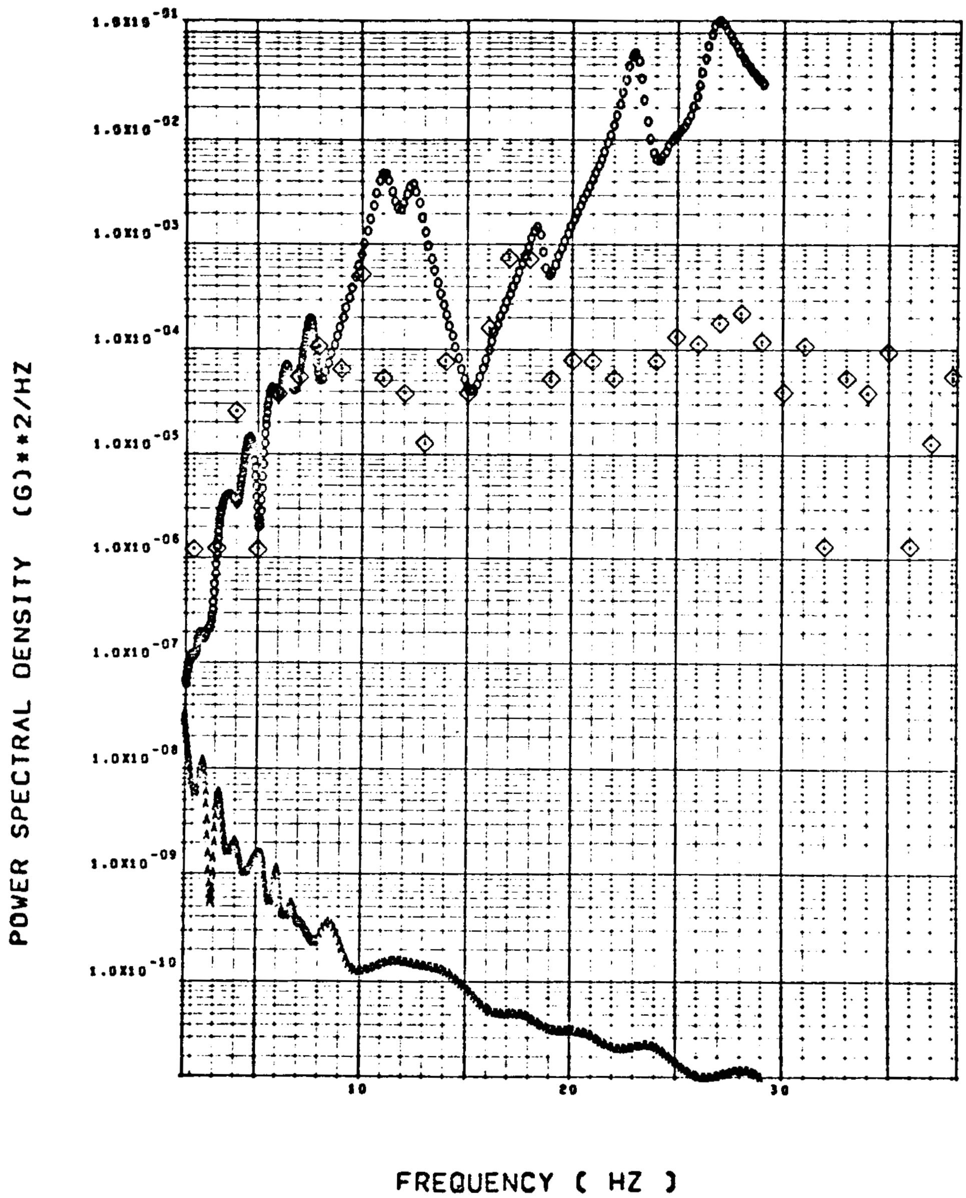

Figure 1.-(e) Pilot seat lateral accelerometer (continued)

△ SW123 $\alpha_{FLT} = 6.9^{o}$

F-111A WING ALONE BUFFET RESPONSE. FLT 77. SC-R
SWEEP=26 DEG. MACH=.8. ALT=6035(M). ALPHA= 6.6
WING SHEAR (N) AT SPAN STATION 75
CIRCLE = UPPER BOUNDS SQUARE = LOWER BOUNDS

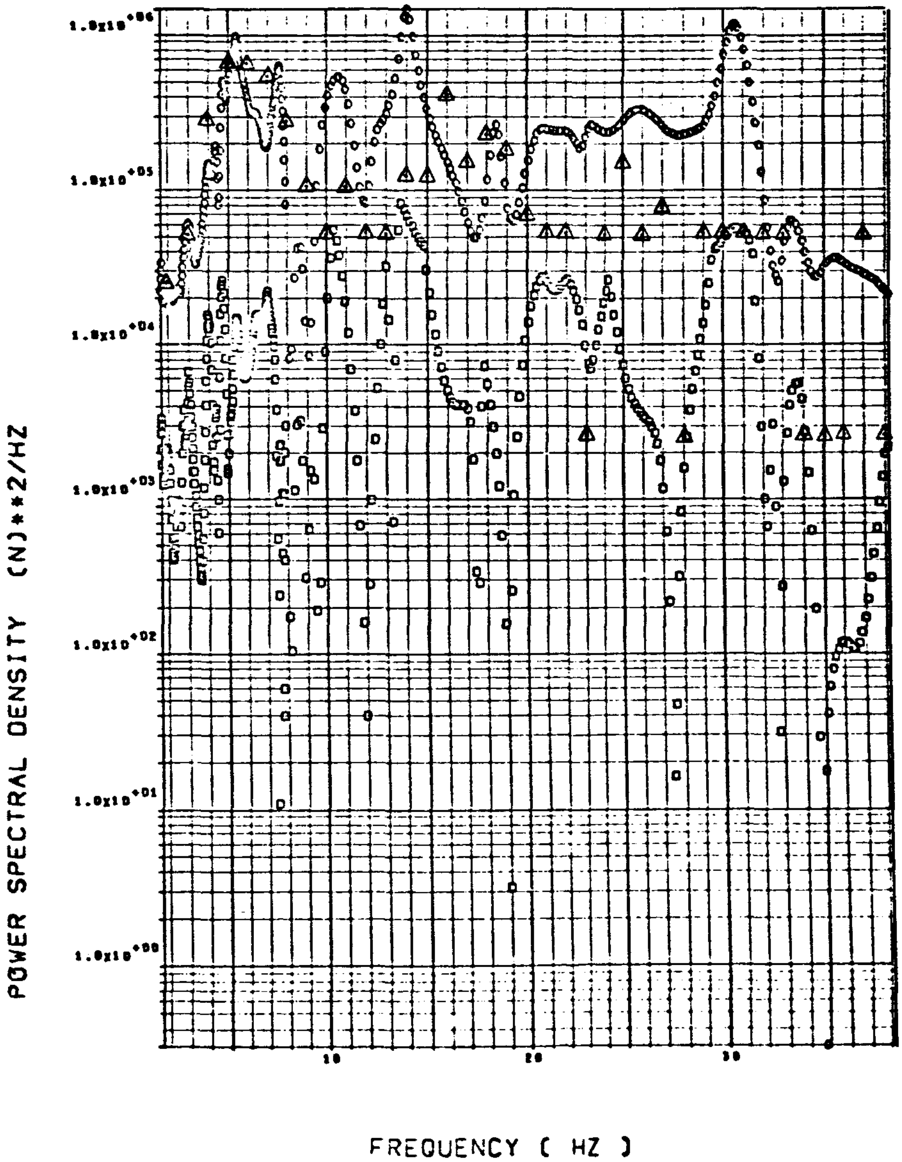

Figure 1.-(f) Wing shear

△ SW123 $\alpha_{FLT} = 11.7^{o}$

F-111A WING ALONE BUFFET RESPONSE. FLT 77. SC-R
SWEEP=26 DEG. MACH=.8. ALT=6035(M). ALPHA= 11.1
WING SHEAR (N) AT SPAN STATION 75
CIRCLE = UPPER BOUNDS SQUARE = LOWER BOUNDS

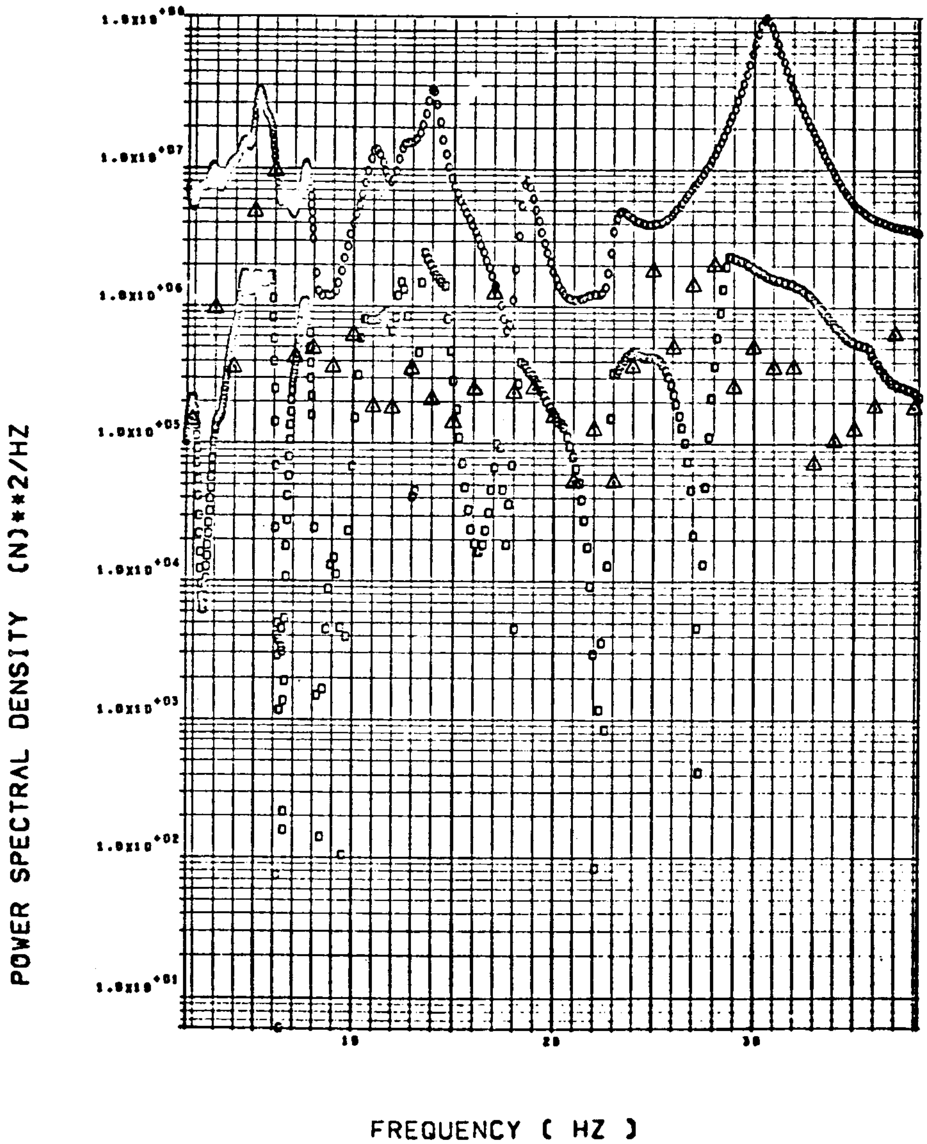

Figure 1.-(f) Wing shear (continued)

△ SW123 $\alpha_{FLT} = 14.1^{o}$

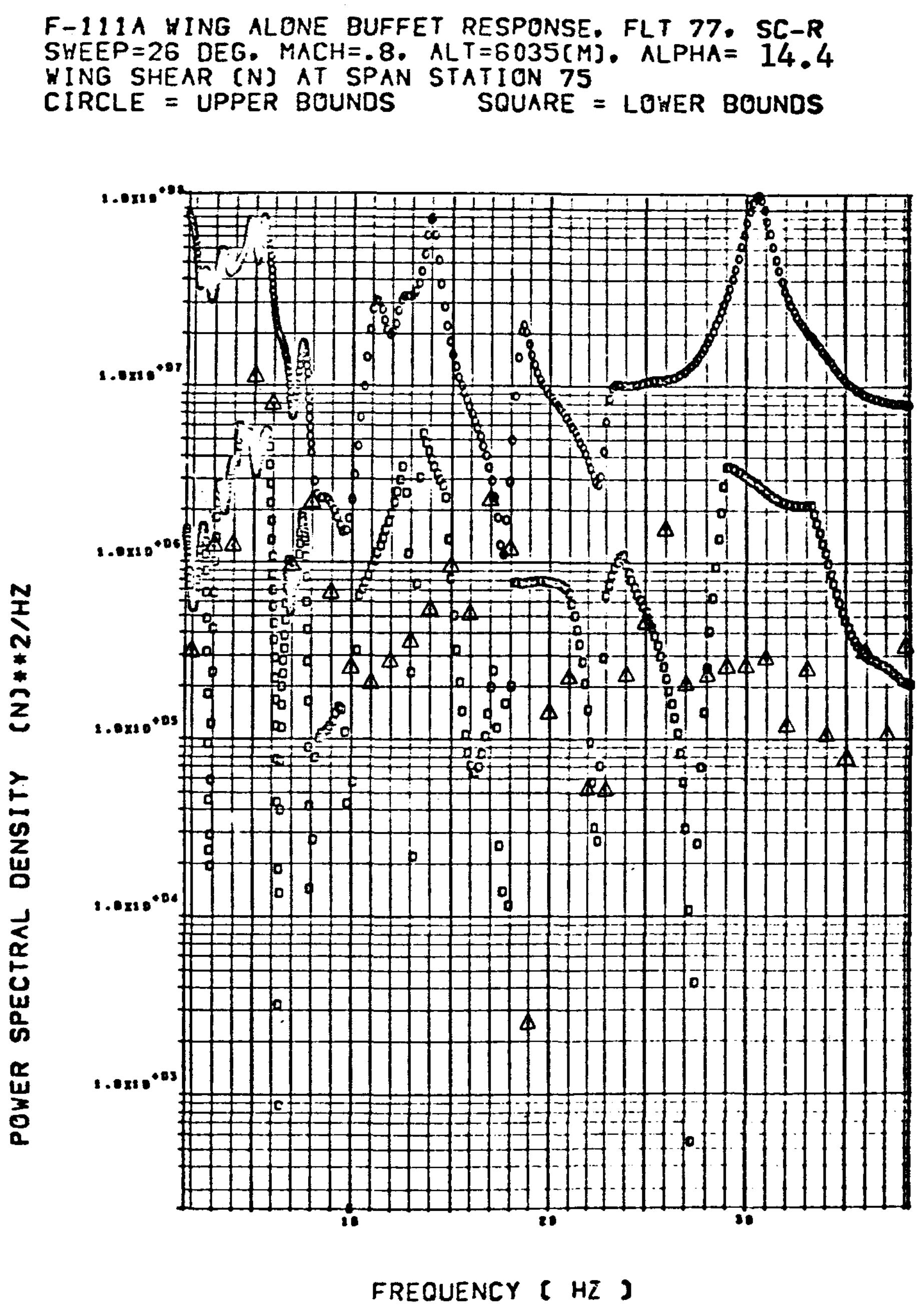

Figure 1.-(f) Wing shear (continued)

▲ SW124 $\alpha_{FLT} = 6.9^{o}$

F-111A WING ALONE BUFFET RESPONSE, FLT 77, SC-R
SWEEP=26 DEG, MACH=.8, ALT=6035(M), ALPHA=6.6
WING BENDING MOMENT (M-N) AT SPAN STATION 75
CIRCLE = UPPER BOUNDS SQUARE = LOWER BOUNDS

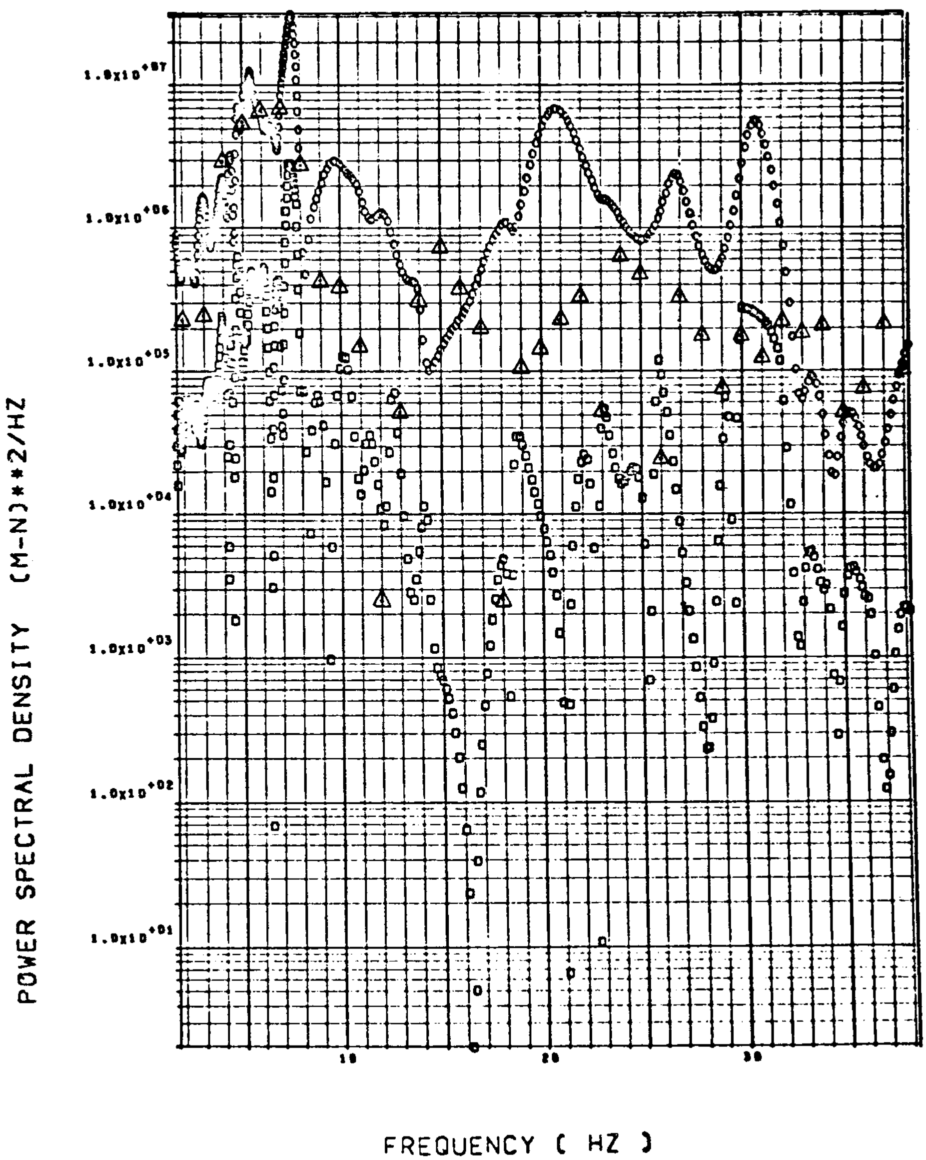

Figure 1.-(g) Wing bending moment

△ SW124 $\alpha_{FLT} = 11.7^{\circ}$

F-111A WING ALONE BUFFET RESPONSE. FLT 77. SC-R
SWEEP=26 DEG. MACH=.8. ALT=6035(M). ALPHA= 11.1
WING BENDING MOMENT (M-N) AT SPAN STATION 75
CIRCLE = UPPER BOUNDS SQUARE = LOWER BOUNDS

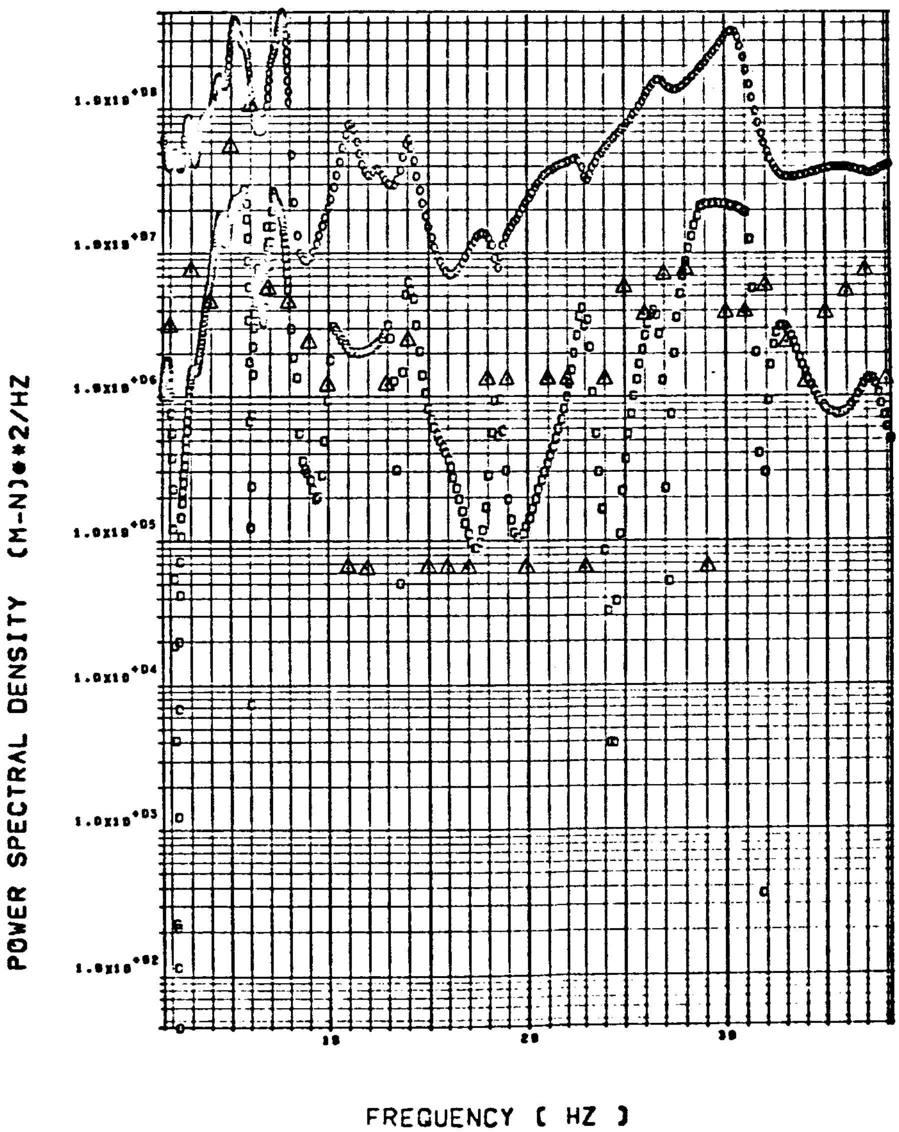

Figure 1.-(g) Wing bending moment (continued)

Δ SW124 $\alpha_{FLT} = 14.1^{\circ}$

F-111A WING ALONE BUFFET RESPONSE. FLT 77. SC-R
SWEEP=26 DEG. MACH=.8. ALT=6035(M). ALPHA= 14.4
WING BENDING MOMENT (M-N) AT SPAN STATION 75
CIRCLE = UPPER BOUNDS SQUARE = LOWER BOUNDS

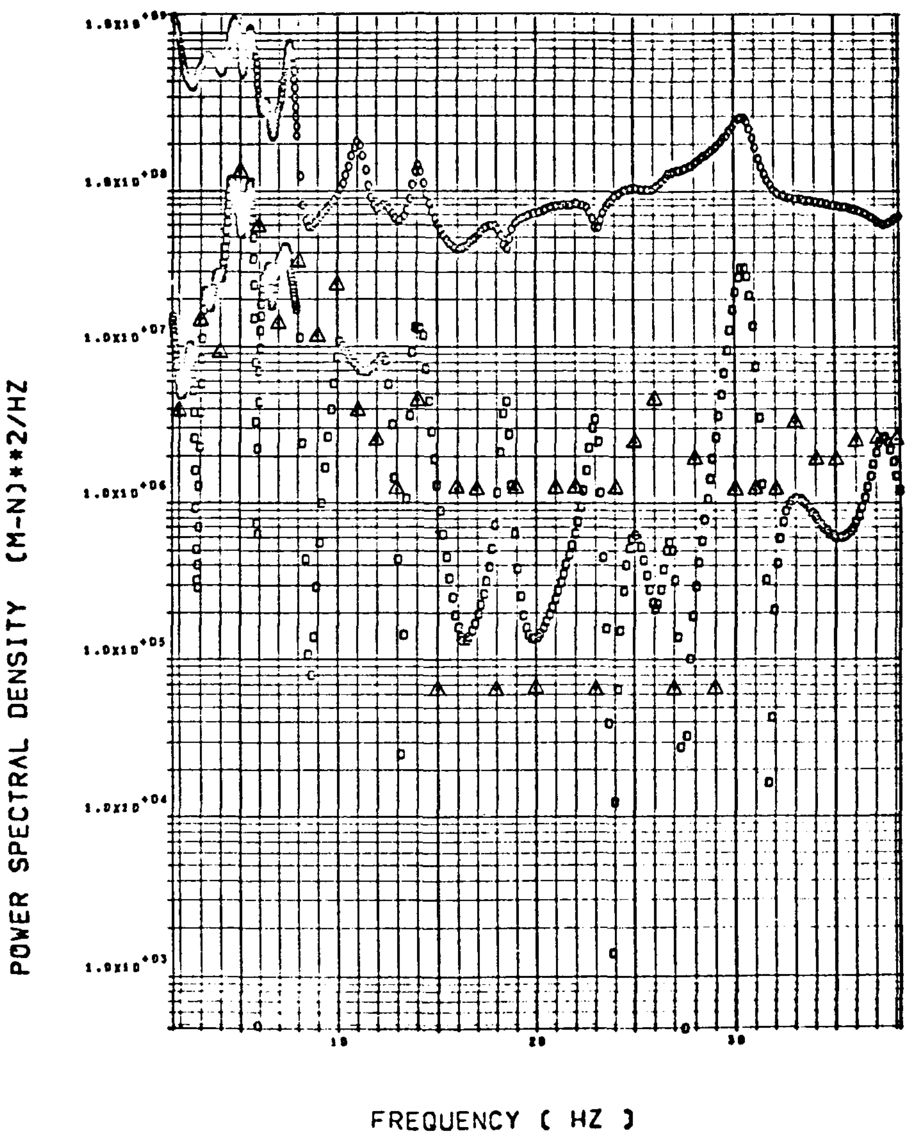

Figure 1. Wing bending moment (continued)

▲ SW125 $\alpha_{FLT} = 6.9^{o}$

F-111A WING ALONE BUFFET RESPONSE, FLT 77, SC-R
SWEEP=26 DEG, MACH=.8, ALT=6035(M), ALPHA= 6.6
WING TORQUE (M-N) AT SPAN STATION 75
CIRCLE = UPPER BOUNDS SQUARE = LOWER BOUNDS

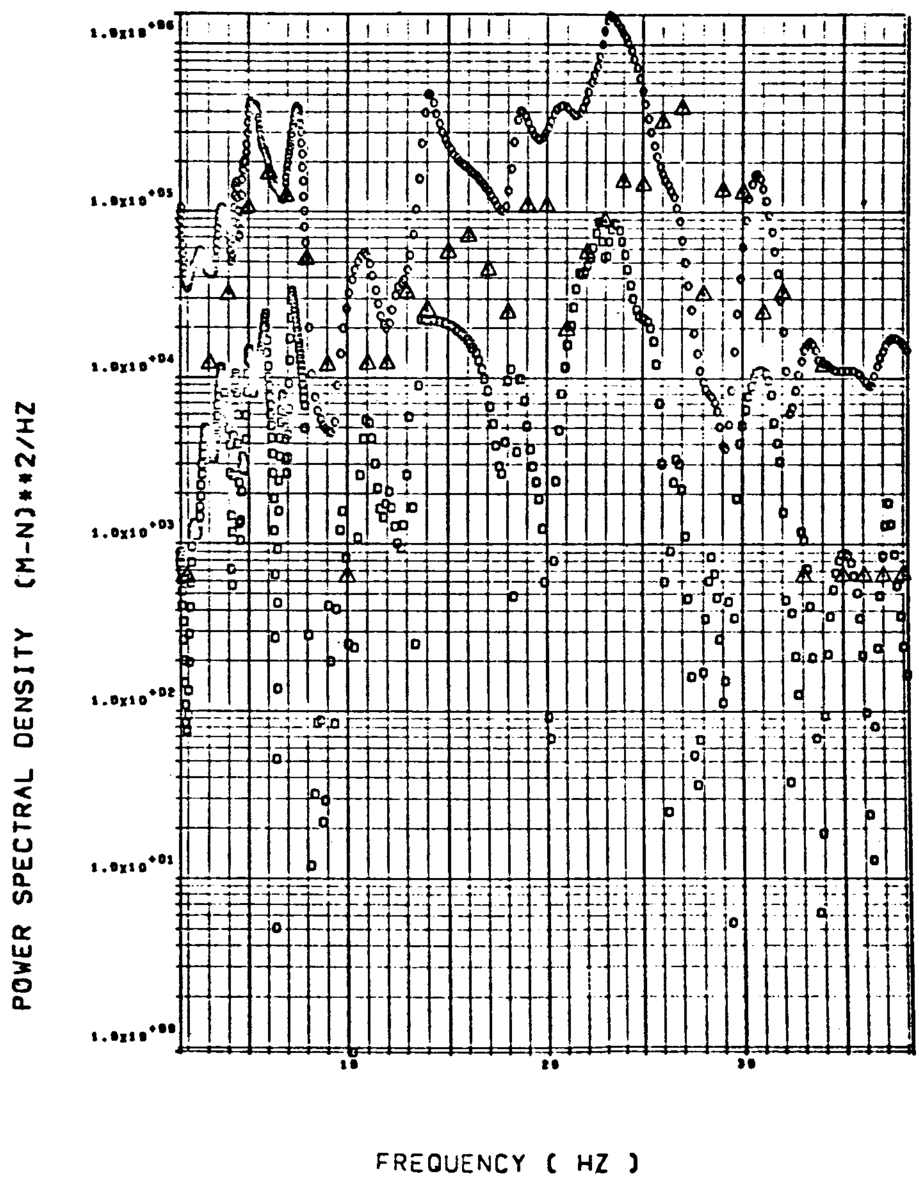

Figure 1.-(h) Wing torsion

△ SW125 $\alpha_{FLT} = 11.7^{o}$

F-111A WING ALONE BUFFET RESPONSE. FLT 77. SC-R
SWEEP=26 DEG. MACH=.8. ALT=6035(M). ALPHA= 11.1
WING TORQUE (M-N) AT SPAN STATION 75
CIRCLE = UPPER BOUNDS SQUARE = LOWER BOUNDS

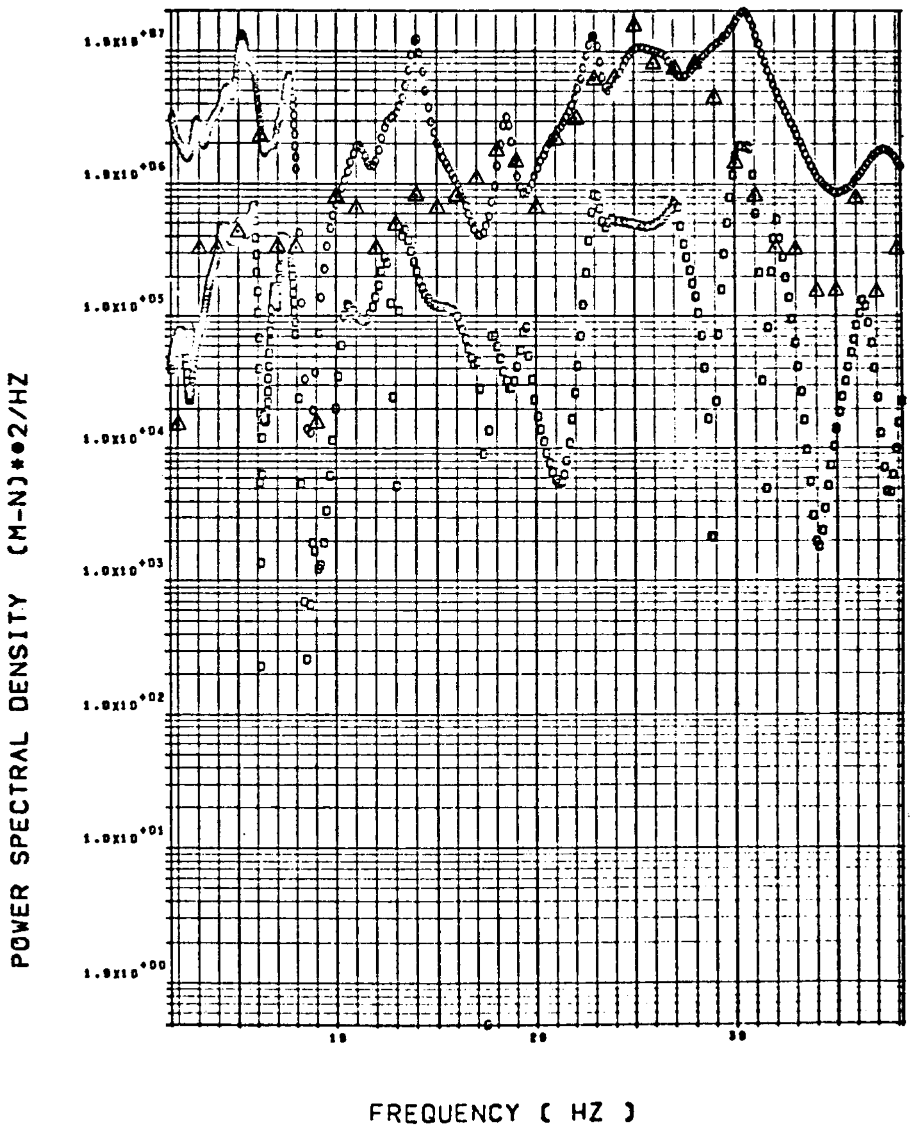

Figure 1.-(h) Wing torsion (continued)

△ SW125 $\alpha_{FLT} = 14.1^{\circ}$

F-111A WING ALONE BUFFET RESPONSE, FLT 77, SC-R
SWEEP=26 DEG, MACH=.8, ALT=6035(M), ALPHA= 14.4
WING TORQUE (M-N) AT SPAN STATION 75
CIRCLE = UPPER BOUNDS SQUARE = LOWER BOUNDS

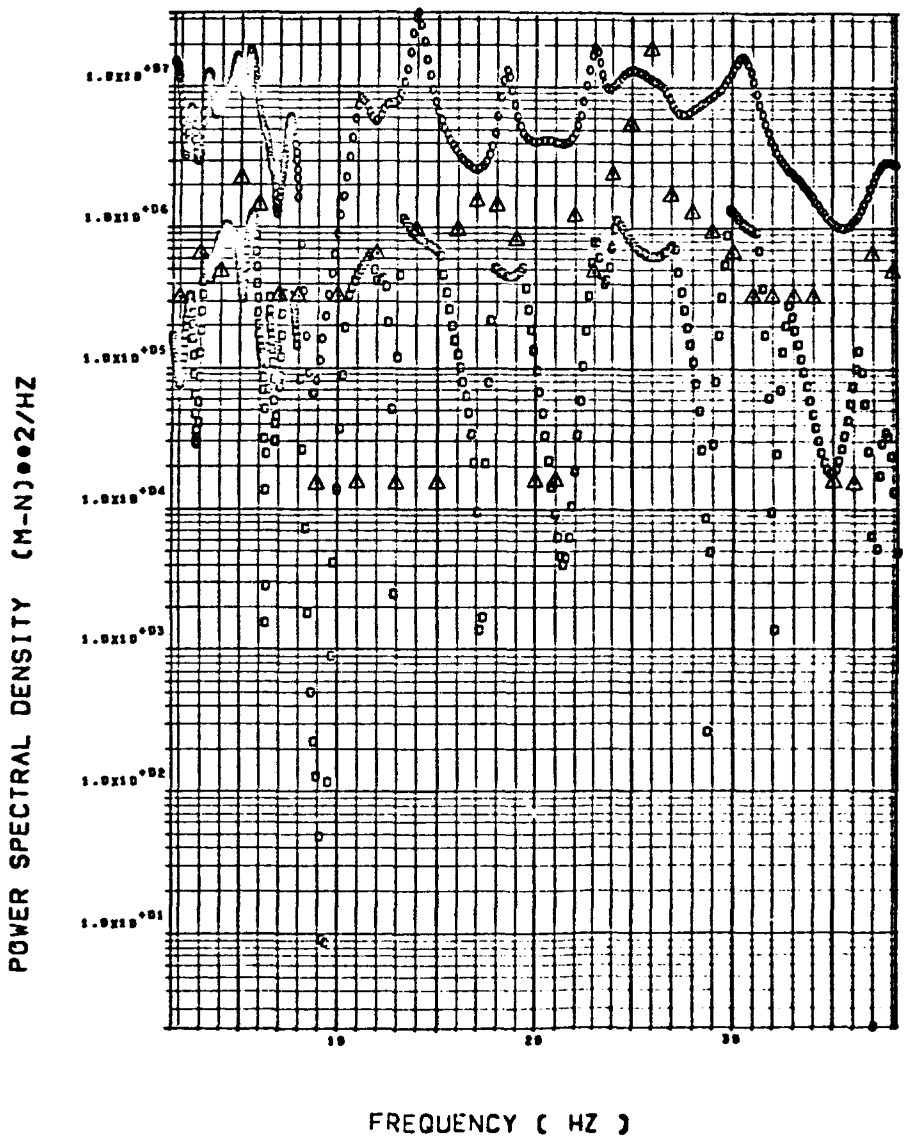

Figure 1.-(h) Wing torsion (continued)

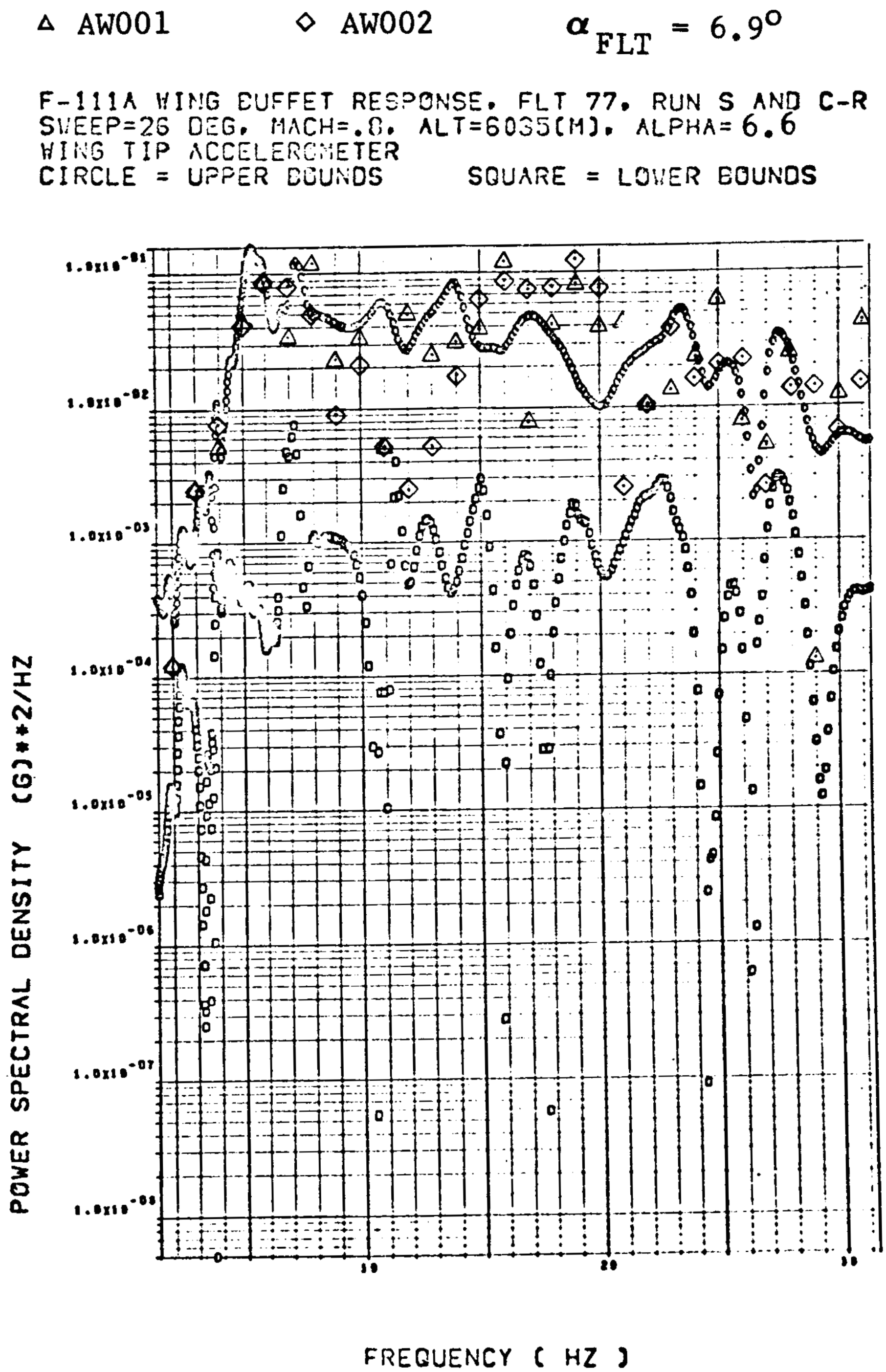

Figure 2.- Power spectra for
Case 2, total airplane (half horizontal tail),
Λ=26°, M=0.80, alt.=6035m (19,800 ft)
(a) wing tip accelerometer

△ AW001 ◇ AW002 $\alpha_{FLT} = 11.7^{\circ}$

F-111A WING BUFFET RESPONSE, FLT 77, RUN S AND C-R
SWEEP=26 DEG, MACH=.8, ALT=6035(M), ALPHA= 11.1
WING TIP ACCELEROMETER
CIRCLE = UPPER BOUNDS SQUARE = LOWER BOUNDS

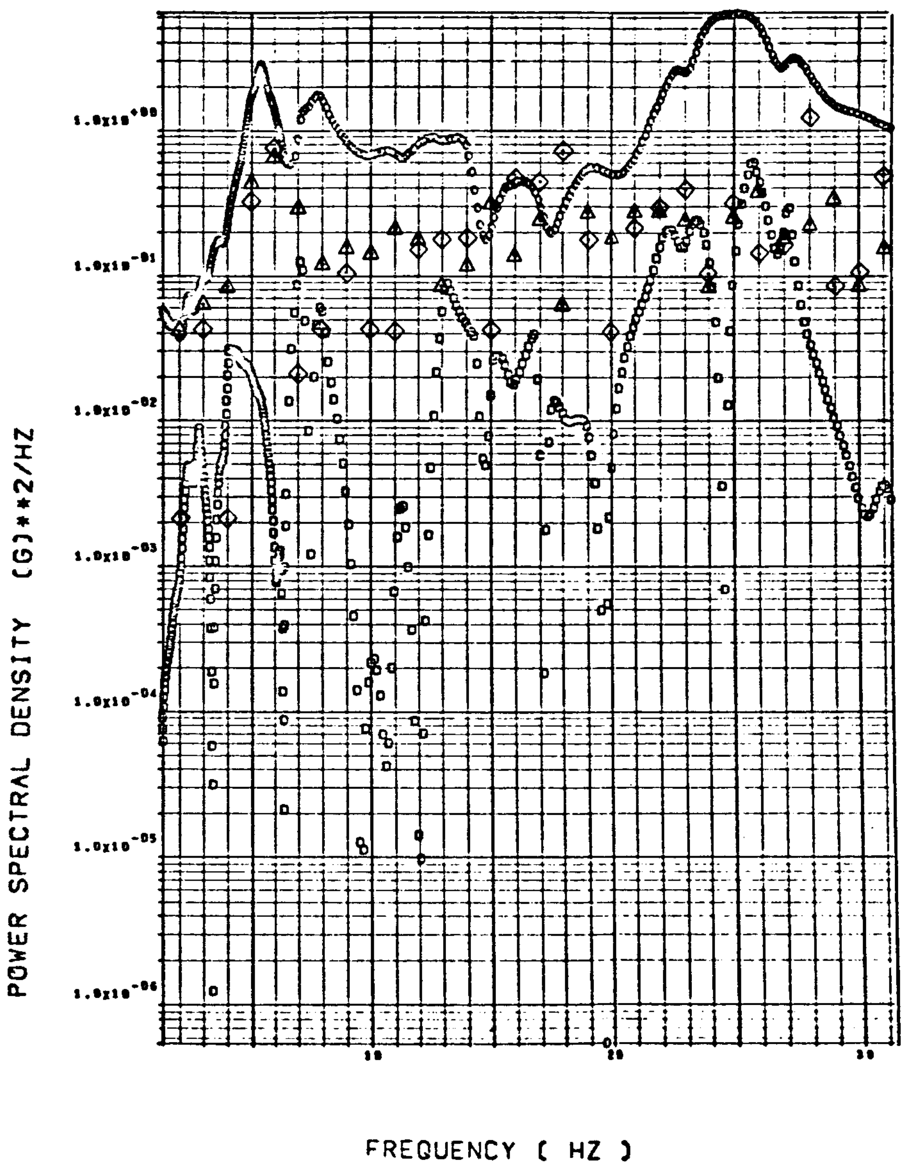

Figure 2.-(a) Wing tip accelerometer (continued)

△ AW001 ◇ AW002 $\alpha_{FLT} = 14.1^{o}$

F-111A WING BUFFET RESPONSE. FLT 77. RUN S AND C-R
SWEEP=26 DEG. MACH=.8. ALT=6035(M). ALPHA= 14.4
WING TIP ACCELEROMETER
CIRCLE = UPPER BOUNDS SQUARE = LOWER BOUNDS

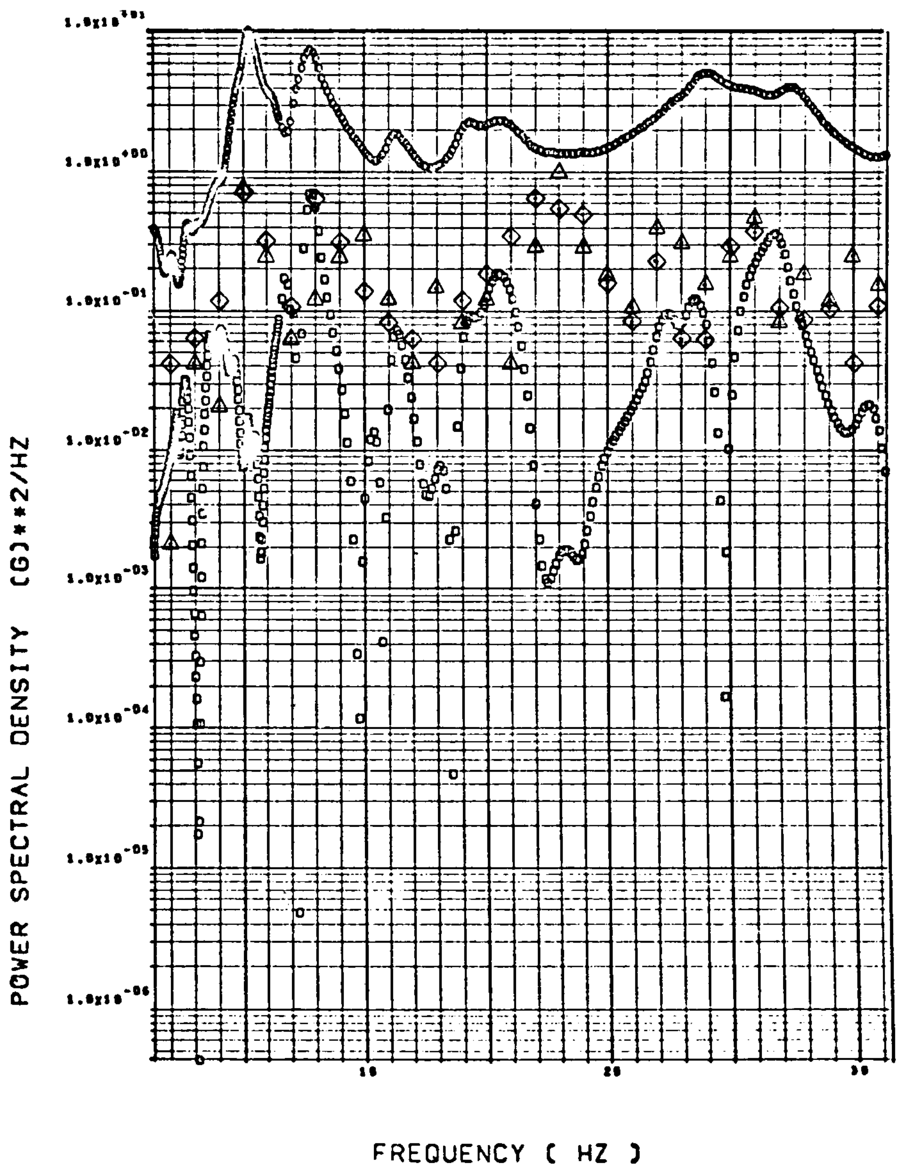

Figure 2.-(a) Wing tip accelerometer (continued)

◇ AB018 $\alpha_{FLT} = 6.9^{o}$

F-111A SYM. AC BUFFET. HALF TAIL. TORSION FREQS.
SWEEP = 26 DEG. MACH= .8. ALT = 19.8K. ALPHA= 6.6
C.G. VERTICAL ACCELEROMETER. FS = 529
SQUARE = 1 DOF A = 2 DOF CIRCLE = 14 DOF

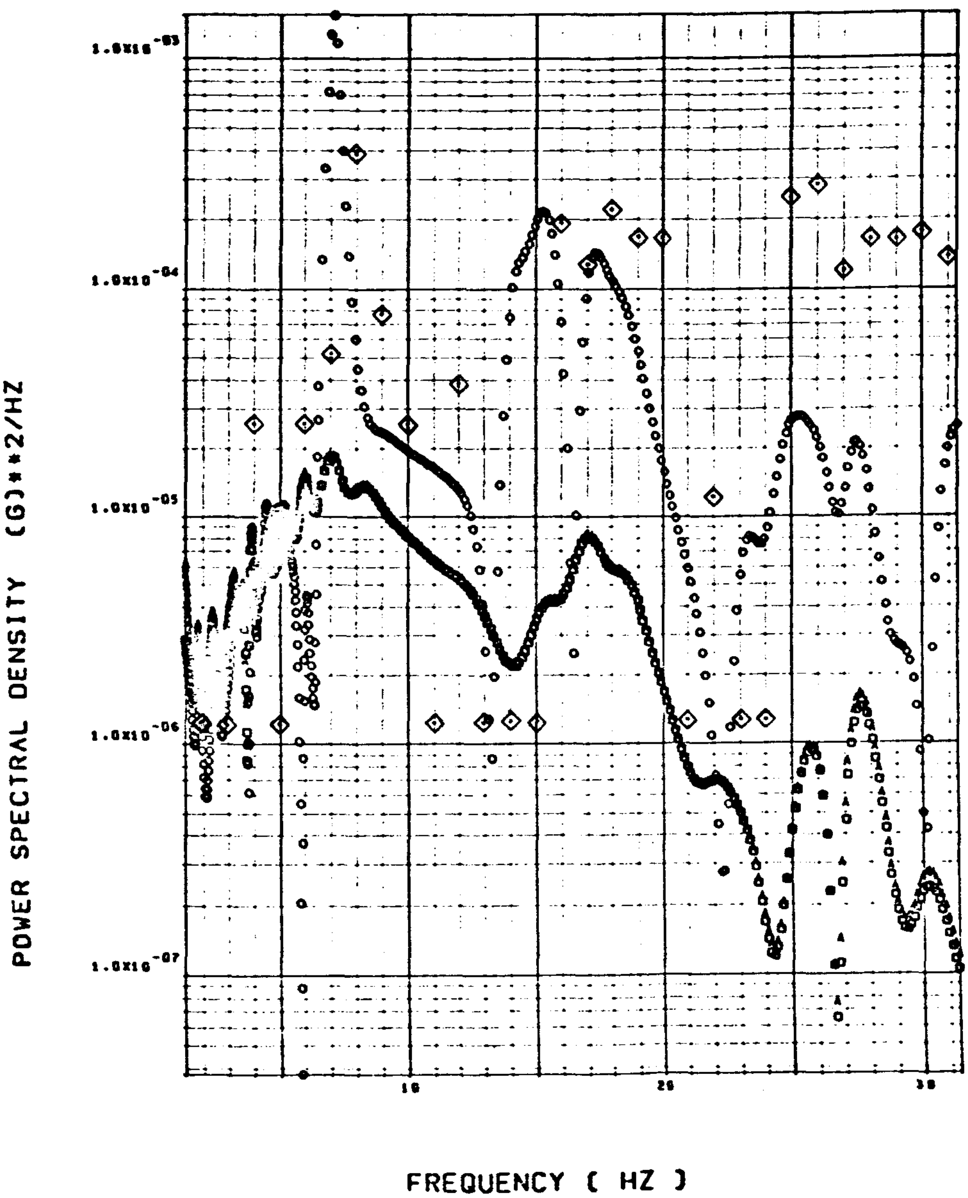

Figure 2.-(b) C.G. vertical accelerometer

◇ AB018 $\alpha_{FLT} = 11.7^{\circ}$

F-111A SYM. AC BUFFET. HALF TAIL. TORSION FREQS.
SWEEP = 26 DEG. MACH= .8. ALT = 19.8K. ALPHA= 11.1
C.G. VERTICAL ACCELEROMETER. FS = 529
SQUARE = 1 DOF A = 2 DOF CIRCLE = 14 DOF

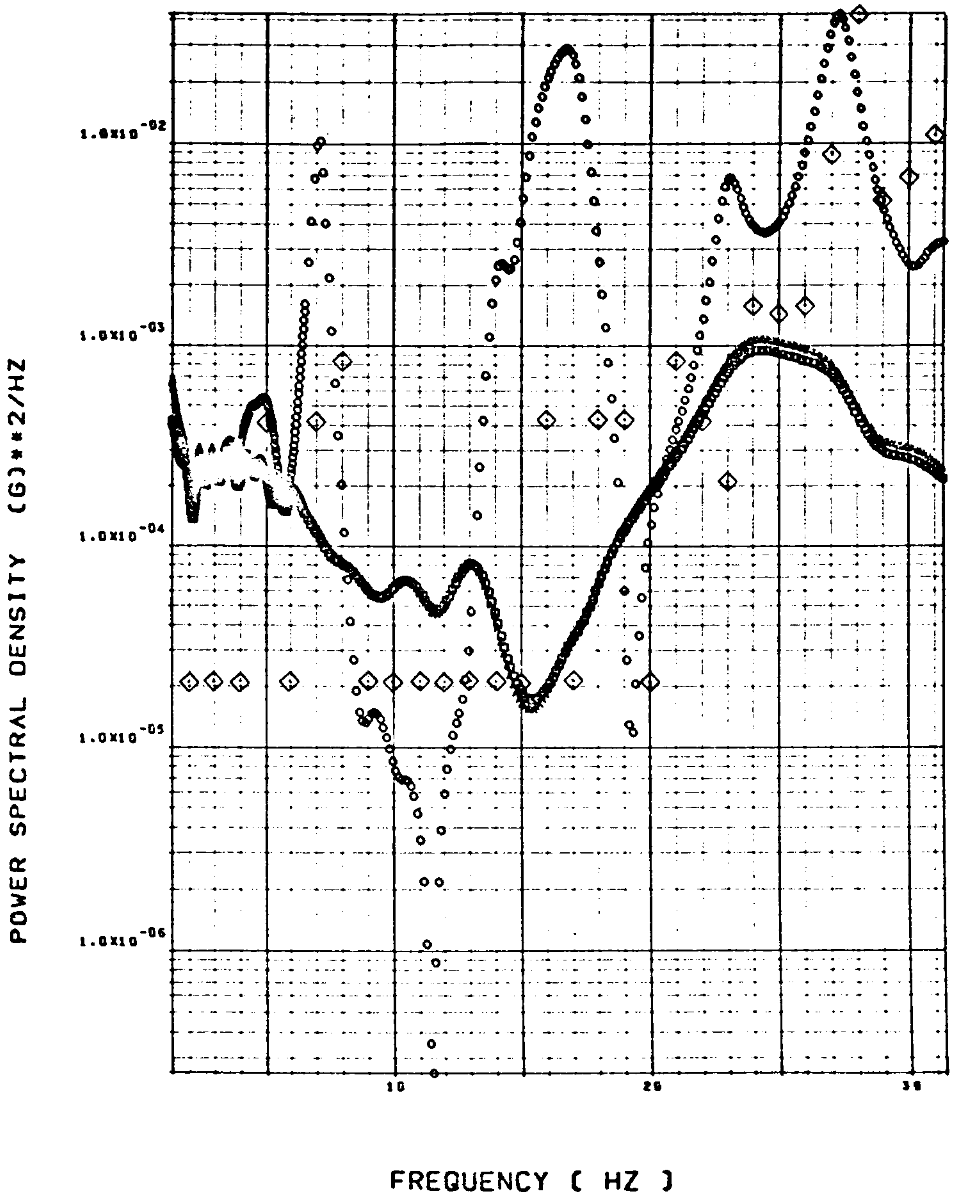

Figure 2.-(b) C.G. vertical accelerometer (continued)

◇ AB018 $\alpha_{FLT} = 14.1^{o}$

F-111A SYM. AC BUFFET. HALF TAIL. TORSION FREQS.
SWEEP = 26 DEG. MACH= .8. ALT = 19.8K. ALPHA= 14.4
C.G. VERTICAL ACCELEROMETER. FS = 529
SQUARE = 1 DOF A = 2 DOF CIRCLE = 14 DOF

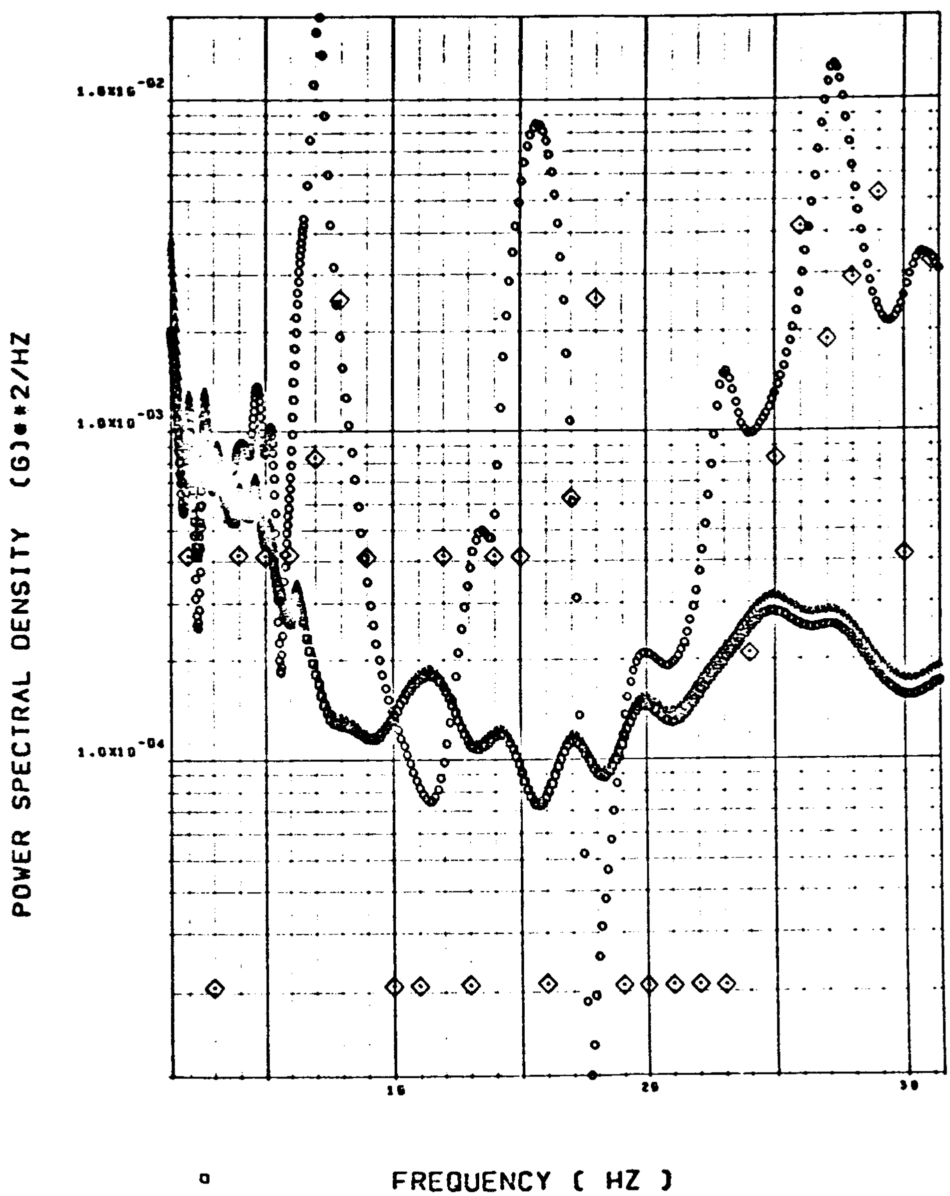

Figure 2.-(b) C.G. vertical accelerometer (continued)

◇ AF009 $\alpha_{FLT} = 6.9^{o}$

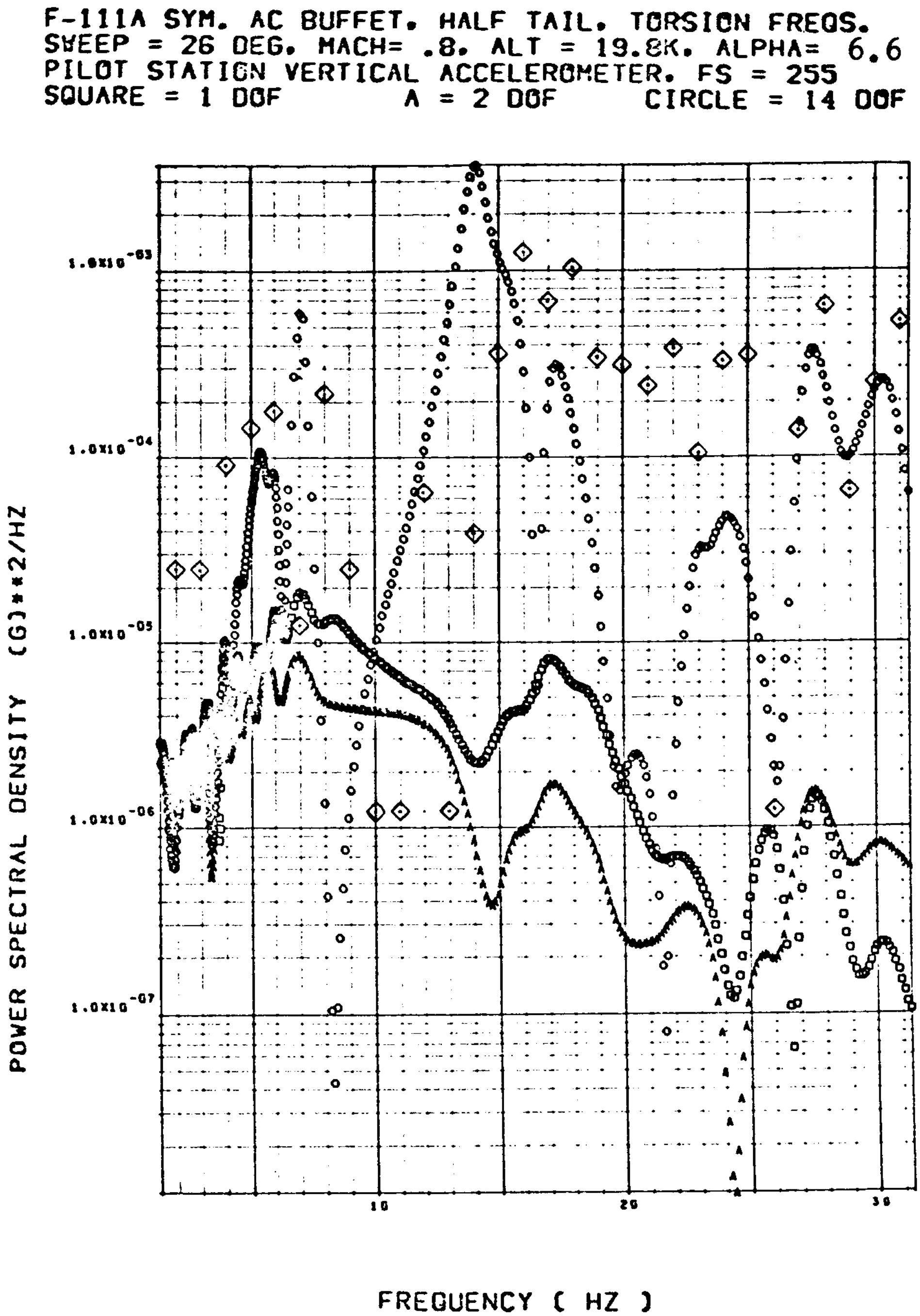

Figure 2.-(c) Pilot seat vertical accelerometer

◇ AF009 $\alpha_{FLT} = 11.7^{o}$

F-111A SYM. AC BUFFET. HALF TAIL. TORSION FREQS.
SWEEP = 26 DEG. MACH= .8. ALT = 19.8K. ALPHA= 11.1
PILOT STATION VERTICAL ACCELEROMETER. FS = 255
SQUARE = 1 DOF A = 2 DOF CIRCLE = 14 DOF

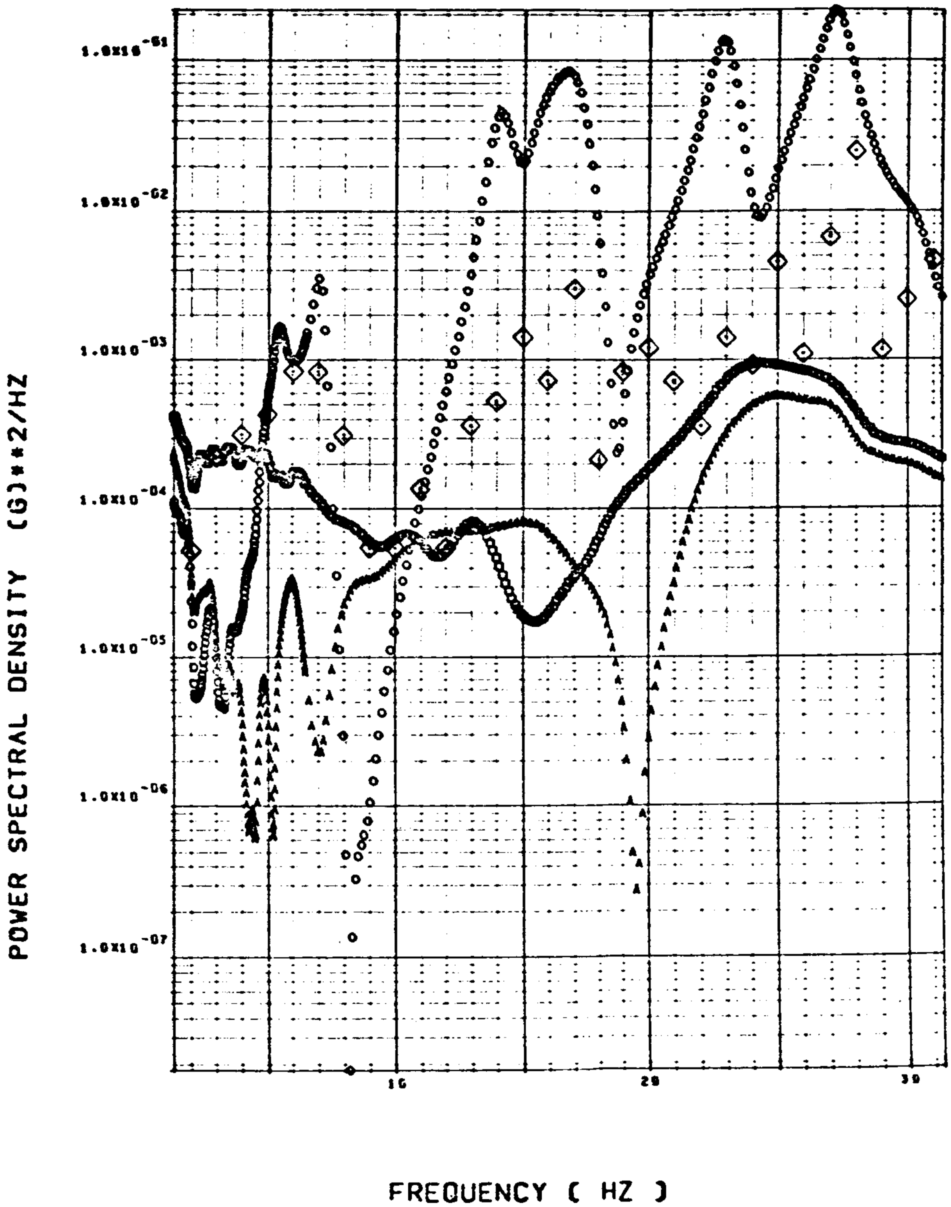

Figure 2.-(c) Pilot seat vertical accelerometer (continued)

◇ AF009 $\alpha_{FLT} = 14.1^{\circ}$

F-111A SYM. AC BUFFET. HALF TAIL. TORSION FREQS.
SWEEP = 26 DEG. MACH= .8. ALT = 19.8K. ALPHA= 14.4
PILOT STATION VERTICAL ACCELEROMETER. FS = 255
SQUARE = 1 DOF A = 2 DOF CIRCLE = 14 DOF

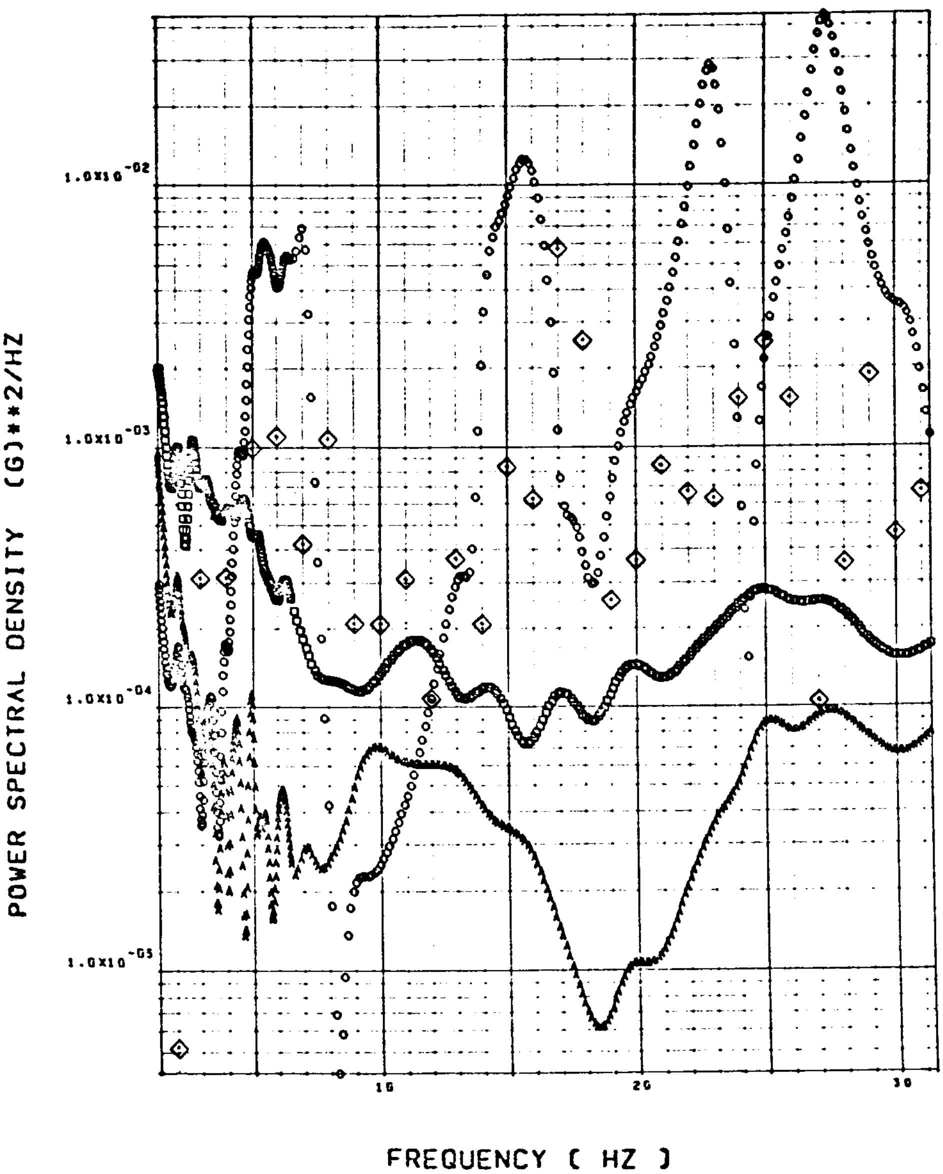

Figure 2.-(c) Pilot seat vertical accelerometer (continued)

◇ AB020 $\alpha_{FLT} = 6.9^{o}$

F-111A ANTI AC BUFFET. HALF TAIL. TORSION FREQS.
SWEEP = 26 DEG. MACH= .8. ALT = 19.8K. ALPHA= 6.6
C.G. LATERAL ACCELEROMETER. FS = 529
SQUARE = 1 DOF A = 3 DOF CIRCLE = 18 DOF

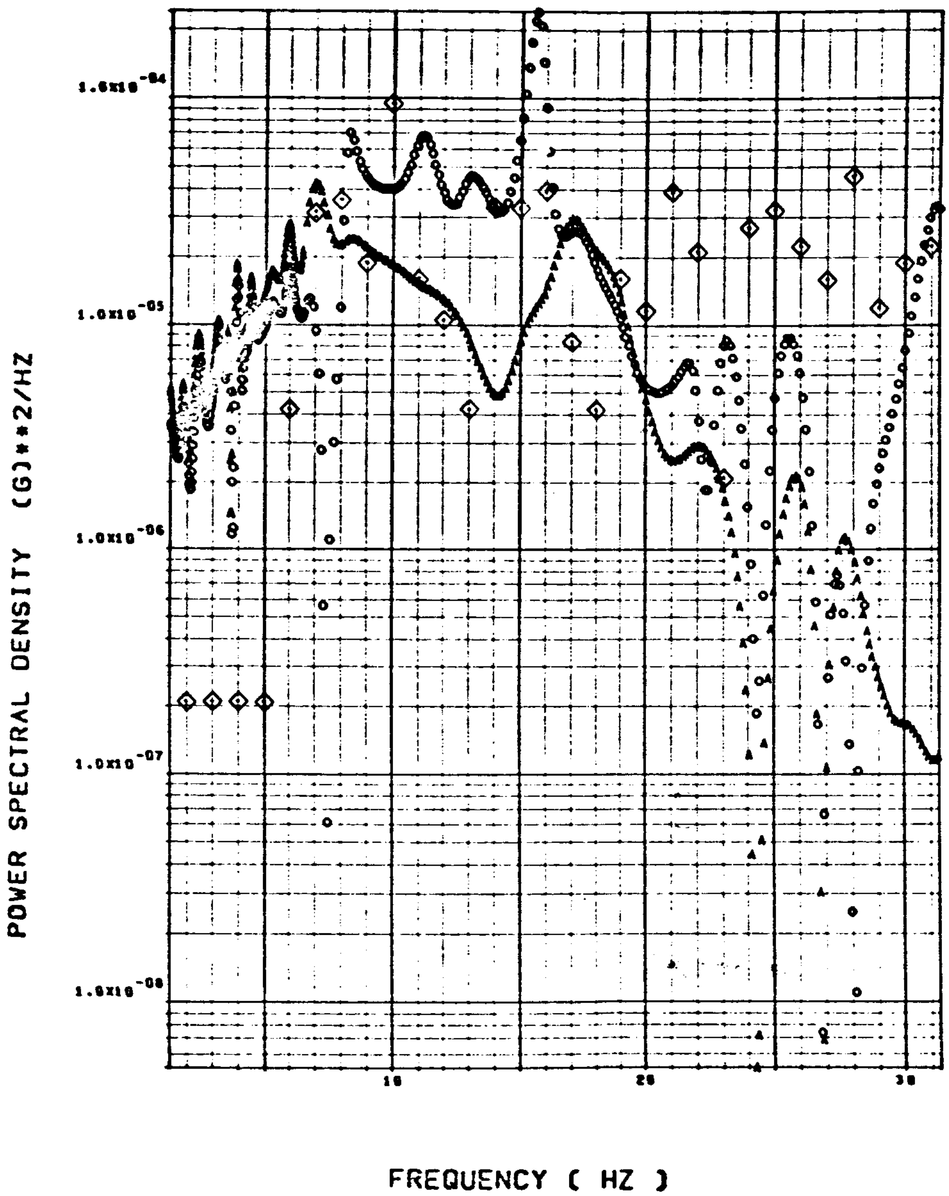

Figure 2.-(d) C.G. lateral accelerometer

◇ AB020 $\alpha_{FLT} = 11.7^{\circ}$

F-111A ANTI AC BUFFET. HALF TAIL. TORSION FREQS.
SWEEP = 26 DEG. MACH= .8. ALT = 19.8K. ALPHA= 11.1
C.G. LATERAL ACCELEROMETER. FS = 529
SQUARE = 1 DOF A = 3 DOF CIRCLE = 18 DOF

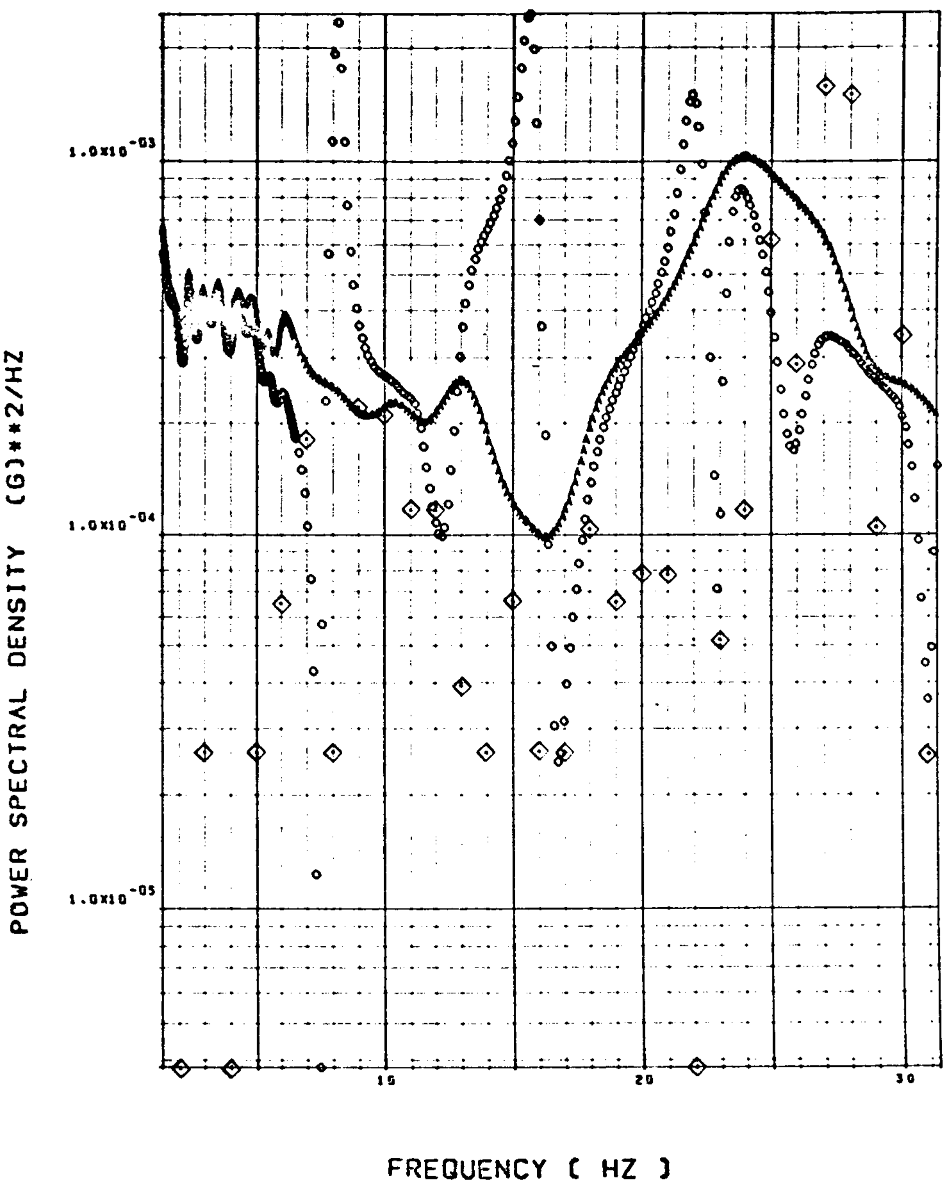

Figure 2.-(d) C.G. lateral accelerometer (continued)

◇ AB020 $\alpha_{FLT} = 14.1^{o}$

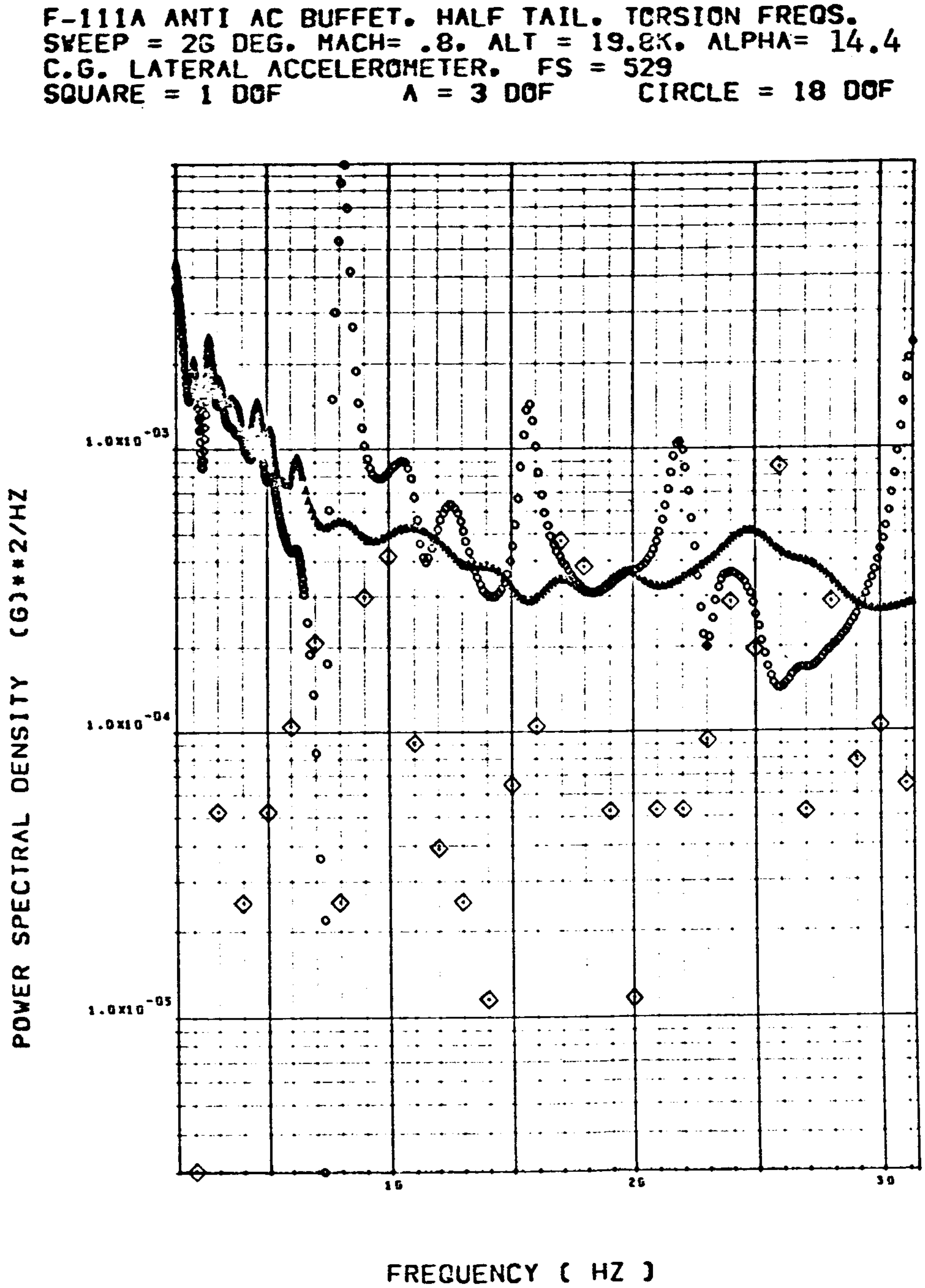

Figure 2.-(d) C.G. lateral accelerometer (continued)

◇ AF010 $\alpha_{FLT} = 6.9^{\circ}$

F-111A ANTI AC BUFFET. HALF TAIL. TORSION FREQS.
SWEEP = 26 DEG. MACH= .8. ALT = 19.8K. ALPHA= 6.6
PILOT STATION LATERAL ACCELEROMETER. FS = 255
SQUARE = 1 DOF A = 3 DOF CIRCLE = 18 DOF

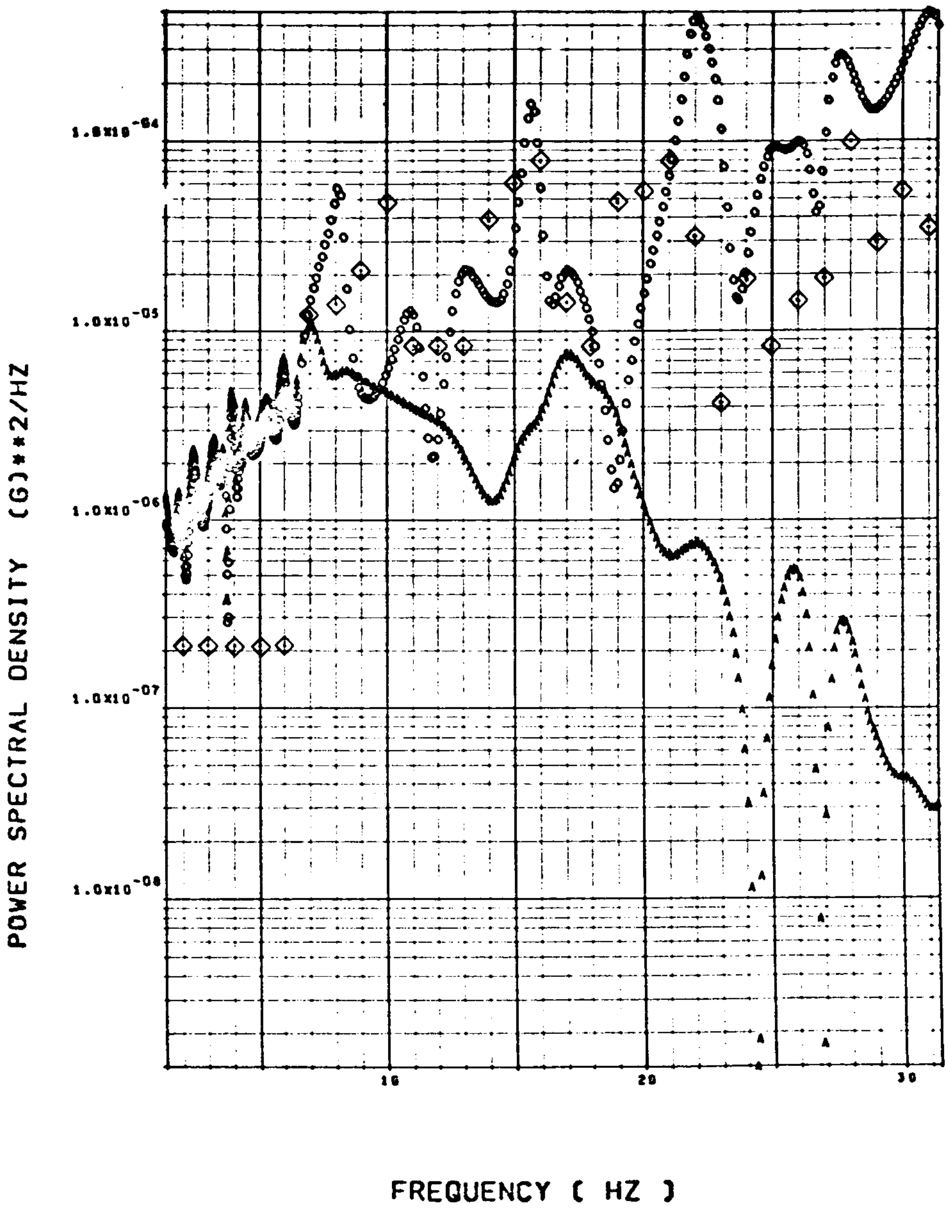

Figure 2.-(e) Pilot seat lateral accelerometer

◇ AF010 $\alpha_{FLT} = 11.7^{o}$

F-111A ANTI AC BUFFET. HALF TAIL. TORSION FREQS.
SWEEP = 26 DEG. MACH= .8. ALT = 19.8K. ALPHA= 11.1
PILOT STATION LATERAL ACCELEROMETER. FS = 255
SQUARE = 1 DOF A = 3 DOF CIRCLE = 18 DOF

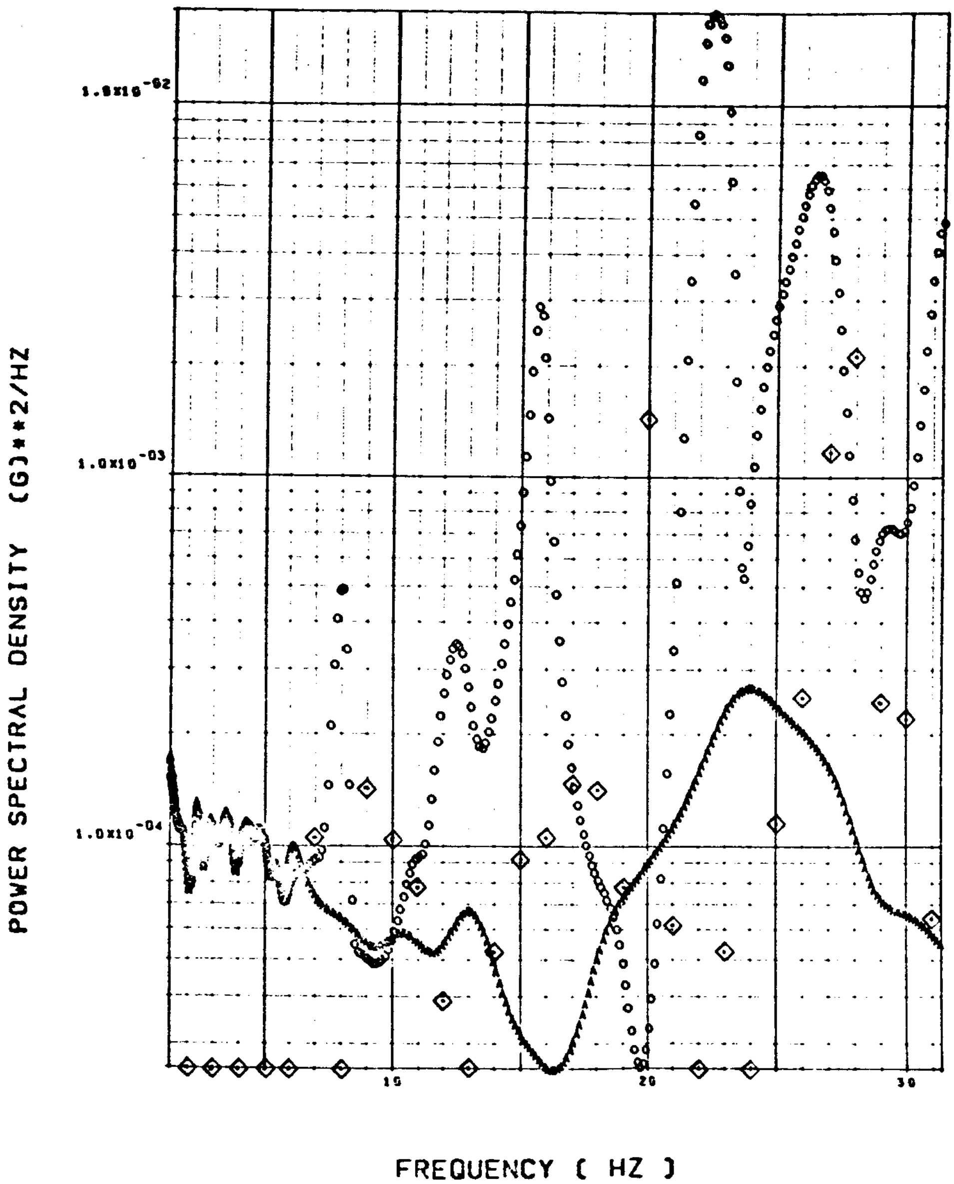

Figure 2.-(e) Pilot seat lateral accelerometer (continued)

◇ AF010 $\alpha_{FLT} = 14.1^{o}$

F-111A ANTI AC BUFFET. HALF TAIL. TORSION FREQS.
SWEEP = 26 DEG. MACH= .8. ALT = 19.8K. ALPHA= 14.4
PILOT STATION LATERAL ACCELEROMETER. FS = 255
SQUARE = 1 DOF A = 3 DOF CIRCLE = 18 DOF

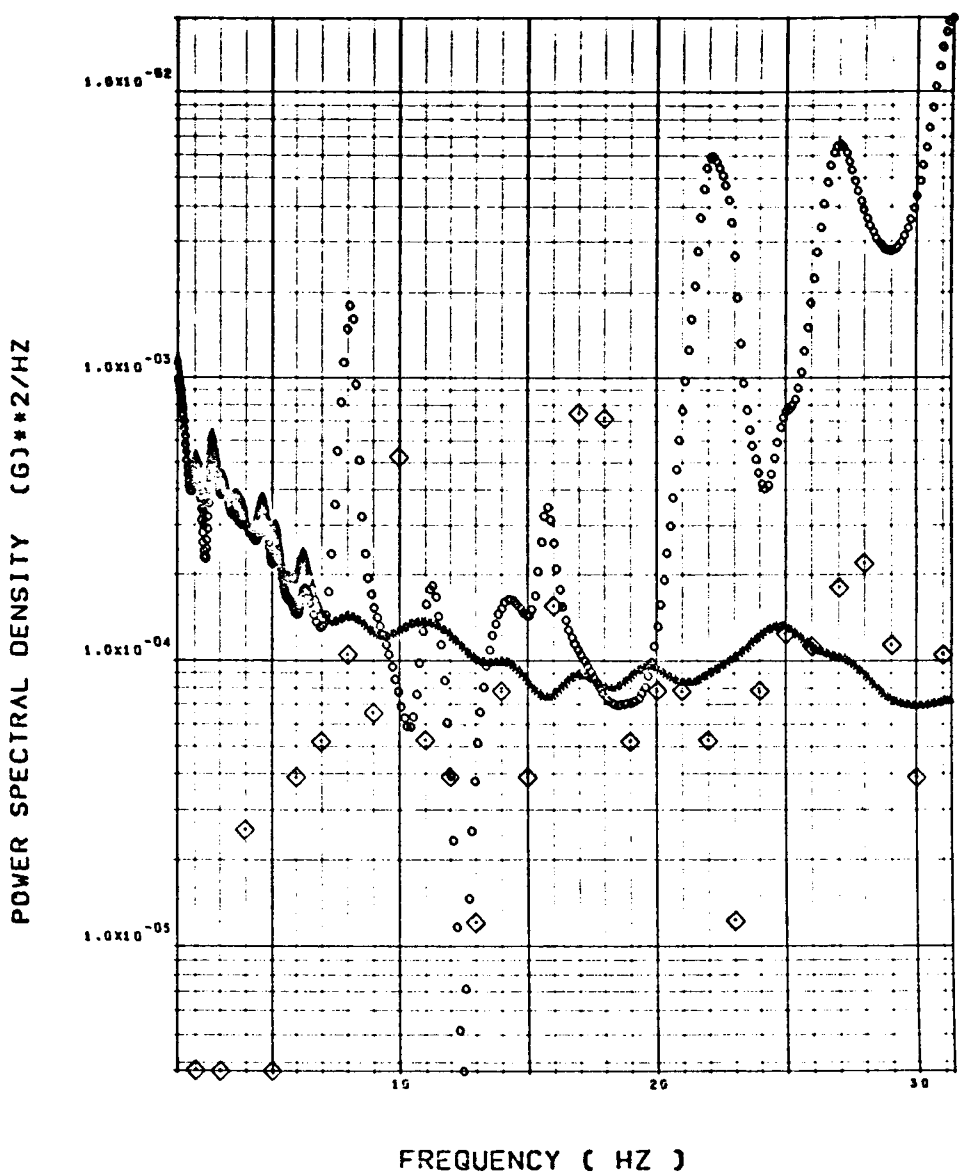

Figure 2.-(e) Pilot seat lateral accelerometer (continued)

△ SW123 $\alpha_{FLT} = 6.9^{\circ}$

F-111A WING BUFFET RESPONSE. FLT 77. RUN S AND C-R
SWEEP=26 DEG. MACH=.8. ALT=6035(M). ALPHA= 6.6
WING SHEAR (N) AT SPAN STATION 75
CIRCLE = UPPER BOUNDS SQUARE = LOWER BOUNDS

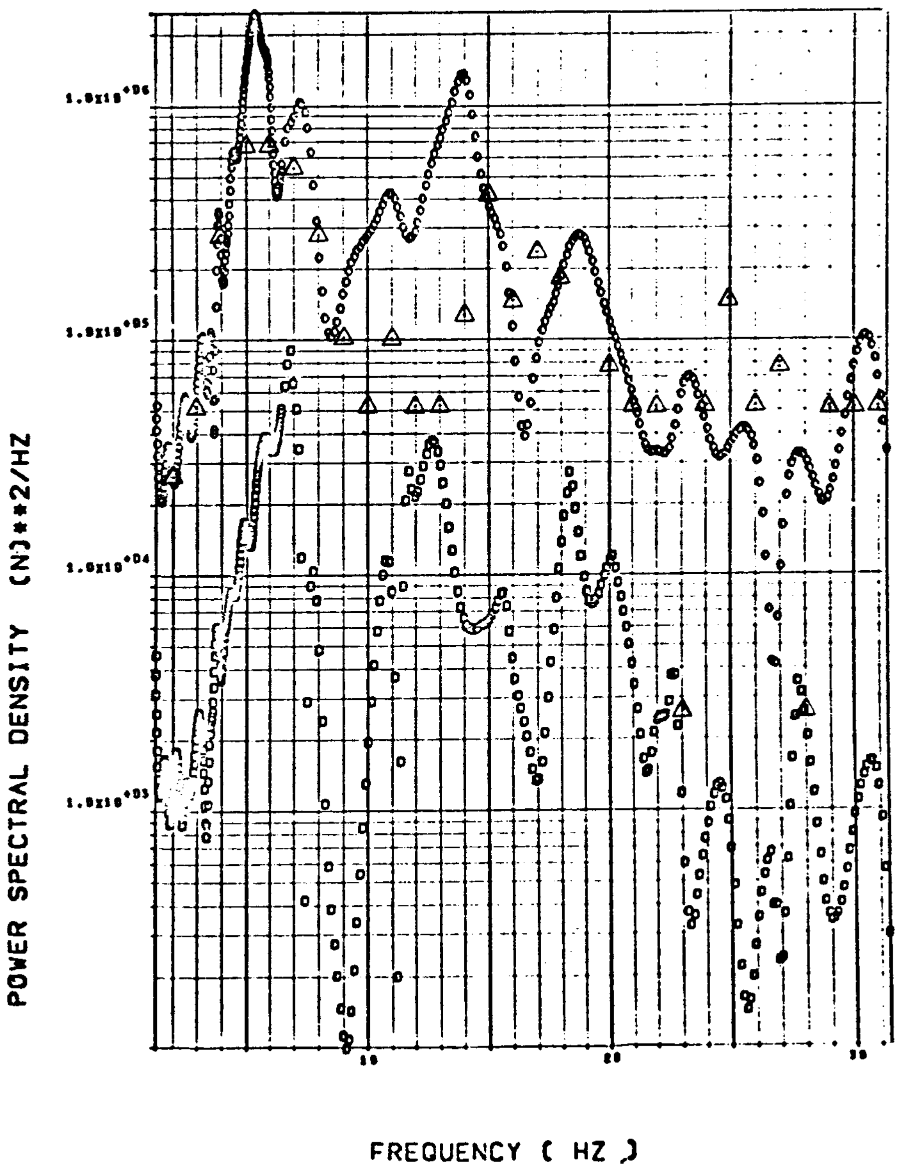

Figure 2.-(f) Wing shear

△ SW123 $\alpha_{FLT} = 11.7^{\circ}$

F-111A WING BUFFET RESPONSE. FLT 77. RUN S AND C-R
SWEEP=26 DEG. MACH=.8. ALT=6035(M). ALPHA= 11.1
WING SHEAR (N) AT SPAN STATION 75
CIRCLE = UPPER BOUNDS SQUARE = LOWER BOUNDS

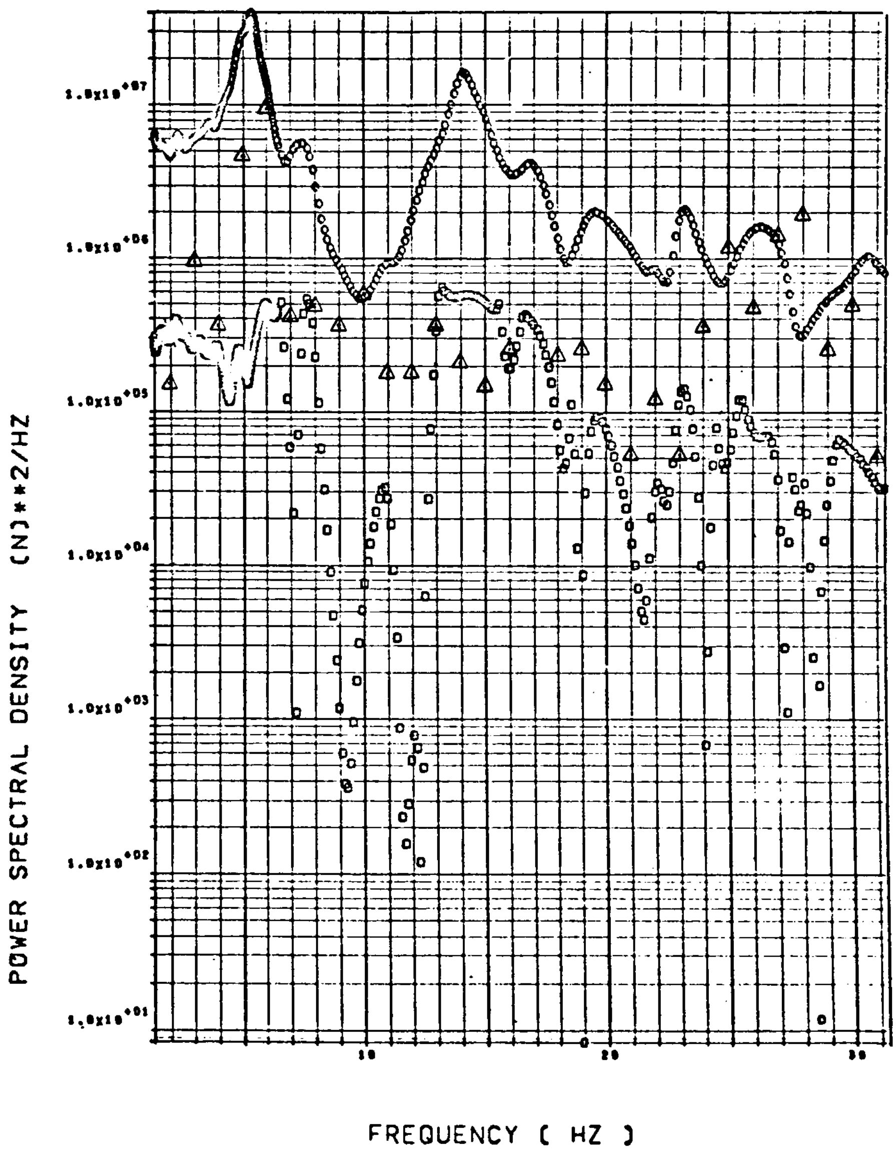

Figure 2.-(f) Wing shear (continued)

Δ SW123 $\alpha_{FLT} = 14.1^{o}$

F-111A WING BUFFET RESPONSE. FLT 77. RUN S AND C-R
SWEEP=26 DEG. MACH=.8. ALT=6035(M). ALPHA= 14.4
WING SHEAR (N) AT SPAN STATION 75
CIRCLE = UPPER BOUNDS SQUARE = LOWER BOUNDS

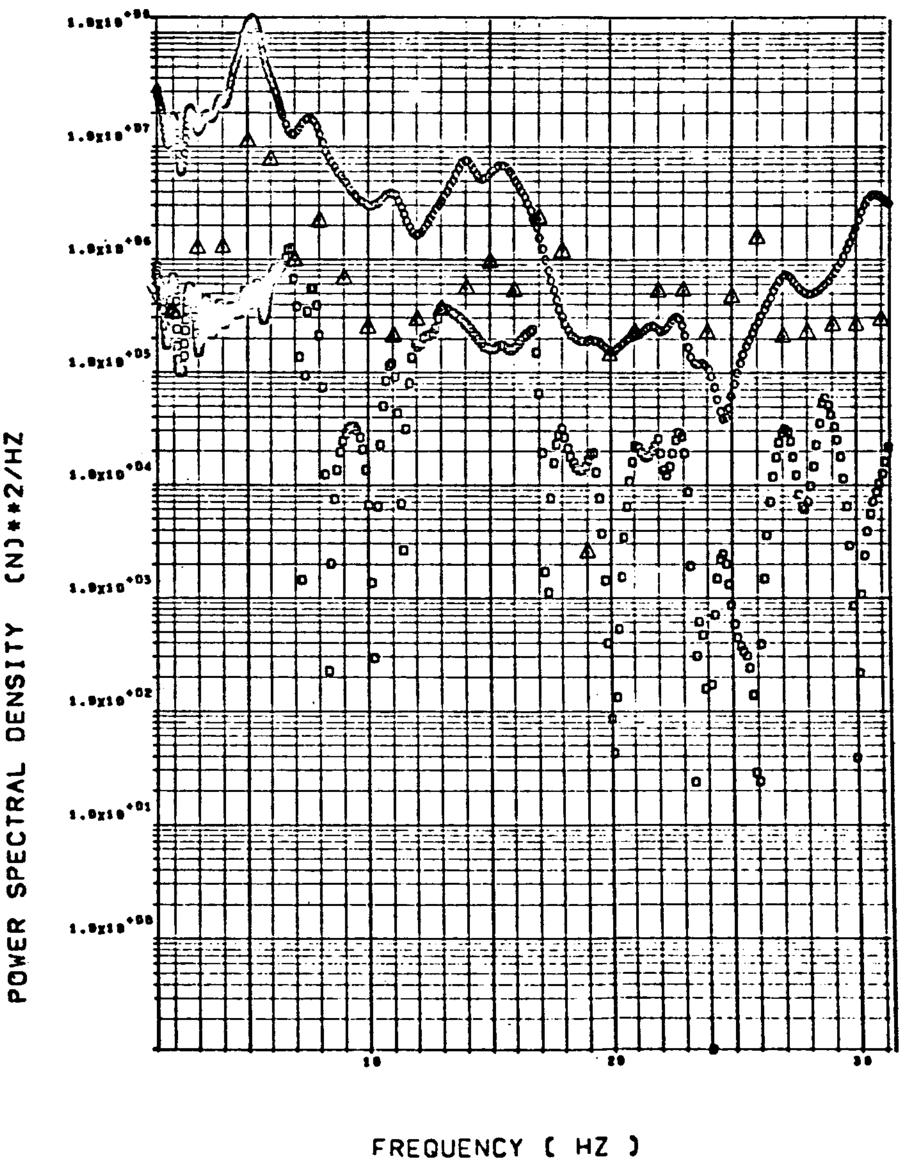

Figure 2.-(f) Wing shear (continued)

△ SW124 $\alpha_{FLT} = 6.9^{o}$

F-111A WING BUFFET RESPONSE, FLT 77, RUN S AND C-R
SWEEP=26 DEG, MACH=.8, ALT=6035(M), ALPHA= 6.6
WING BENDING MOMENT (M-N) AT SPAN STATION 75
CIRCLE = UPPER BOUNDS SQUARE = LOWER BOUNDS

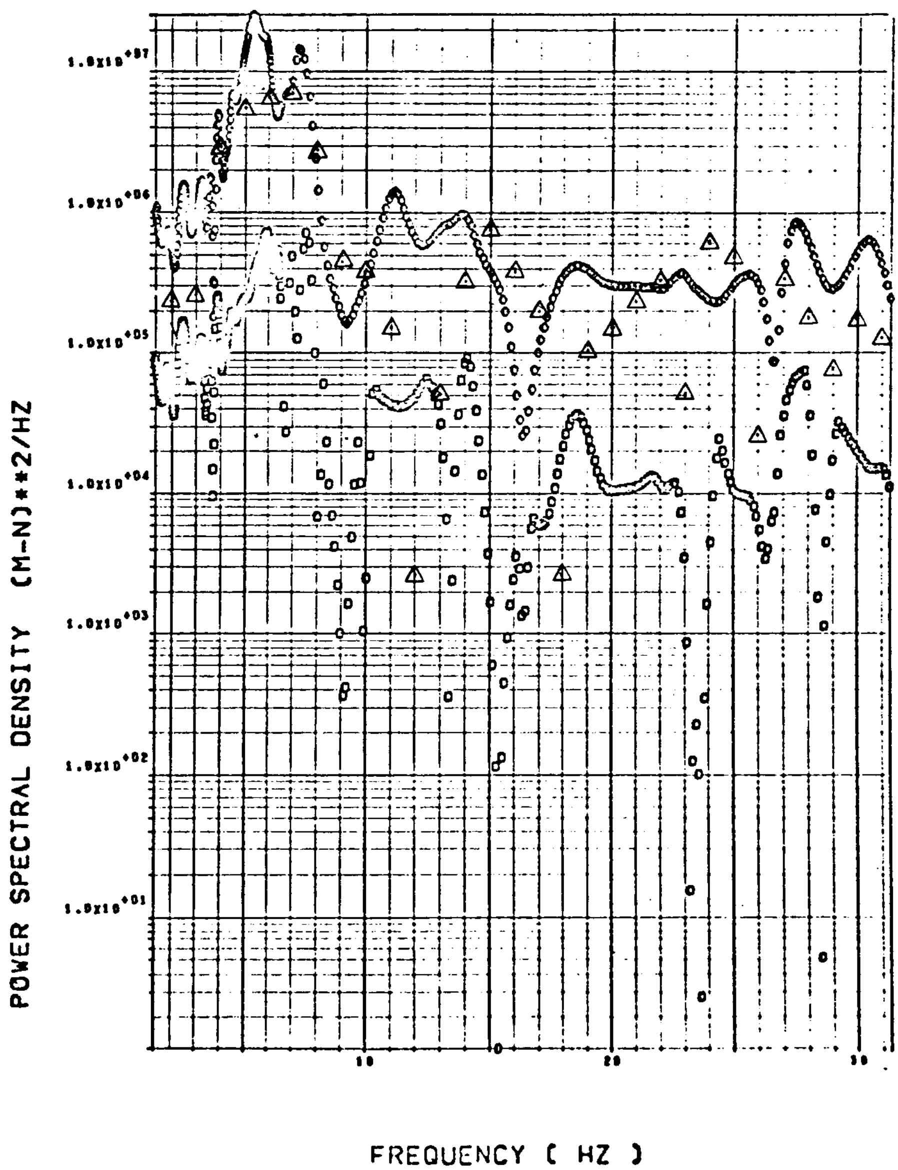

Figure 2.-(g) Wing bending moment

△ SW124 $\alpha_{FLT} = 11.7^{o}$

F-111A WING BUFFET RESPONSE, FLT 77, RUN S AND C-R
SWEEP=26 DEG, MACH=.8, ALT=6035(M), ALPHA= 11.1
WING BENDING MOMENT (M-N) AT SPAN STATION 75
CIRCLE = UPPER BOUNDS SQUARE = LOWER BOUNDS

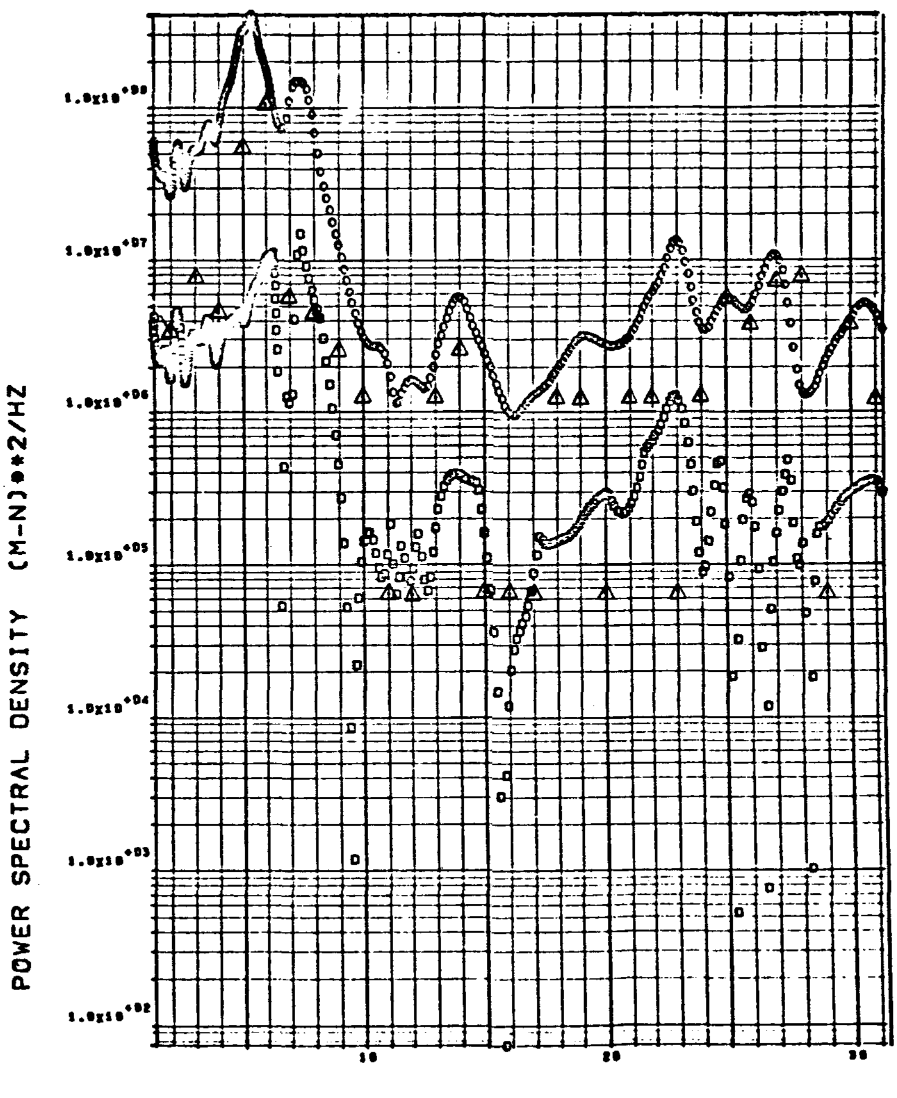

Figure 2.-(g) Wing bending moment (continued)

△ SW124 $\alpha_{FLT} = 14.1^{o}$

F-111A WING BUFFET RESPONSE. FLT 77. RUN S AND C-R
SWEEP=26 DEG. MACH=.8. ALT=6035(M). ALPHA= 14.4
WING BENDING MOMENT (M-N) AT SPAN STATION 75
CIRCLE = UPPER BOUNDS SQUARE = LOWER BOUNDS

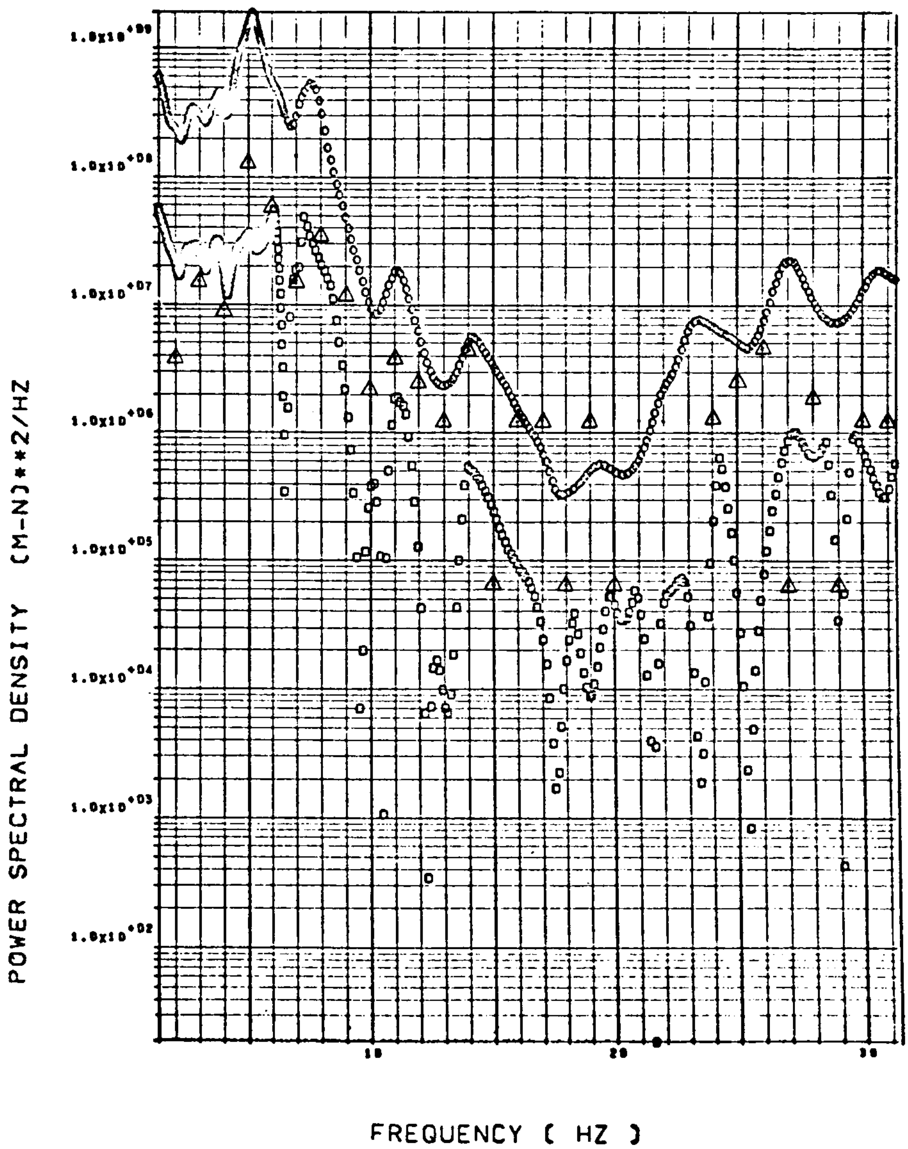

Figure 2.-(g) Wing bending moment (continued)

△ SW125 $\alpha_{FLT} = 6.9^{o}$

F-111A WING BUFFET RESPONSE, FLT 77, RUN S AND C-R
SWEEP=26 DEG, MACH=.8, ALT=6035(M), ALPHA= 6.6
WING TORQUE (M-N) AT SPAN STATION 75
CIRCLE = UPPER BOUNDS SQUARE = LOWER BOUNDS

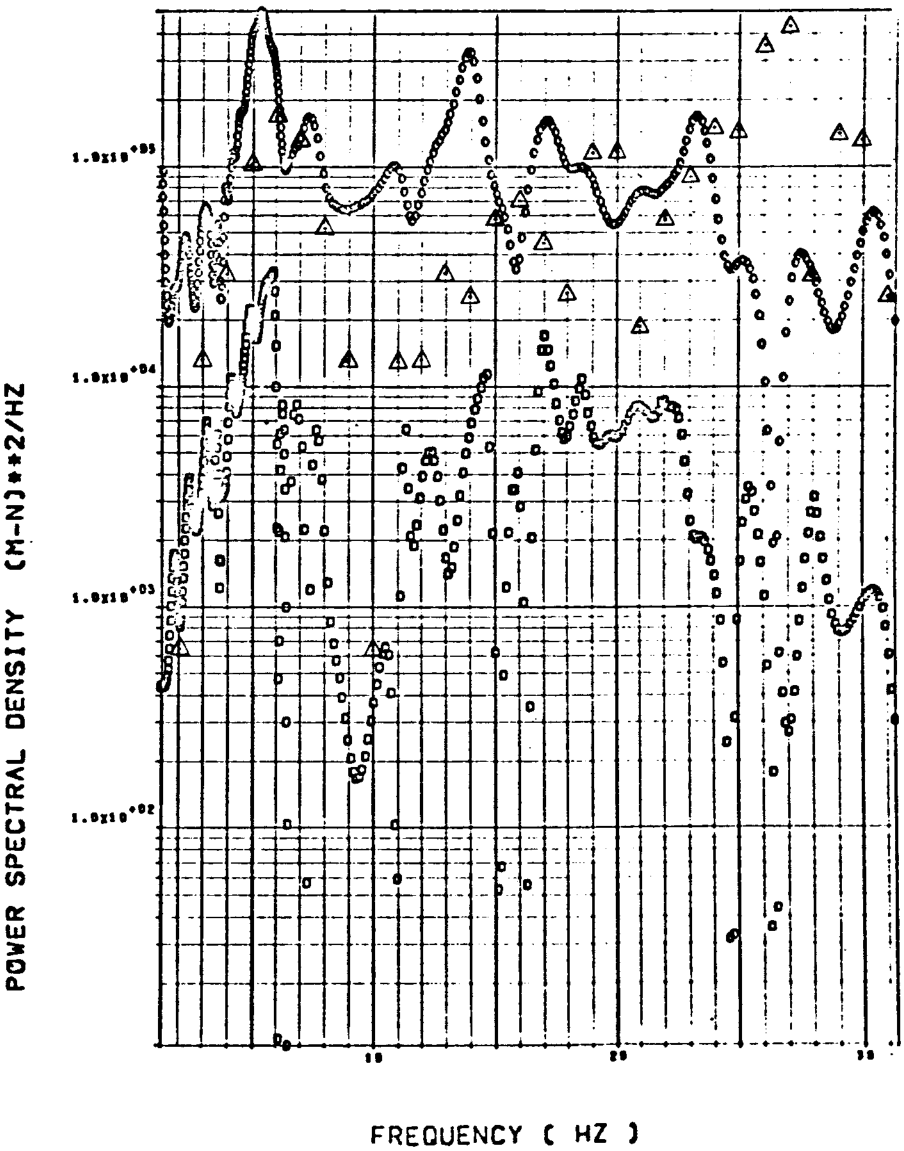

Figure 2.-(h) Wing torsion

△ SW125 $\alpha_{FLT} = 11.7^{\circ}$

F-111A WING BUFFET RESPONSE, FLT 77, RUN S AND C-R
SWEEP=26 DEG, MACH=.8, ALT=6035(M), ALPHA= 11.1
WING TORQUE (M-N) AT SPAN STATION 75
CIRCLE = UPPER BOUNDS SQUARE = LOWER BOUNDS

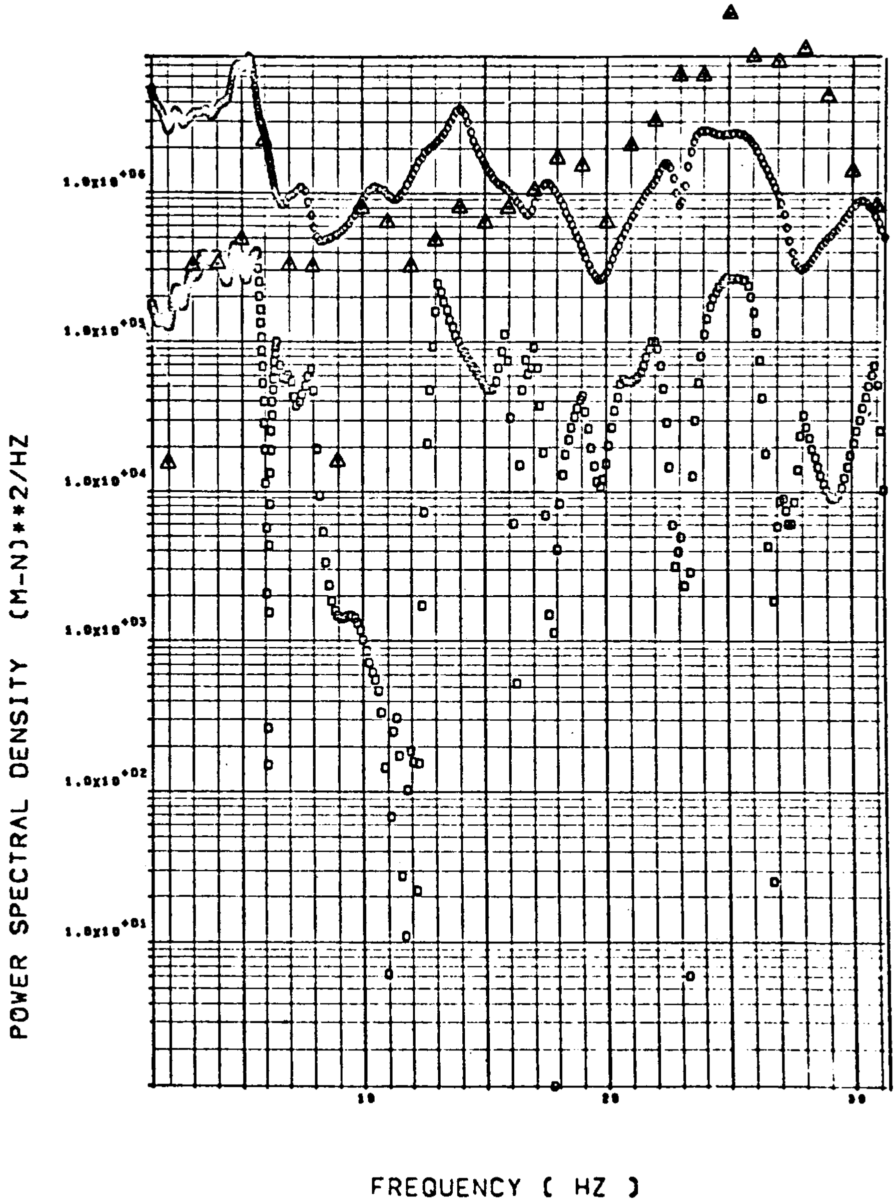

Figure 2.-(h) Wing torsion (continued)

△ SW125 $\alpha_{FLT} = 14.1^{\circ}$

F-111A WING BUFFET RESPONSE, FLT 77, RUN S AND C-R
SWEEP=26 DEG, MACH=.8, ALT=6035(M), ALPHA= 14.4
WING TORQUE (M-N) AT SPAN STATION 75
CIRCLE = UPPER BOUNDS SQUARE = LOWER BOUNDS

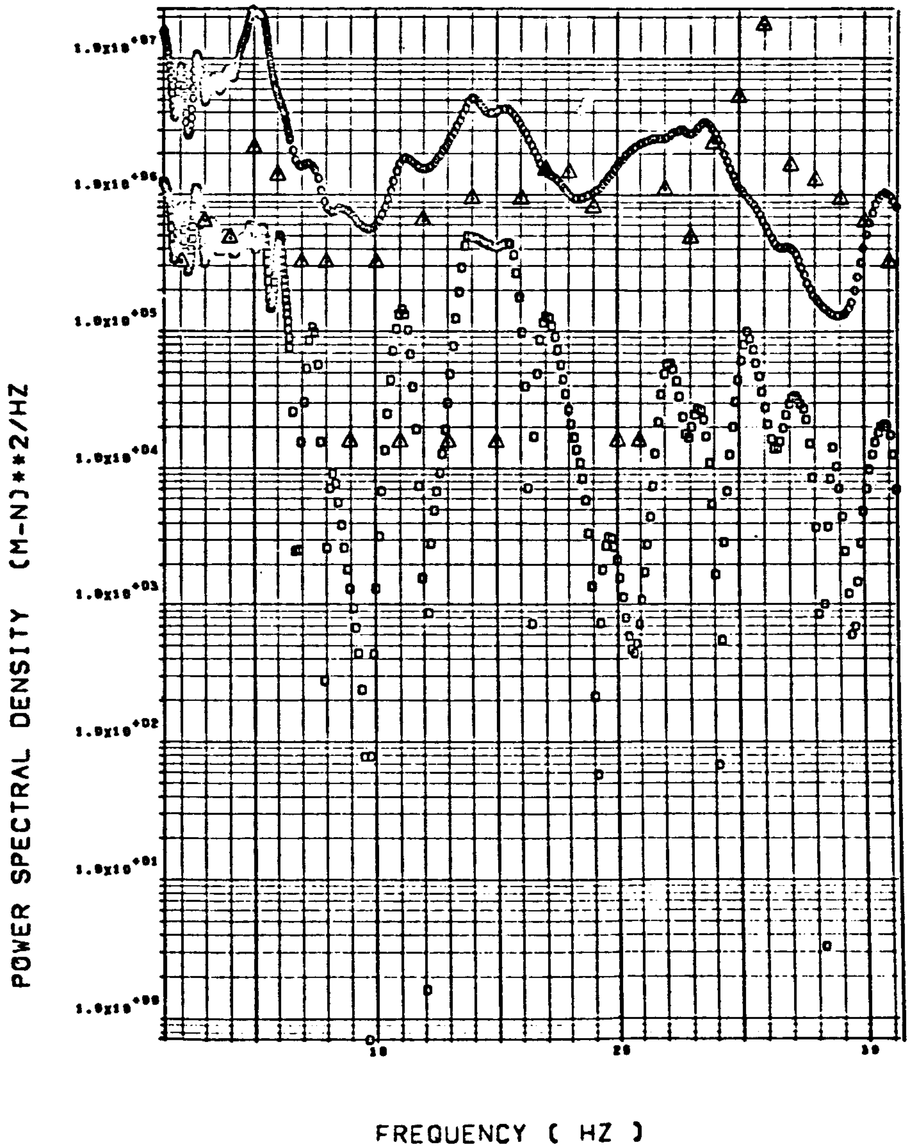

Figure 2.-(h) Wing torsion (continued)

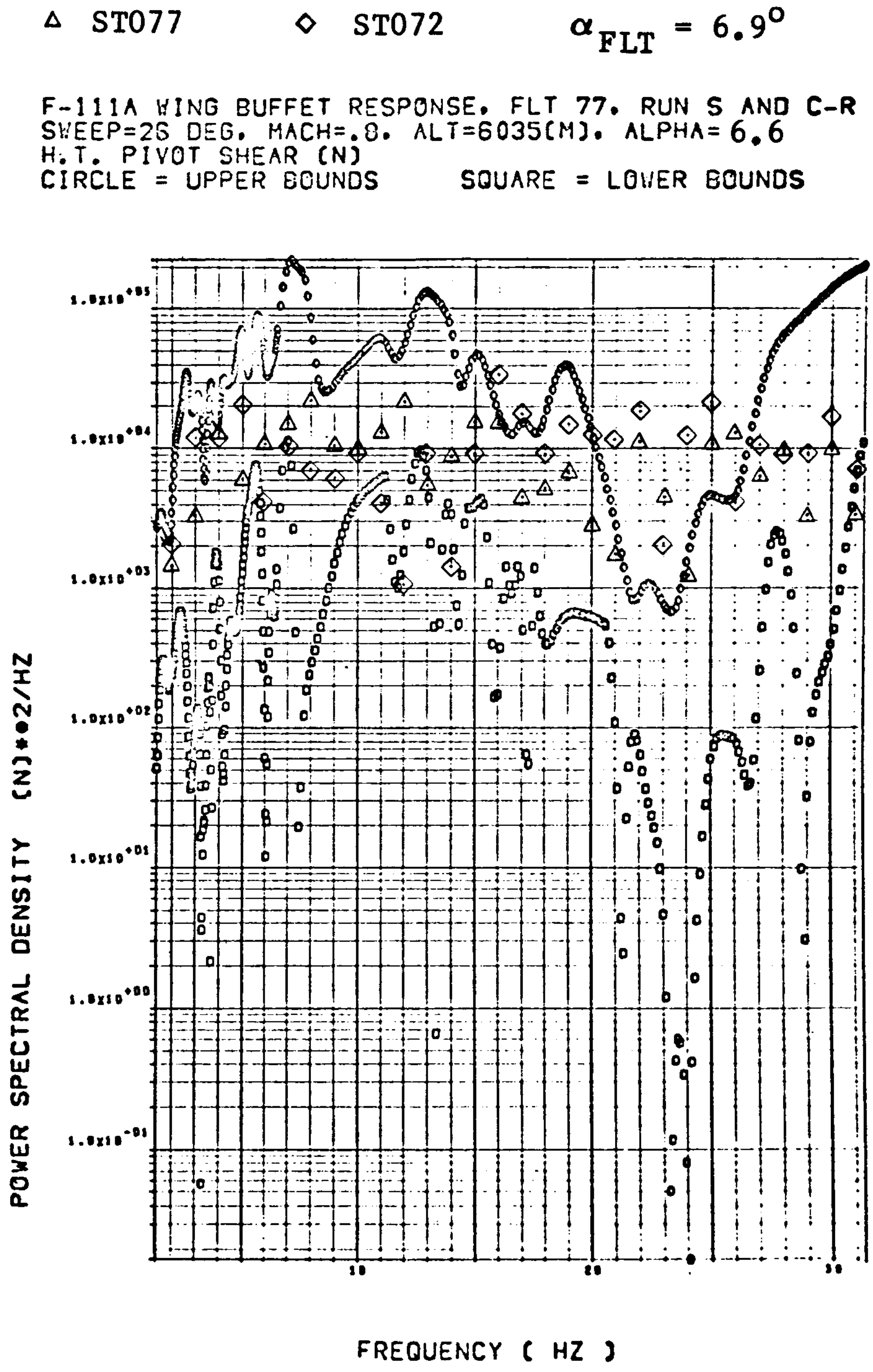

Figure 2.-(i) Horizontal tail shear

△ ST077 ◇ ST072 $\alpha_{FLT} = 11.7^{o}$

F-111A WING BUFFET RESPONSE. FLT 77. RUN S AND C-R
SWEEP=26 DEG. MACH=.8. ALT=6035(M). ALPHA= 11.1
H.T. PIVOT SHEAR (N)
CIRCLE = UPPER BOUNDS SQUARE = LOWER BOUNDS

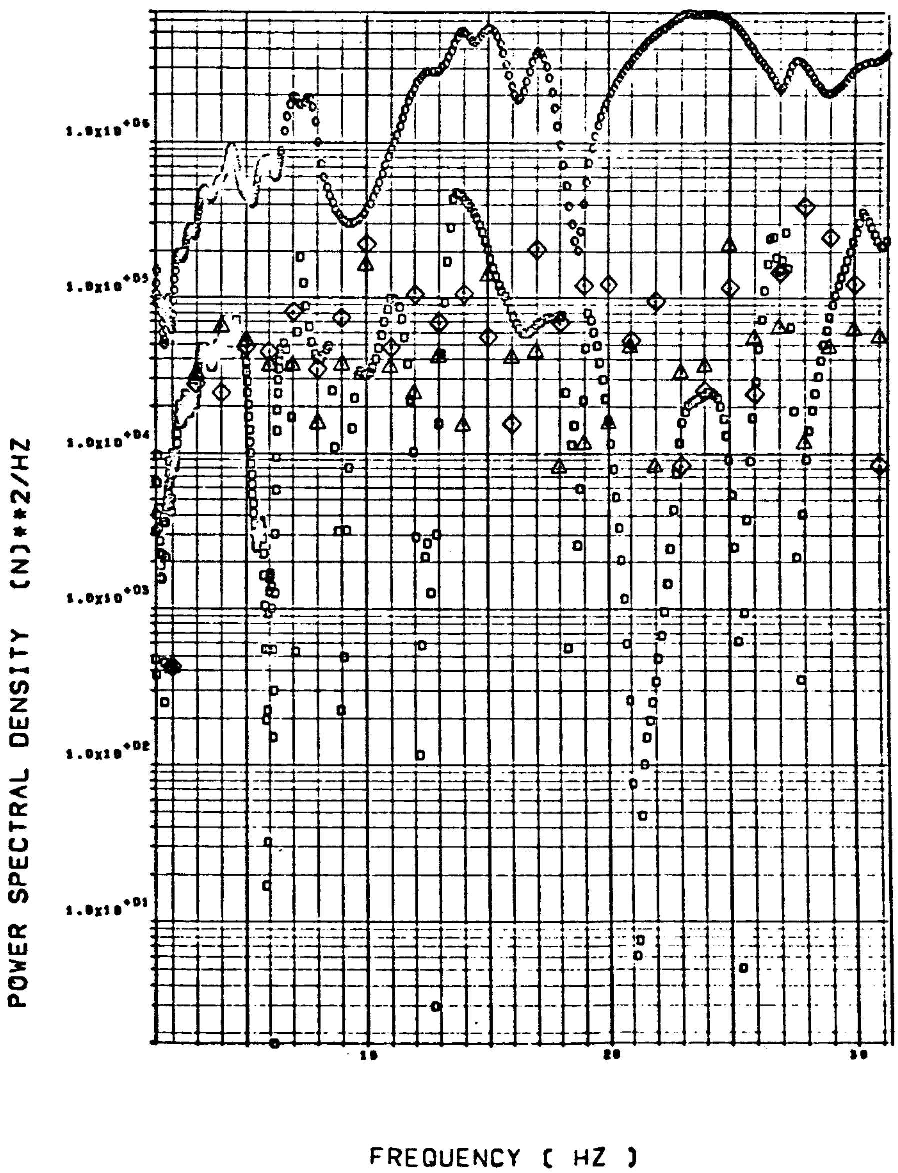

Figure 2.-(i) Horizontal tail shear (continued)

△ ST077 ◇ ST072 $\alpha_{FLT} = 14.1^{\circ}$

F-111A WING BUFFET RESPONSE, FLT 77, RUN S AND C-R
SWEEP=26 DEG, MACH=.8, ALT=6035(M), ALPHA= 14.4
H.T. PIVOT SHEAR (N)
CIRCLE = UPPER BOUNDS SQUARE = LOWER BOUNDS

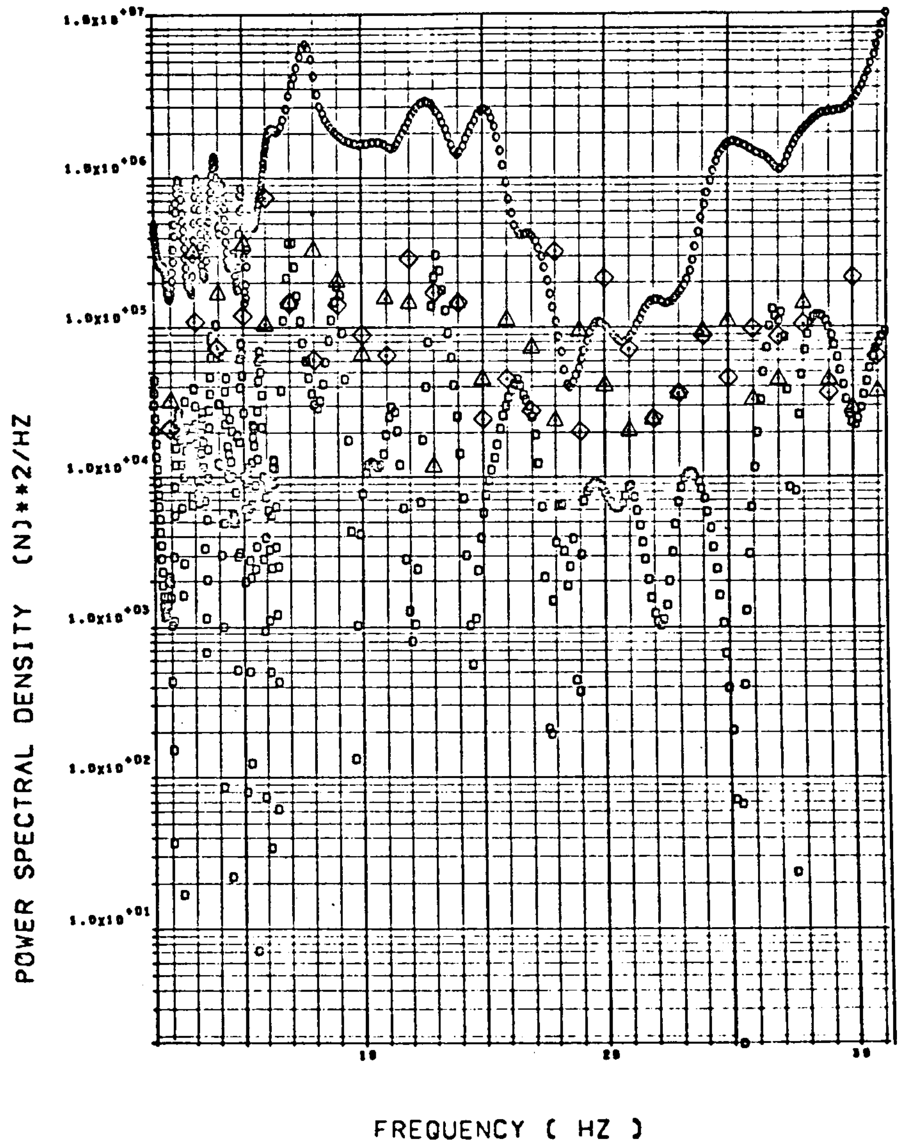

Figure 2.-(i) Horizontal tail shear (continued)

△ ST078 ◇ ST073 $\alpha_{FLT} = 6.9^{o}$

F-111A WING BUFFET RESPONSE. FLT 77. RUN S AND C-R
SWEEP=26 DEG. MACH=.8. ALT=6035(M). ALPHA= 6.6
H.T. PIVOT BENDING MOMENT (M-N)
CIRCLE = UPPER BOUNDS SQUARE = LOWER BOUNDS

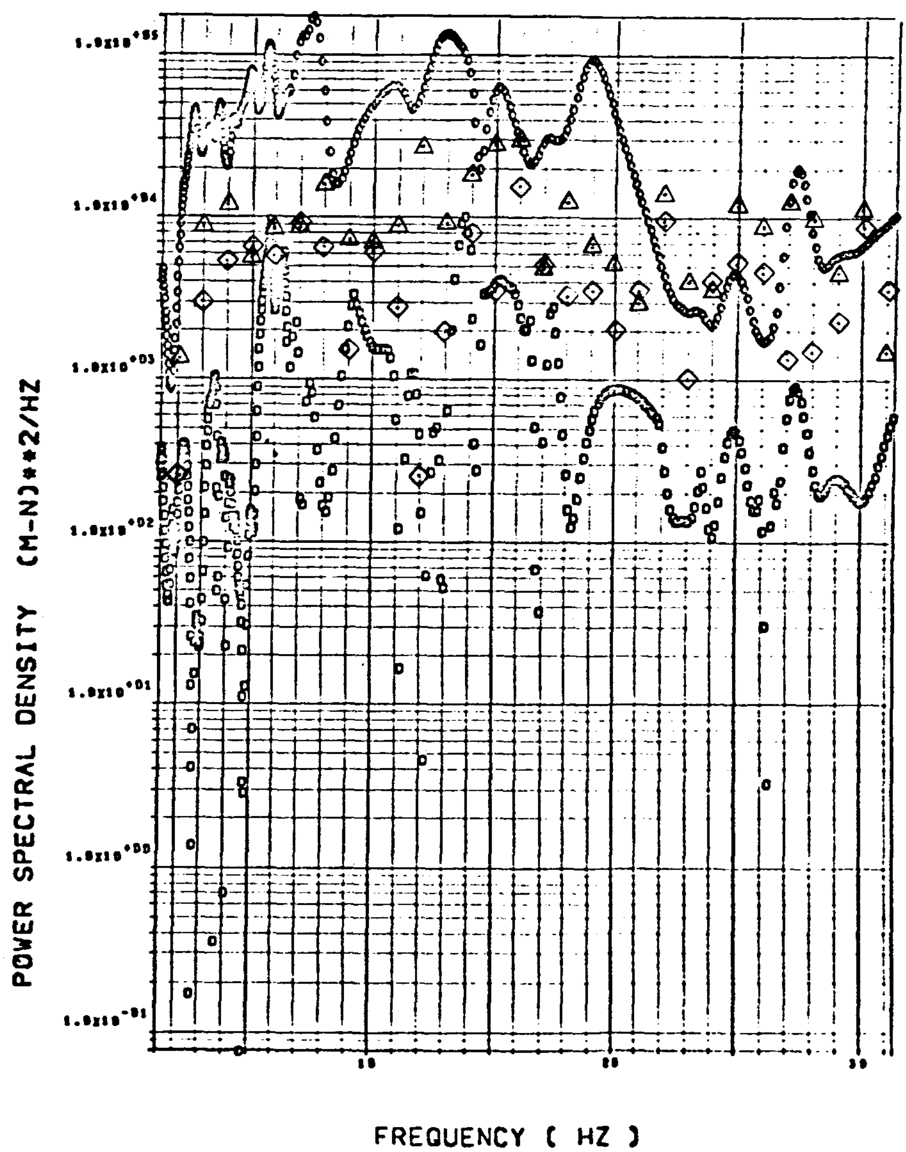

Figure 2.-(j) Horizontal tail bending moment

△ ST078 ◇ ST073 $\alpha_{FLT} = 11.7^{o}$

F-111A WING BUFFET RESPONSE. FLT 77. RUN S AND C-R
SWEEP=26 DEG. MACH=.8. ALT=6035(M). ALPHA= 11.1
H.T. PIVOT BENDING MOMENT (M-N)
CIRCLE = UPPER BOUNDS SQUARE = LOWER BOUNDS

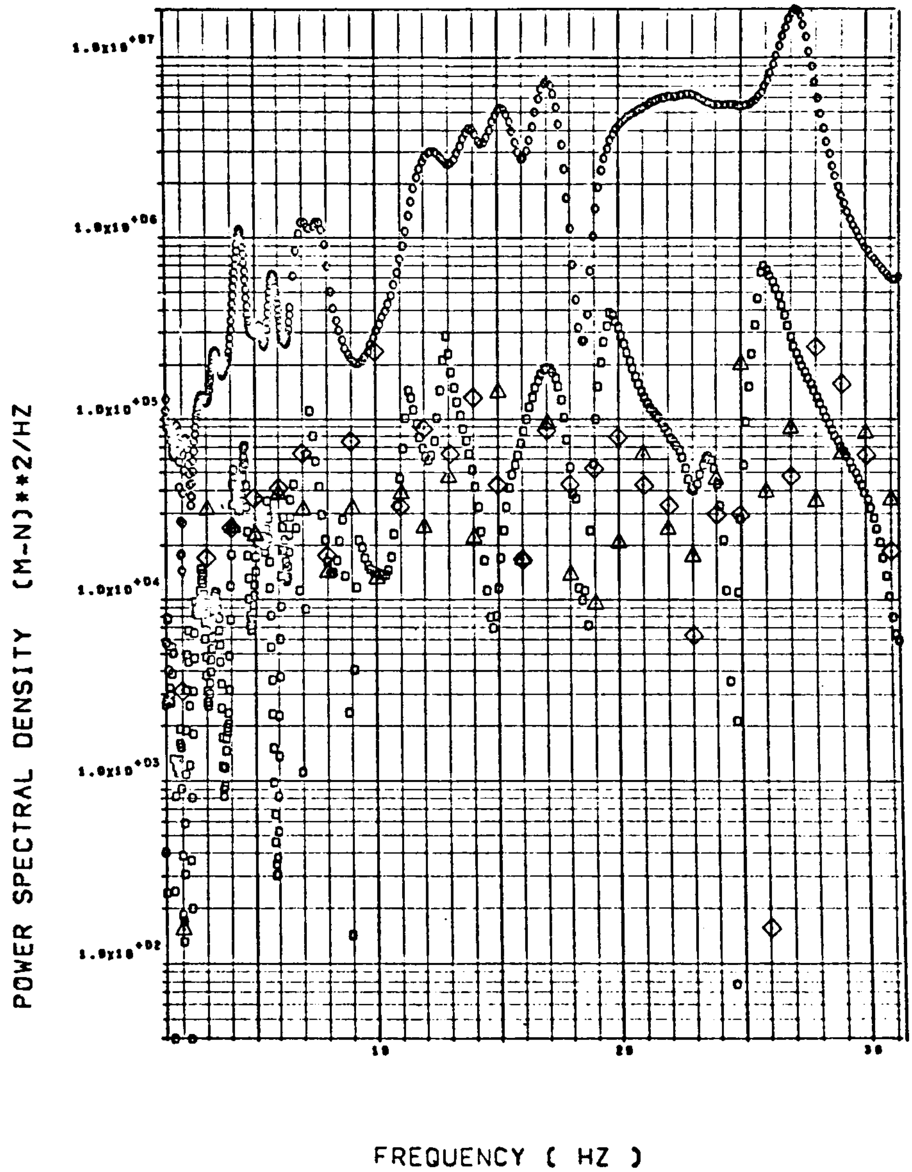

Figure 2.-(j) Horizontal tail bending moment (continued)

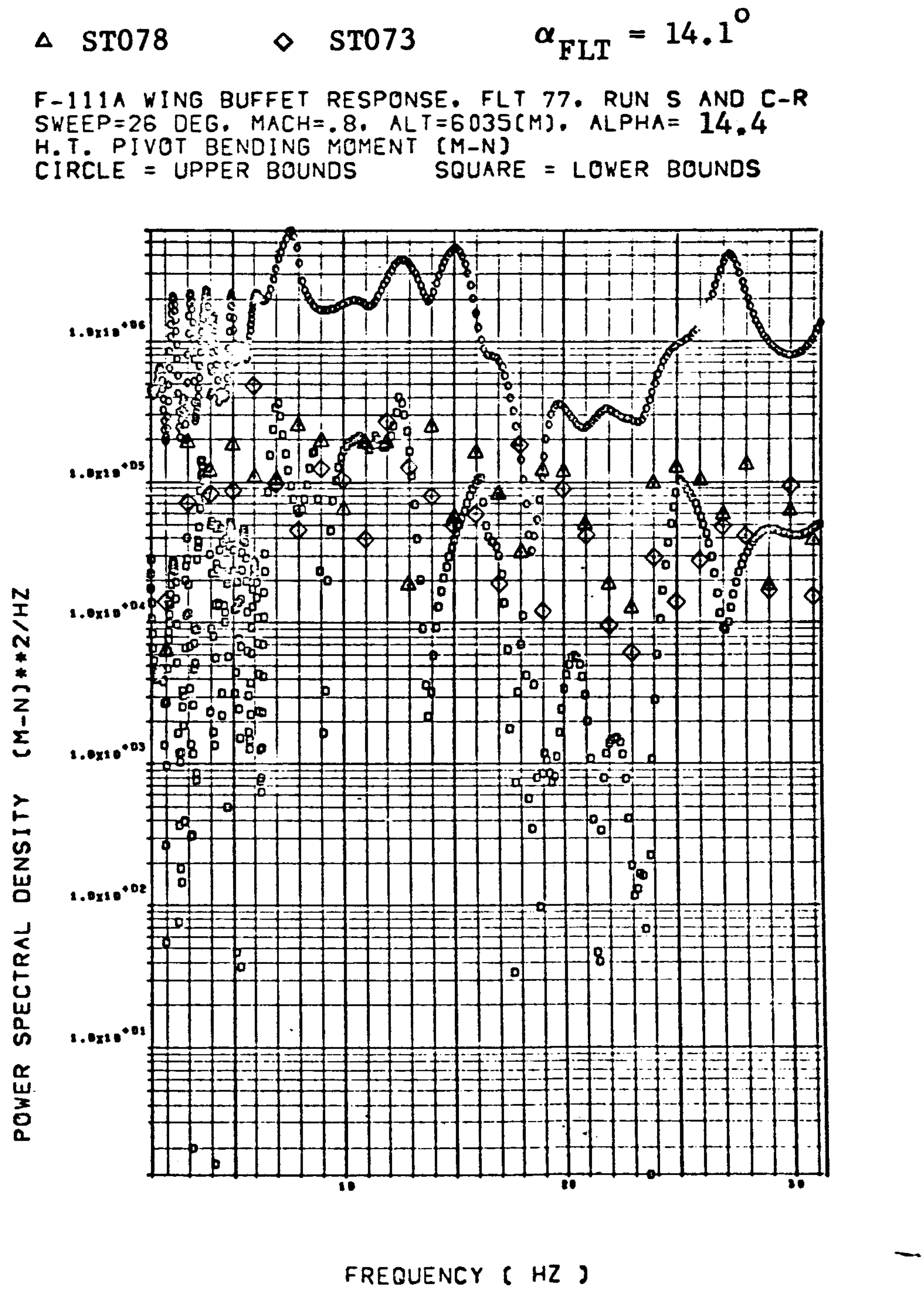

Figure 2.-(j) Horizontal tail bending moment (continued)

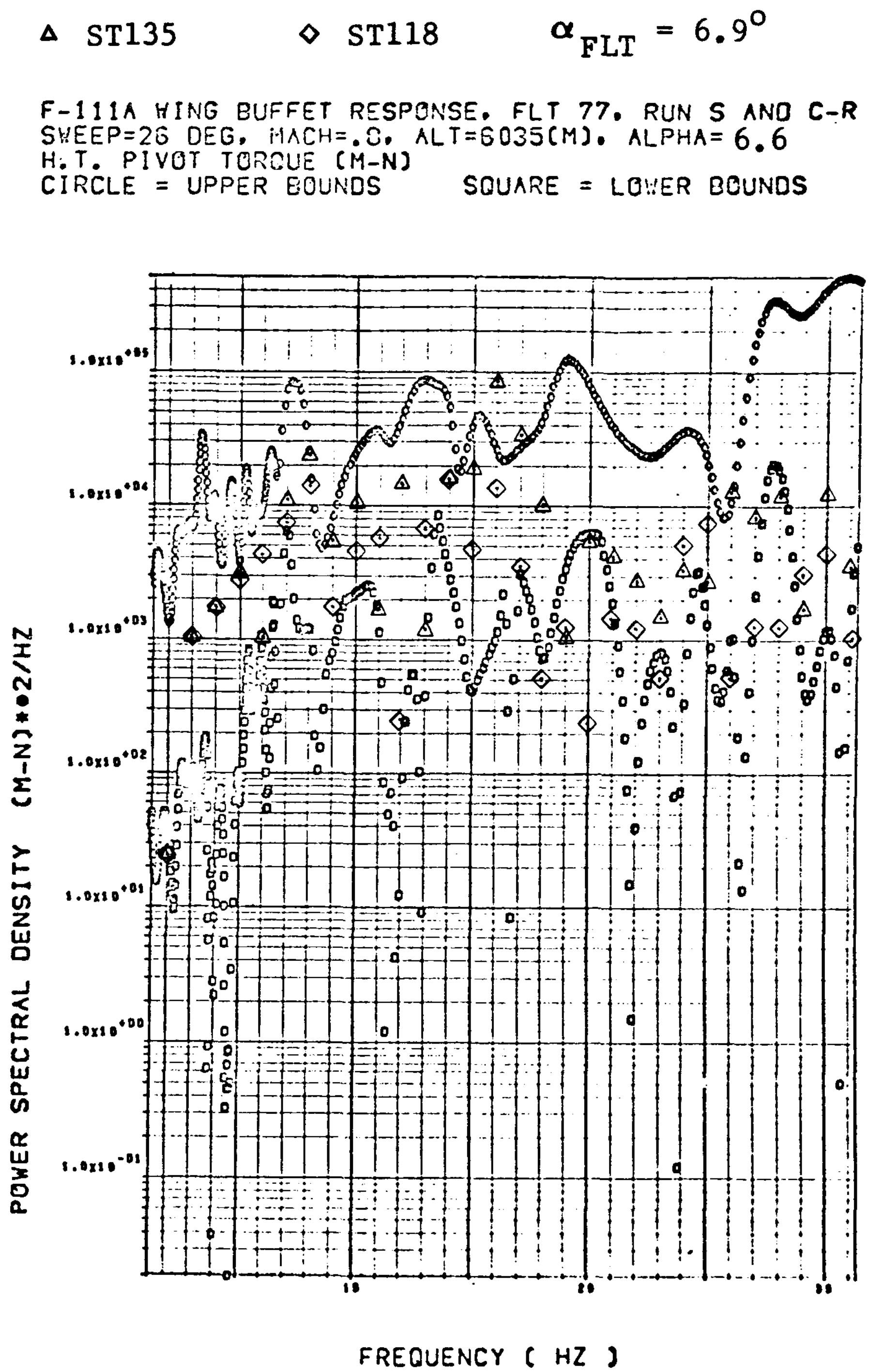

Figure 2.-(k) Horizontal tail torsion

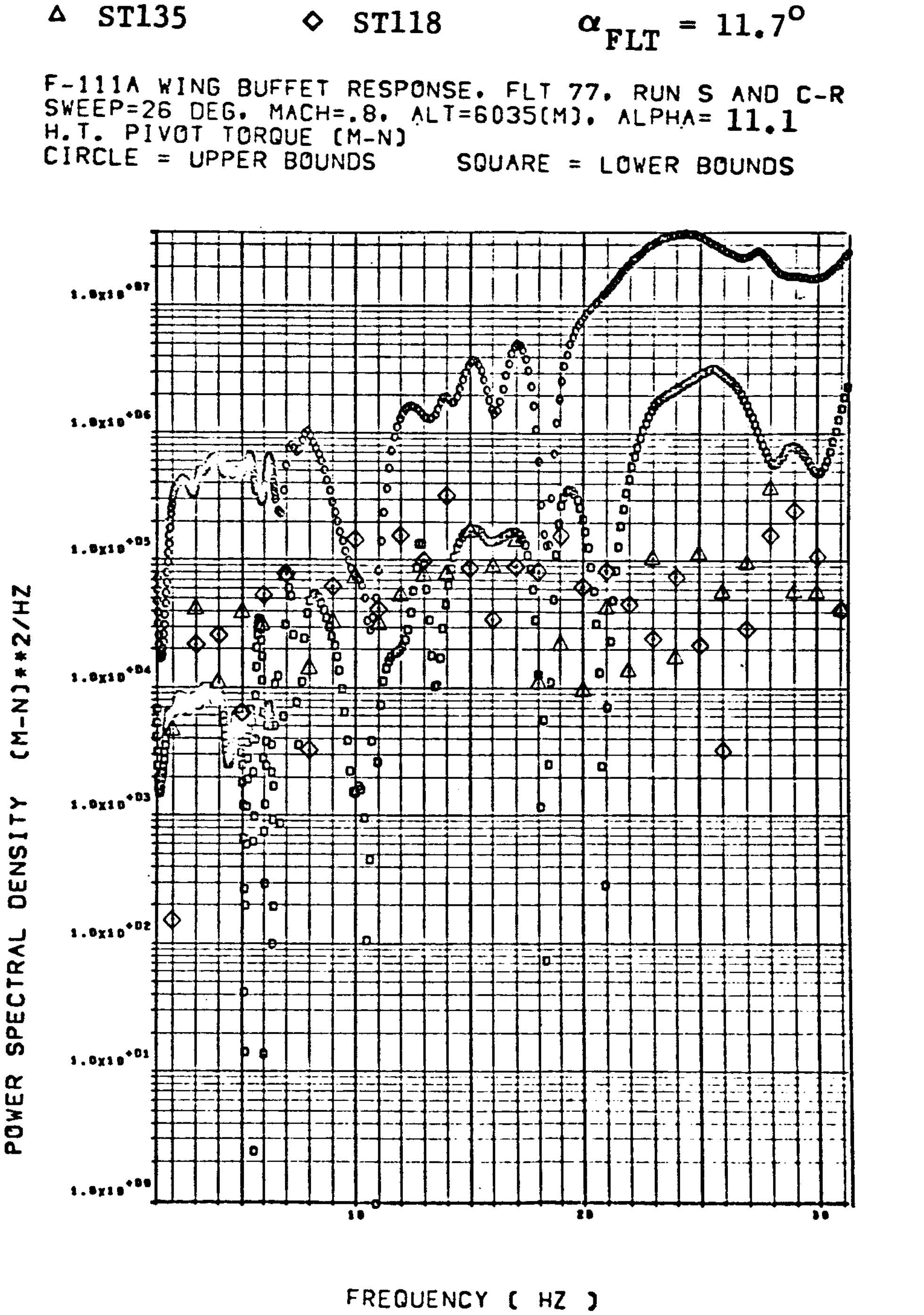

Figure 2.-(k) Horizontal tail torsion (continued)

△ ST135 ◇ ST118 $\alpha_{FLT} = 14.1^{o}$

F-111A WING BUFFET RESPONSE, FLT 77, RUN S AND C-R
SWEEP=26 DEG, MACH=.8, ALT=6035(M), ALPHA= 14.4
H.T. PIVOT TORQUE (M-N)
CIRCLE = UPPER BOUNDS SQUARE = LOWER BOUNDS

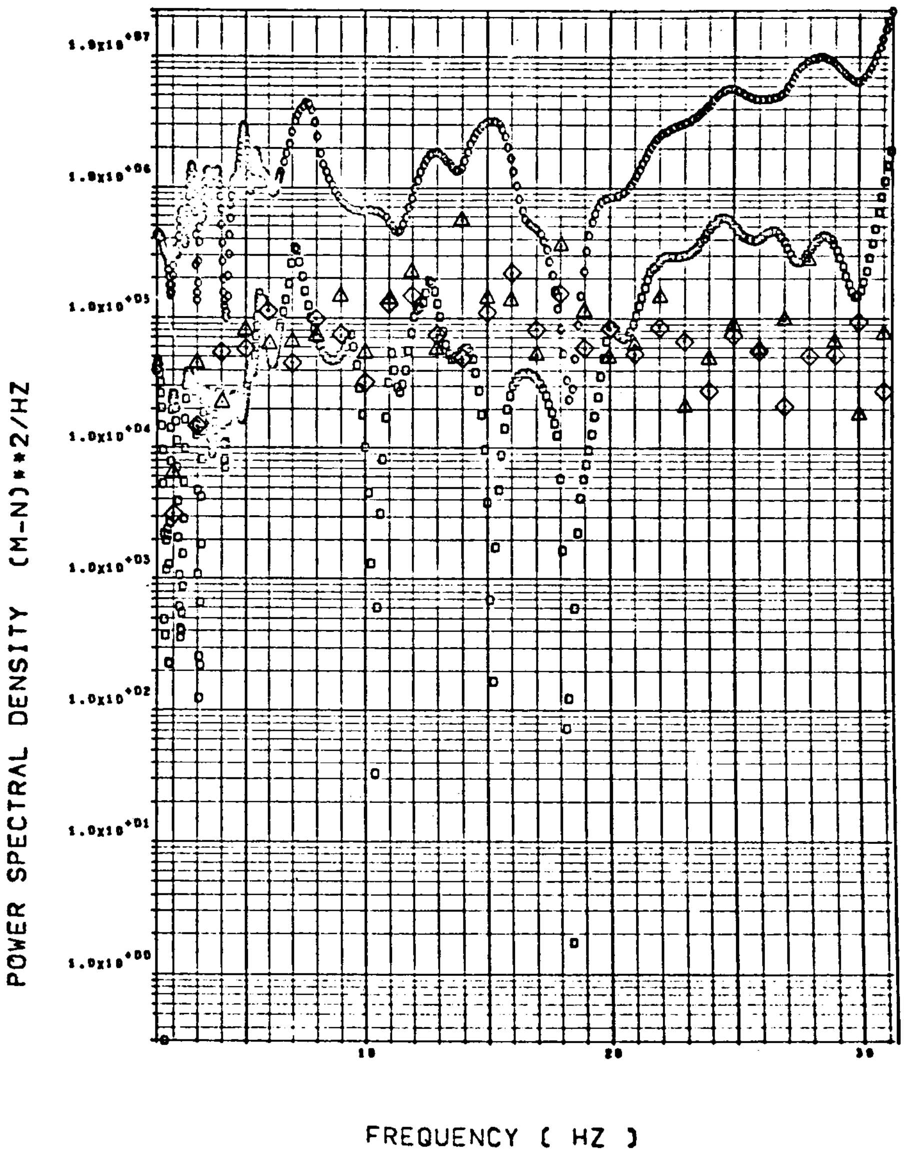

Figure 2.-(k) Horizontal tail torsion (continued)

△ AW001 ◇ AW002 $\alpha_{FLT} = 8.8^{o}$

F-111A WING BUFFET RESPONSE. FLT.48. RUN 6
SWEEP=26 DEG. MACH=.7. ALT=7559 METERS. ALPHA= 9.6
WING TIP ACCELEROMETER
CIRCLE = UPPER BOUNDS SQUARE = LOWER BOUNDS

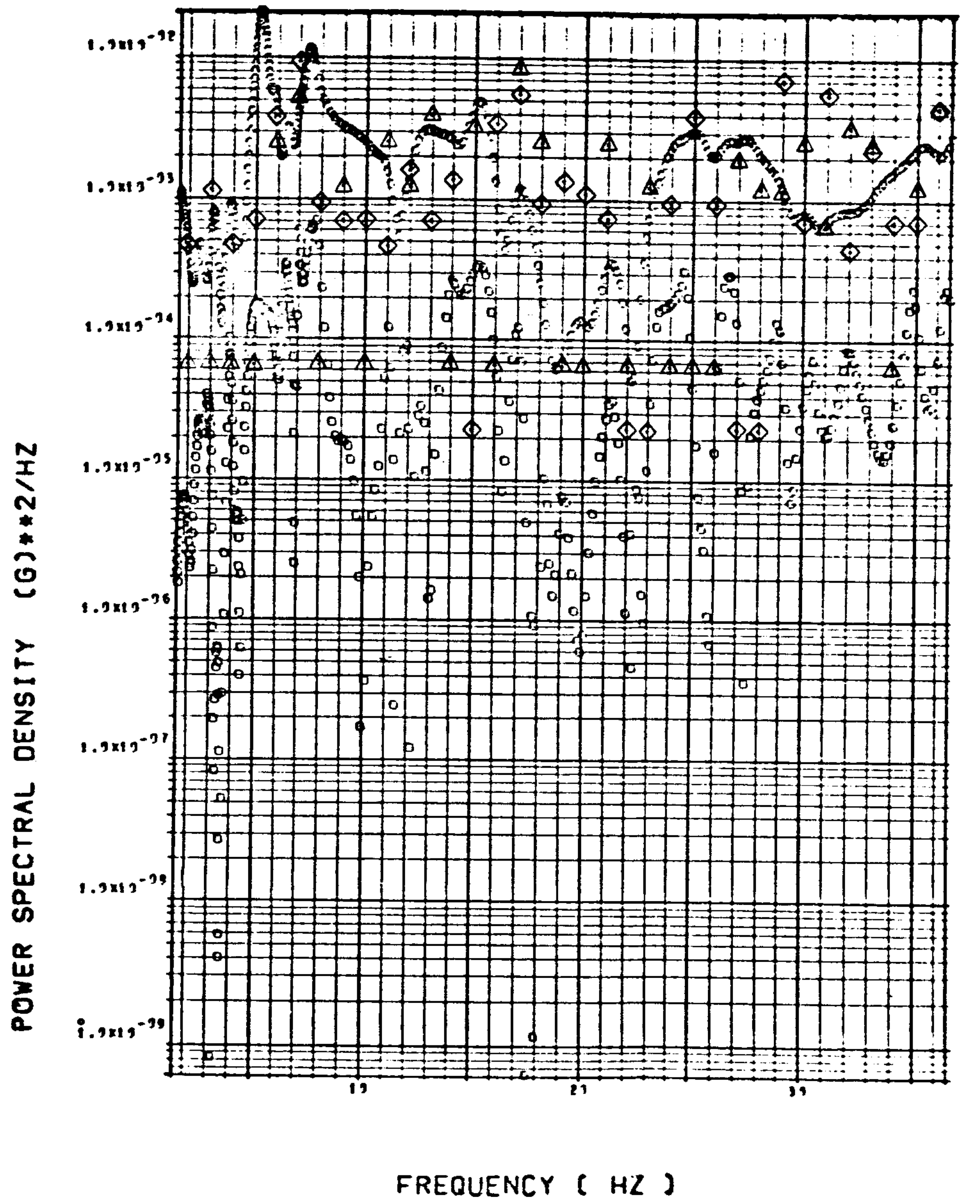

Figure 3.- Power spectra for
Case 3, total airplane (final method),
$\Lambda=26^{o}$, M=0.70, alt.=7559m (24,800 ft)
(a) wing tip accelerometer

△ AW001 ◇ AW002 $\alpha_{FLT} = 9.8^{o}$

F-111A WING BUFFET RESPONSE. FLT.48. RUN 6
SWEEP=26 DEG. MACH=.7. ALT=7559 METERS. ALPHA= 10.7
WING TIP ACCELEROMETER
CIRCLE = UPPER BOUNDS SQUARE = LOWER BOUNDS

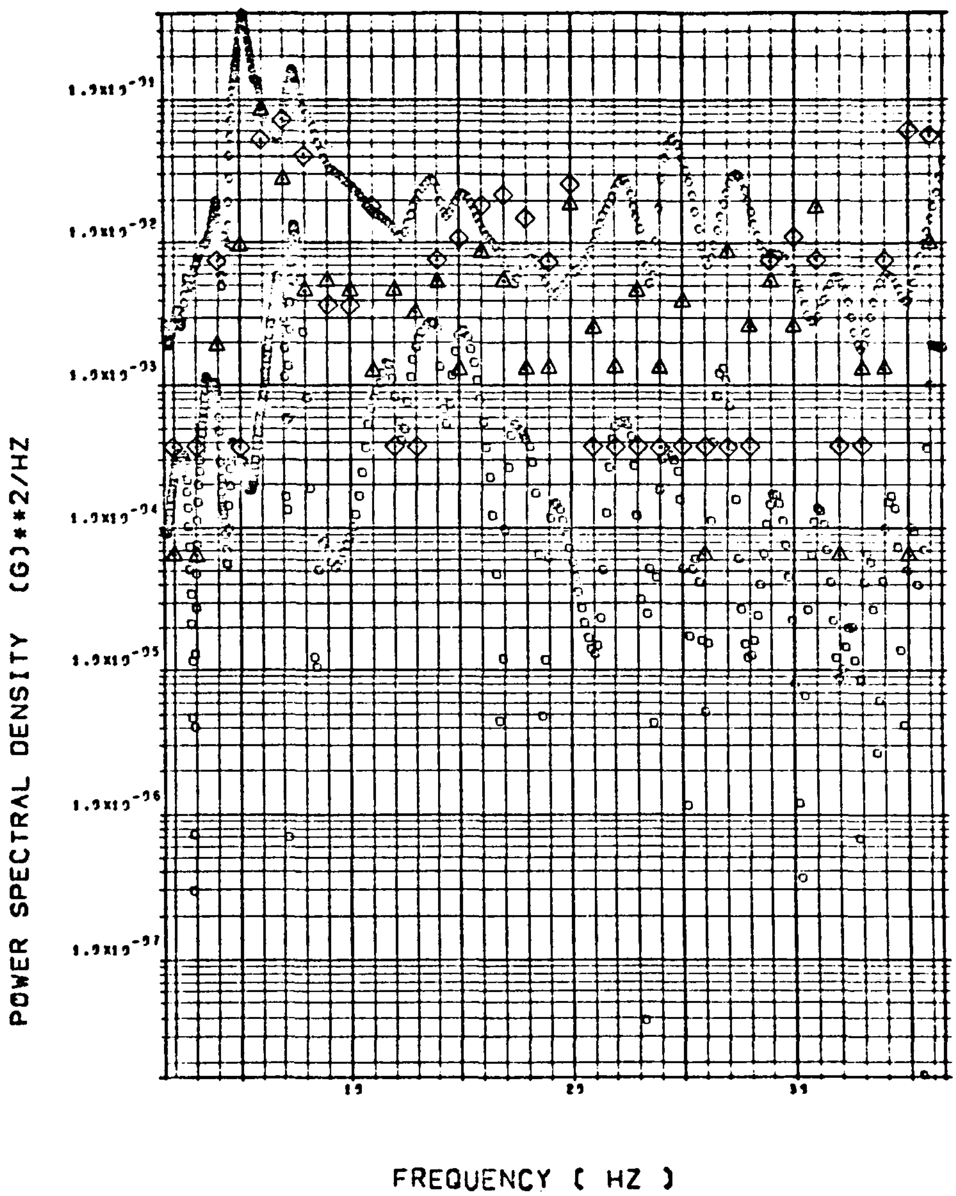

Figure 3.-(a) Wing tip accelerometer (continued)

▲ AW001 ◇ AW002 $\alpha_{FLT} = 10.7^{o}$

F-111A WING BUFFET RESPONSE. FLT.48. RUN 6
SWEEP=26 DEG. MACH=.7. ALT=7559 METERS. ALPHA=11.8
WING TIP ACCELEROMETER
CIRCLE = UPPER BOUNDS SQUARE = LOWER BOUNDS

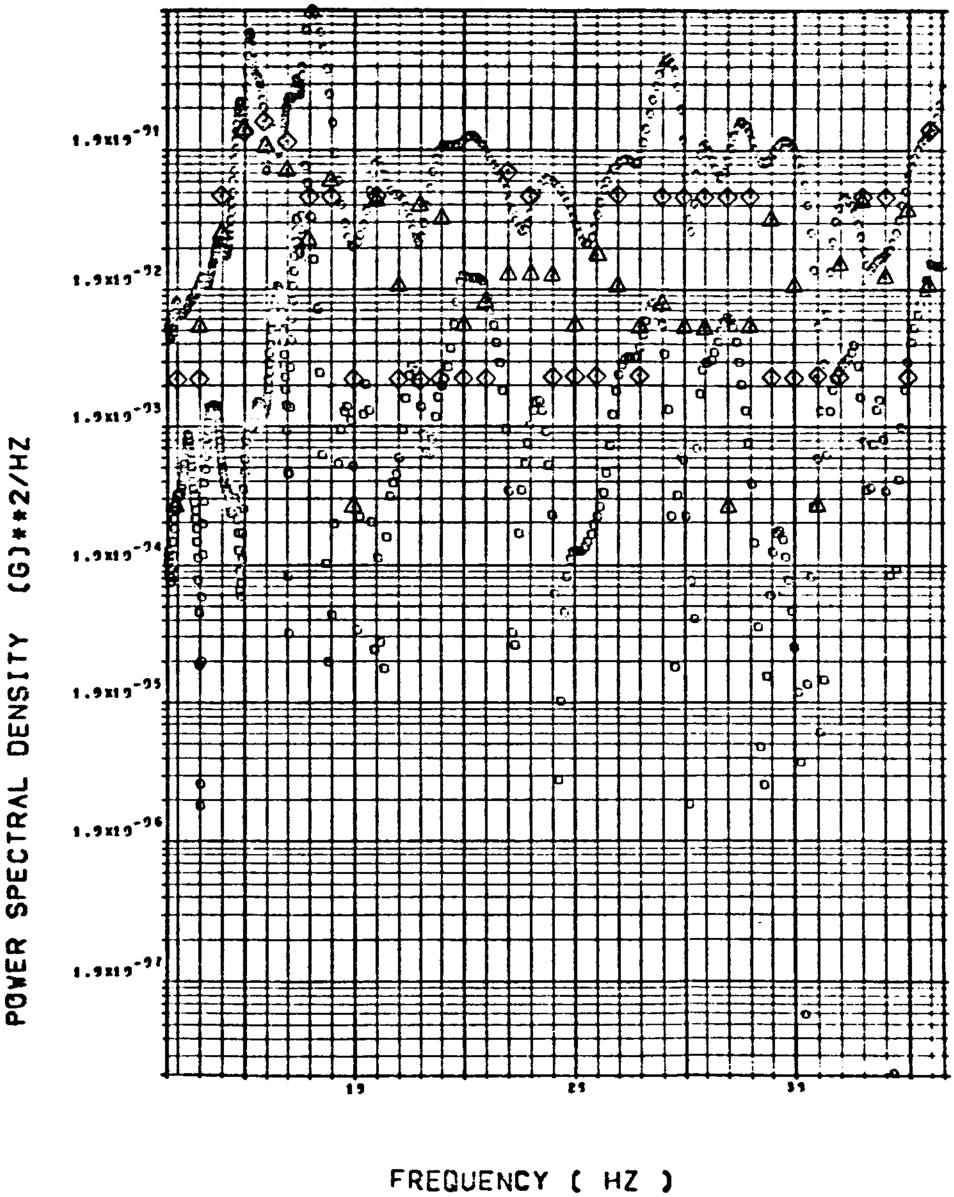

Figure 3.-(a) Wing tip accelerometer (continued)

△ AW001 ◇ AW002 $\alpha_{FLT} = 11.8^{\circ}$

F-111A WING BUFFET RESPONSE. FLT.48. RUN 6
SWEEP=26 DEG. MACH=.7. ALT=7559 METERS. ALPHA=12.8
WING TIP ACCELEROMETER
CIRCLE = UPPER BOUNDS SQUARE = LOWER BOUNDS

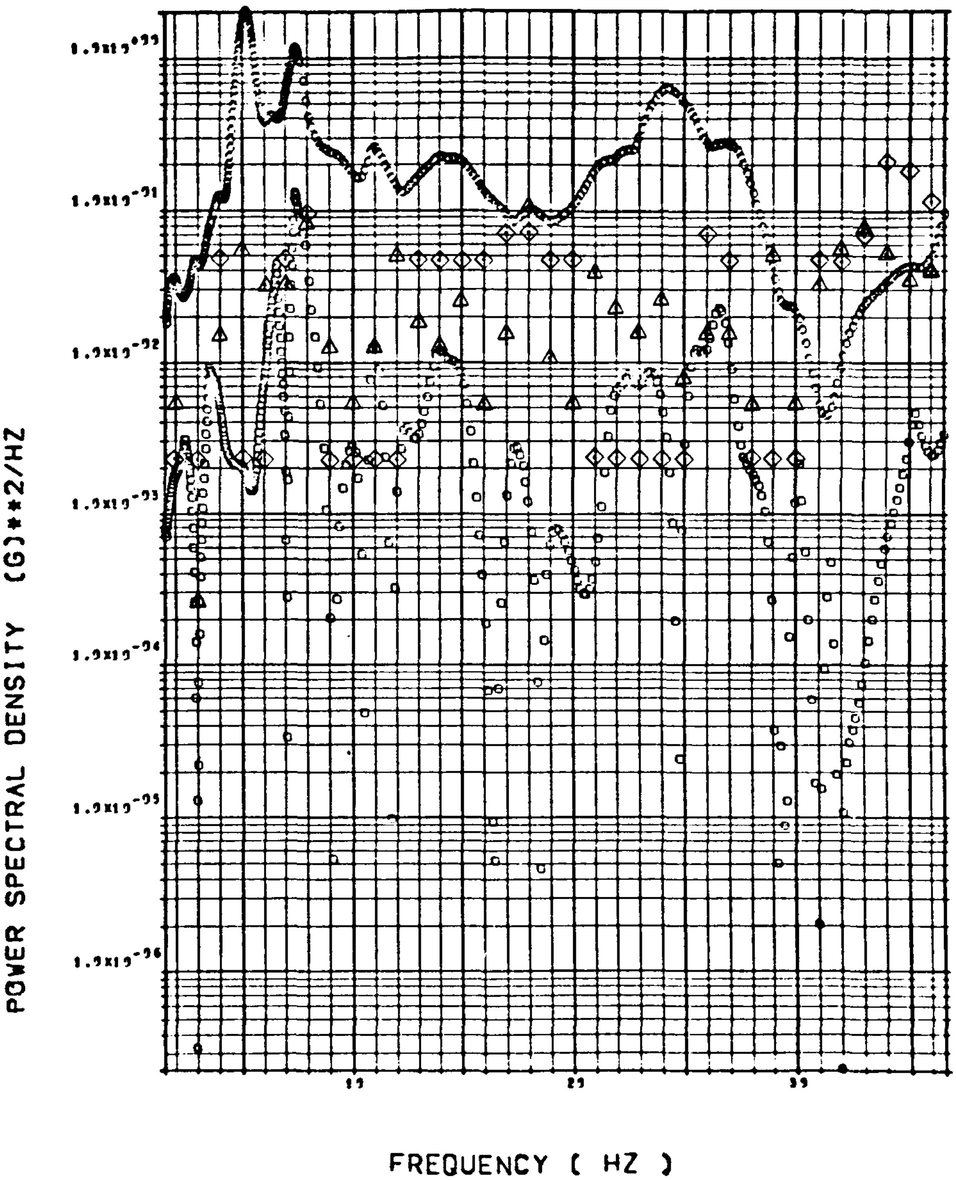

Figure 3.-(a) Wing tip accelerometer (continued)

▲ AW001 ◇ AW002 $\alpha_{FLT} = 14.6^{o}$

F-111A WING BUFFET RESPONSE. FLT.48. RUN 6
SWEEP=26 DEG. MACH=.7. ALT=7559 METERS. ALPHA= 17.1
WING TIP ACCELEROMETER
CIRCLE = UPPER BOUNDS SQUARE = LOWER BOUNDS

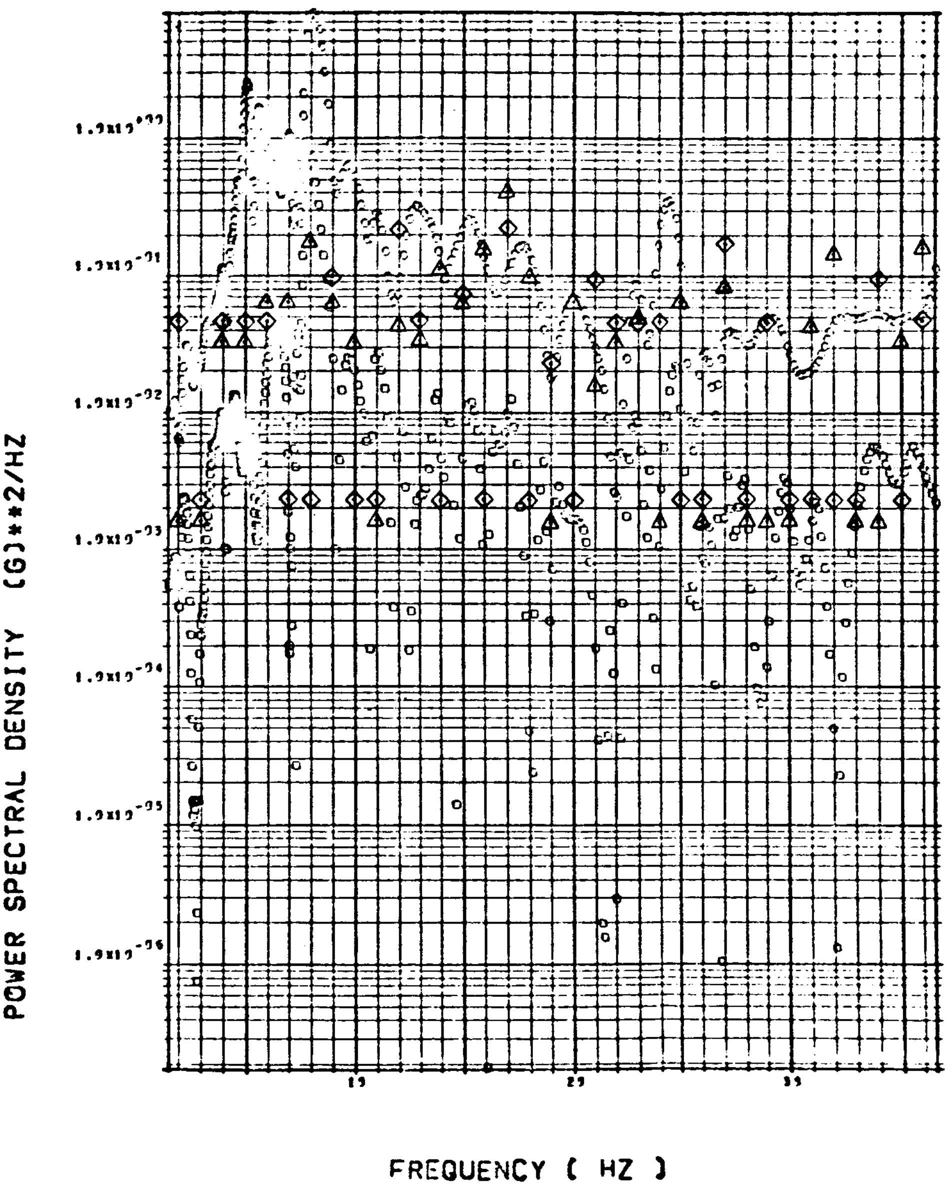

Figure 3.-(a) Wing tip accelerometer (continued)

◇ AB018 $\alpha_{FLT} = 8.8^{\circ}$

SYM F-111A WING BUFFET RESPONSE. FLT 48. RUN 6
SWEEP=26 DEG. MACH=.7. ALT=7559 METERS. ALPHA=9.6
C.G. VERTICAL ACCELEROMETER. FS = 529
SQUARE = 1 DOF A = 2 DOF CIRCLE = 14 DOF

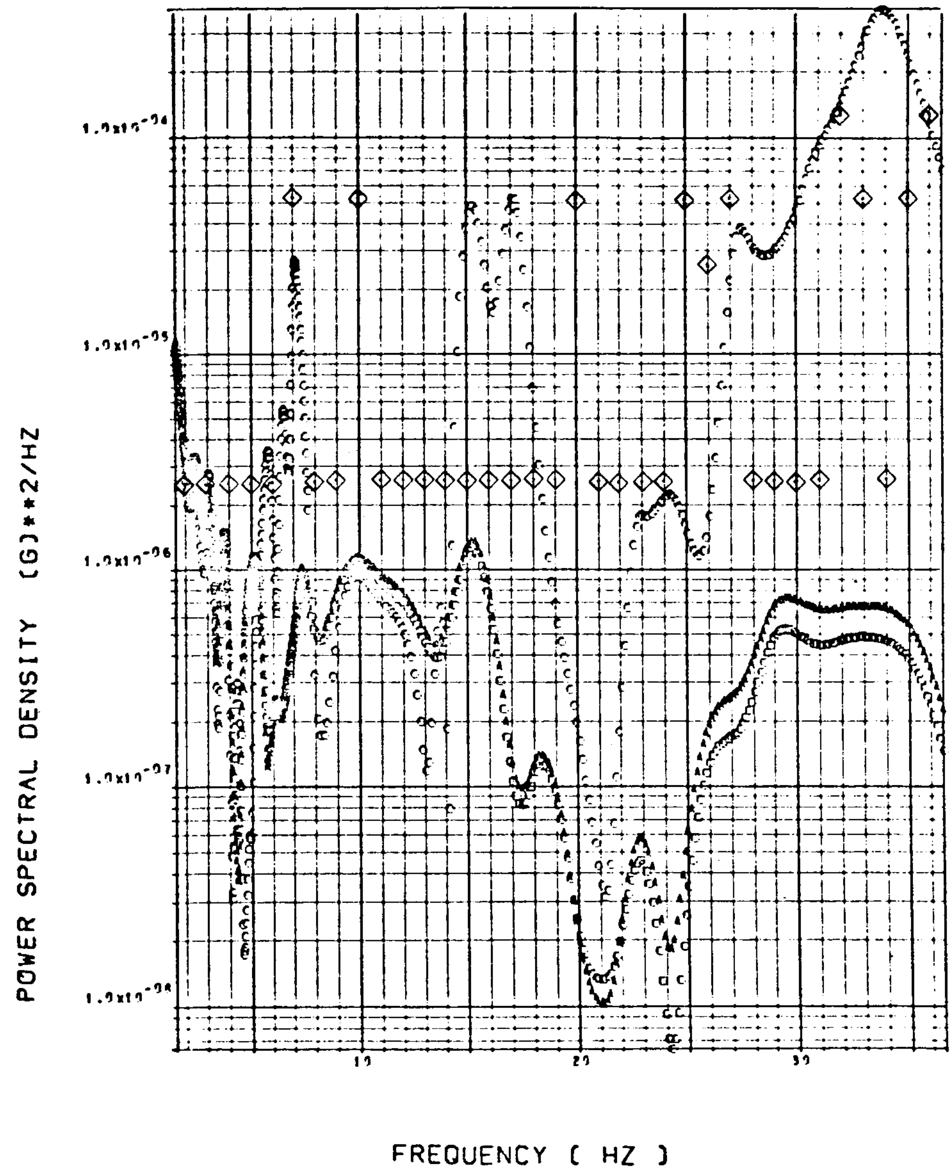

Figure 3.-(b) C.G. vertical accelerometer

◇ AB018 $\alpha_{FLT} = 9.8^{o}$

SYM F-111A WING BUFFET RESPONSE. FLT 48. RUN 6
SWEEP=26 DEG. MACH=.7. ALT=7559 METERS. ALPHA= 10.7
C.G. VERTICAL ACCELEROMETER. FS = 529
SQUARE = 1 DOF A = 2 DOF CIRCLE = 14 DOF

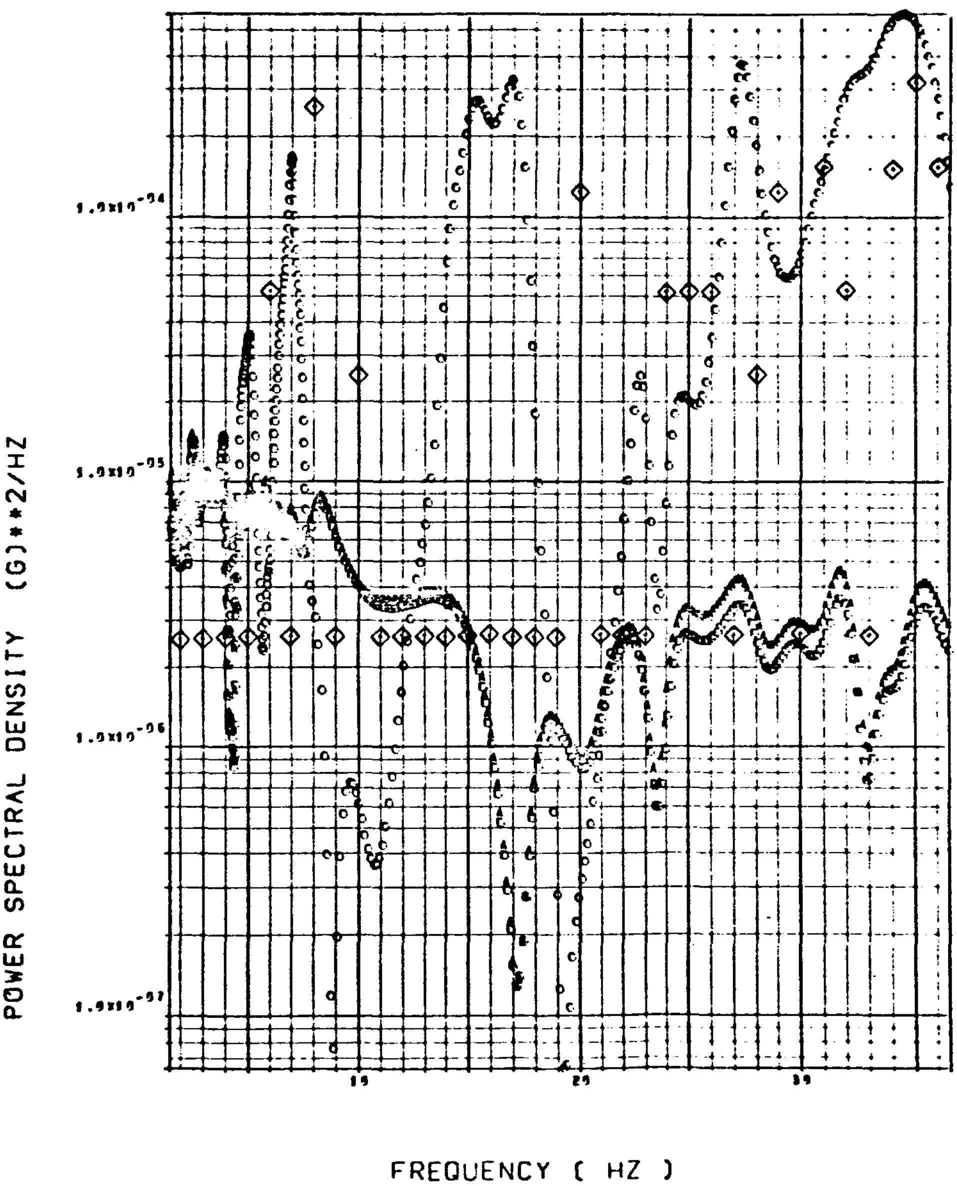

Figure 3.-(b) C.G. vertical accelerometer (continued)

◇ AB018 $\alpha_{FLT} = 10.7^{\circ}$

SYM F-111A WING BUFFET RESPONSE. FLT 48. RUN 6
SWEEP=26 DEG. MACH=.7. ALT=7559 METERS. ALPHA=11.8
C.G. VERTICAL ACCELEROMETER. FS = 529
SQUARE = 1 DOF A = 2 DOF CIRCLE = 14 DOF

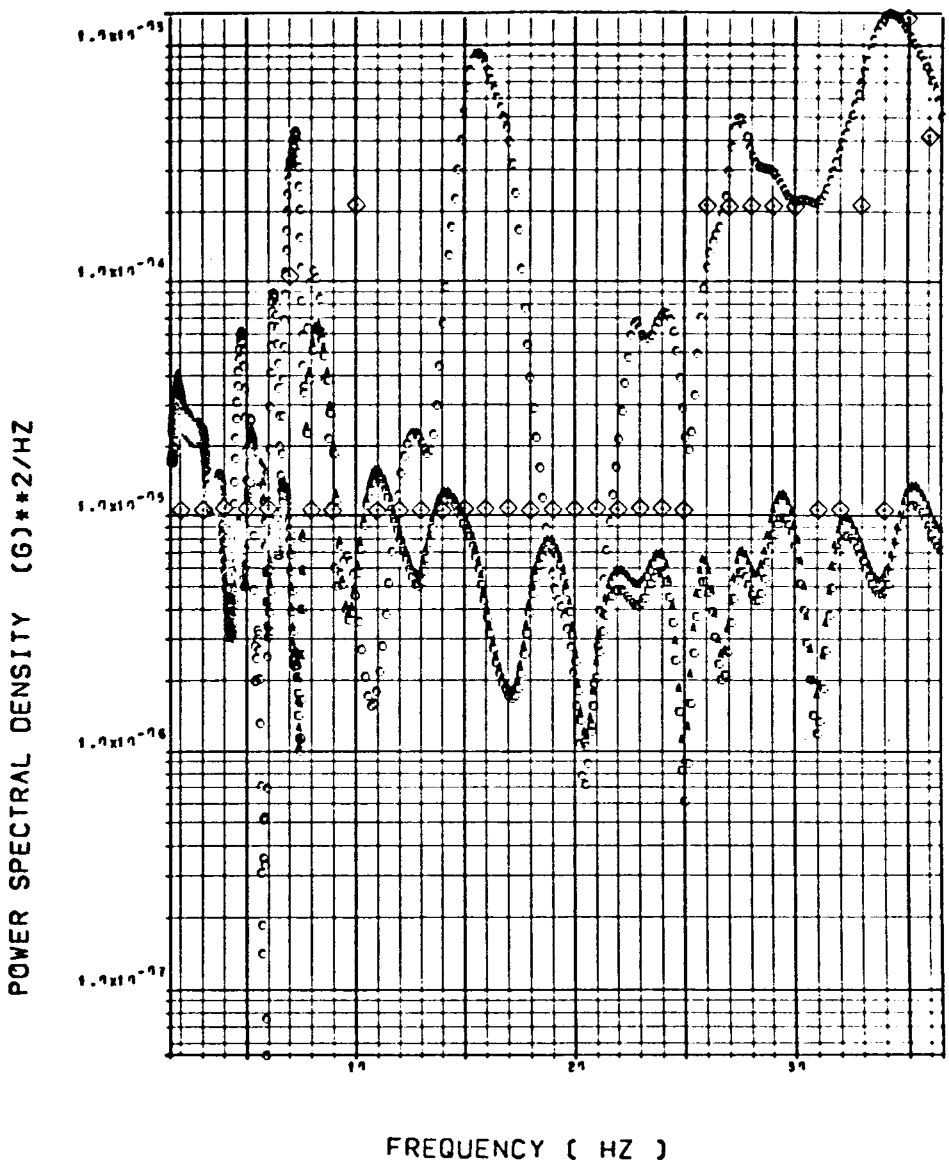

Figure 3.-(b) C.G. vertical accelerometer (continued)

◇ AB018 $\alpha_{FLT} = 11.8^{o}$

SYM F-111A WING BUFFET RESPONSE. FLT 48. RUN 6
SWEEP=26 DEG. MACH=.7. ALT=7559 METERS. ALPHA=12.8
C.G. VERTICAL ACCELEROMETER. FS = 529
SQUARE = 1 DOF A = 2 DOF CIRCLE = 14 DOF

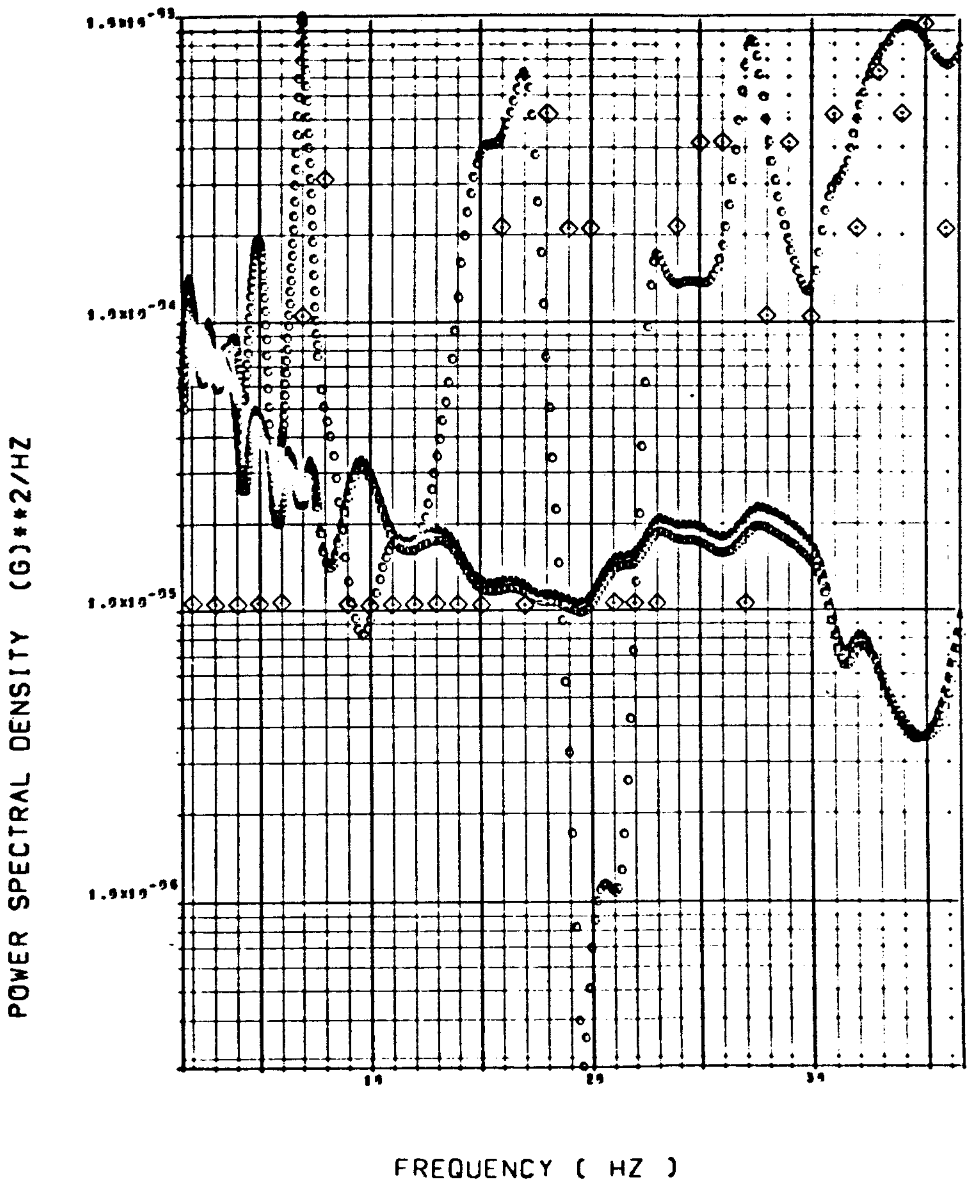

Figure 3.-(b) C.G. vertical accelerometer (continued)

◇ AB018 $\alpha_{FLT} = 14.6^{o}$

SYM F-111A WING BUFFET RESPONSE. FLT 48. RUN 6
SWEEP=26 DEG. MACH=.7. ALT=7559 METERS. ALPHA= 17.1
C.G. VERTICAL ACCELEROMETER. FS = 529
SQUARE = 1 DOF A = 2 DOF CIRCLE = 14 DOF

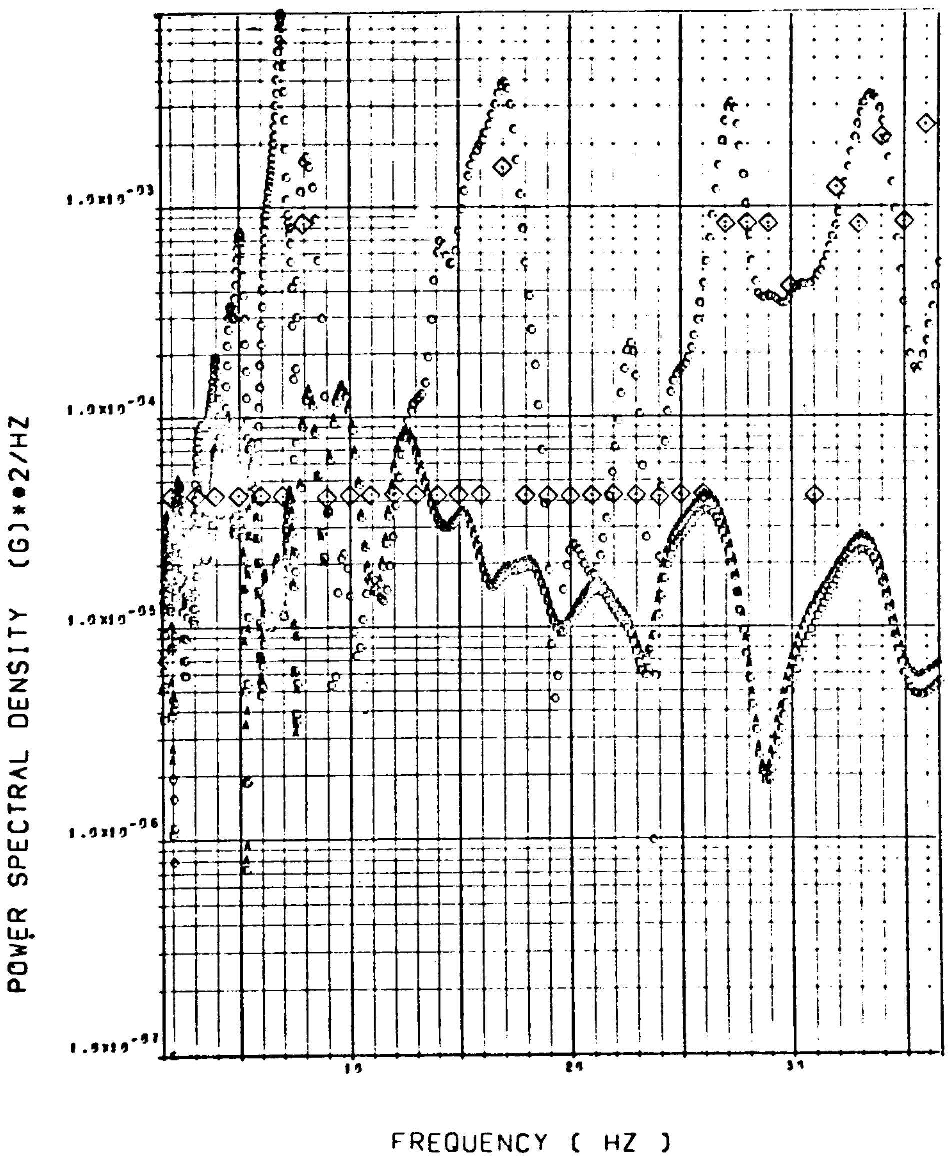

Figure 3.-(b) C.G. vertical accelerometer (continued)

◇ AF009 $\alpha_{FLT} = 8.8^{o}$

SYM F-111A WING BUFFET RESPONSE. FLT 48. RUN 6
SWEEP=26 DEG. MACH=.7. ALT=7559 METERS. ALPHA= 9.6
PILOT STATION VERTICAL ACCELEROMETER. FS = 255
SQUARE = 1 DOF A = 2 DOF CIRCLE = 14 DOF

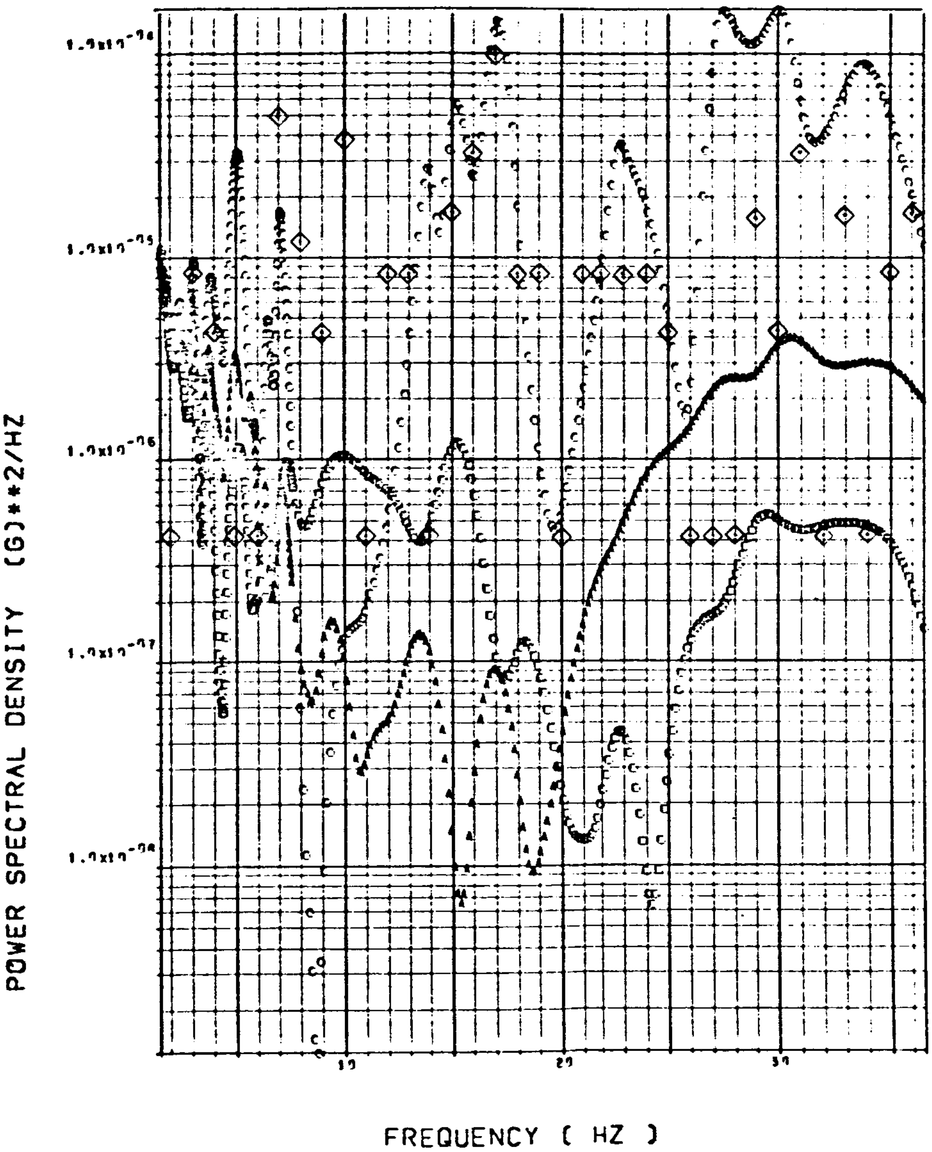

Figure 3.-(c) Pilot seat vertical accelerometer

◇ AF009 $\alpha_{FLT} = 9.8^{o}$

SYM F-111A WING BUFFET RESPONSE. FLT 48. RUN 6
SWEEP=26 DEG. MACH=.7. ALT=7559 METERS. ALPHA=10.7
PILOT STATION VERTICAL ACCELEROMETER. FS = 255
SQUARE = 1 DOF A = 2 DOF CIRCLE = 14 DOF

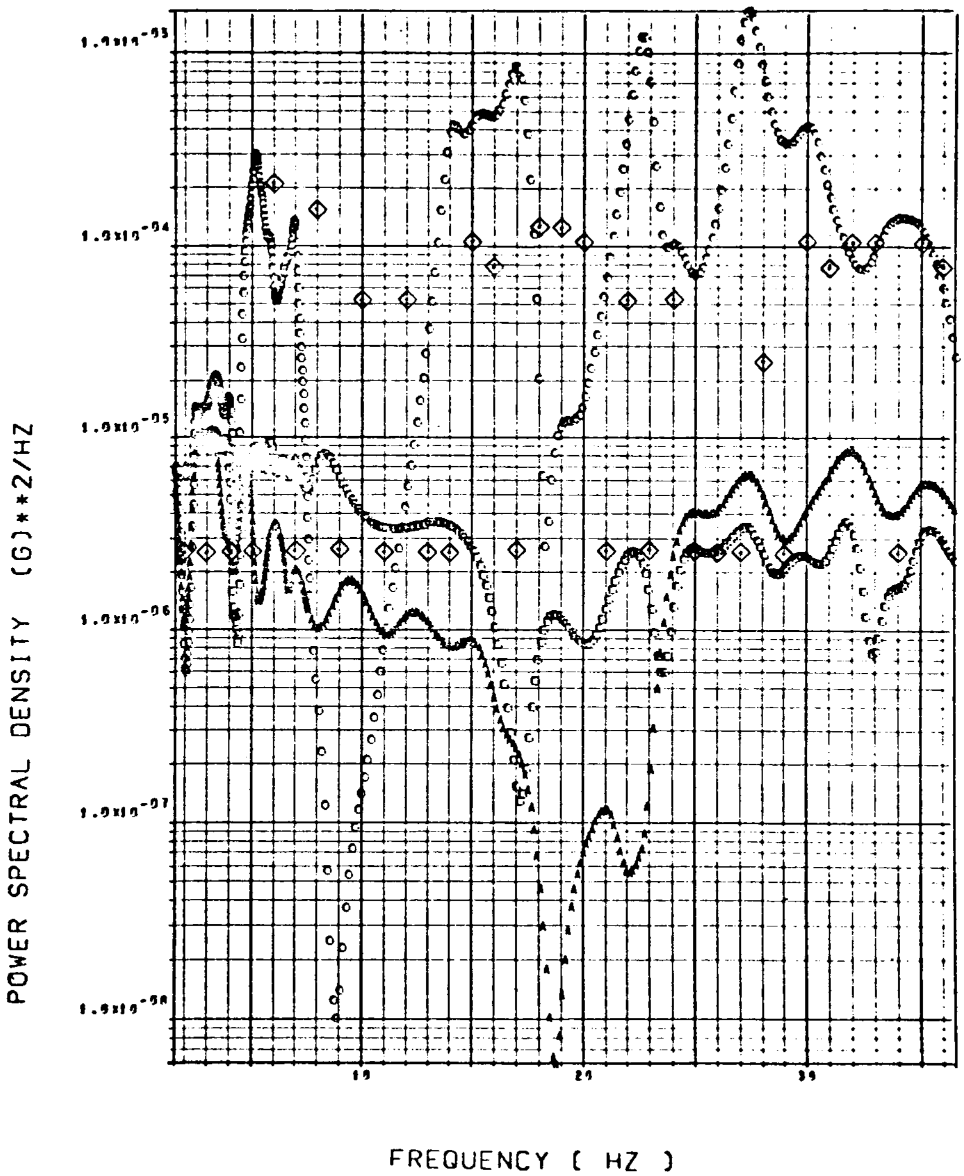

Figure 3.-(c) Pilot seat vertical accelerometer (continued)

◇ AF009 $\alpha_{FLT} = 10.7^{o}$

SYM F-111A WING BUFFET RESPONSE, FLT 48, RUN 6
SWEEP=26 DEG, MACH=.7, ALT=7559 METERS, ALPHA=11.8
PILOT STATION VERTICAL ACCELEROMETER, FS = 255
SQUARE = 1 DOF A = 2 DOF CIRCLE = 14 DOF

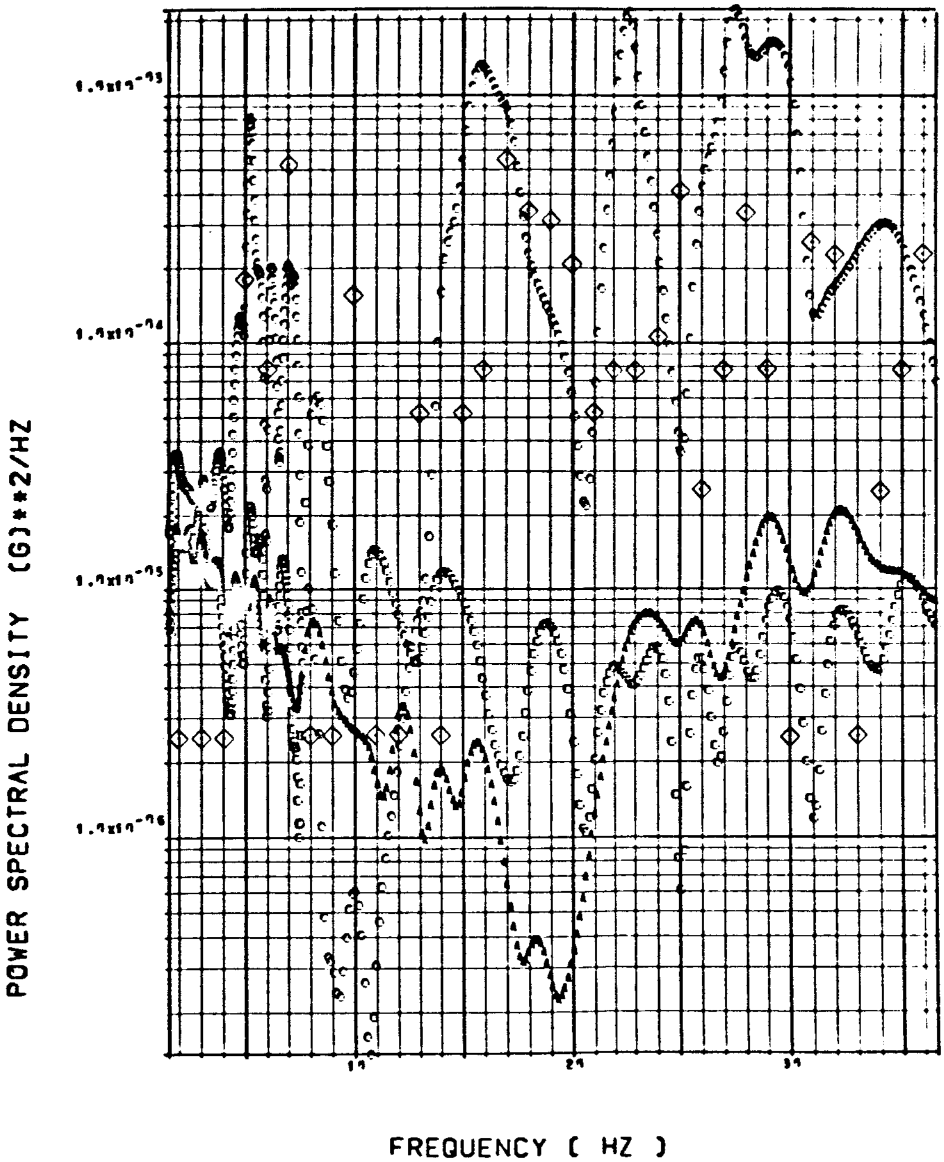

Figure 3.-(c) Pilot seat vertical accelerometer (continued)

◇ AF009 $\alpha_{FLT} = 11.8^{o}$

SYM F-111A WING BUFFET RESPONSE. FLT 48. RUN 6
SWEEP=26 DEG. MACH=.7. ALT=7559 METERS. ALPHA= 12.8
PILOT STATION VERTICAL ACCELEROMETER. FS = 255
SQUARE = 1 DOF A = 2 DOF CIRCLE = 14 DOF

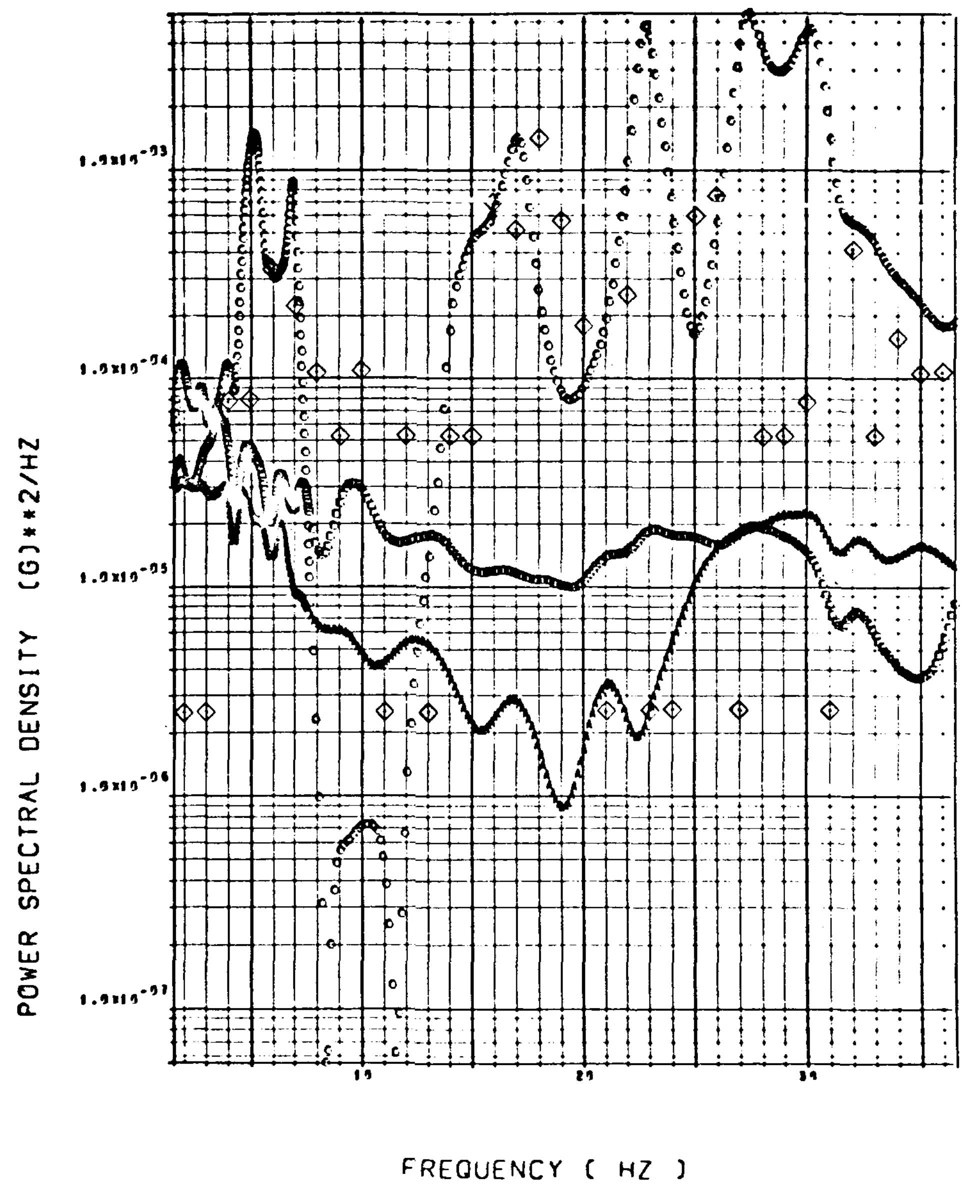

Figure 3.-(c) Pilot seat vertical accelerometer (continued)

◇ AF009 $\alpha_{FLT} = 14.6^{o}$

SYM F-111A WING BUFFET RESPONSE. FLT 48. RUN 6
SWEEP=26 DEG. MACH=.7. ALT=7559 METERS. ALPHA= 17.1
PILOT STATION VERTICAL ACCELEROMETER. FS = 255
SQUARE = 1 DOF A = 2 DOF CIRCLE = 14 DOF

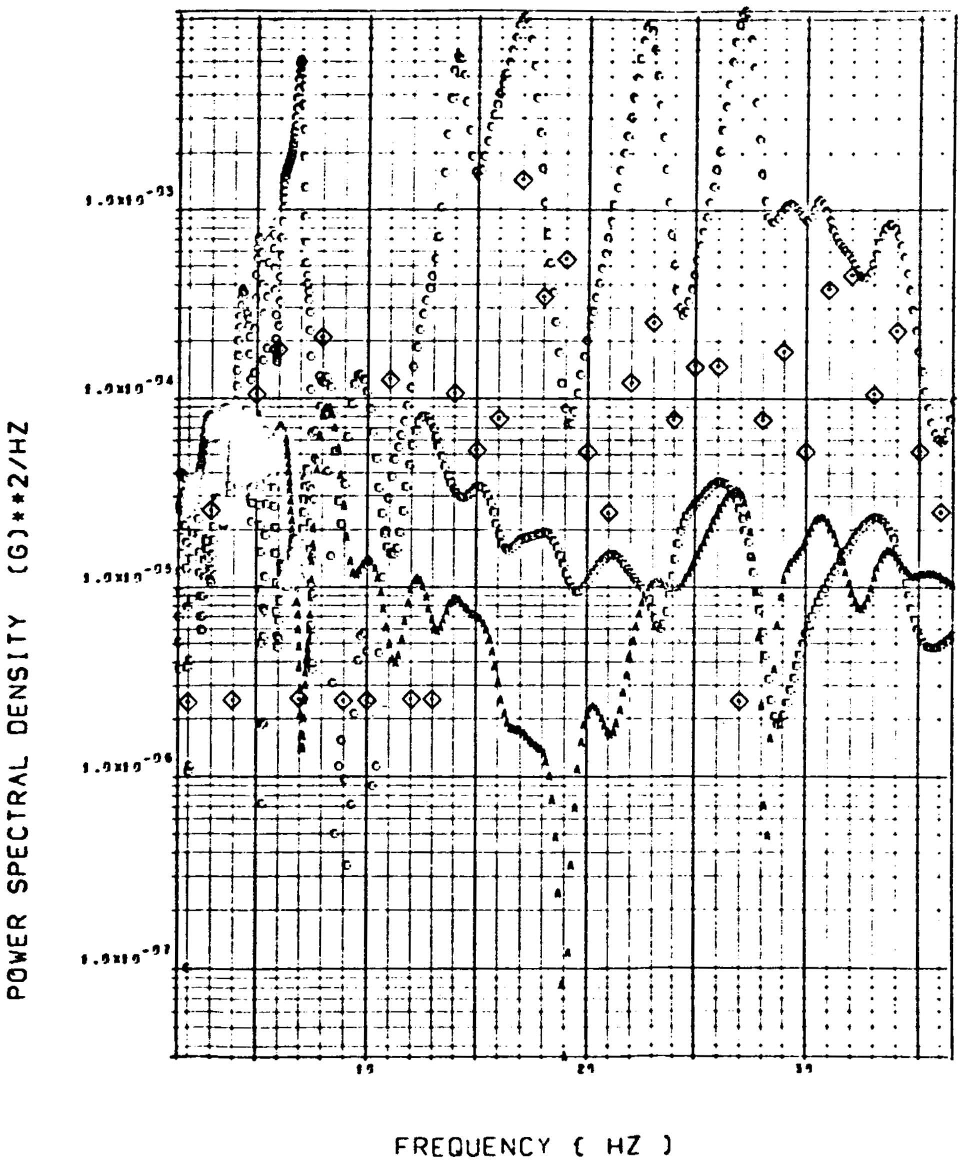

Figure 3.-(c) Pilot seat vertical accelerometer (continued)

◇ AB020 $\alpha_{FLT} = 8.8^{o}$

ANTI F-111A WING BUFFET RESPONSE, FLT 48, RUN 6
SWEEP=26 DEG, MACH=.7, ALT=7559 METERS, ALPHA= 9.6
C.G. LATERAL ACCELEROMETER, FS = 529
SQUARE = 1 DOF A = 3 DOF CIRCLE = 18 DOF

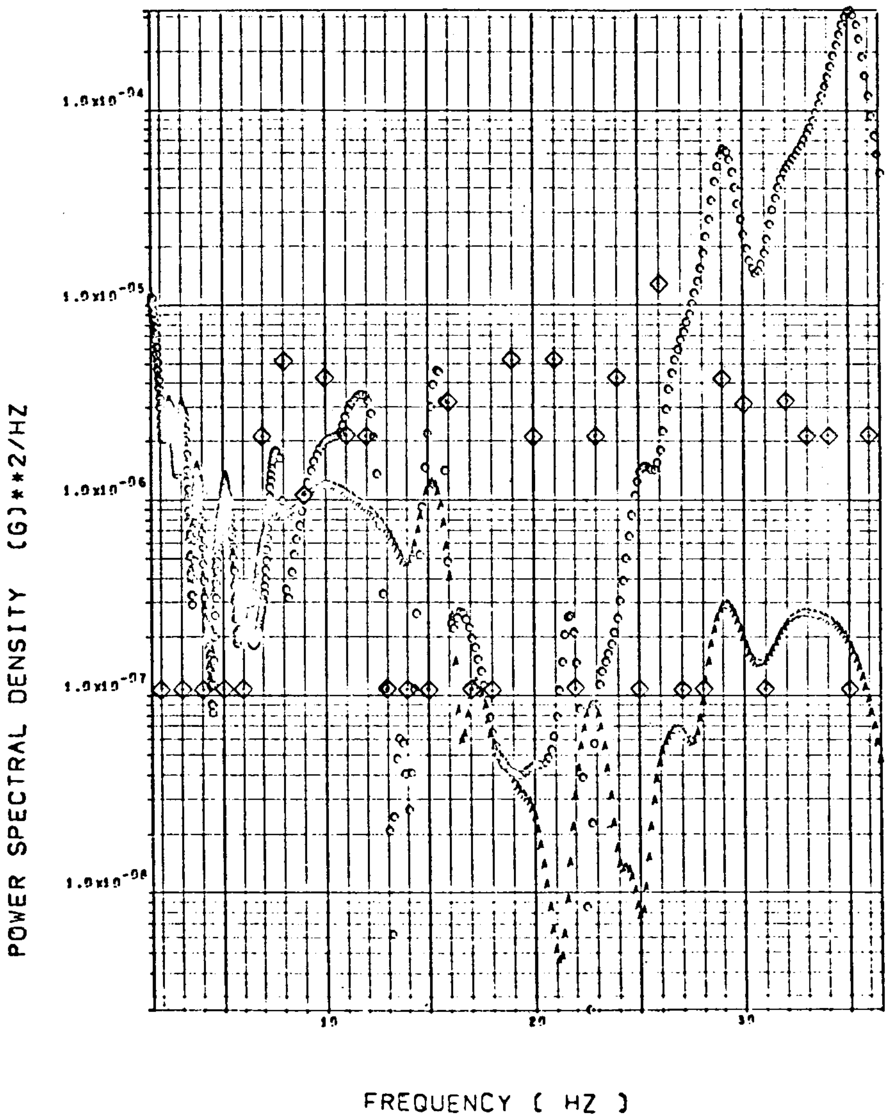

Figure 3.-(d) C.G. lateral accelerometer

◇ AB020 $\alpha_{FLT} = 9.8^{o}$

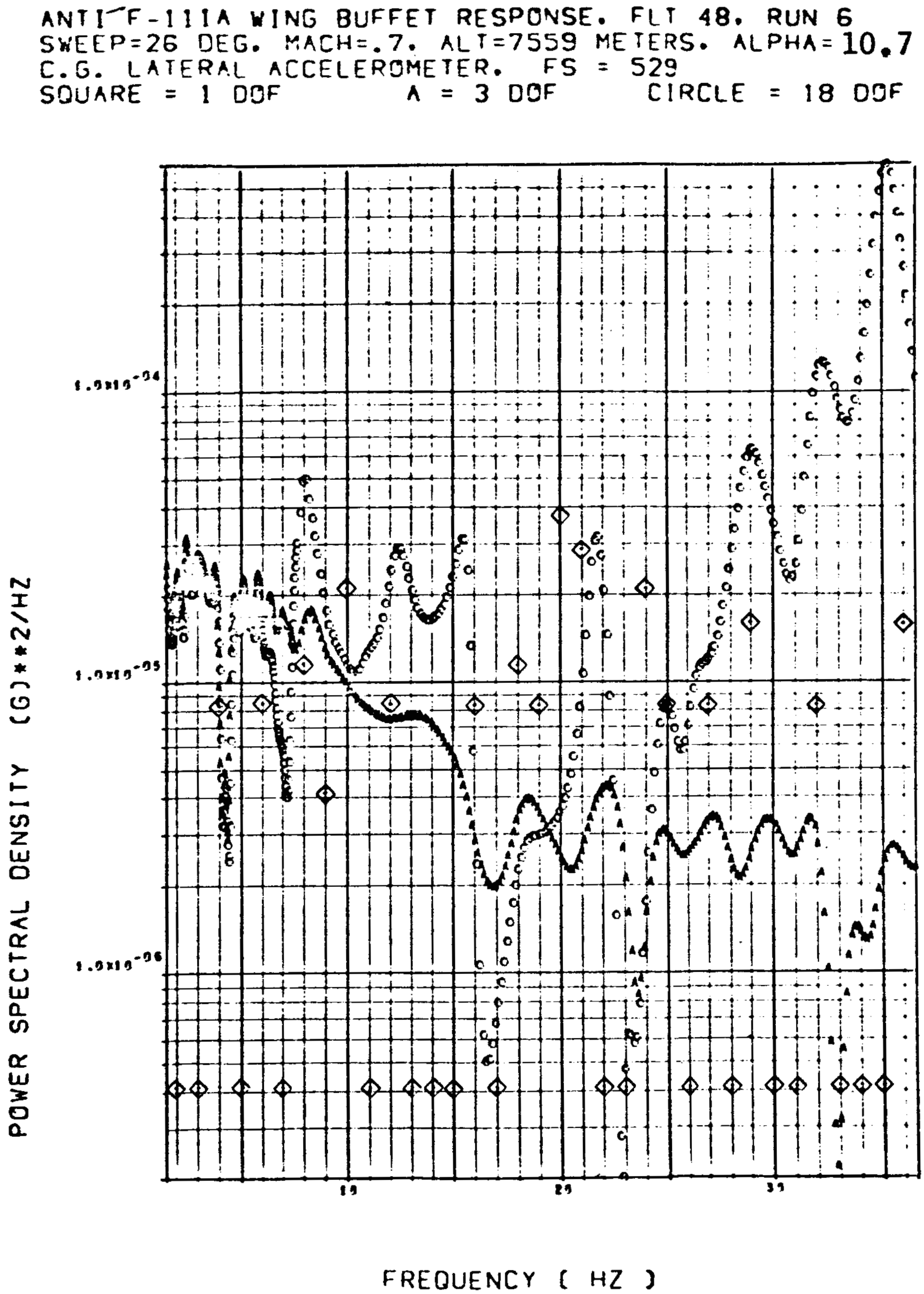

Figure 3.-(d) C.G. lateral accelerometer (continued)

◇ AB020 $\alpha_{FLT} = 10.7^{o}$

ANTI F-111A WING BUFFET RESPONSE. FLT 48. RUN 6
SWEEP=26 DEG. MACH=.7. ALT=7559 METERS. ALPHA= 11.8
C.G. LATERAL ACCELEROMETER. FS = 529
SQUARE = 1 DOF A = 3 DOF CIRCLE = 18 DOF

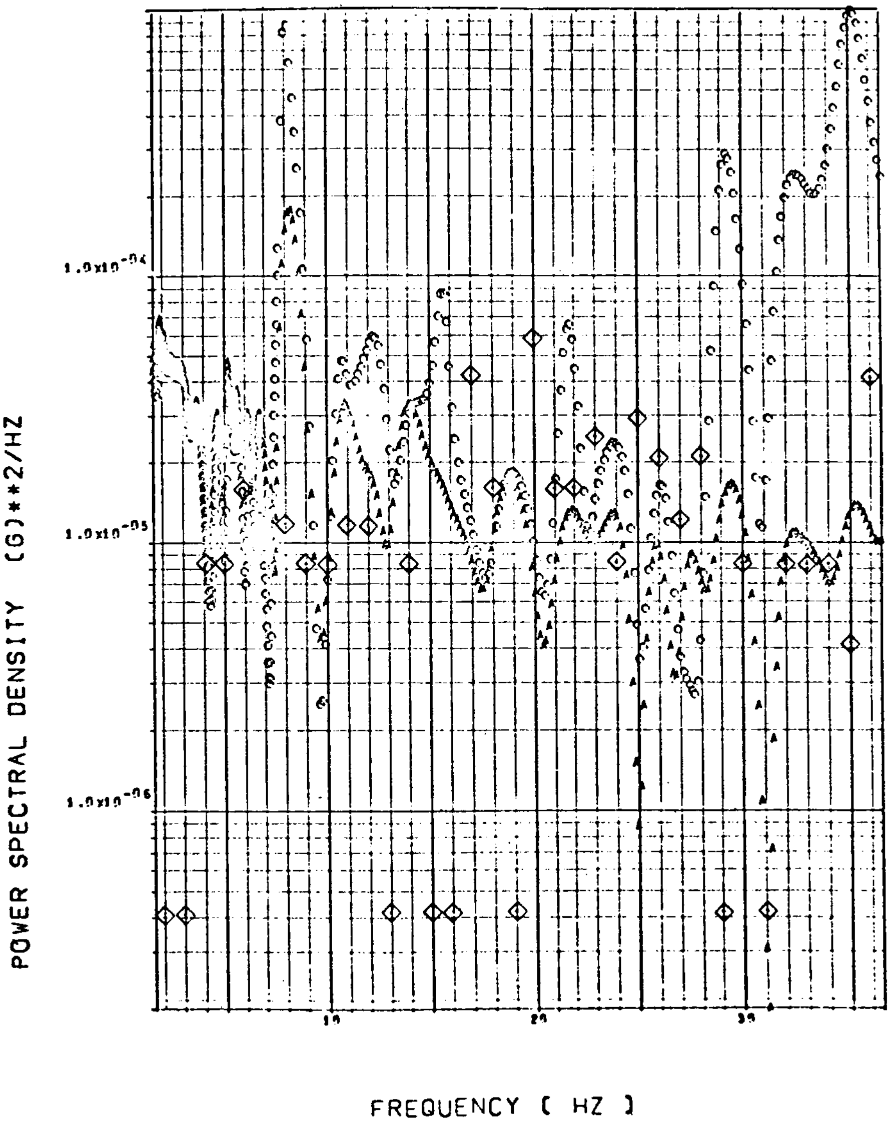

Figure 3.-(d) C.G. lateral accelerometer (continued)

◇ AB020 $\alpha_{FLT} = 11.8^{o}$

ANTI F-111A WING BUFFET RESPONSE. FLT 48. RUN 6
SWEEP=26 DEG. MACH=.7. ALT=7559 METERS. ALPHA=12.8
C.G. LATERAL ACCELEROMETER. FS = 529
SQUARE = 1 DOF A = 3 DOF CIRCLE = 18 DOF

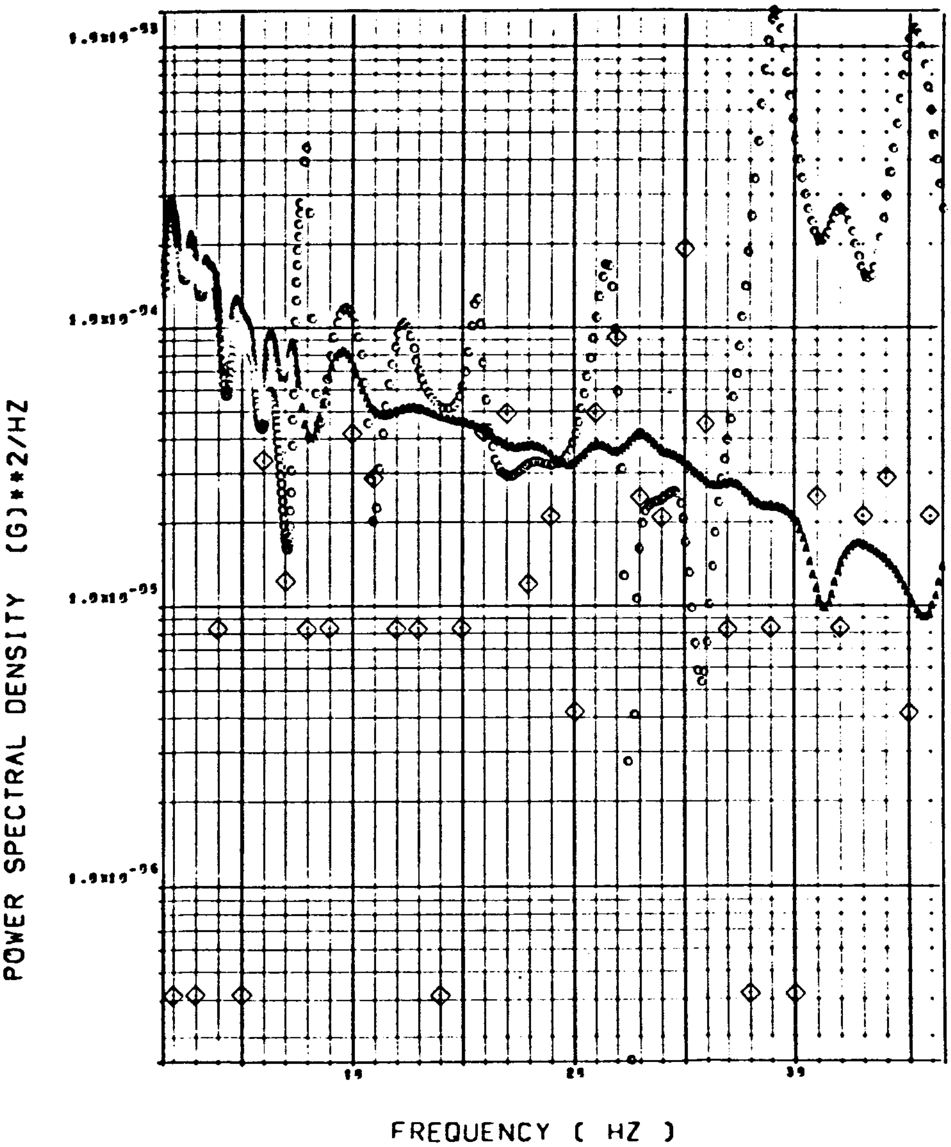

Figure 3.-(d) C.G. lateral accelerometer (continued)

◇ AB020 $\alpha_{FLT} = 14.6^{\circ}$

ANTI F-111A WING BUFFET RESPONSE. FLT 48. RUN 6
SWEEP=26 DEG. MACH=.7. ALT=7559 METERS. ALPHA=17.1
C.G. LATERAL ACCELEROMETER. FS = 529
SQUARE = 1 DOF A = 3 DOF CIRCLE = 18 DOF

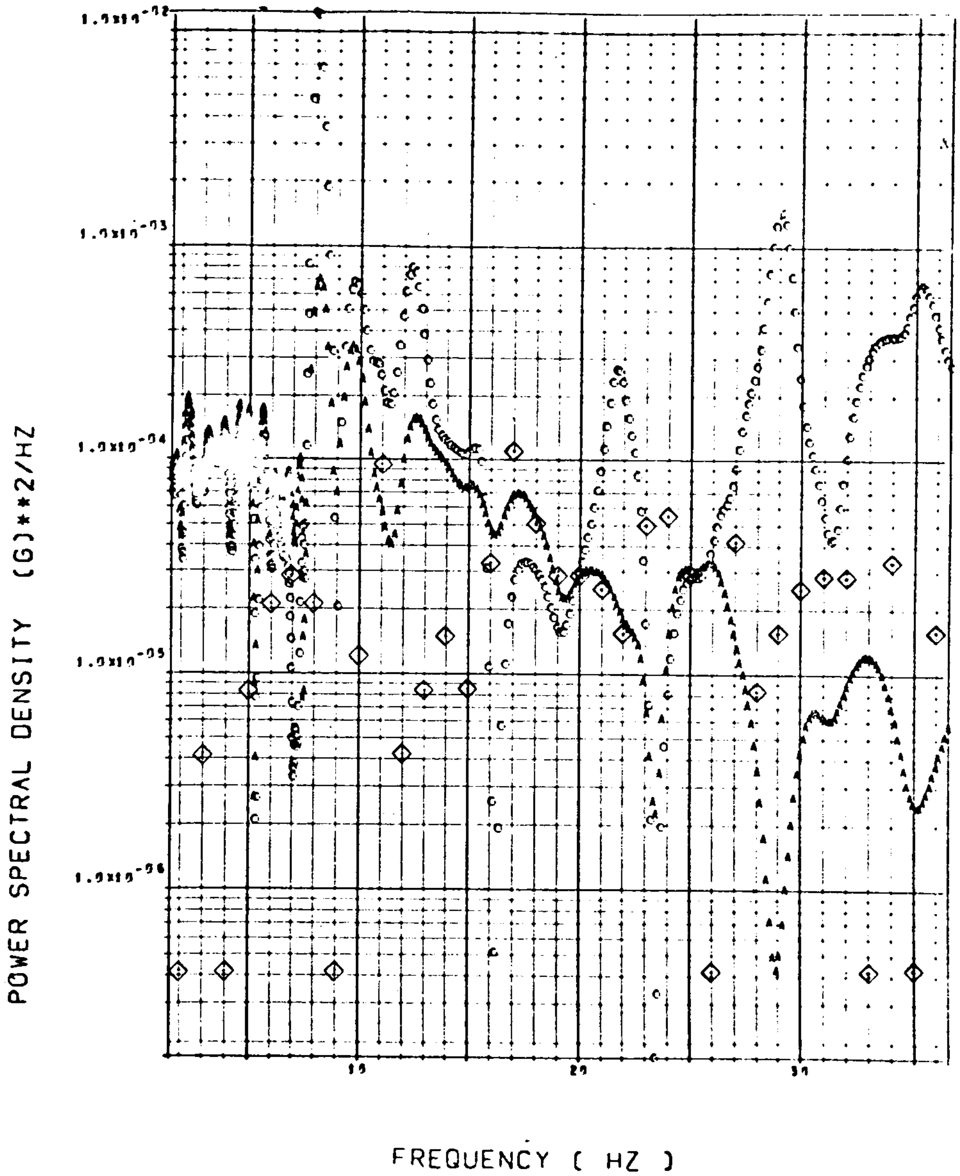

Figure 3.-(d) C.G. lateral accelerometer (continued)

◇ AF010 $\alpha_{FLT} = 8.8^{o}$

ANTI F-111A WING BUFFET RESPONSE. FLT 48. RUN 6
SWEEP=26 DEG. MACH=.7. ALT=7559 METERS. ALPHA= 9.6
PILOT STATION LATERAL ACCELEROMETER. FS = 255
SQUARE = 1 DOF A = 3 DOF CIRCLE = 18 DOF

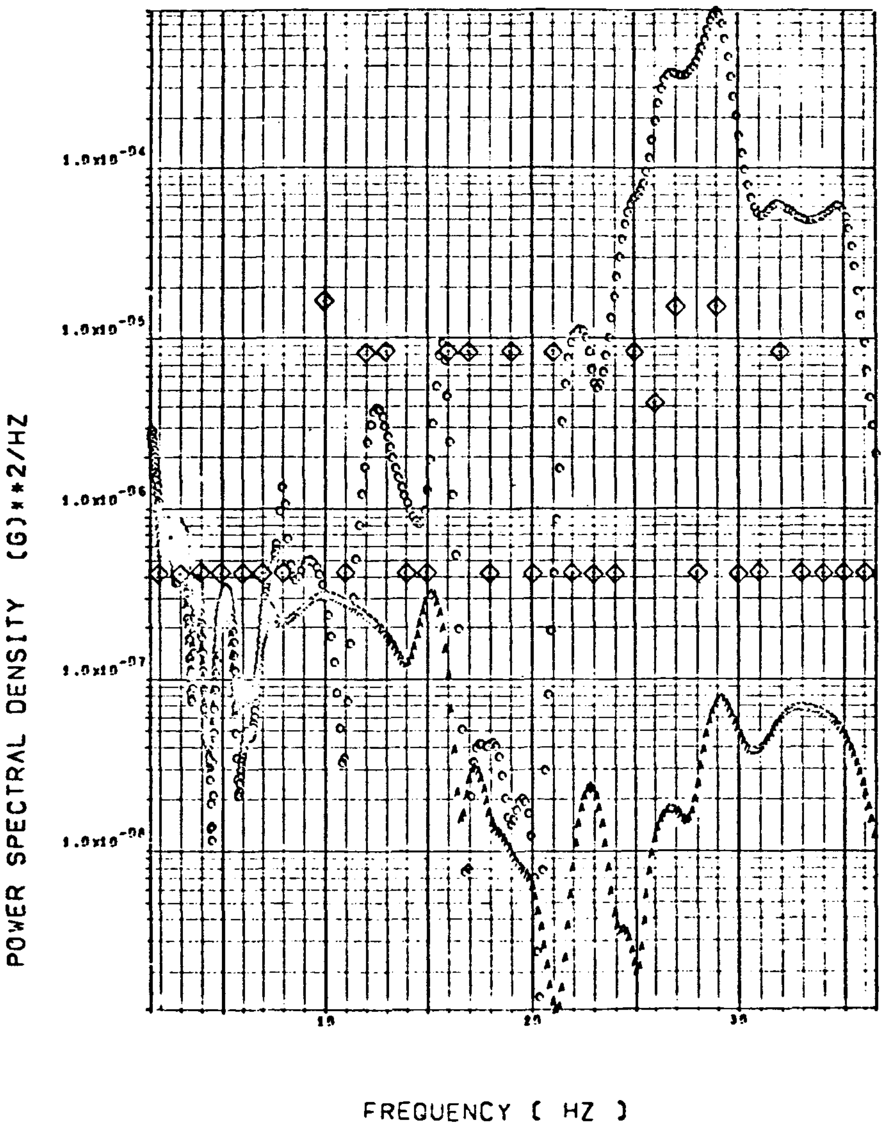

Figure 3.-(e) Pilot seat lateral accelerometer

◇ AF010 $\alpha_{FLT} = 9.8^{o}$

ANTI F-111A WING BUFFET RESPONSE. FLT 48. RUN 6
SWEEP=26 DEG. MACH=.7. ALT=7559 METERS. ALPHA=10.7
PILOT STATION LATERAL ACCELEROMETER. FS = 255
SQUARE = 1 DOF A = 3 DOF CIRCLE = 18 DOF

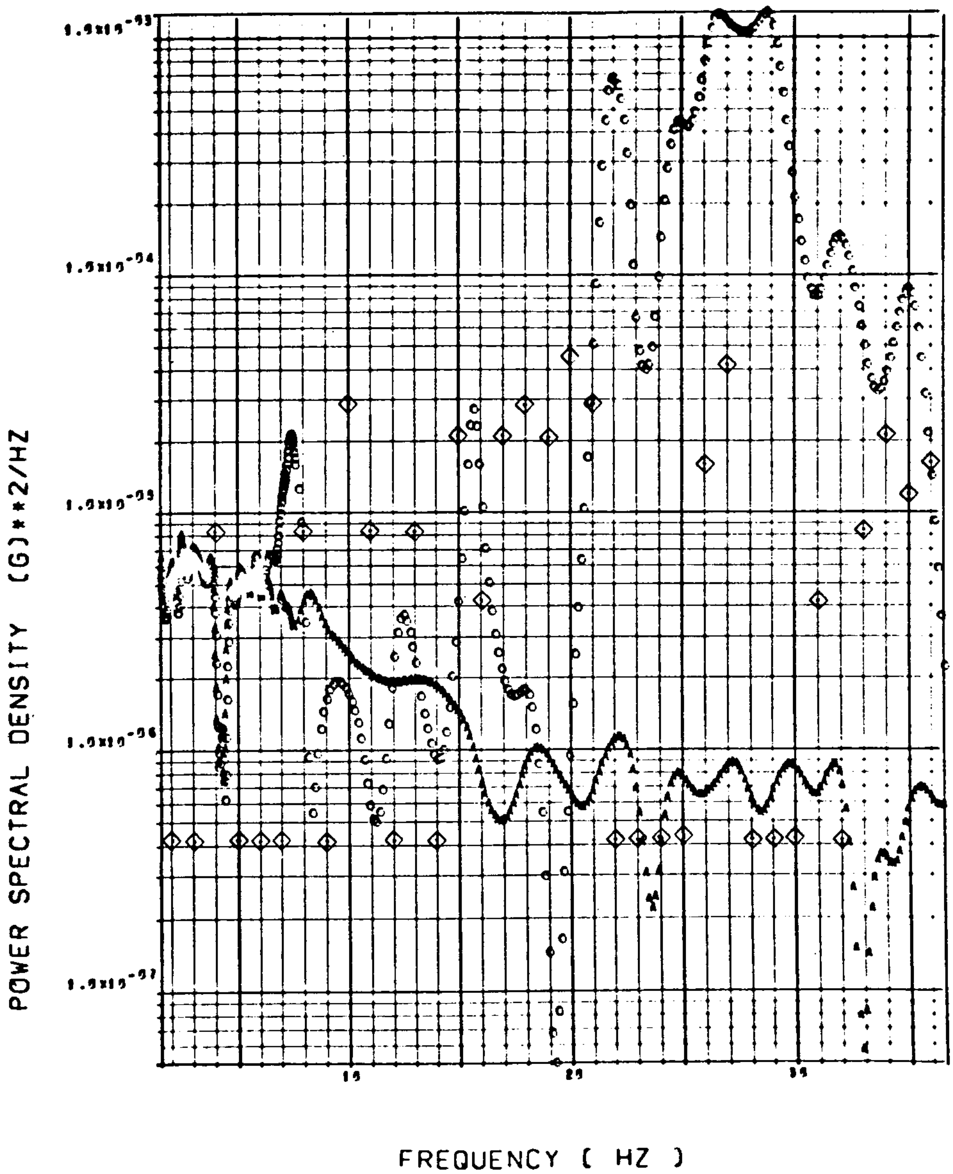

Figure 3.-(e) Pilot seat lateral accelerometer (continued)

◇ AF010 $\alpha_{FLT} = 10.7^{o}$

ANTI F-111A WING BUFFET RESPONSE, FLT 48, RUN 6
SWEEP=26 DEG, MACH=.7, ALT=7559 METERS, ALPHA= 11.8
PILOT STATION LATERAL ACCELEROMETER, FS = 255
SQUARE = 1 DOF A = 3 DOF CIRCLE = 18 DOF

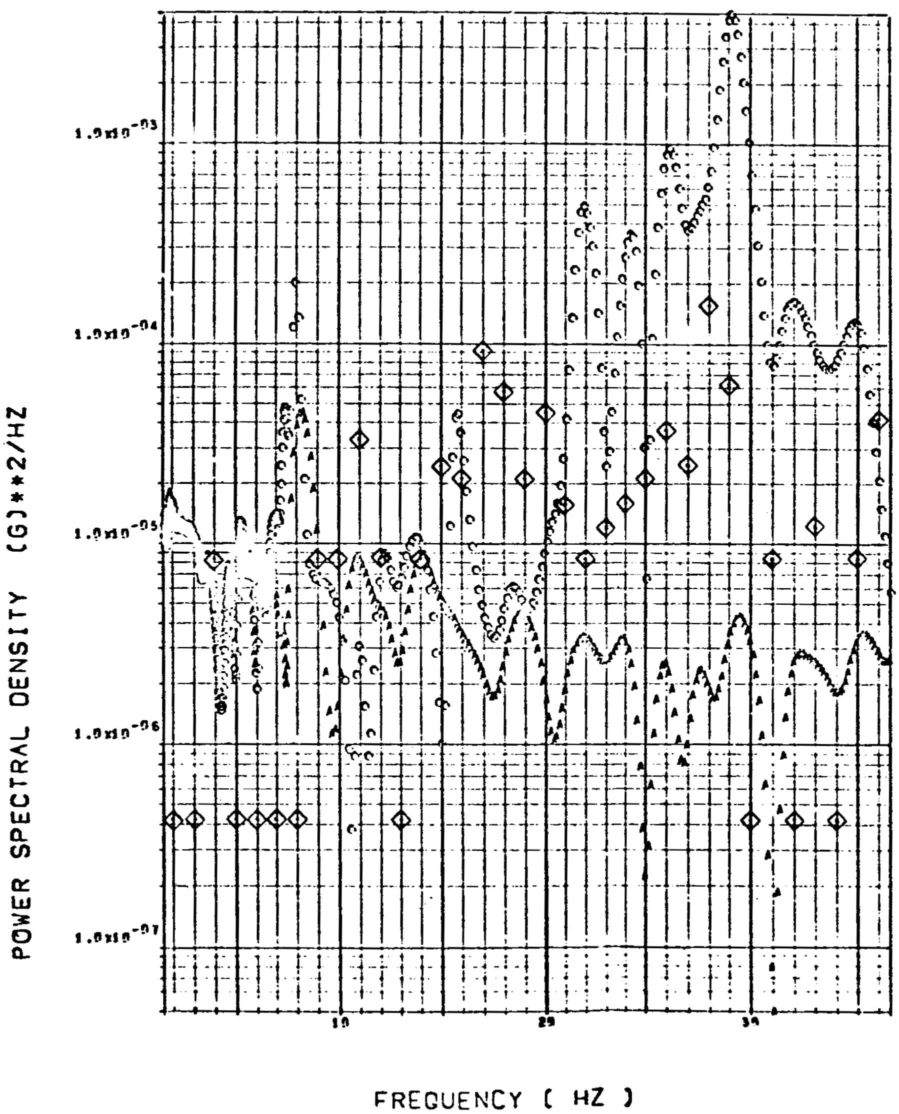

Figure 3.-(e) Pilot seat lateral accelerometer (continued)

◇ AF010 $\alpha_{FLT} = 11.8^{o}$

ANTI F-111A WING BUFFET RESPONSE. FLT 48. RUN 6
SWEEP=26 DEG. MACH=.7. ALT=7559 METERS. ALPHA= 12.8
PILOT STATION LATERAL ACCELEROMETER. FS = 255
SQUARE = 1 DOF A = 3 DOF CIRCLE = 18 DOF

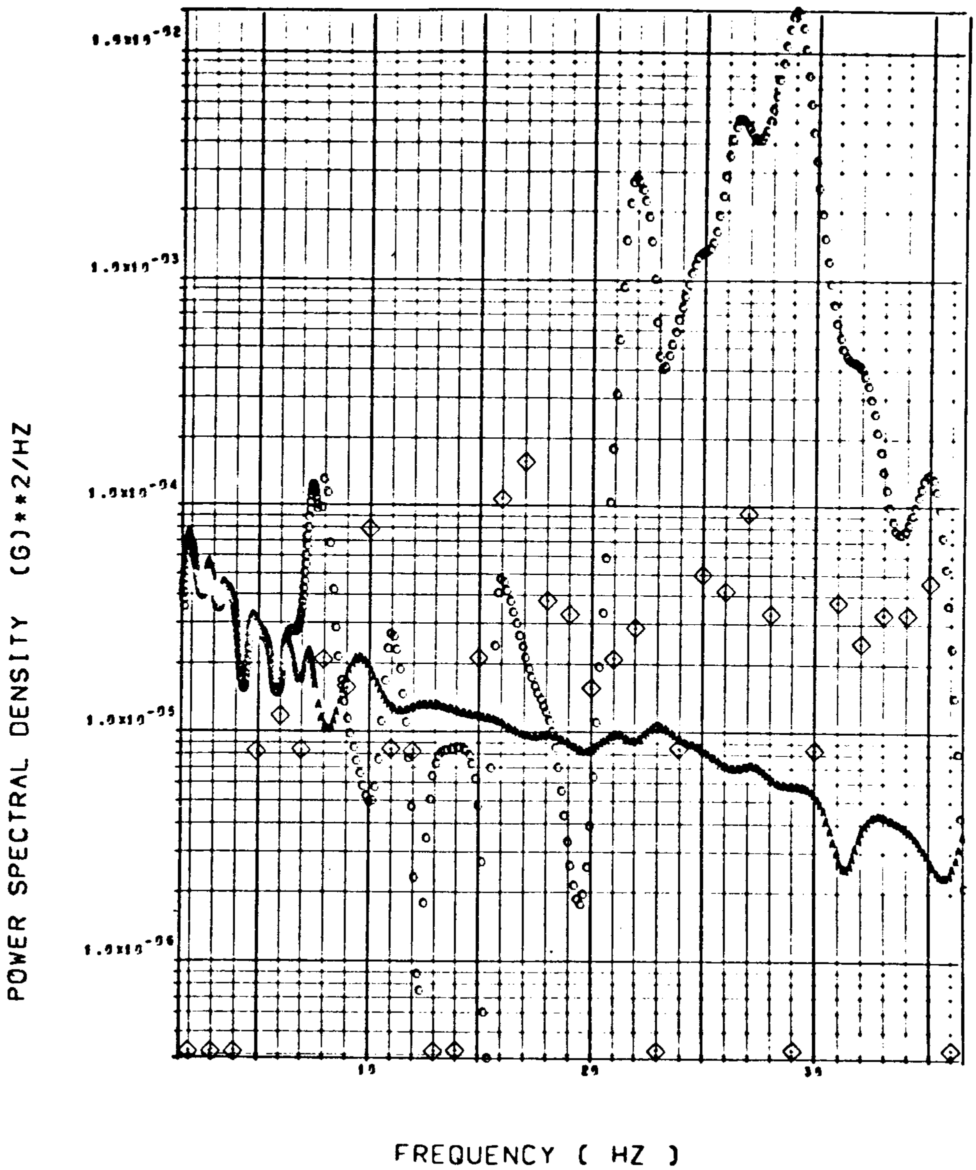

Figure 3.-(e) Pilot seat lateral accelerometer (continued)

◇ AF010 $\alpha_{FLT} = 14.6^{o}$

ANTI F-111A WING BUFFET RESPONSE. FLT 48. RUN 6
SWEEP=26 DEG. MACH=.7. ALT=7559 METERS. ALPHA= 17.1
PILOT STATION LATERAL ACCELEROMETER. FS = 255
SQUARE = 1 DOF A = 3 DOF CIRCLE = 18 DOF

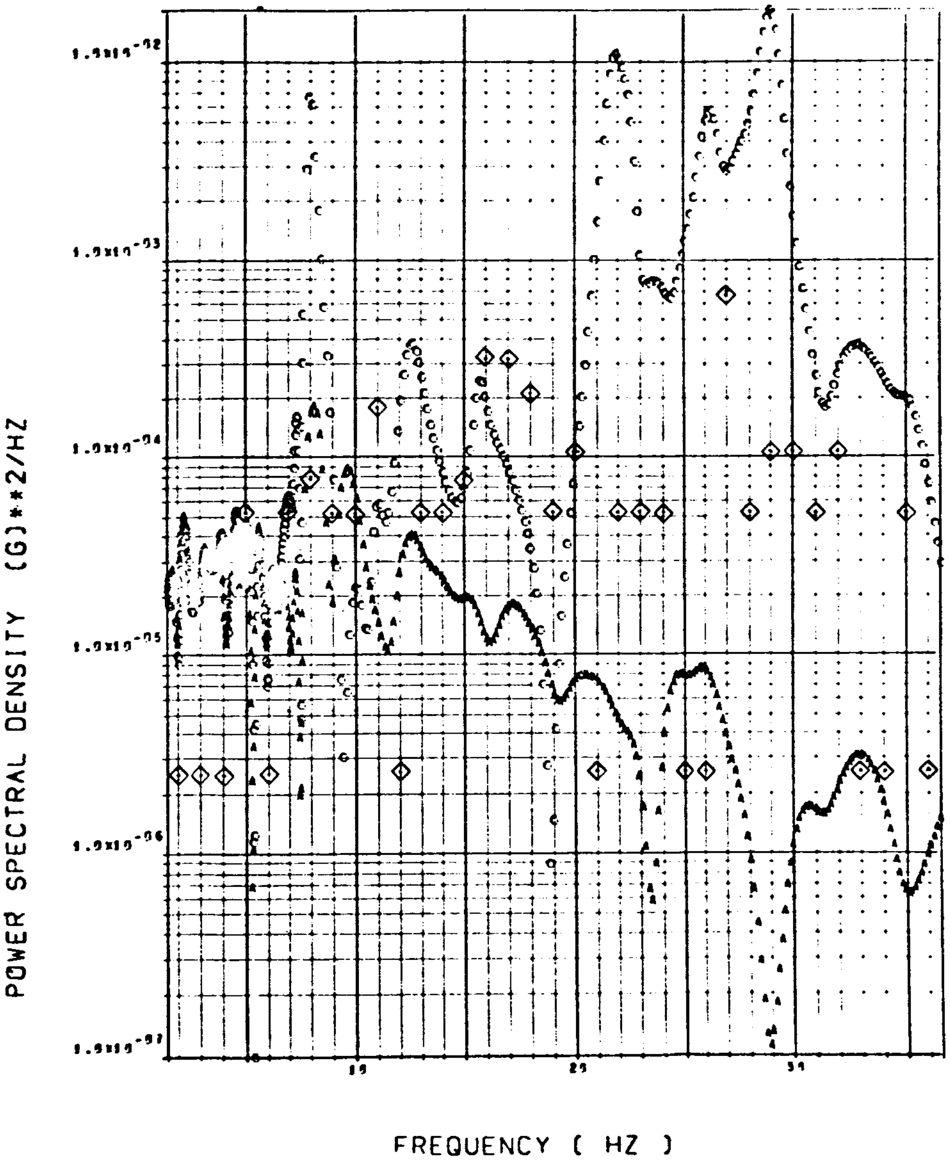

Figure 3.-(e) Pilot seat lateral accelerometer (continued)

△ SW123 $\alpha_{FLT} = 8.8^{o}$

F-111A WING BUFFET RESPONSE. FLT.43. RUN 6
SWEEP=26 DEG. MACH=.7. ALT=7559 METERS. ALPHA=9.6
WING SHEAR (N) AT SPAN STATION 75
CIRCLE = UPPER BOUNDS SQUARE = LOWER BOUNDS

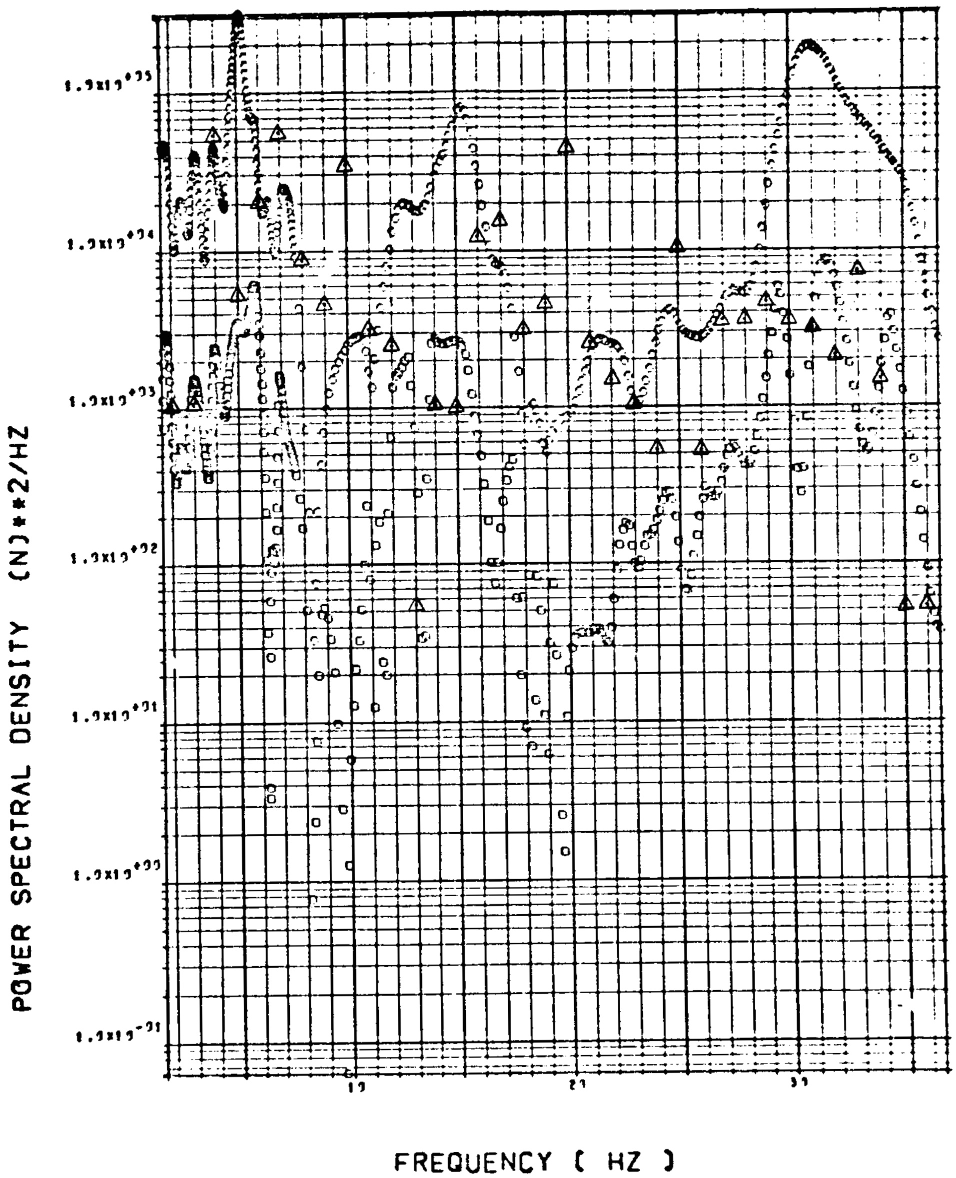

Figure 3.-(f) Wing shear

▲ SW123 $\alpha_{FLT} = 9.8^{o}$

F-111A WING BUFFET RESPONSE. FLT.48. RUN 6
SWEEP=26 DEG. MACH=.7. ALT=7559 METERS. ALPHA= 10.7
WING SHEAR (N) AT SPAN STATION 75
CIRCLE = UPPER BOUNDS SQUARE = LOWER BOUNDS

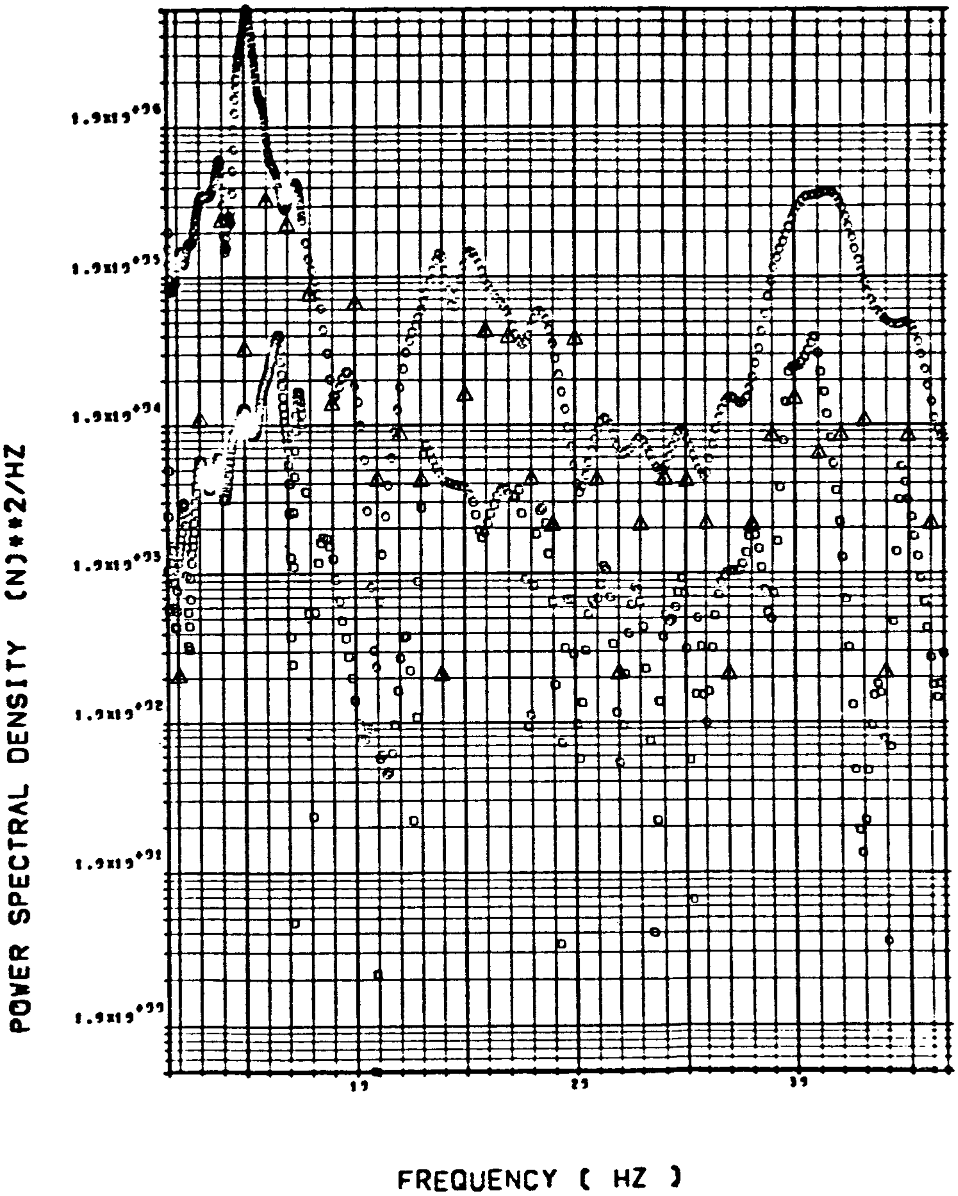

Figure 3.-(f) Wing shear (continued)

▲ SW123 $\alpha_{FLT} = 10.7^{o}$

F-111A WING BUFFET RESPONSE. FLT.48. RUN 6
SWEEP=26 DEG. MACH=.7. ALT=7559 METERS. ALPHA=11.8
WING SHEAR (N) AT SPAN STATION 75
CIRCLE = UPPER BOUNDS SQUARE = LOWER BOUNDS

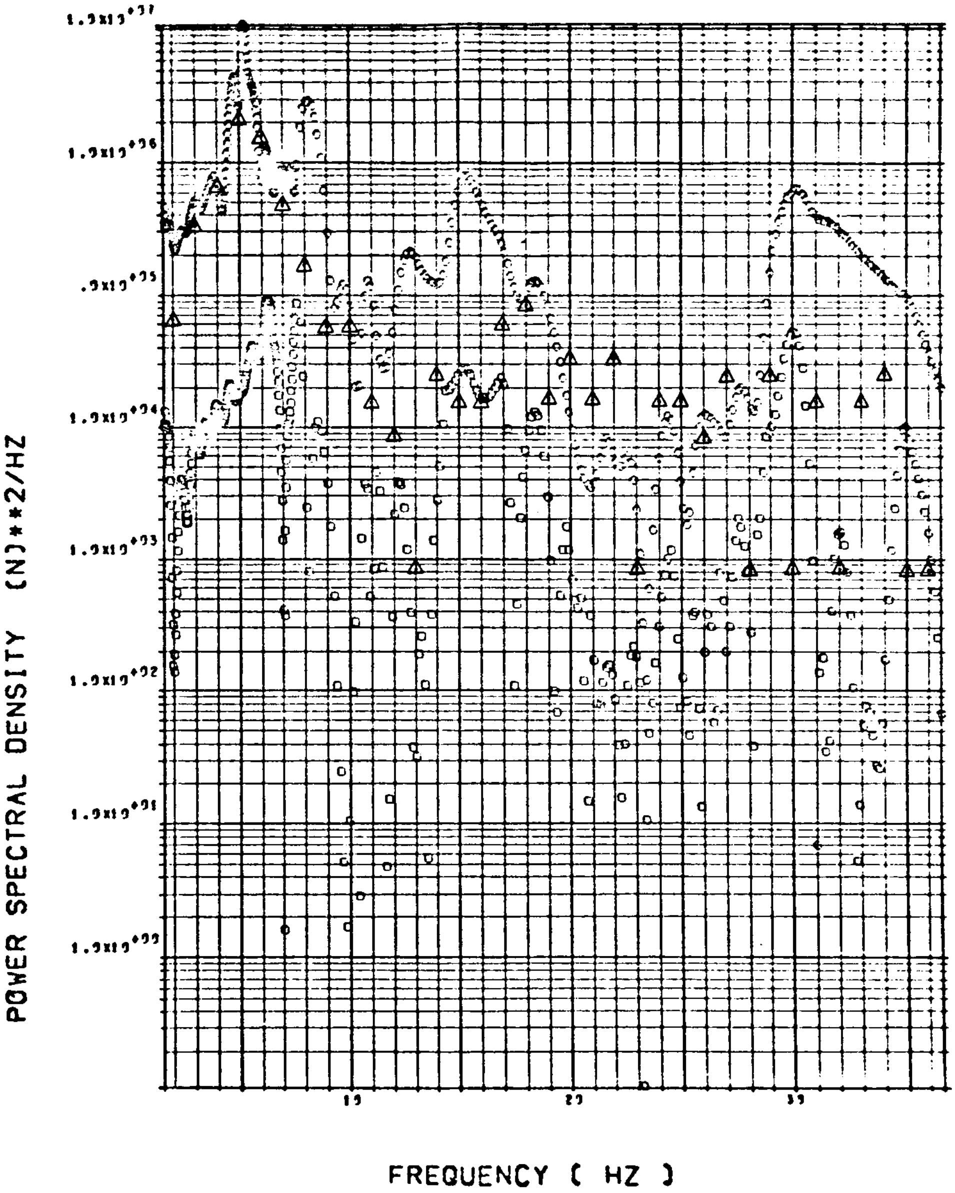

Figure 3.-(f) Wing shear (continued)

▲ SW123 $\alpha_{FLT} = 11.8^{\circ}$

F-111A WING BUFFET RESPONSE. FLT.48. RUN 6
SWEEP=26 DEG. MACH=.7. ALT=7559 METERS. ALPHA= 12.8
WING SHEAR (N) AT SPAN STATION 75
CIRCLE = UPPER BOUNDS SQUARE = LOWER BOUNDS

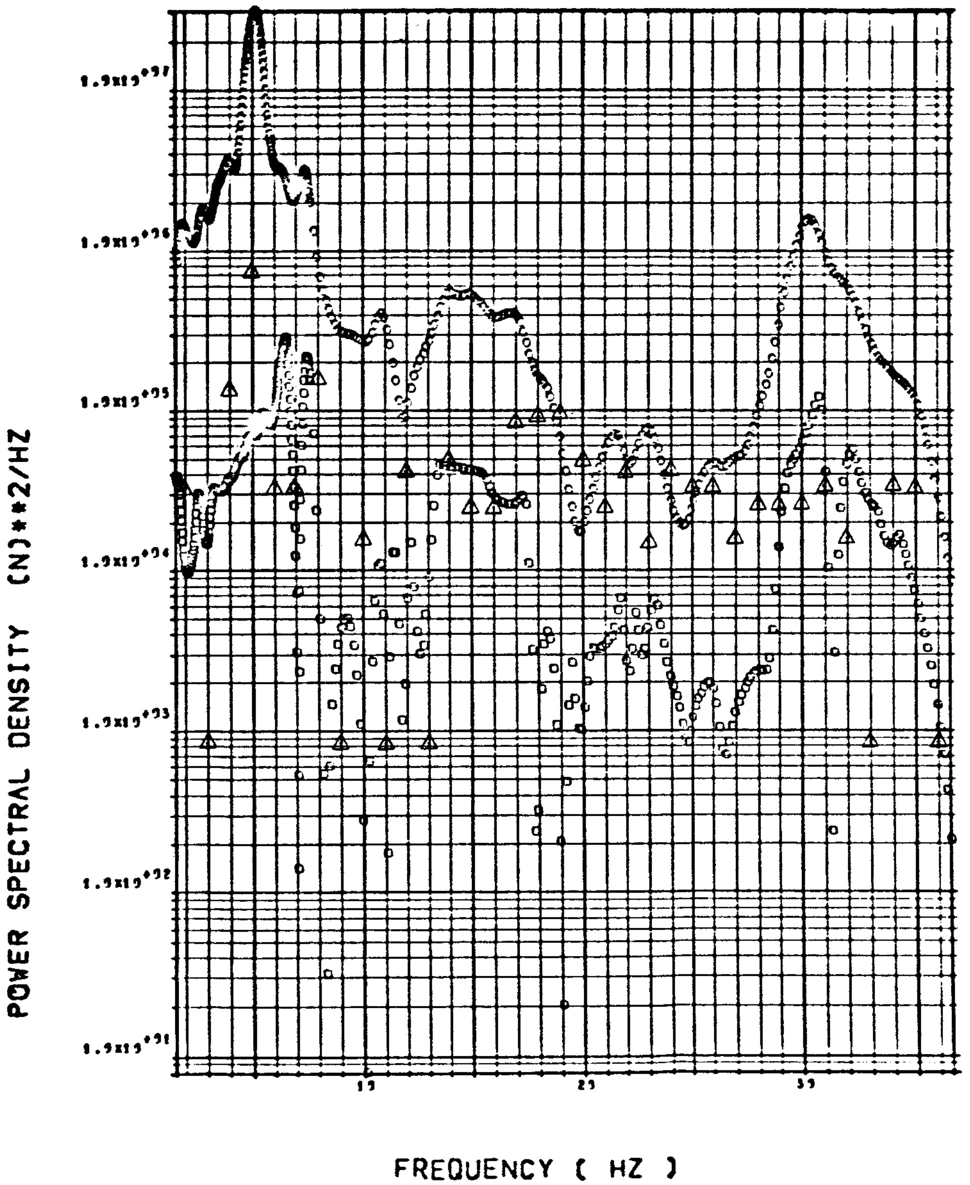

Figure 3.-(f) Wing shear (continued)

△ SW123 $\alpha_{FLT} = 14.6^{o}$

F-111A WING BUFFET RESPONSE, FLT.48, RUN 6
SWEEP=26 DEG, MACH=.7, ALT=7559 METERS, ALPHA=17.1
WING SHEAR (N) AT SPAN STATION 75
CIRCLE = UPPER BOUNDS SQUARE = LOWER BOUNDS

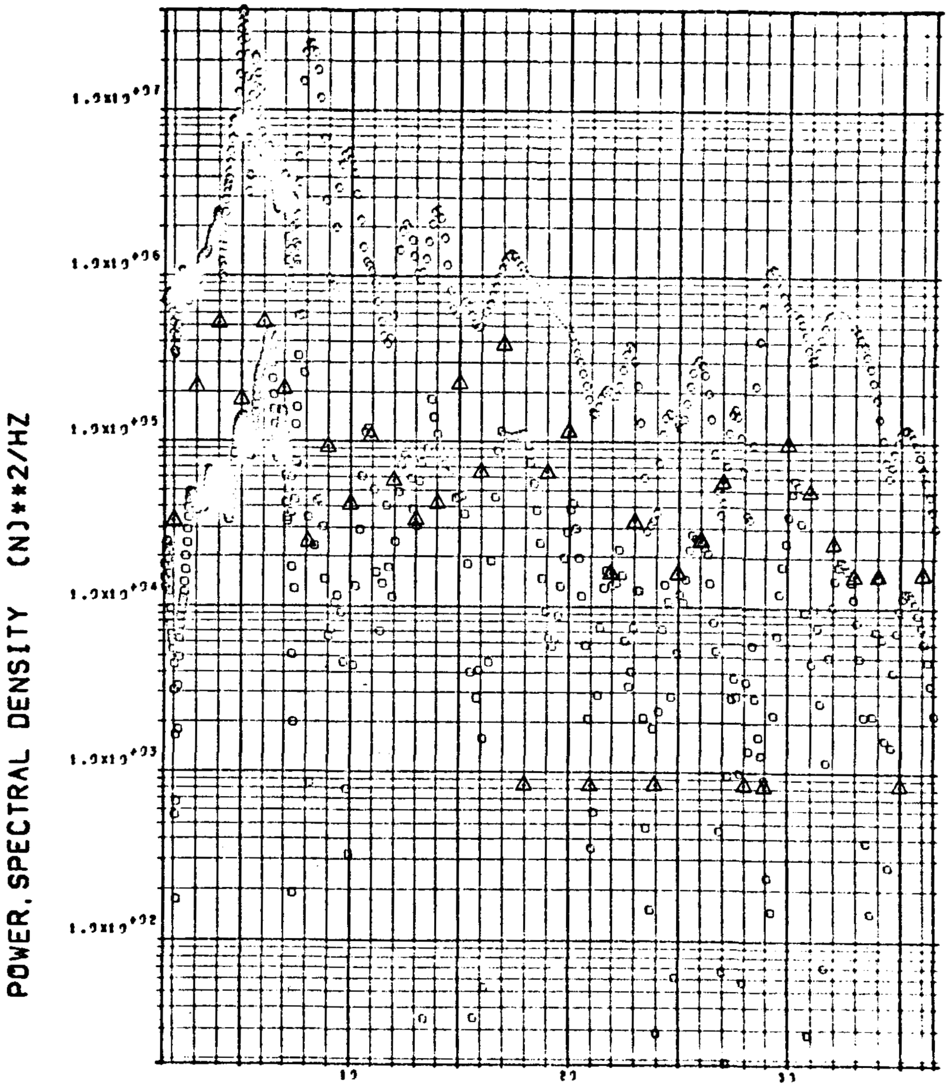

Figure 3.-(f) Wing shear (continued)

Δ SW124 $\alpha_{FLT} = 8.8^{o}$

F-111A WING BUFFET RESPONSE. FLT.48. RUN 6
SWEEP=26 DEG. MACH=.7. ALT=7559 METERS. ALPHA=9.6
WING BENDING MOMENT (M-N) AT SPAN STATION 75
CIRCLE = UPPER BOUNDS SQUARE = LOWER BOUNDS

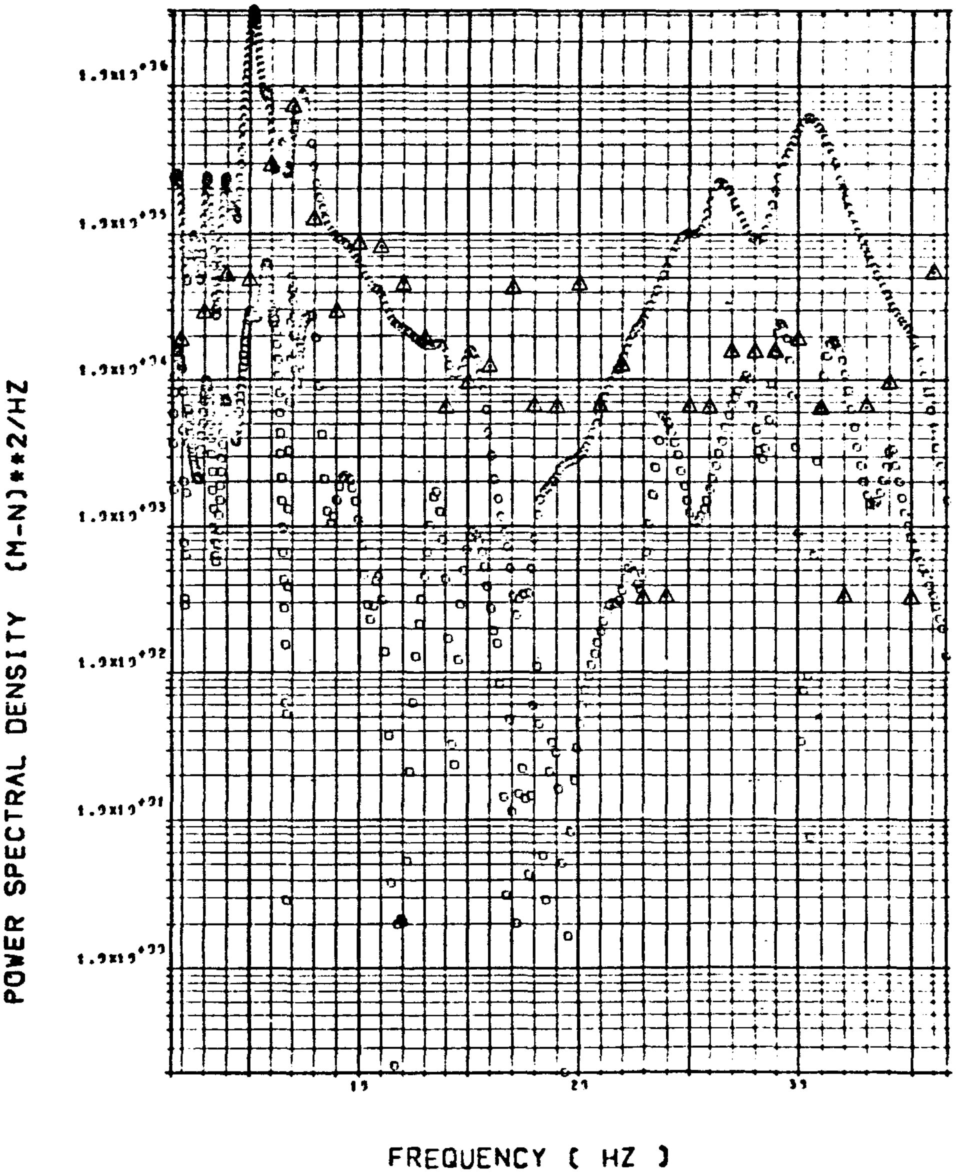

Figure 3.-(g) Wing bending moment

△ SW124 $\alpha_{FLT} = 9.8^{\circ}$

F-111A WING BUFFET RESPONSE. FLT.48. RUN 6
SWEEP=26 DEG. MACH=.7. ALT=7559 METERS. ALPHA=10.7
WING BENDING MOMENT (M-N) AT SPAN STATION 75
CIRCLE = UPPER BOUNDS SQUARE = LOWER BOUNDS

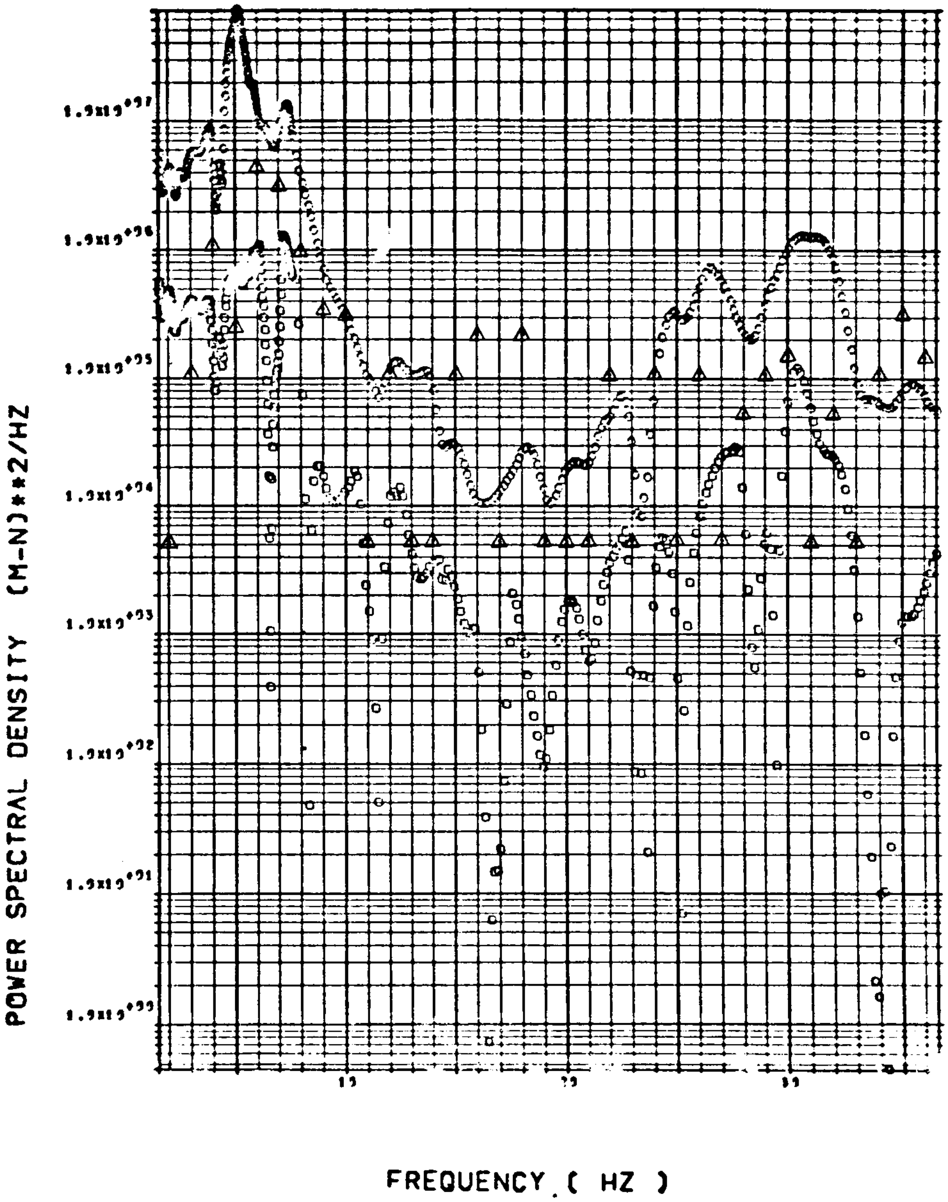

Figure 3.-(g) Wing bending moment (continued)

▲ SW124 $\alpha_{FLT} = 10.7^{\circ}$

F-111A WING BUFFET RESPONSE. FLT.48. RUN 6
SWEEP=26 DEG. MACH=.7. ALT=7559 METERS. ALPHA= 11.8
WING BENDING MOMENT (M-N) AT SPAN STATION 75
CIRCLE = UPPER BOUNDS SQUARE = LOWER BOUNDS

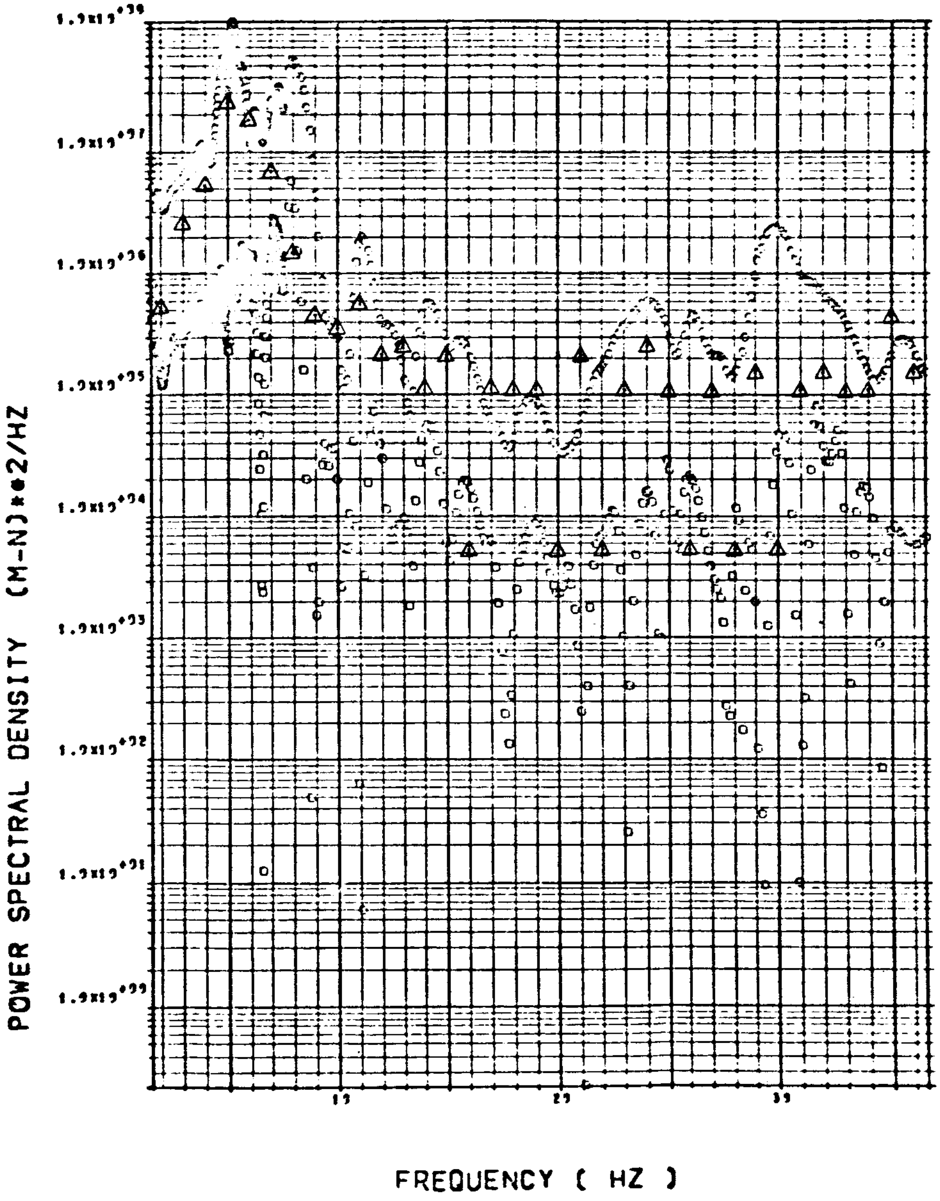

Figure 3.-(g) Wing bending moment (continued)

△ SW124 $\alpha_{FLT} = 11.8^{o}$

F-111A WING BUFFET RESPONSE. FLT.48. RUN 6
SWEEP=26 DEG. MACH=.7. ALT=7559 METERS. ALPHA= 12.8
WING BENDING MOMENT (M-N) AT SPAN STATION 75
CIRCLE = UPPER BOUNDS SQUARE = LOWER BOUNDS

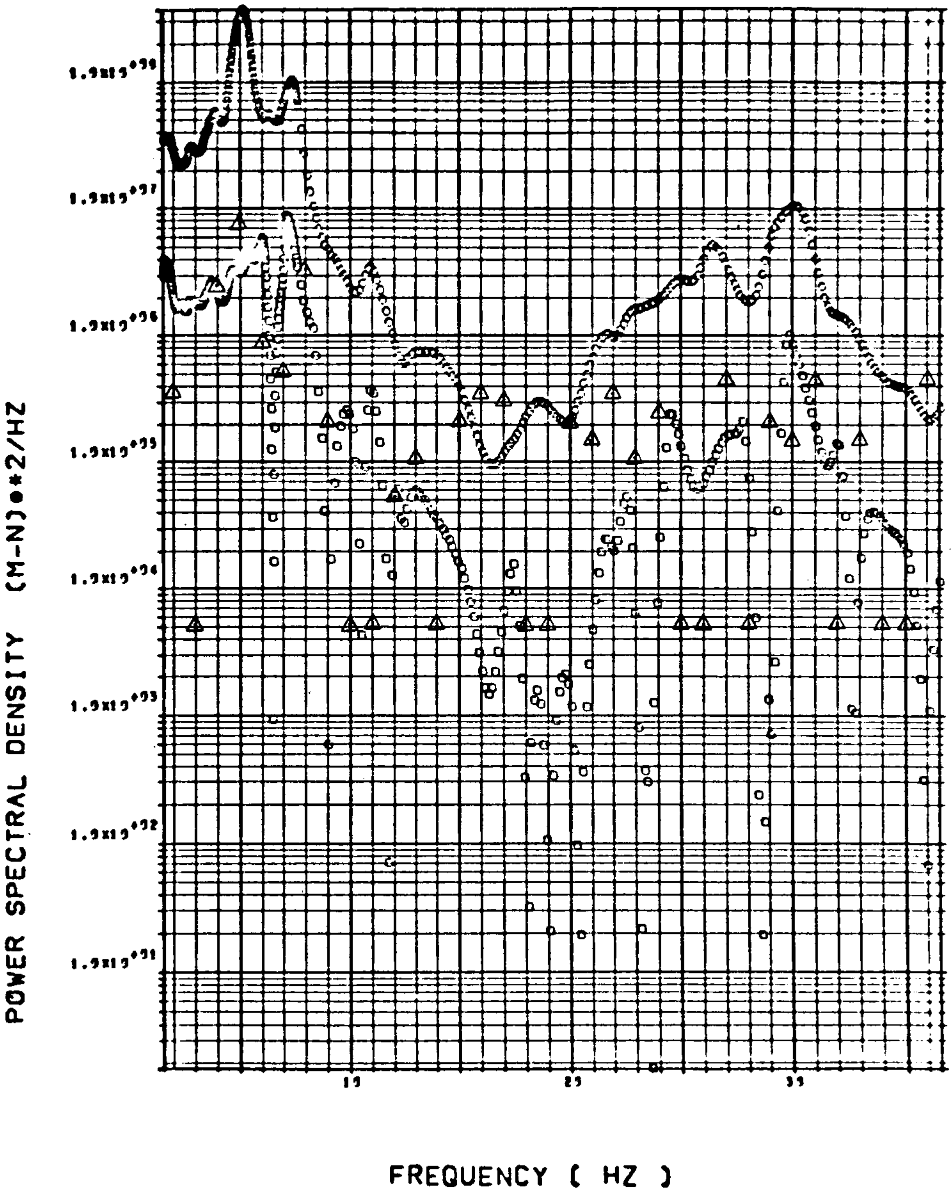

Figure 3.-(g) Wing bending moment (continued)

▲ SW124 $\alpha_{FLT} = 14.6^{\circ}$

F-111A WING BUFFET RESPONSE, FLT.40, RUN 6
SWEEP=26 DEG.-MACH=.7, ALT=7550 METERS, ALPHA= 17.1
WING BENDING MOMENT (M-N) AT SPAN STATION 75
CIRCLE = UPPER BOUNDS SQUARE = LOWER BOUNDS

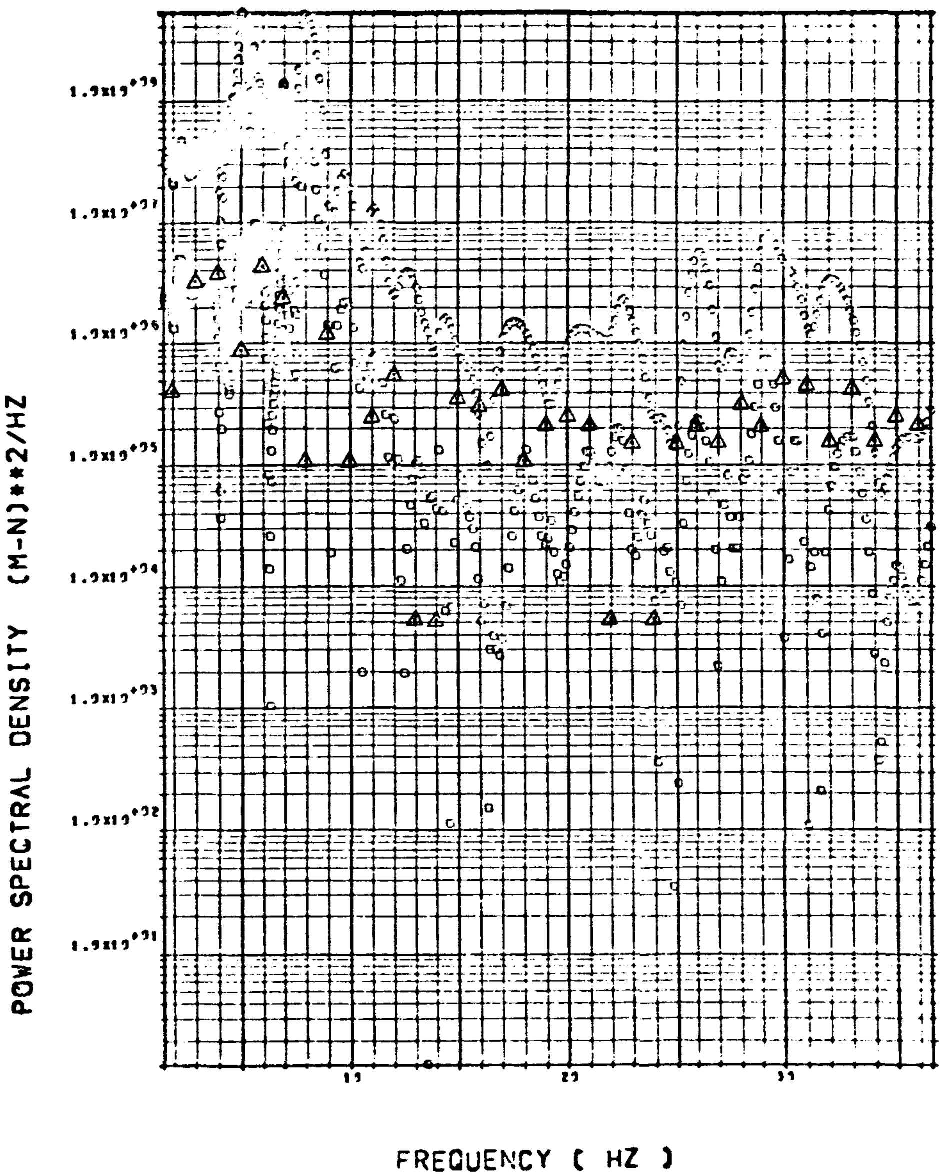

Figure 3.-(g) Wing bending moment (continued)

△ SW125 $\alpha_{FLT} = 8.8^{\circ}$

F-111A WING BUFFET RESPONSE. FLT.48. RUN 6
SWEEP=26 DEG. MACH=.7. ALT=7553 METERS. ALPHA= 9.6
WING TORQUE (M-N) AT SPAN STATION 75
CIRCLE = UPPER BOUNDS SQUARE = LOWER BOUNDS

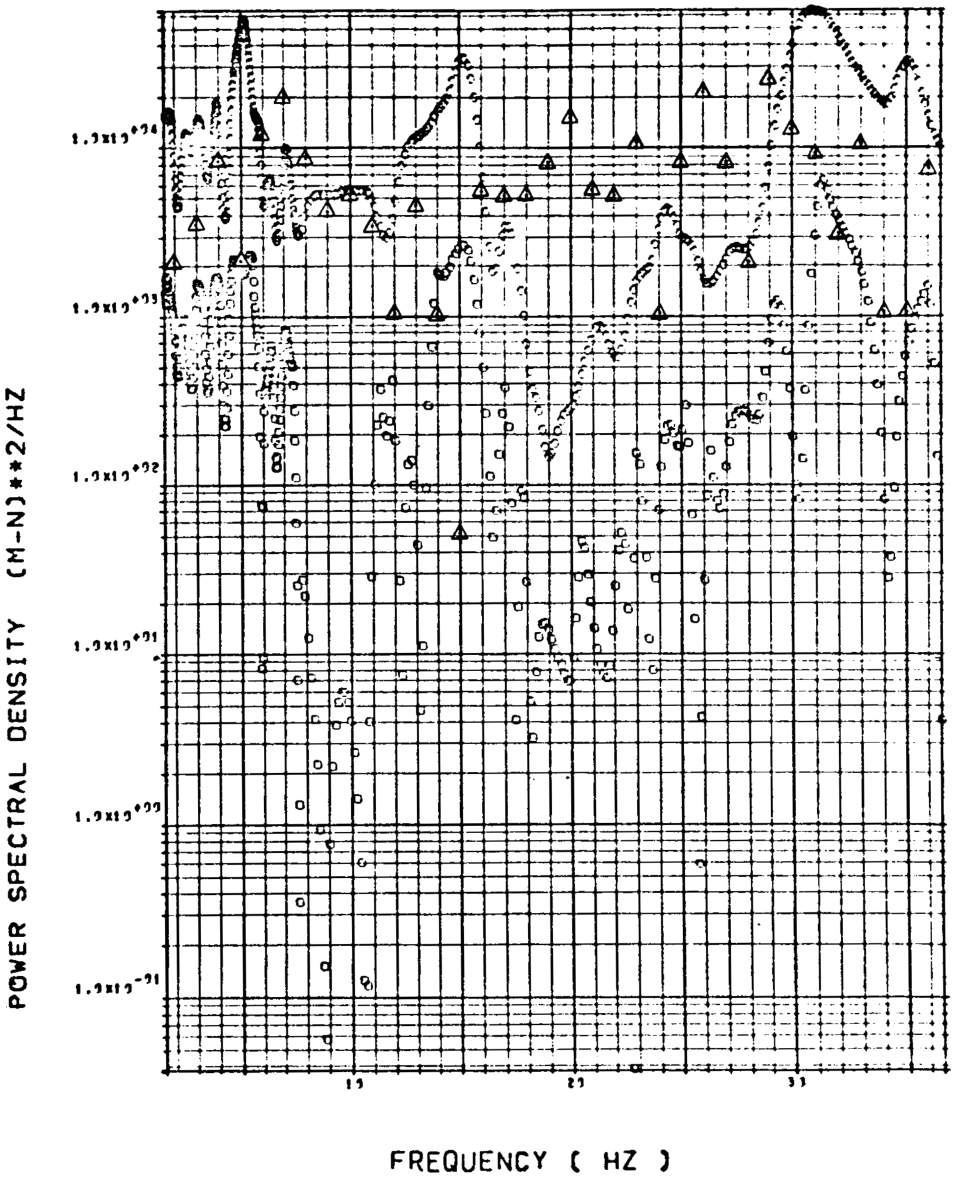

Figure 3.-(h) Wing torsion

▲ SW125 $\alpha_{FLT} = 9.8^{o}$

F-111A WING BUFFET RESPONSE. FLT.48. RUN 6
SWEEP=26 DEG. MACH=.7. ALT=7559 METERS. ALPHA= 10.7
WING TORQUE (M-N) AT SPAN STATION 75
CIRCLE = UPPER BOUNDS SQUARE = LOWER BOUNDS

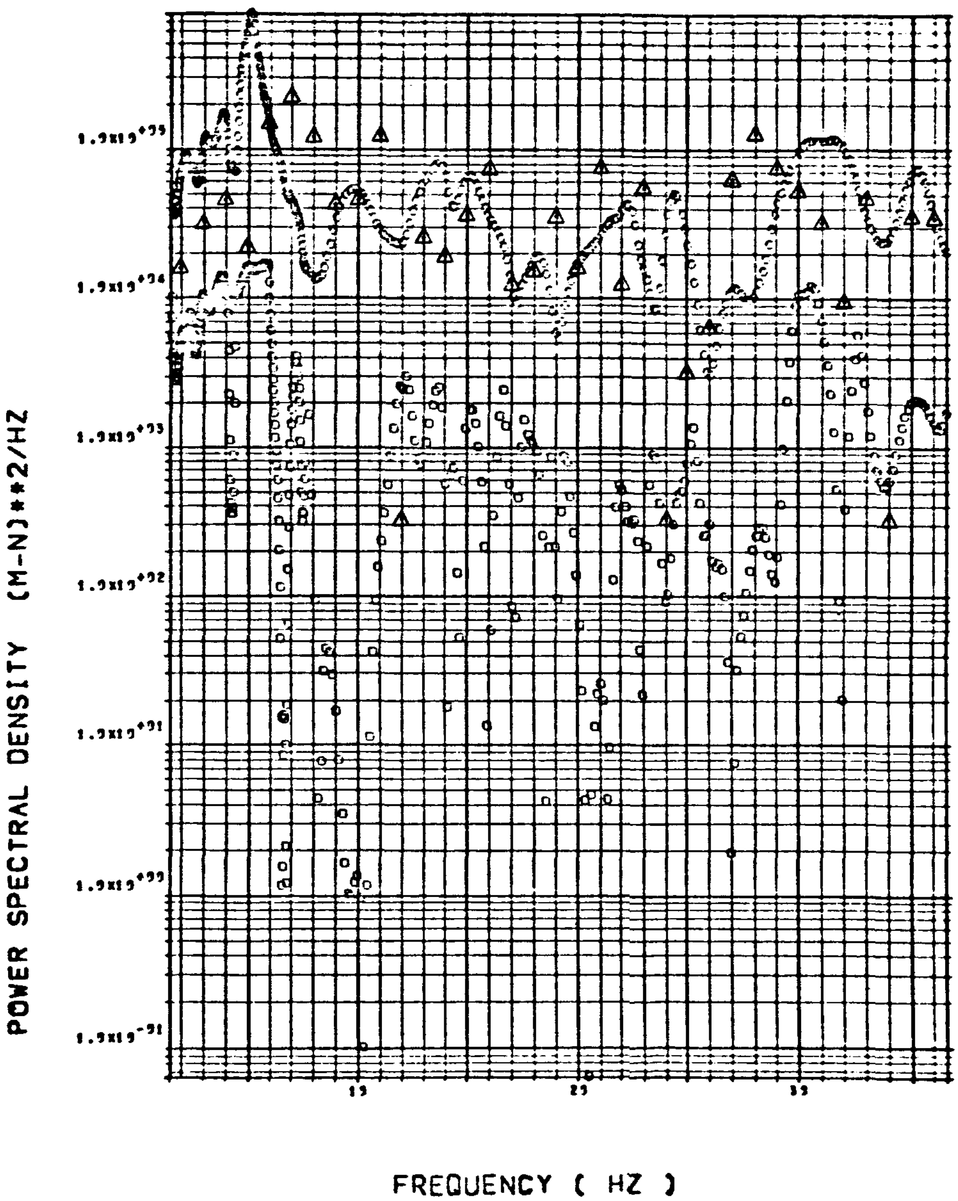

Figure 3.-(h) Wing torsion (continued)

△ SW125 $\alpha_{FLT} = 10.7^{\circ}$

F-111A WING BUFFET RESPONSE. FLT.48. RUN 6
SWEEP=26 DEG. MACH=.7. ALT=7559 METERS. ALPHA=11.8
WING TORQUE (M-N) AT SPAN STATION 75
CIRCLE = UPPER BOUNDS SQUARE = LOWER BOUNDS

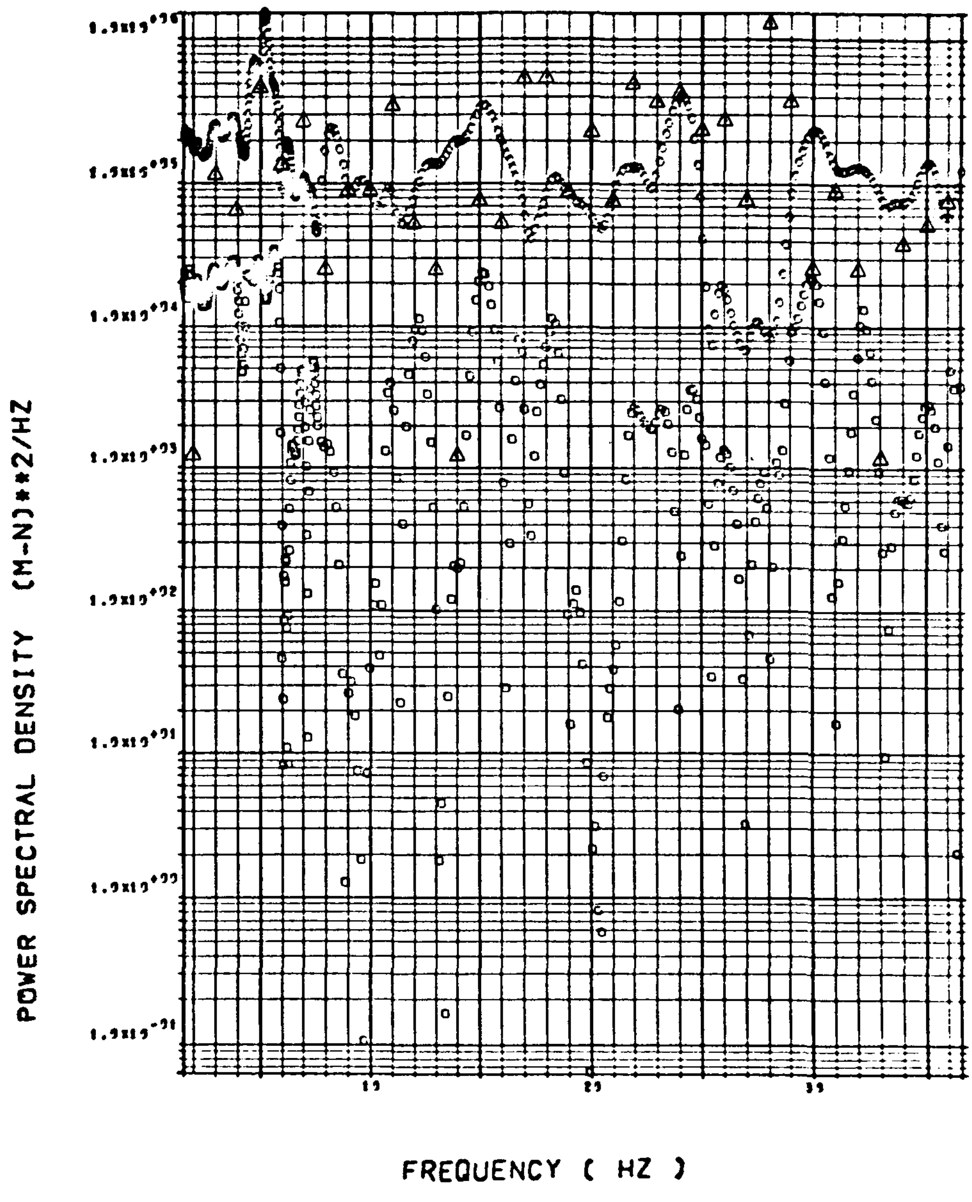

Figure 3.-(h) Wing torsion (continued)

▲ SW125 $\alpha_{FLT} = 11.8^{o}$

F-111A WING BUFFET RESPONSE. FLT.48. RUN 6
SWEEP=26 DEG. MACH=.7. ALT=7559 METERS. ALPHA=12.8
WING TORQUE (M-N) AT SPAN STATION 75
CIRCLE = UPPER BOUNDS SQUARE = LOWER BOUNDS

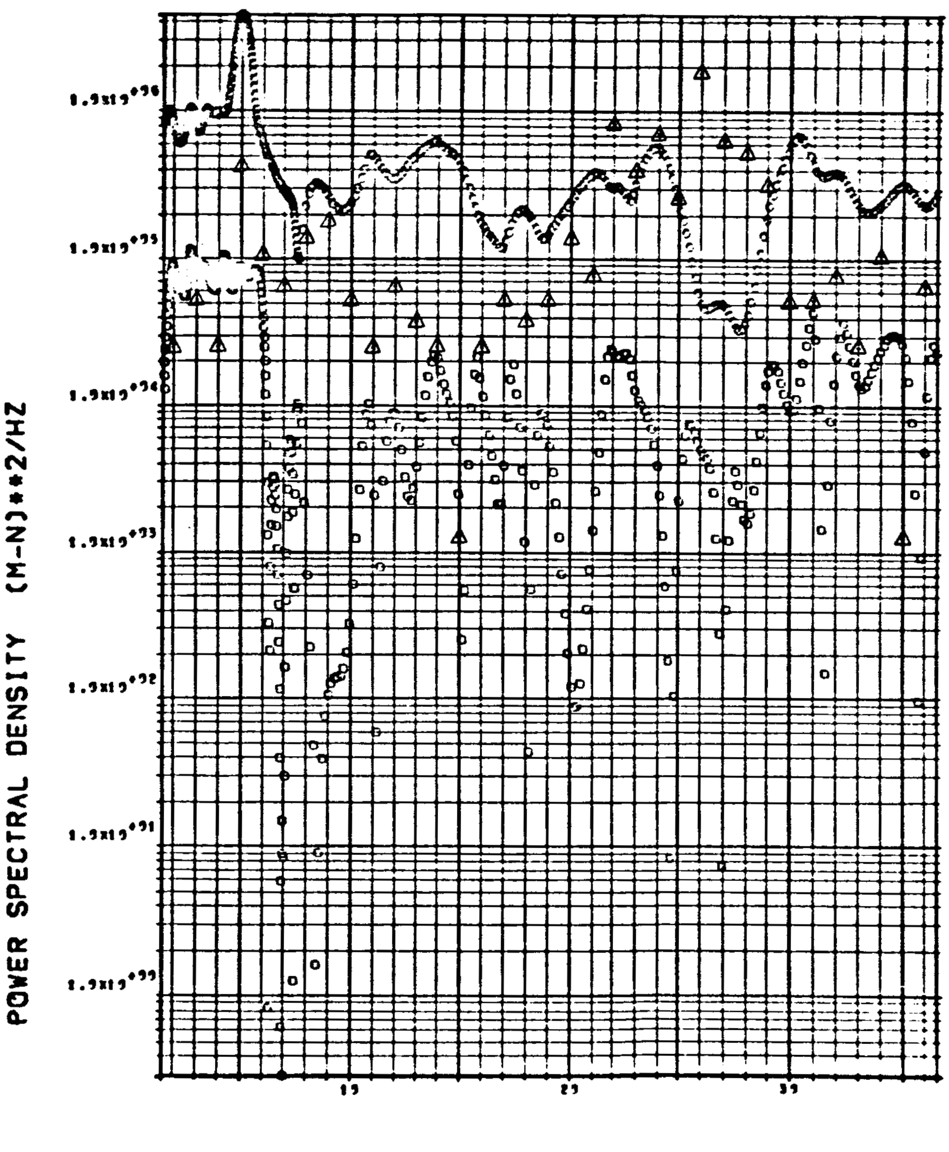

Figure 3.-(h) Wing torsion (continued)

Δ SW125

$\alpha_{FLT} = 14.6^{\circ}$

F-111A WING BUFFET RESPONSE, FLT.43, RUN 6
SWEEP=26 DEG, MACH=.7, ALT=7559 METERS, ALPHA=17.1
WING TORQUE (M-N) AT SPAN STATION 75
CIRCLE = UPPER BOUNDS   SQUARE = LOWER BOUNDS

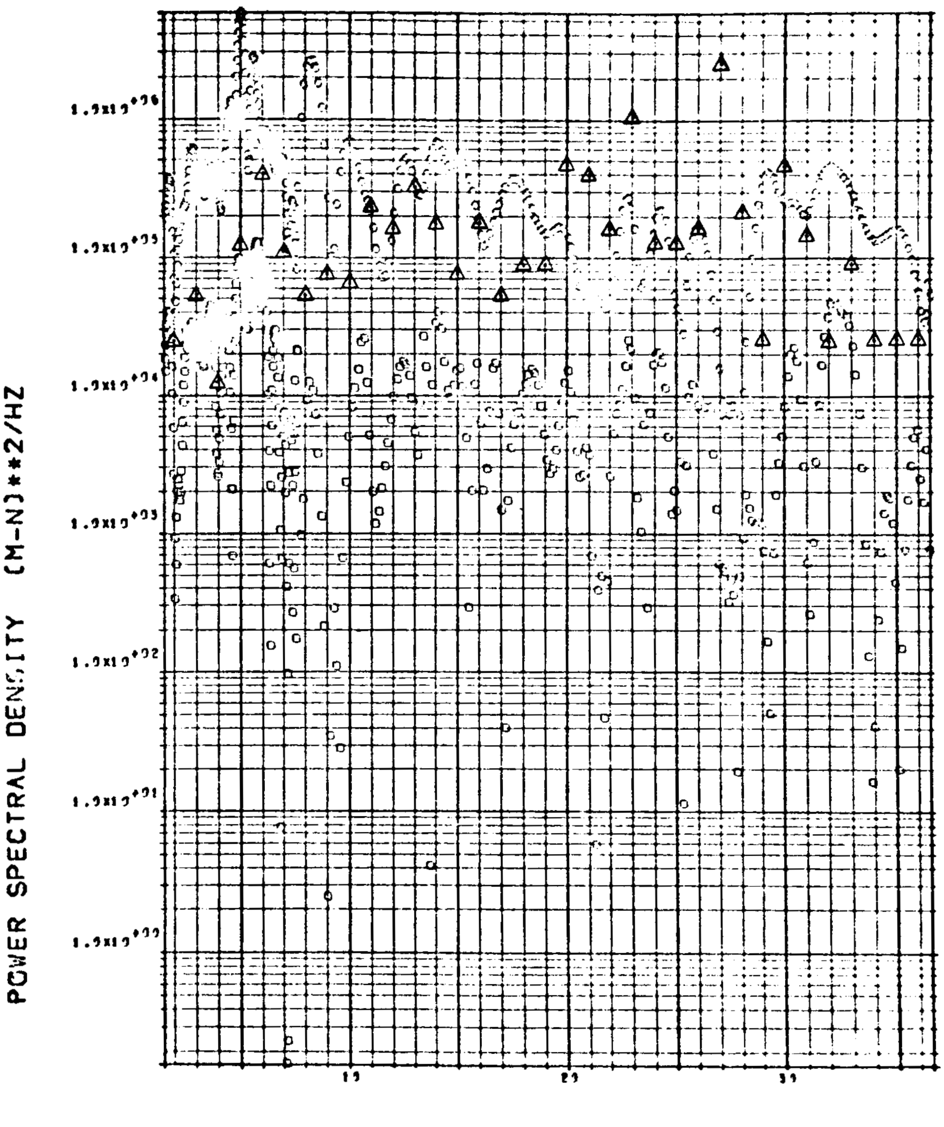

Figure 3.-(h) Wing torsion (continued)

▲ ST077 ◇ ST072 $\alpha_{FLT} = 8.8^{\circ}$

F-111A WING BUFFET RESPONSE, FLT.48, RUN 6
SWEEP=26 DEG. MACH=.7, ALT=7559 METERS. ALPHA= 9.6
H.T. PIVOT SHEAR (N)
CIRCLE = UPPER BOUNDS SQUARE = LOWER BOUNDS

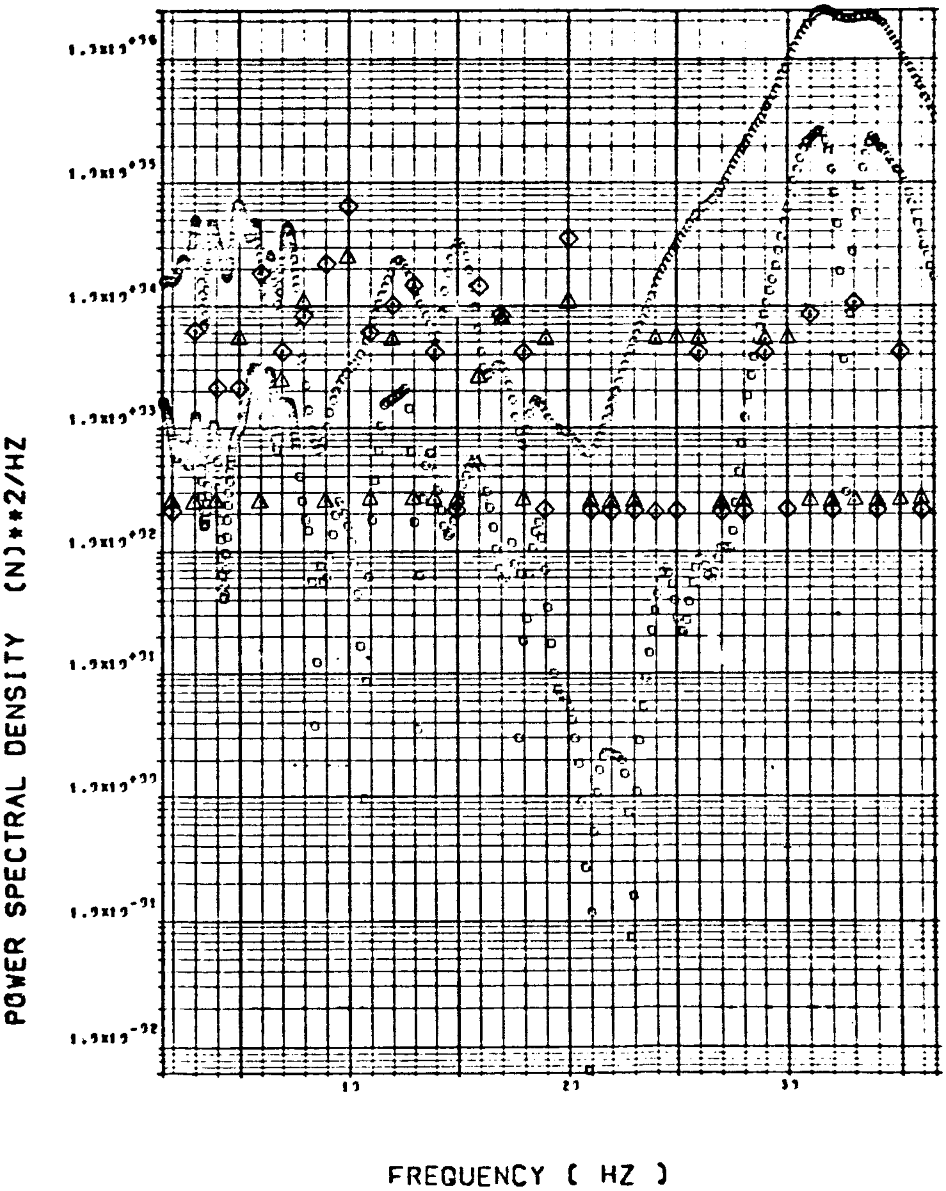

Figure 3.-(i) Horizontal tail shear

△ ST077 ◇ ST072 $\alpha_{FLT} = 9.8^{o}$

F-111A WING BUFFET RESPONSE. FLT.48. RUN 6
SWEEP=26 DEG. MACH=.7. ALT=7553 METERS. ALPHA=10.7
H.T. PIVOT SHEAR (N)
CIRCLE = UPPER BOUNDS SQUARE = LOWER BOUNDS

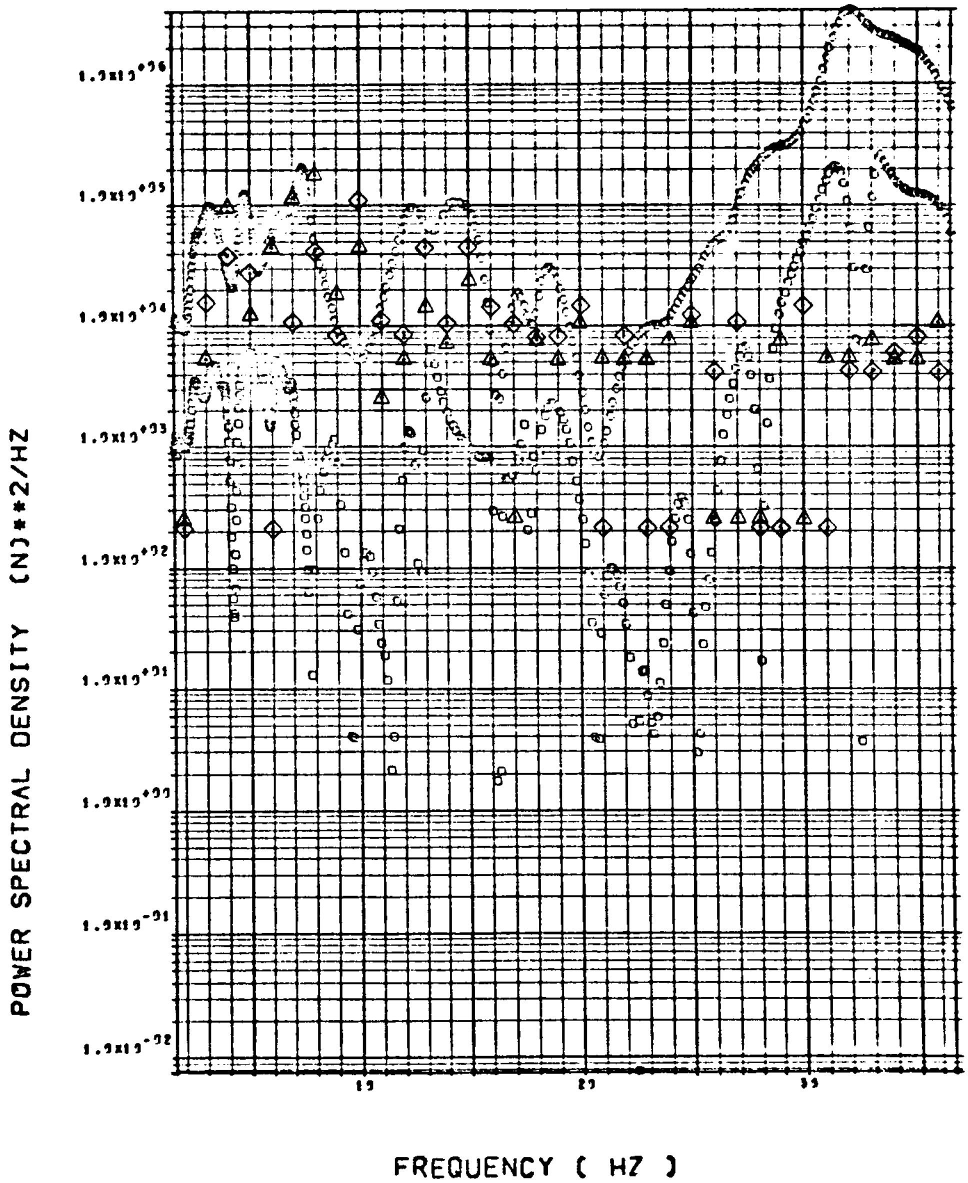

Figure 3.-(i) Horizontal tail shear (continued)

△ ST077 ◇ ST072 $\alpha_{FLT} = 10.7^{\circ}$

F-111A WING BUFFET RESPONSE. FLT.48. RUN 6
SWEEP=26 DEG. MACH=.7. ALT=7559 METERS. ALPHA= 11.8
H.T. PIVOT SHEAR (N)
CIRCLE = UPPER BOUNDS SQUARE = LOWER BOUNDS

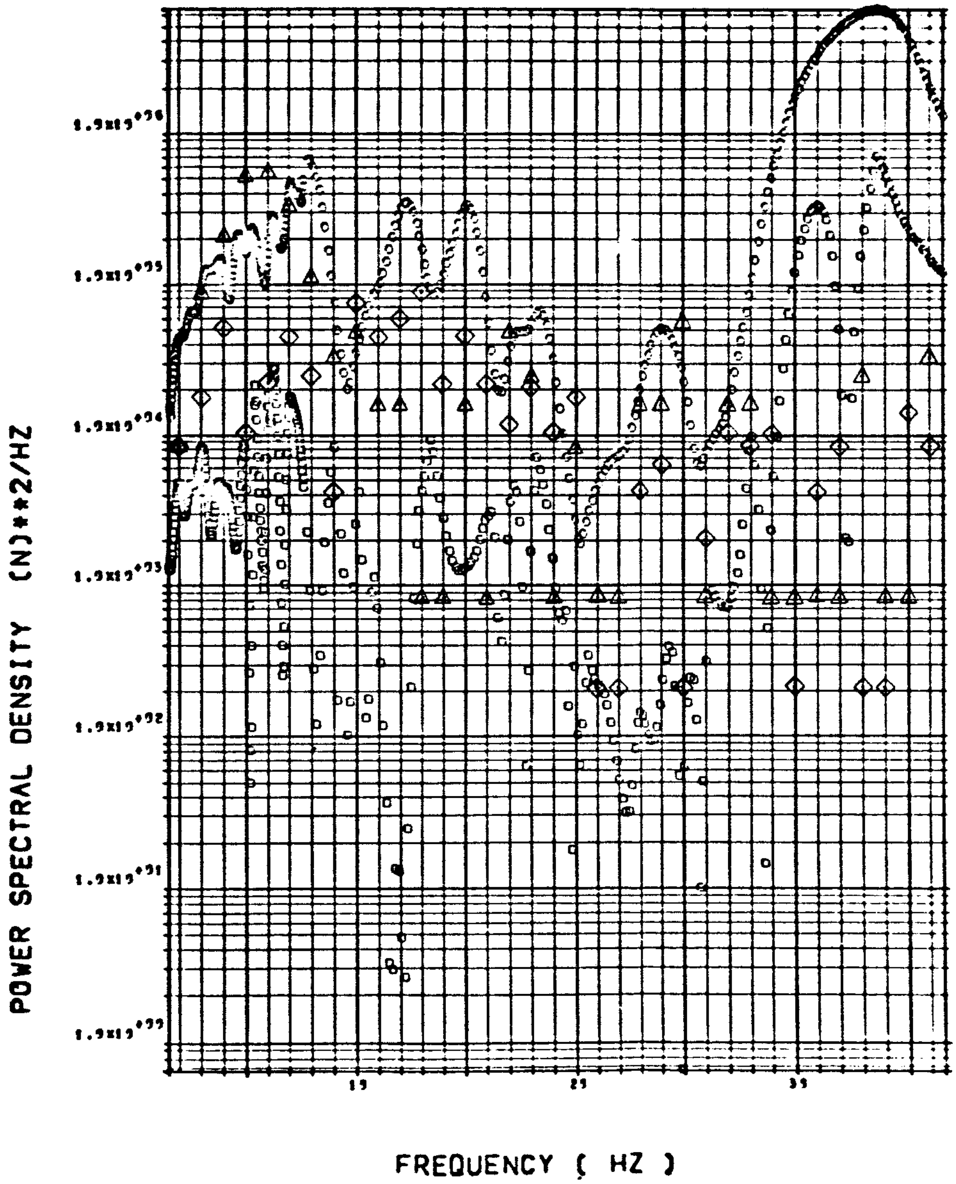

Figure 3.-(i) Horizontal tail shear (continued)

△ ST077 ◇ ST072 $\alpha_{FLT} = 11.8^{\circ}$

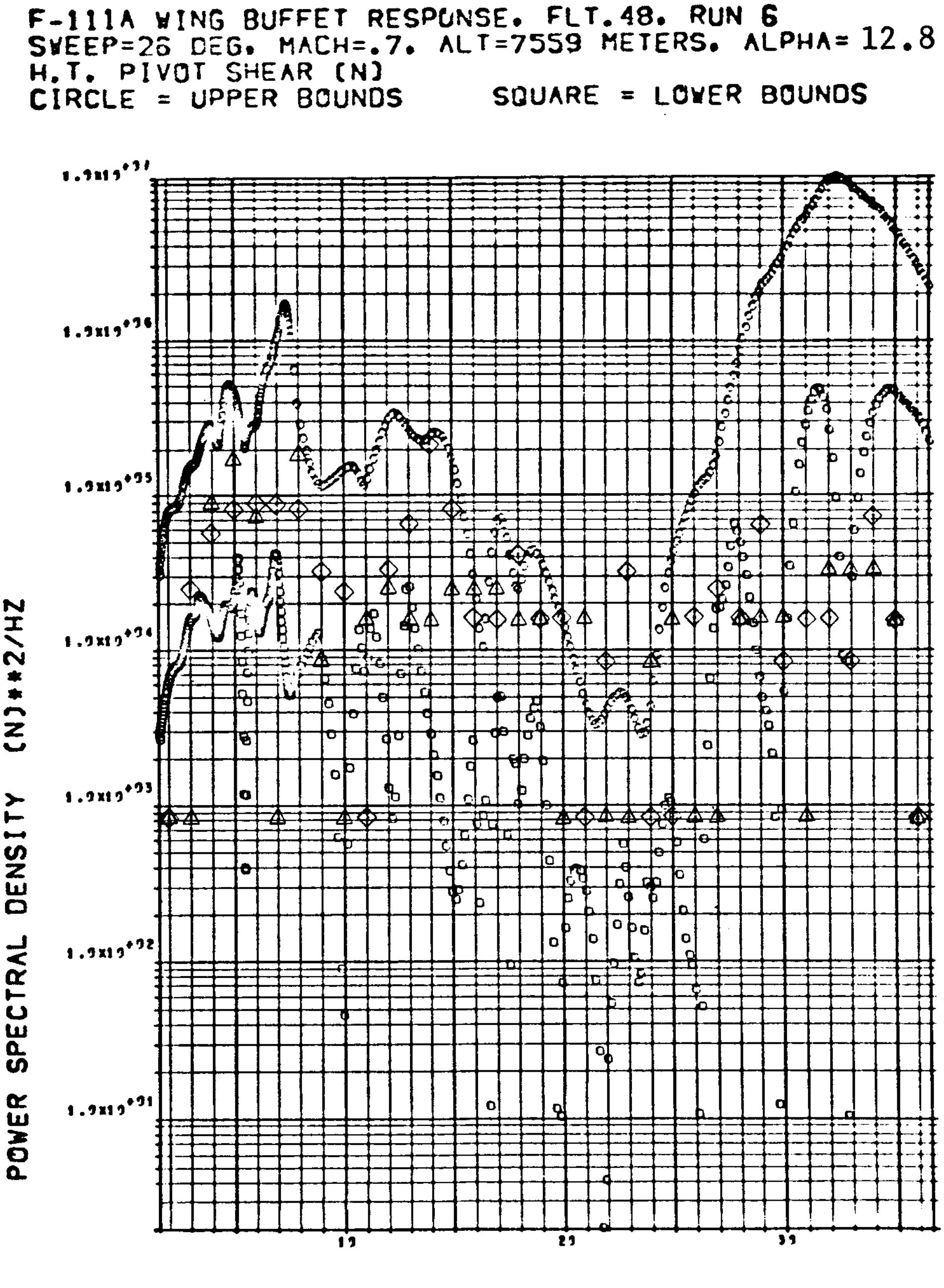

Figure 3.-(i) Horizontal tail shear (continued)

△ ST077 ◇ ST072 $\alpha_{FLT} = 14.6^{o}$

F-111A WING BUFFET RESPONSE, FLT.48, RUN 6
SWEEP=26 DEG, MACH=.7, ALT=7559 METERS, ALPHA= 17.1
H.T. PIVOT SHEAR (N)
CIRCLE = UPPER BOUNDS SQUARE = LOWER BOUNDS

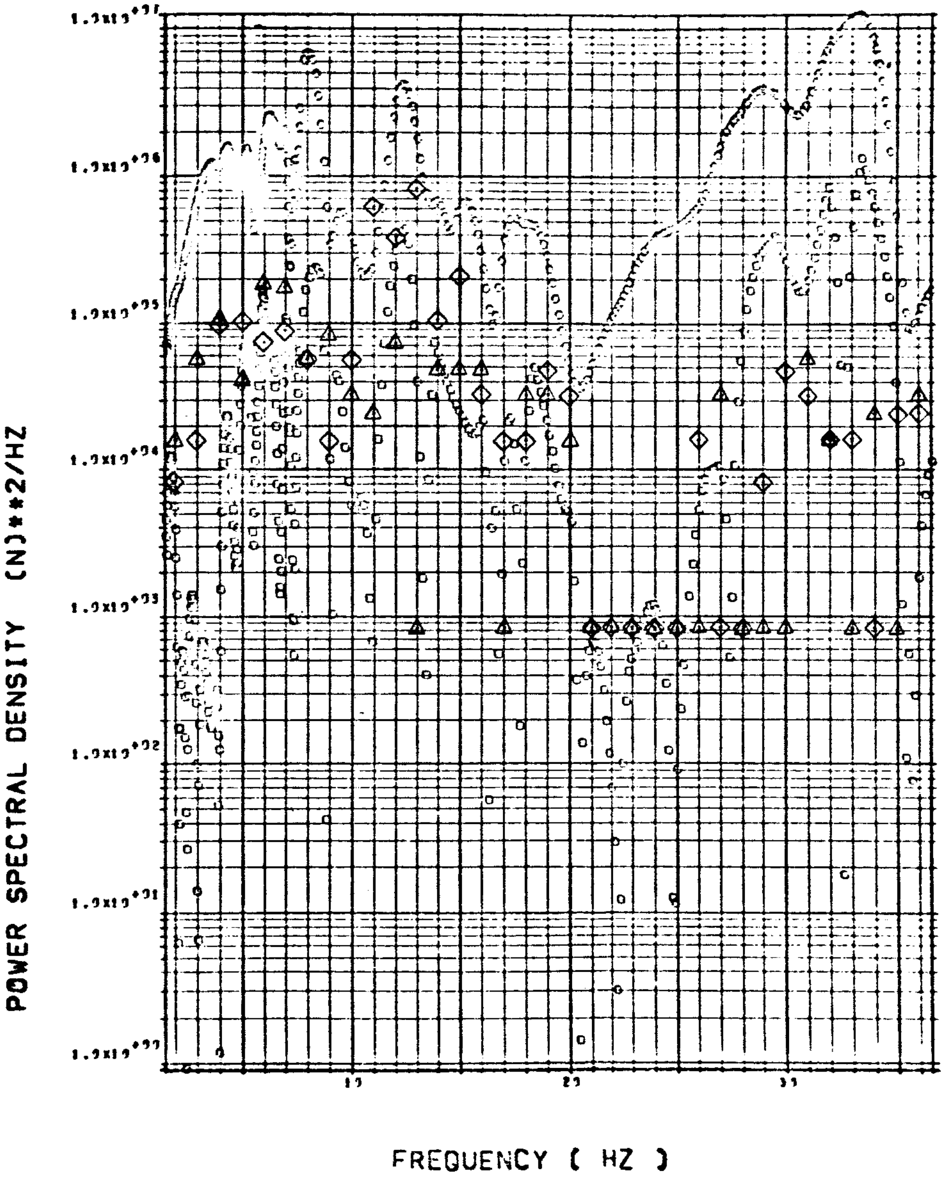

Figure 3.-(i) Horizontal tail shear (continued)

Δ ST078 ◇ ST073 $\alpha_{FLT} = 8.8^{o}$

F-111A WING BUFFET RESPONSE, FLT.48, RUN 6
SWEEP=26 DEG, MACH=.7, ALT=7559 METERS, ALPHA= 9.6
H.T. PIVOT BENDING MOMENT (M-N)
CIRCLE = UPPER BOUNDS SQUARE = LOWER BOUNDS

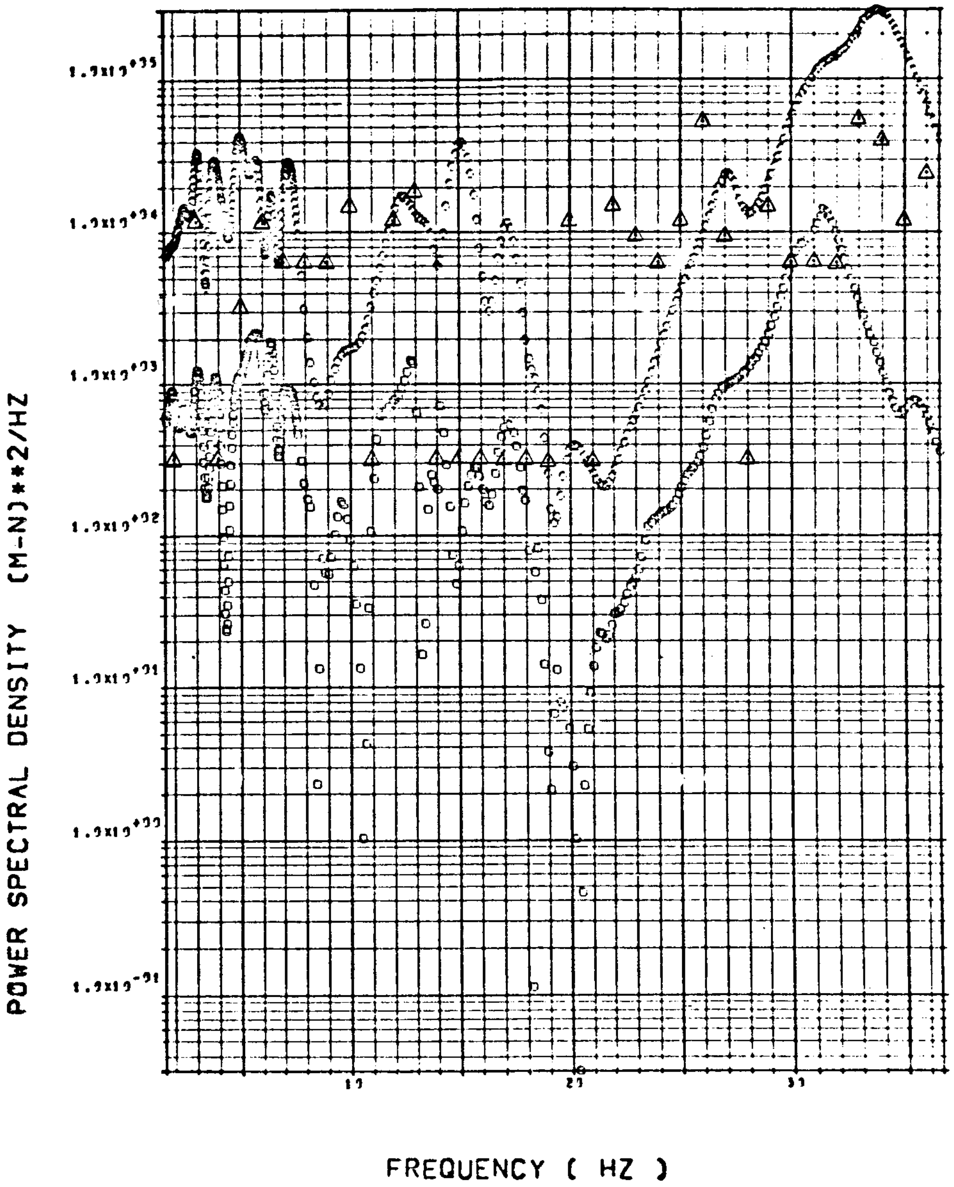

Figure 3.-(j) Horizontal tail bending moment

△ ST078 ◇ ST073 $\alpha_{FLT} = 9.8^{o}$

F-111A WING BUFFET RESPONSE. FLT.48. RUN 6
SWEEP=26 DEG. MACH=.7. ALT=7559 METERS. ALPHA= 10.7
H.T. PIVOT BENDING MOMENT (M-N)
CIRCLE = UPPER BOUNDS SQUARE = LOWER BOUNDS

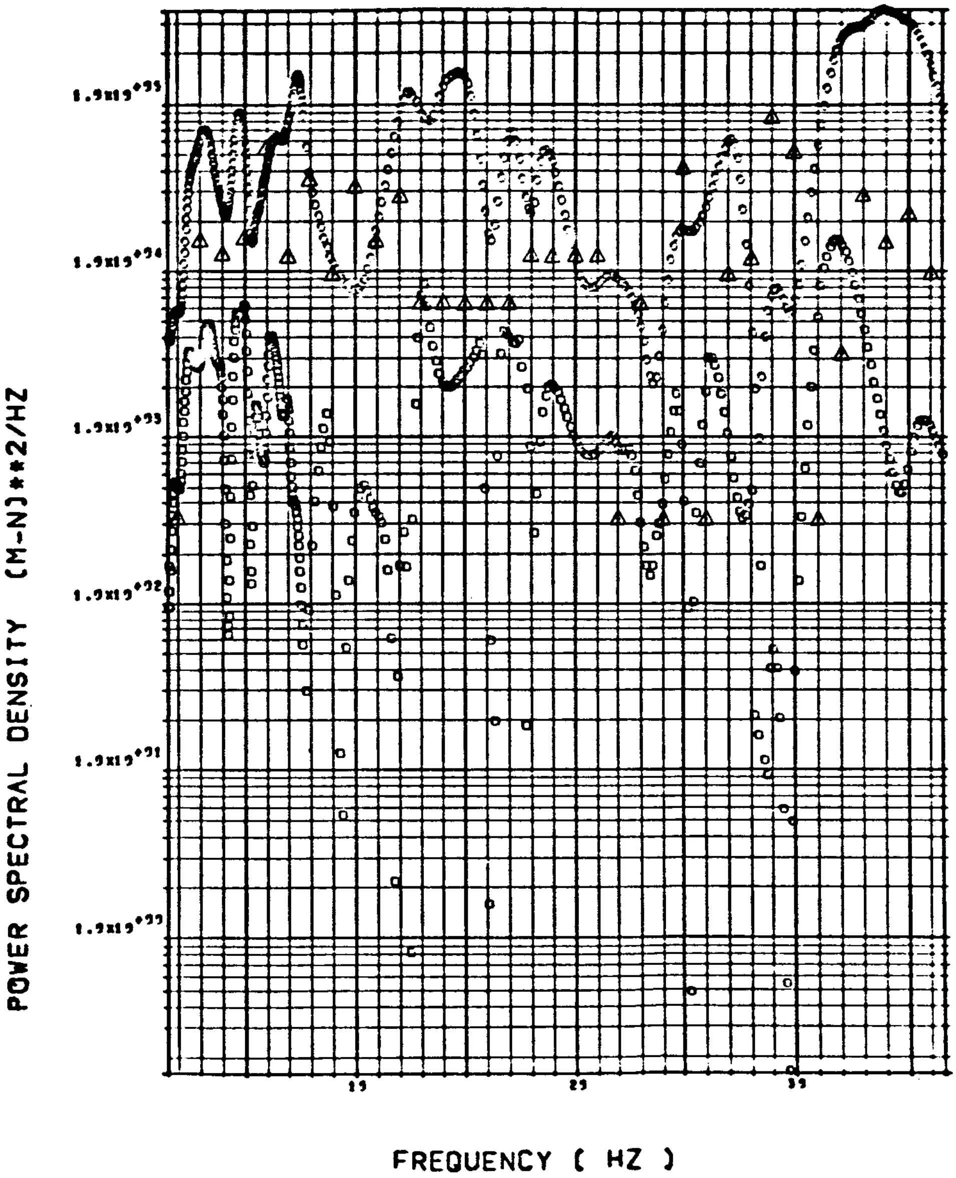

Figure 3.-(j) Horizontal tail bending moment (continued)

△ ST078   ◇ ST073 $\alpha_{FLT} = 10.7^{o}$

F-111A WING BUFFET RESPONSE. FLT.48. RUN 6
SWEEP=26 DEG. MACH=.7. ALT=7559 METERS. ALPHA= 11.8
H.T. PIVOT BENDING MOMENT (M-N)
CIRCLE = UPPER BOUNDS   SQUARE = LOWER BOUNDS

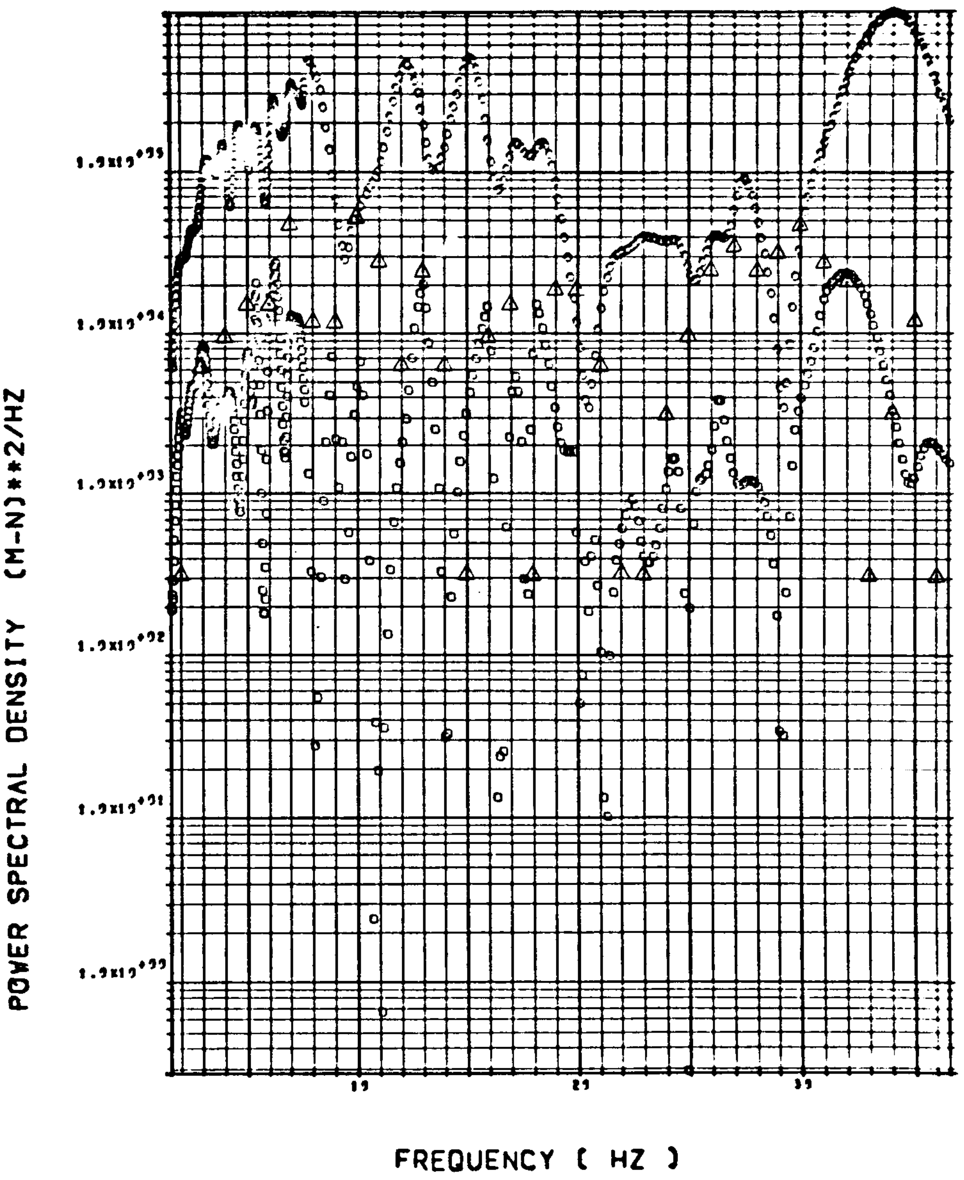

Figure 3.-(j) Horizontal tail bending moment (continued)

△ ST078 ◇ ST073 $\alpha_{FLT} = 11.8^{o}$

F-111A WING BUFFET RESPONSE. FLT.48. RUN 6
SWEEP=26 DEG. MACH=.7. ALT=7559 METERS. ALPHA= 12.8
H.T. PIVOT BENDING MOMENT (M-N)
CIRCLE = UPPER BOUNDS SQUARE = LOWER BOUNDS

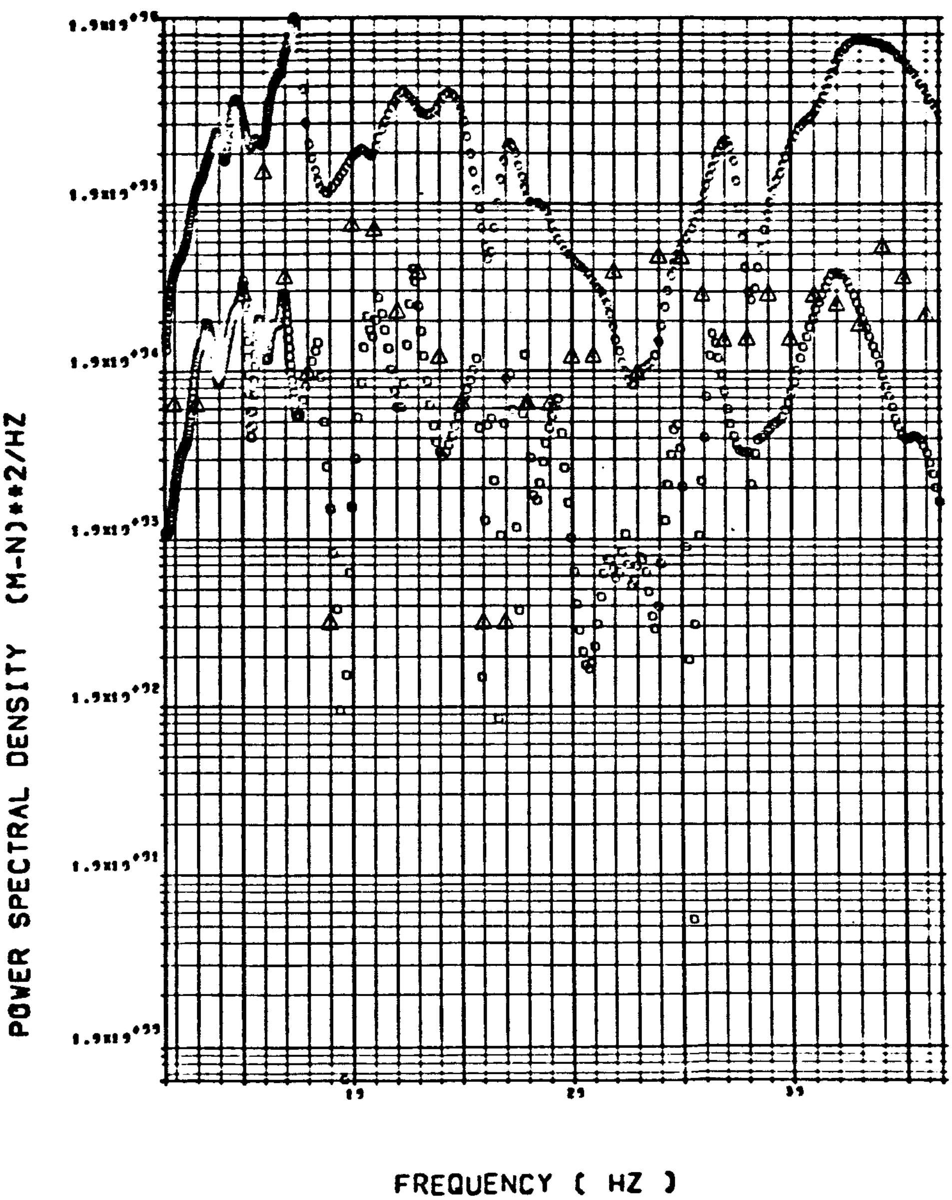

Figure 3.-(j) Horizontal tail bending moment (continued)

△ ST078 ◇ ST073 $\alpha_{FLT} = 14.6^{\circ}$

F-111A WING BUFFET RESPONSE. FLT.43. RUN 6
SWEEP=26 DEG. MACH=.7. ALT=7550 METERS. ALPHA=17.1
H.T. PIVOT BENDING MOMENT (M-N)
CIRCLE = UPPER BOUNDS SQUARE = LOWER BOUNDS

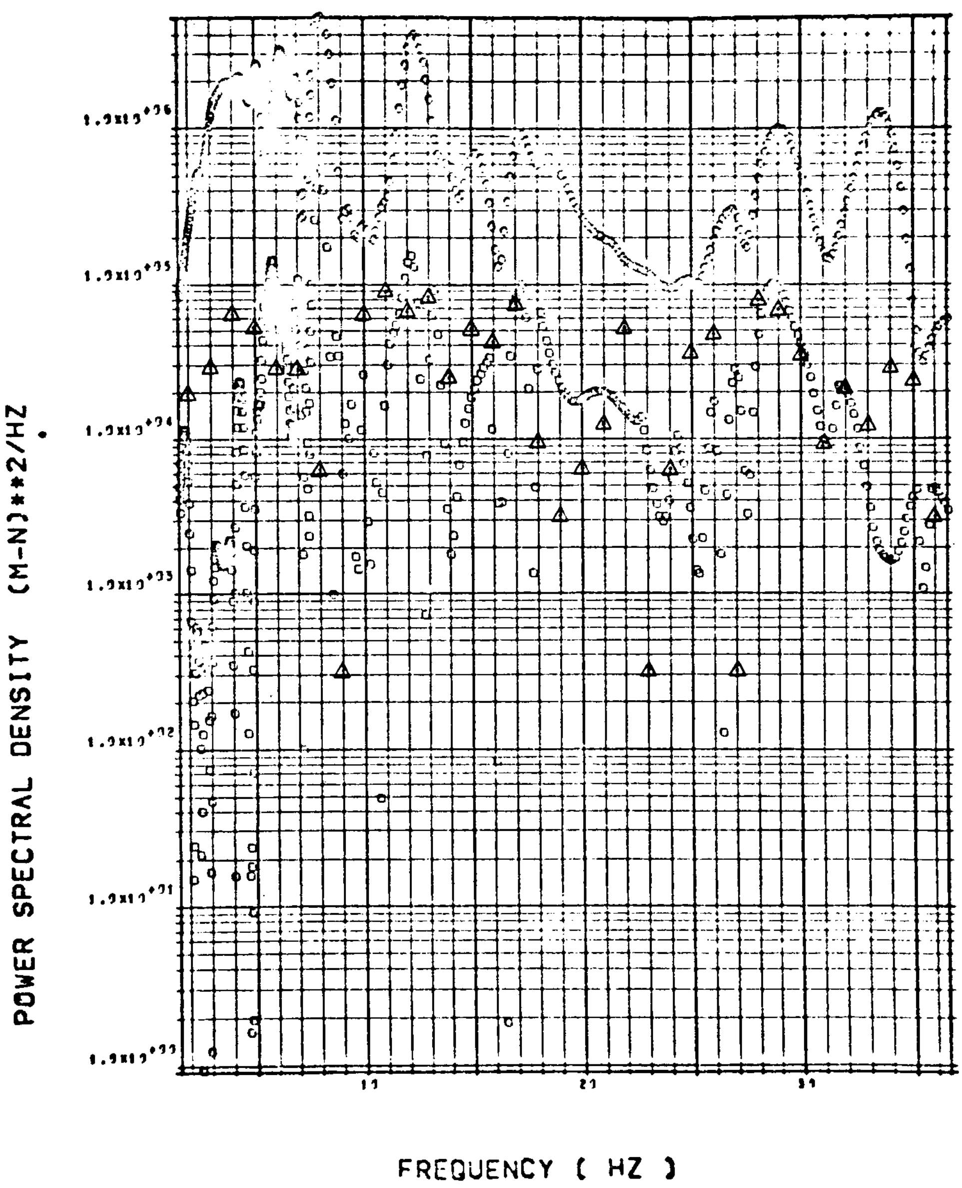

Figure 3.-(j) Horizontal tail bending moment (continued)

△ ST135 ◇ ST118 $\alpha_{FLT} = 8.8^{o}$

F-111A WING BUFFET RESPONSE. FLT.48. RUN 6
SWEEP=26 DEG. MACH=.7. ALT=7559 METERS. ALPHA=9.6
H.T. PIVOT TORQUE (M-N)
CIRCLE = UPPER BOUNDS SQUARE = LOWER BOUNDS

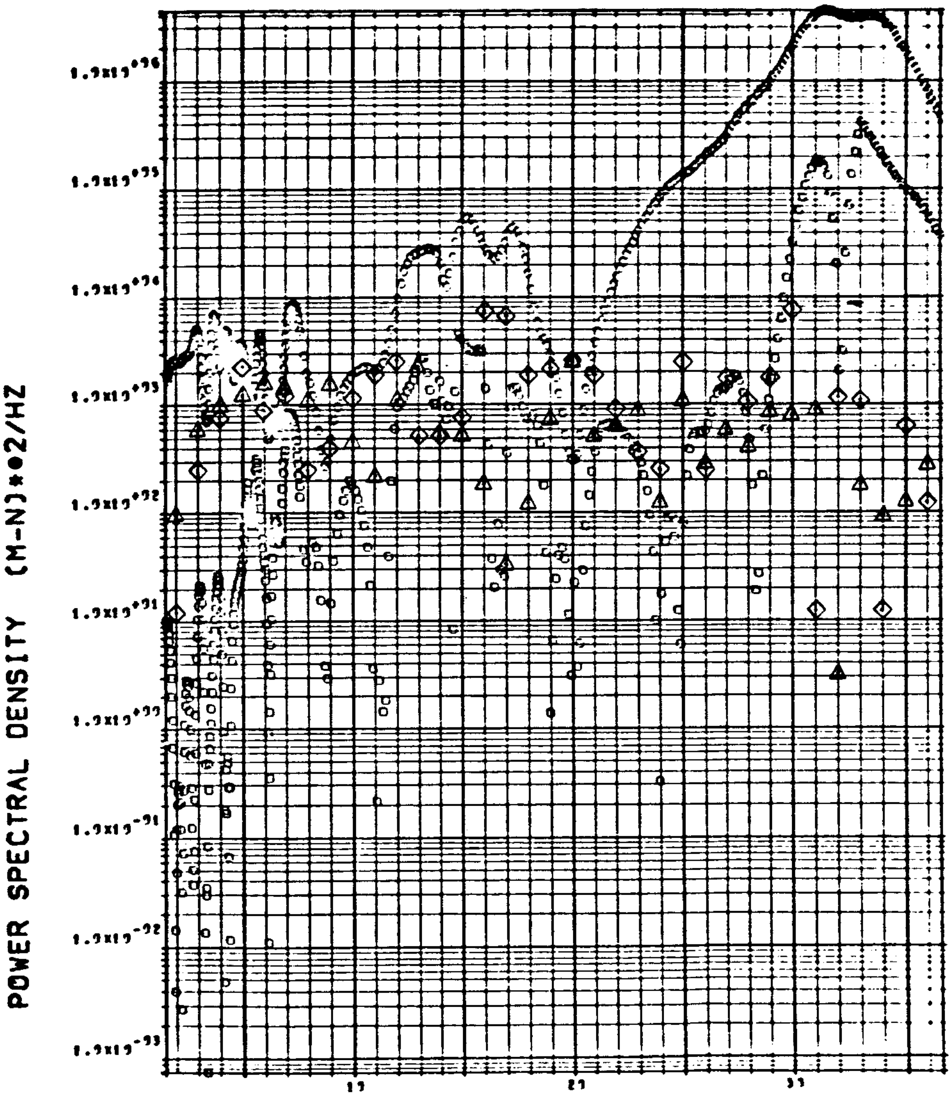

Figure 3.-(k) Horizontal tail torsion

△ ST135 ◇ ST118 $\alpha_{FLT} = 9.8^{o}$

F-111A WING BUFFET RESPONSE, FLT.40, RUN 6
SWEEP=26 DEG, MACH=.7, ALT=7559 METERS, ALPHA=10.7
H.T. PIVOT TORQUE (M-N)
CIRCLE = UPPER BOUNDS SQUARE = LOWER BOUNDS

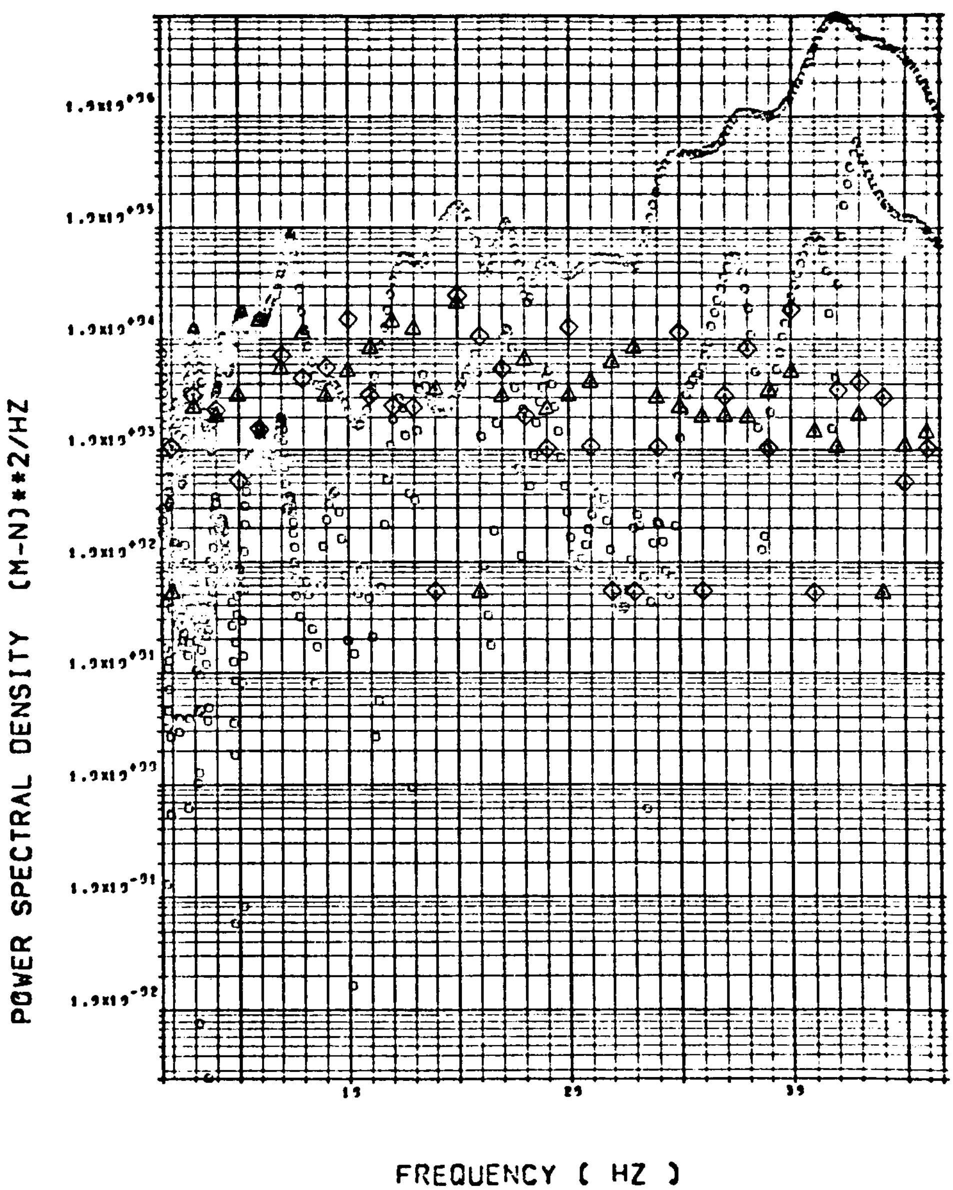

Figure 3.-(k) Horizontal tail torsion (continued)

△ ST135 ◇ ST118 $\alpha_{FLT} = 10.7^{o}$

F-111A WING BUFFET RESPONSE. FLT.48. RUN 6
SWEEP=26 DEG. MACH=.7. ALT=7559 METERS. ALPHA=11.8
H.T. PIVOT TORQUE (M-N)
CIRCLE = UPPER BOUNDS SQUARE = LOWER BOUNDS

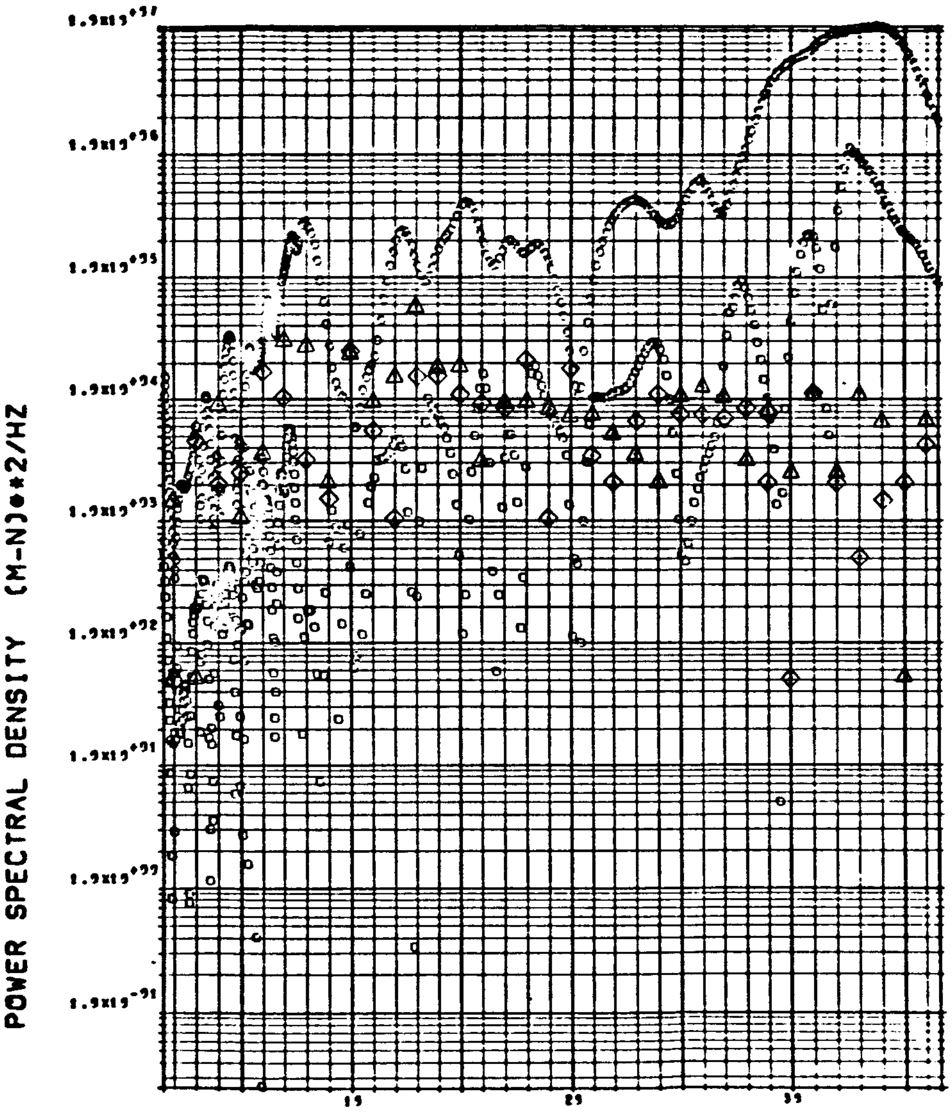

Figure 3.-(k) Horizontal tail torsion (continued)

△ ST135 ◇ ST118 $\alpha_{FLT} = 11.8^{\circ}$

F-111A WING BUFFET RESPONSE, FLT.48, RUN 6
SWEEP=26 DEG, MACH=.7, ALT=7559 METERS, ALPHA= 12.8
H.T. PIVOT TORQUE (M-N)
CIRCLE = UPPER BOUNDS SQUARE = LOWER BOUNDS

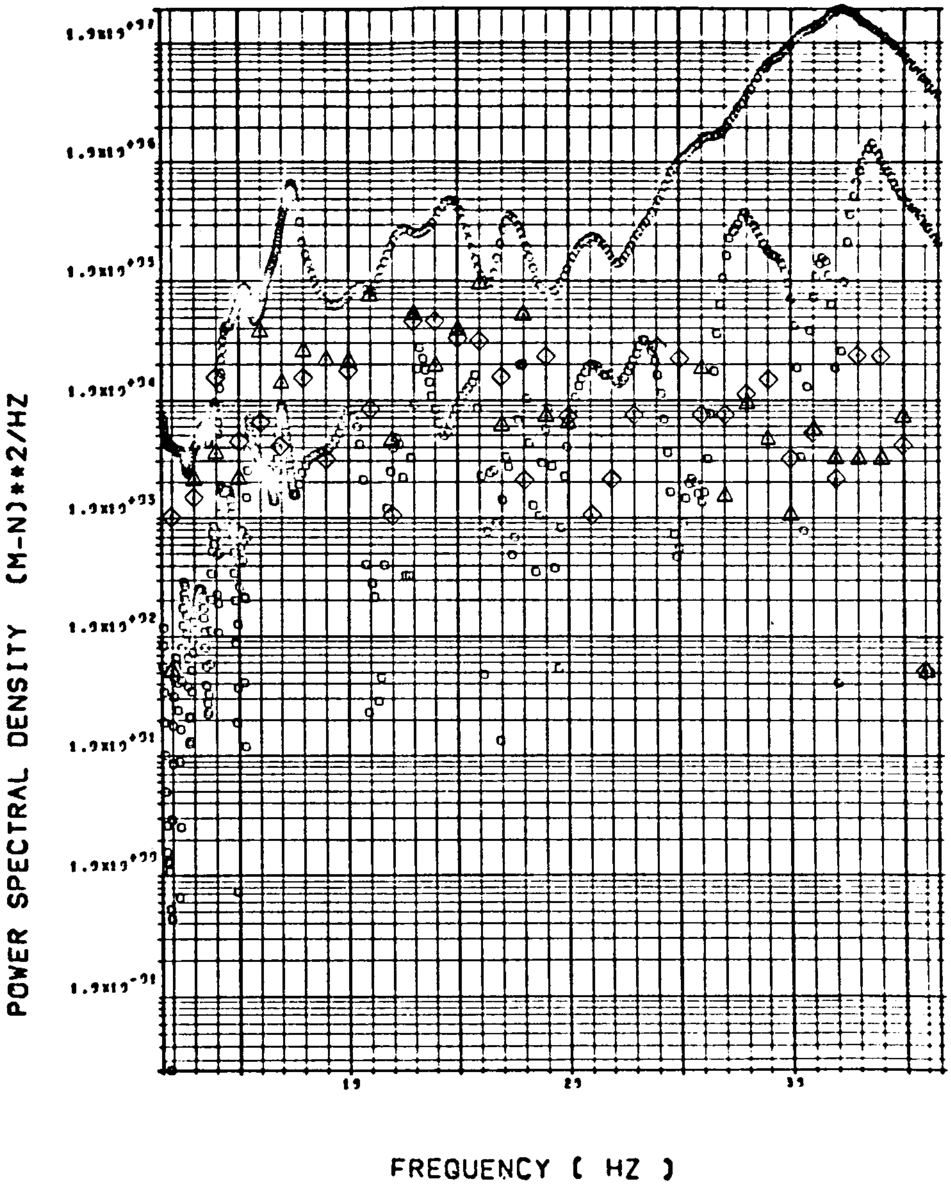

Figure 3.-(k) Horizontal tail torsion (continued)

△ ST135 ◇ ST118 $\alpha_{FLT} = 14.6^{o}$

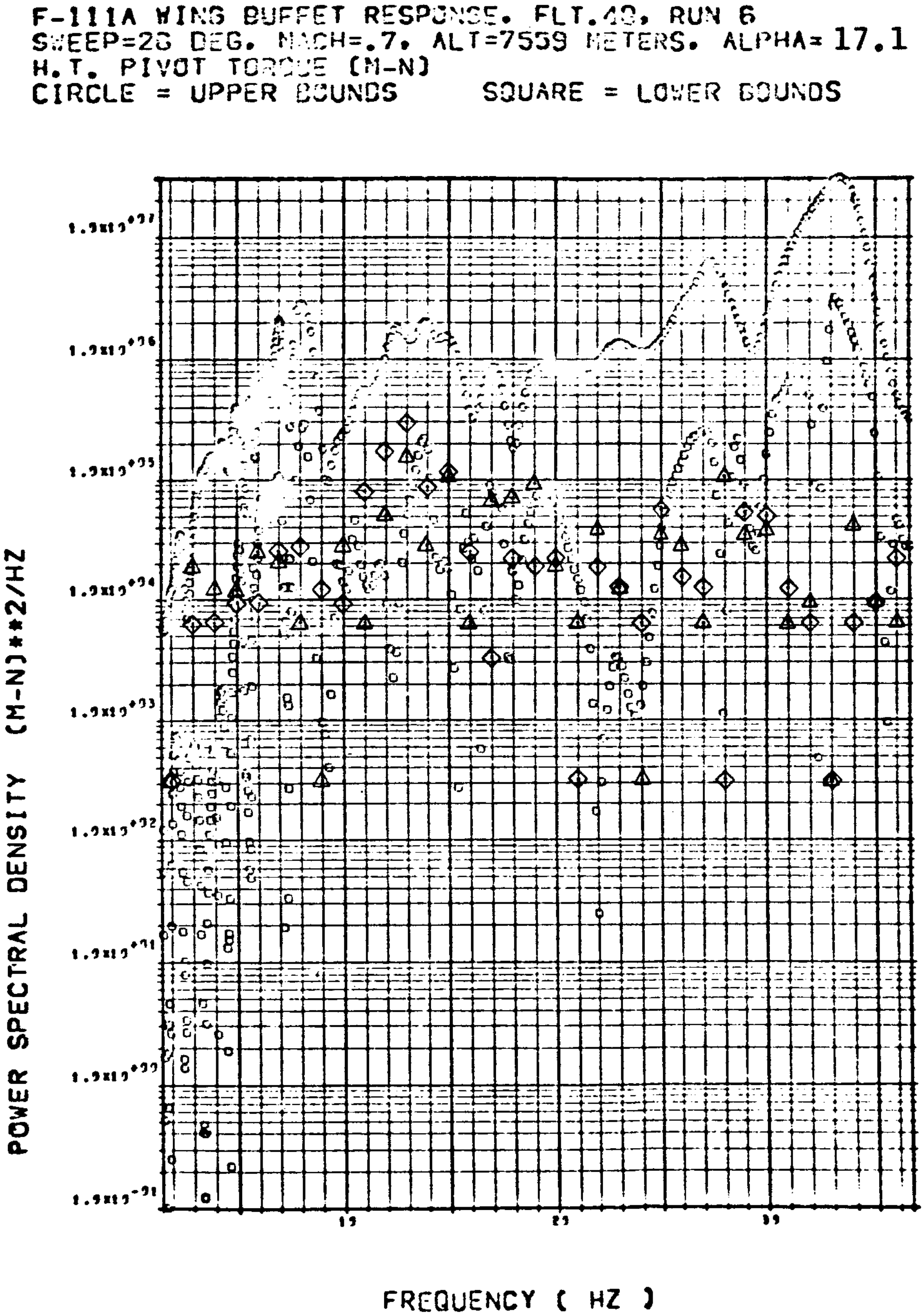

Figure 3.-(k) Horizontal tail torsion (continued)

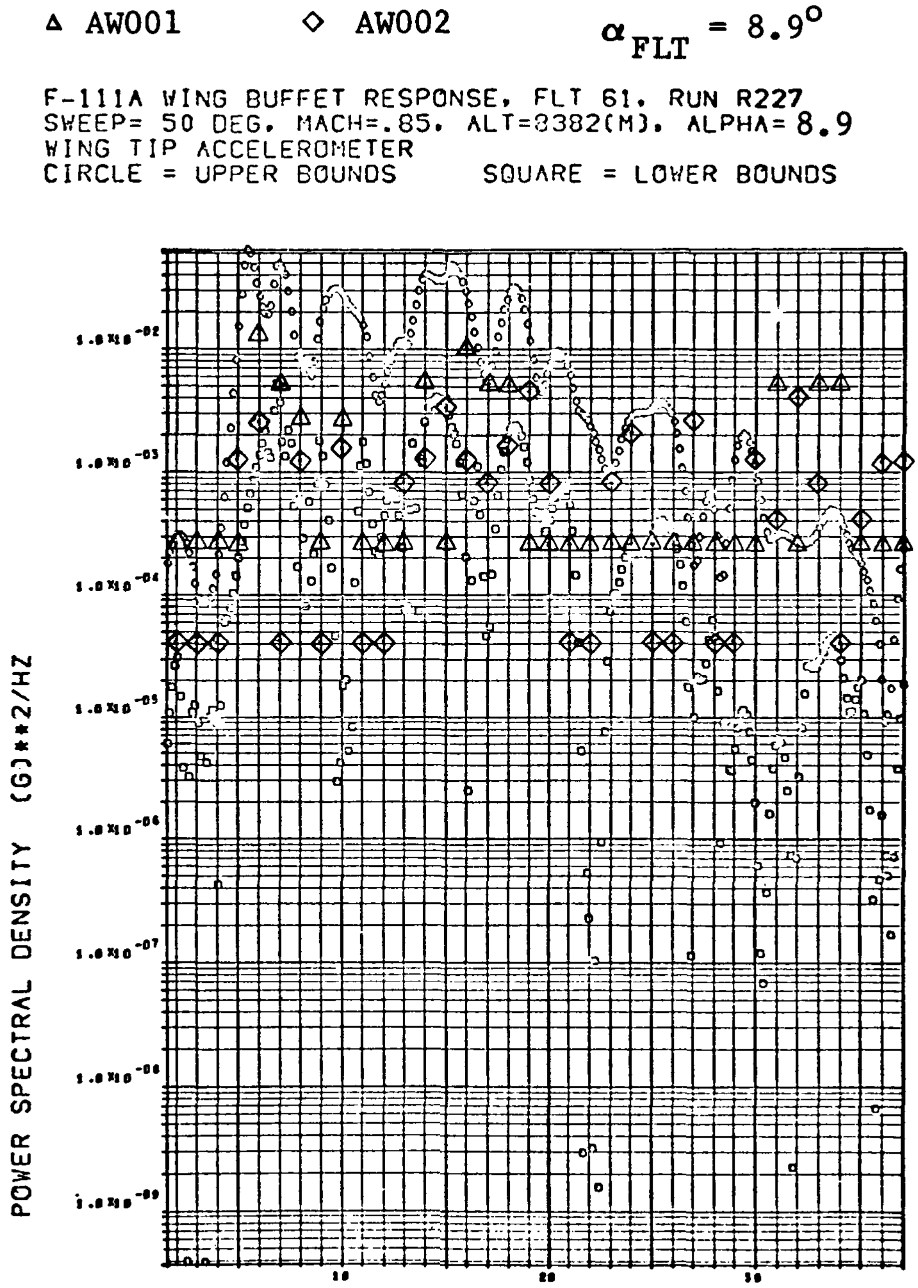

Figure 4.- Power spectra for
Case 4, total airplane (final method),
$\Lambda=50^{\circ}$, M=0.85, alt.=8382m (27,500 ft)
(a) wing tip accelerometer

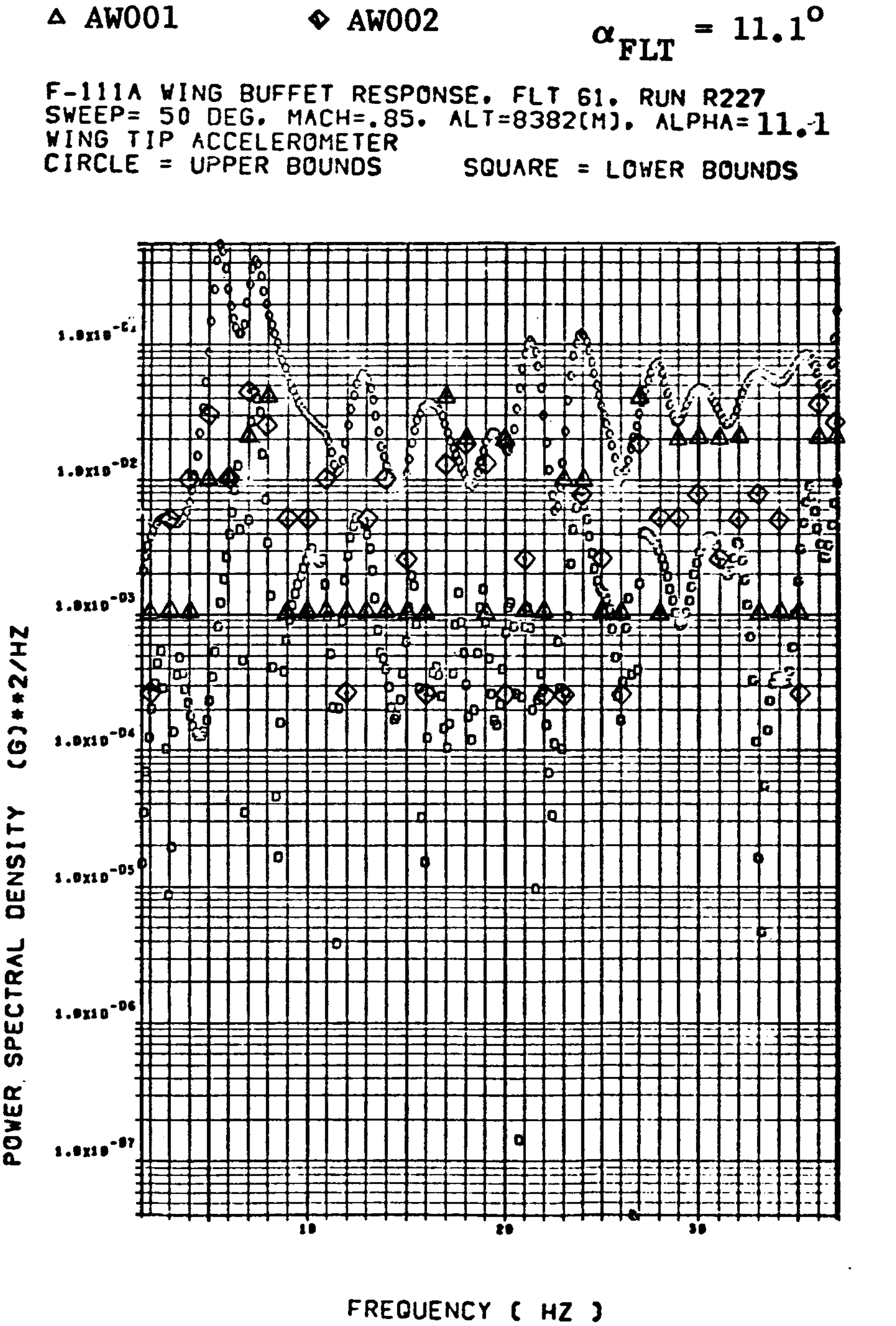

Figure 4.-(a) Wing tip accelerometer (continued)

△ AW001 ◇ AW002 $\alpha_{FLT} = 13.1^{\circ}$

F-111A WING BUFFET RESPONSE, FLT 61, RUN R227
SWEEP= 50 DEG, MACH=.85, ALT=8802(M), ALPHA= 14.4
WING TIP ACCELEROMETER
CIRCLE = UPPER BOUNDS SQUARE = LOWER BOUNDS

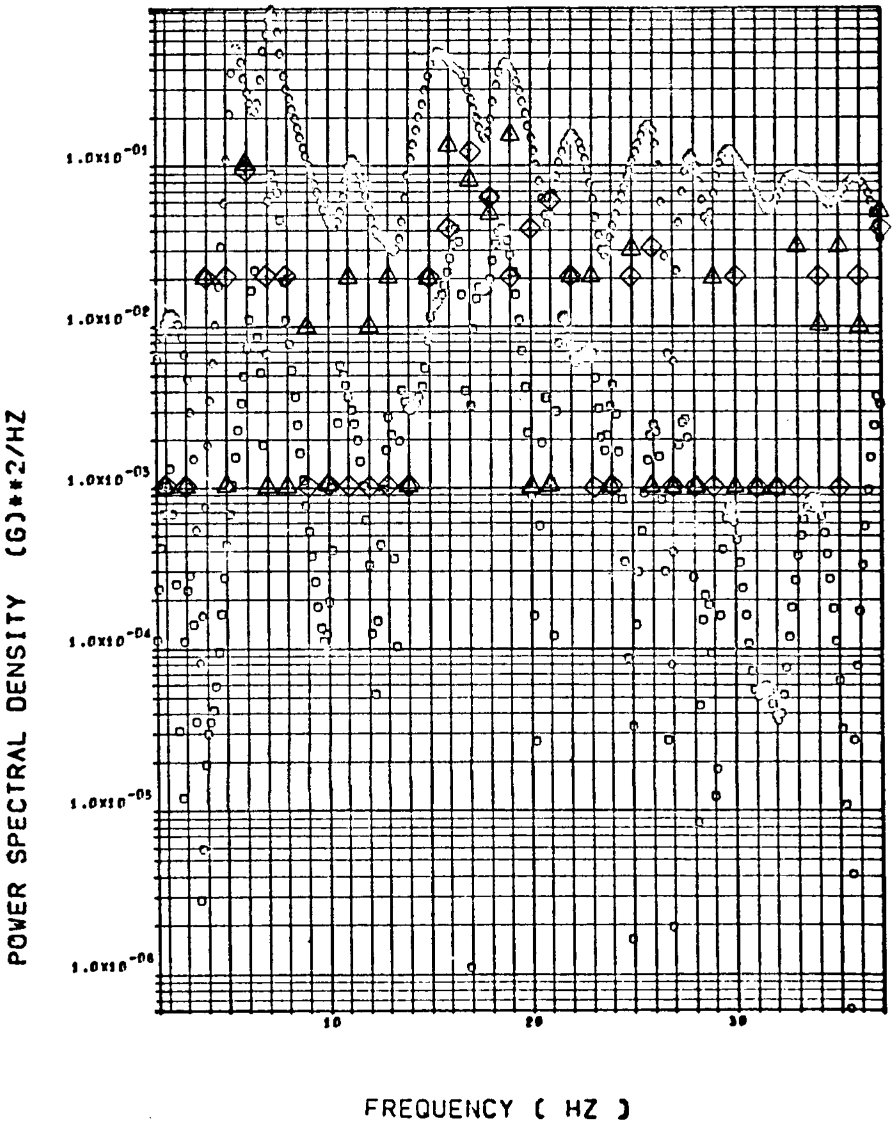

Figure 4.-(a) Wing tip accelerometer (continued)

◇ AB018 $\alpha_{FLT} = 8.9^{\circ}$

SYM F-111A WING BUFFET RESPONSE, FLT 61, RUN R227
SWEEP= 50 DEG. MACH=.85, ALT=8382(M), ALPHA= 8.9
C.G. VERTICAL ACCELEROMETER, FS = 529
SQUARE = 1 DOF A = 2 DOF CIRCLE = 14 DOF

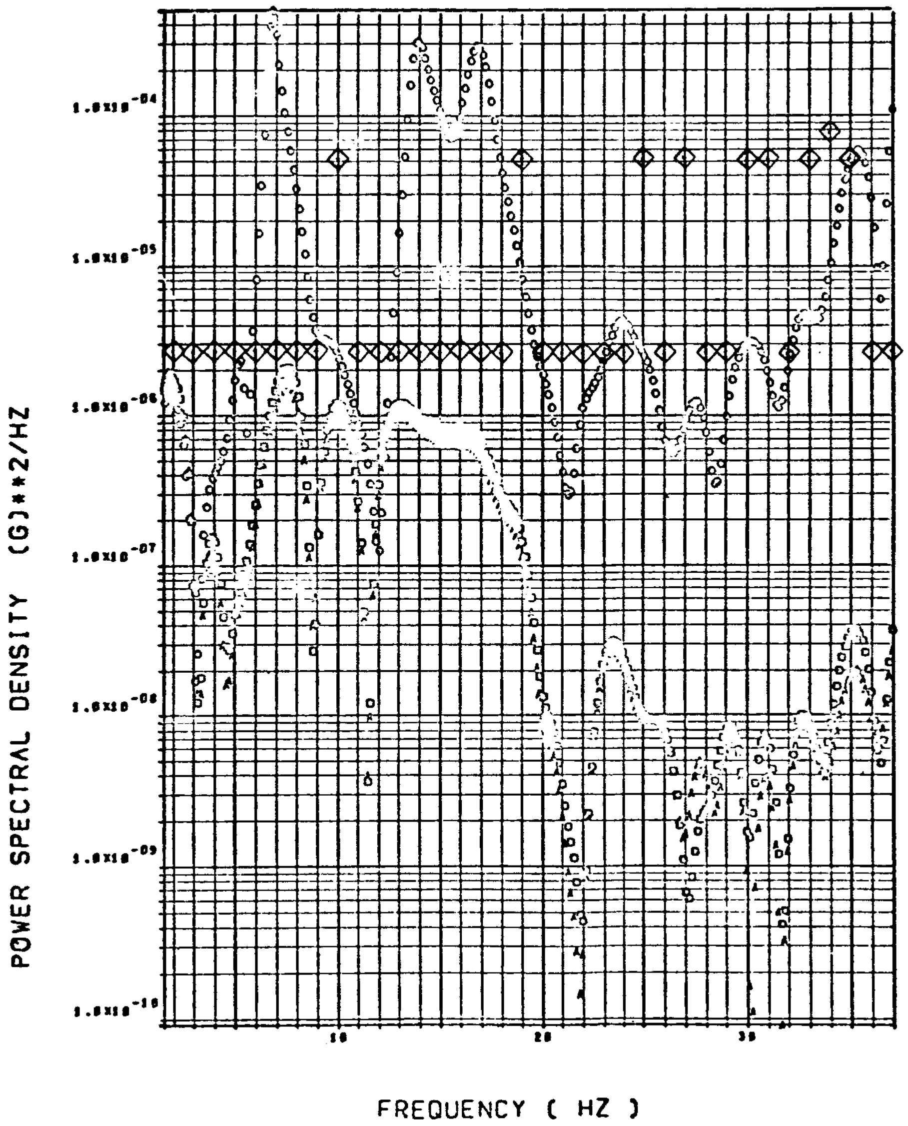

Figure 4.-(b) C.G. vertical accelerometer

AB018 $\alpha_{FLT} = 11.1^{\circ}$

SYM F-111A WING BUFFET RESPONSE, FLT 61, RUN R227
SWEEP= 50 DEG, MACH=.85, ALT=8382(M), ALPHA= 11.1
C.G. VERTICAL ACCELEROMETER, FS = 529
SQUARE = 1 DOF A = 2 DOF CIRCLE = 14 DOF

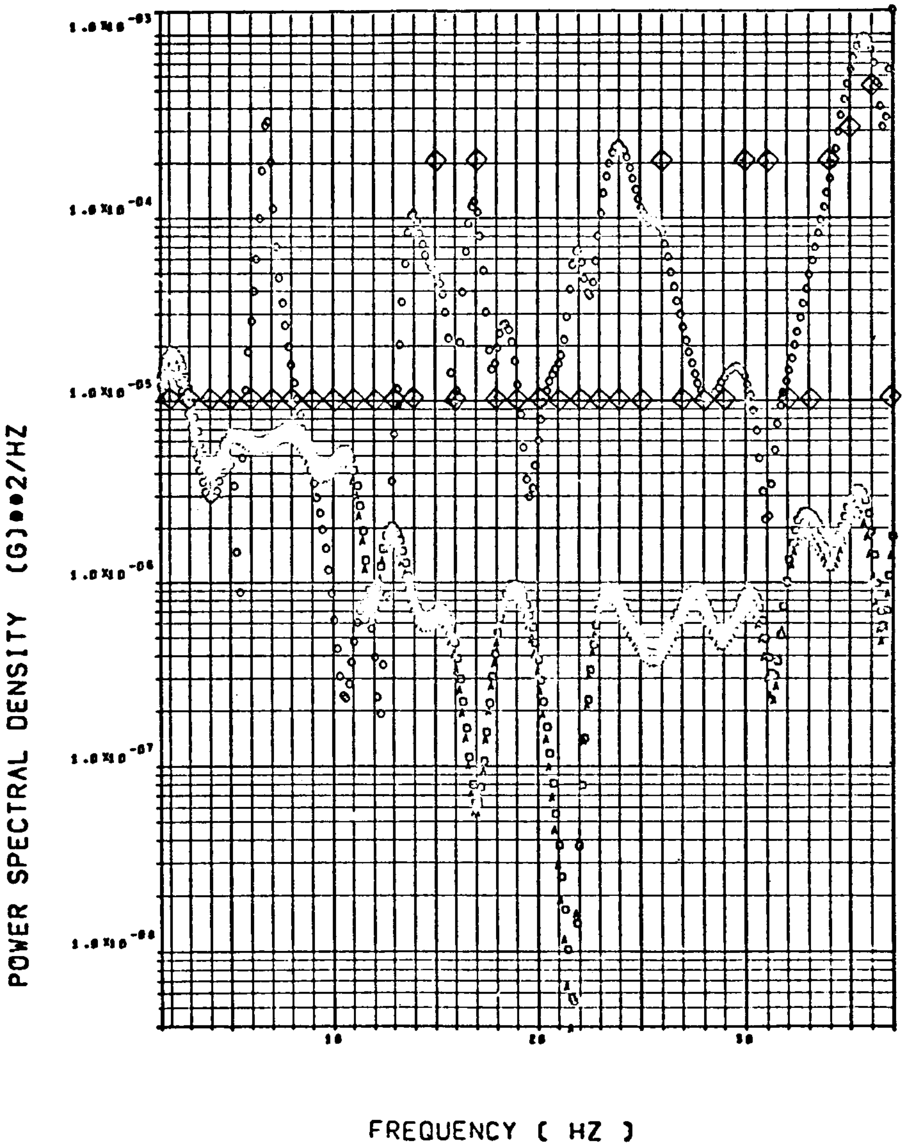

Figure 4.-(b) C.G. vertical accelerometer (continued)

◇ AB018 $\alpha_{FLT} = 13.1^{\circ}$

SYM F-111A WING BUFFET RESPONSE. FLT 61. RUN R227
SWEEP= 50 DEG. MACH=.85. ALT=8382(M).ALPHA= 14.4
C.G. VERTICAL ACCELEROMETER. FS = 529
SQUARE = 1 DOF A = 2 DOF CIRCLE = 14 DOF

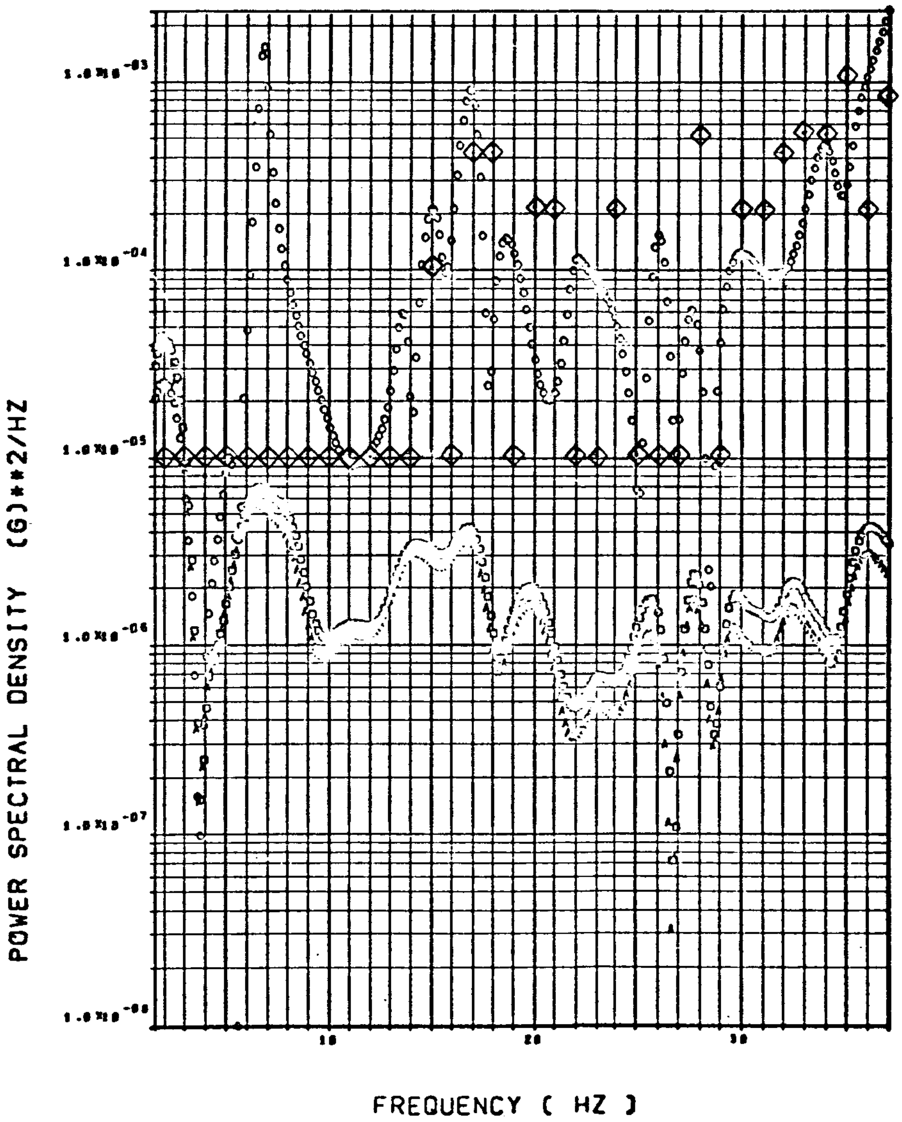

Figure 4.-(b) C.G. vertical accelerometer (continued)

◇ AF009 $\alpha_{FLT} = 8.9^{o}$

SYM F-111A WING BUFFET RESPONSE. FLT 61. RUN R227
SWEEP= 50 DEG. MACH=.85. ALT=8382(M). ALPHA= 8.9
PILOT STATION VERTICAL ACCELEROMETER. FS = 255
SQUARE = 1 DOF A = 2 DOF CIRCLE = 14 DOF

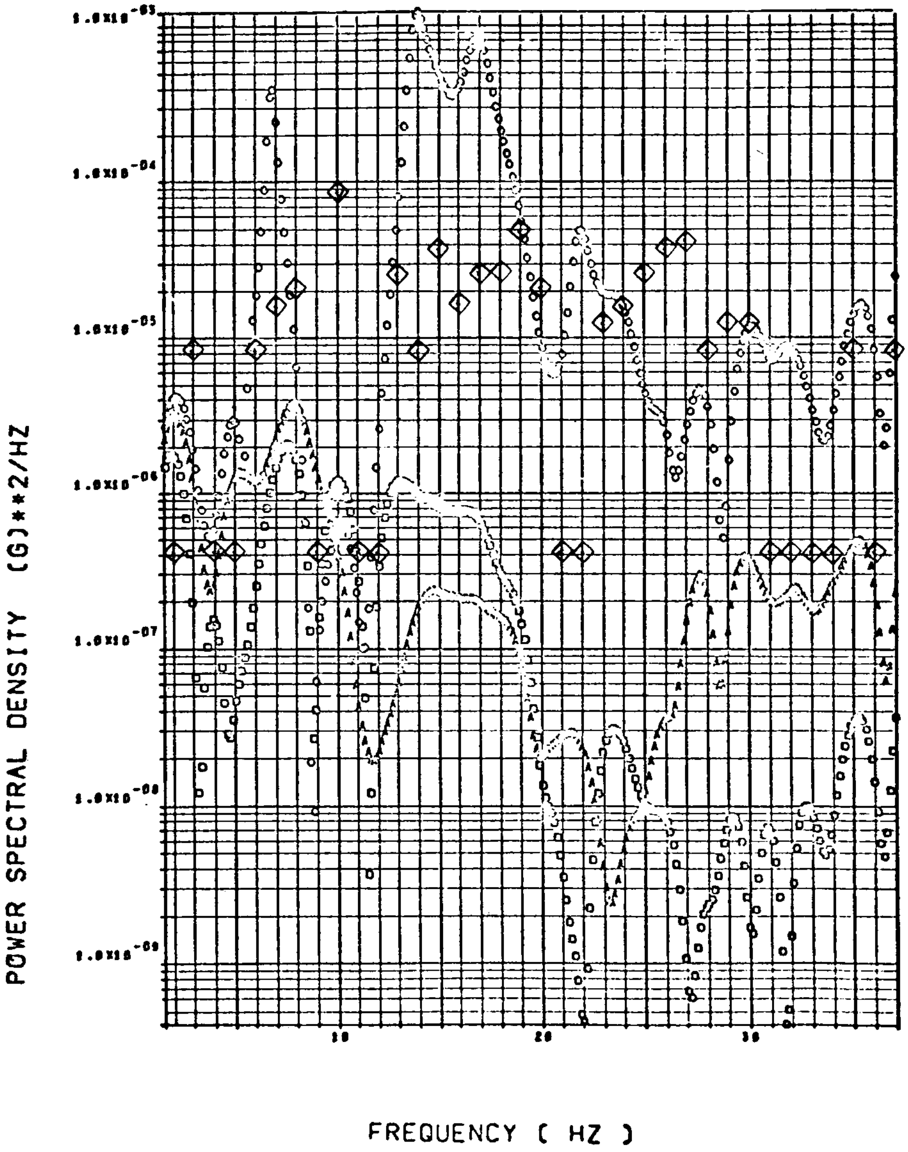

Figure 4.-(c) Pilot seat vertical accelerometer

◇ AF009 $\alpha_{FLT} = 11.1^{o}$

SYM F-111A WING BUFFET RESPONSE, FLT 61, RUN R227
SWEEP= 50 DEG, MACH=.85, ALT=8302(M), ALPHA= 11.1
PILOT STATION VERTICAL ACCELEROMETER, FS = 255
SQUARE = 1 DOF A = 2 DOF CIRCLE = 14 DOF

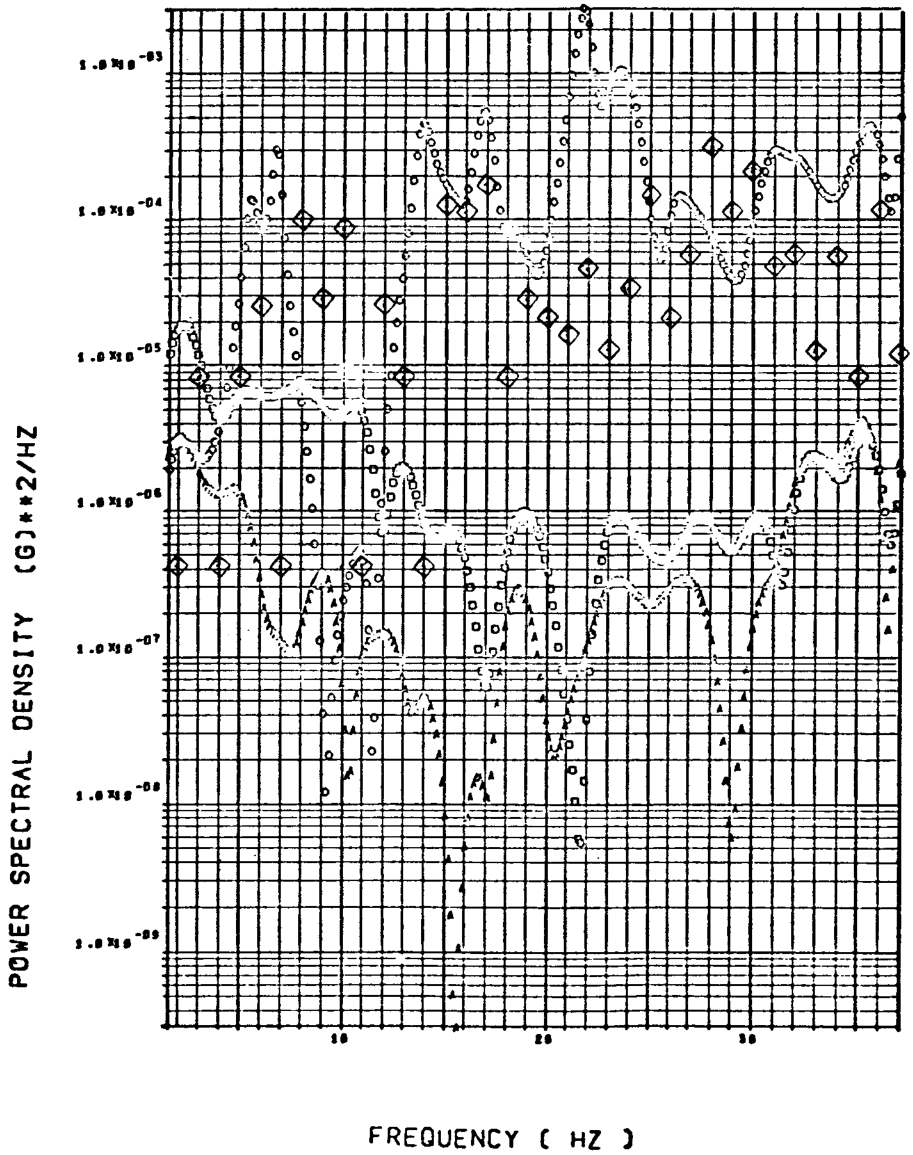

Figure 4.-(c) Pilot seat vertical accelerometer (continued)

◇ AF009 $\alpha_{FLT} = 13.1^{o}$

SYM F-111A WING BUFFET RESPONSE. FLT 61. RUN R227
SWEEP= 50 DEG. MACH=.85. ALT=8382(M).ALPHA= 14.4
PILOT STATION VERTICAL ACCELEROMETER. FS = 255
SQUARE = 1 DOF A = 2 DOF CIRCLE = 14 DOF

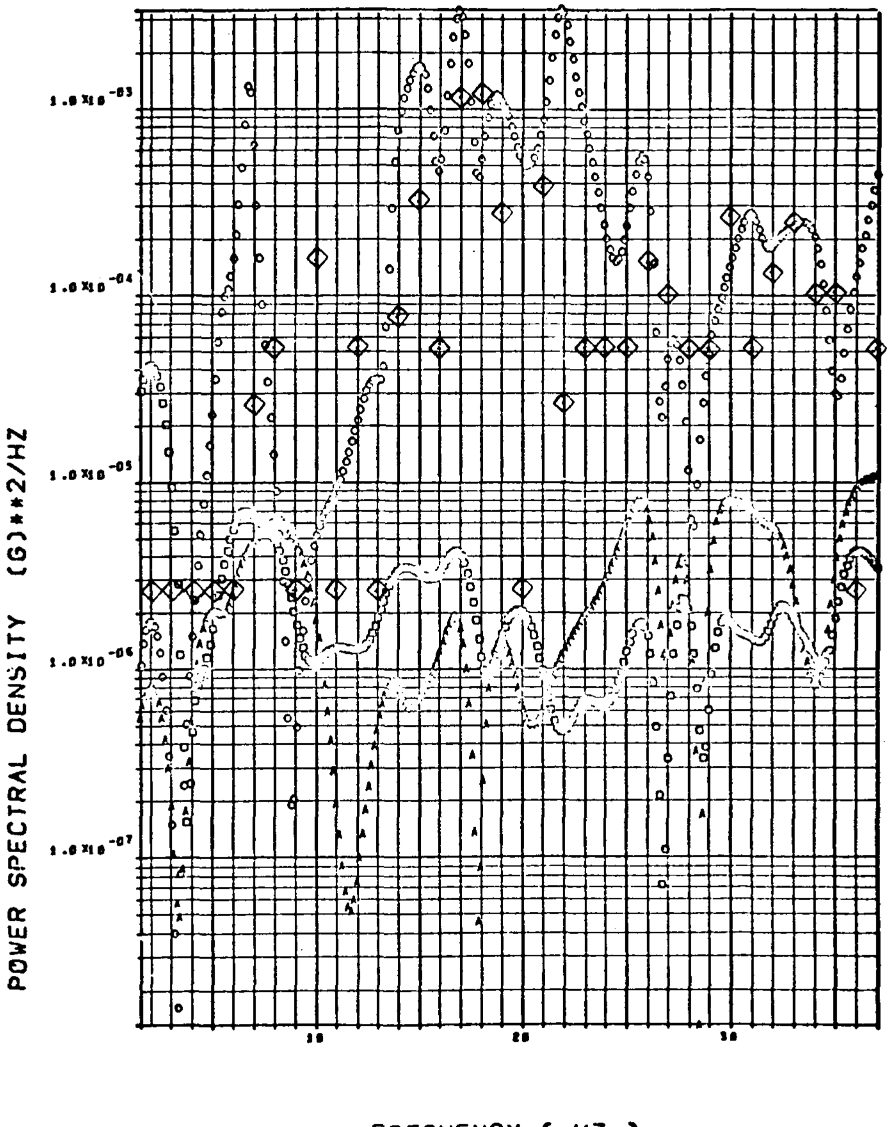

Figure 4.-(c) Pilot seat vertical accelerometer (continued)

◇ AB020 $\alpha_{FLT} = 8.9^{o}$

ANTI F-111A WING BUFFET RESPONSE. FLT 61. RUN R227
SWEEP= 50 DEG. MACH=.85. ALT=8382(M). ALPHA= 8.9
C.G. LATERAL ACCELEROMETER. FS = 529
SQUARE = 1 DOF A = 3 DOF CIRCLE = 18 DOF

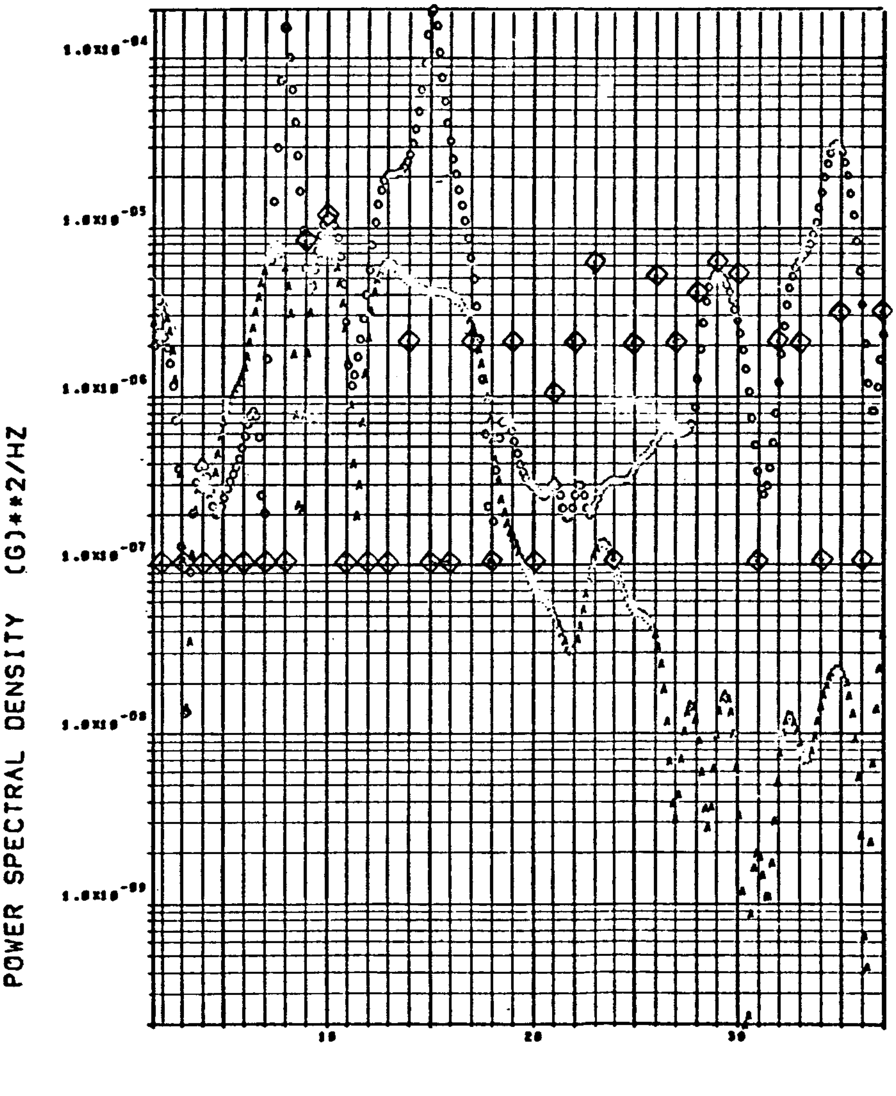

Figure 4.-(d) C.G. lateral accelerometer

◇ AB020 $\alpha_{FLT} = 11.1^{o}$

ANTI F-111A WING BUFFET RESPONSE, FLT 61, RUN R227
SWEEP= 50 DEG, MACH=.85, ALT=8382(M), ALPHA= 11.1
C.G. LATERAL ACCELEROMETER, FS = 529
SQUARE = 1 DOF A = 3 DOF CIRCLE = 18 DOF

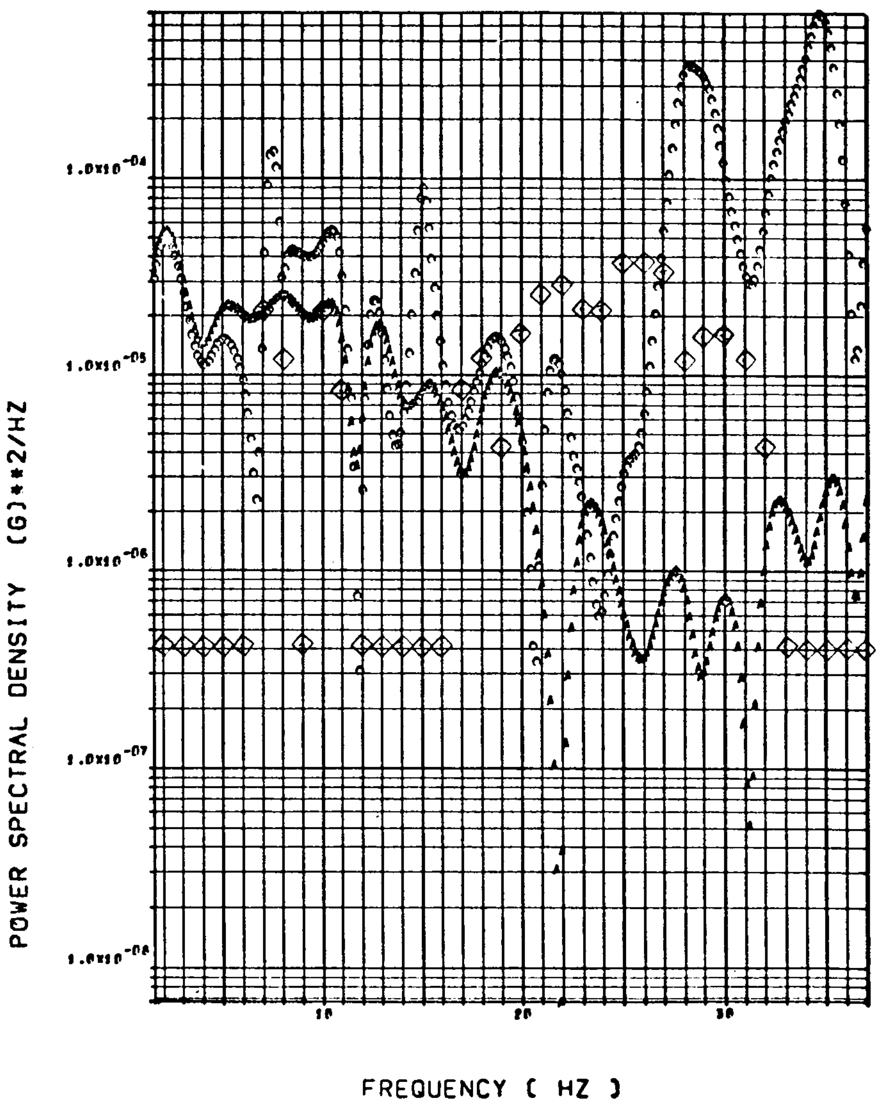

Figure 4.-(d) C.G. lateral accelerometer (continued)

◇ AB020 $\alpha_{FLT} = 13.1^{\circ}$

ANTI F-111A WING BUFFET RESPONSE. FLT 61. RUN R227
SWEEP= 50 DEG. MACH=.85. ALT=8332(M). ALPHA= 14.4
C.G. LATERAL ACCELEROMETER. FS = 529
SQUARE = 1 DOF A = 3 DOF CIRCLE = 18 DOF

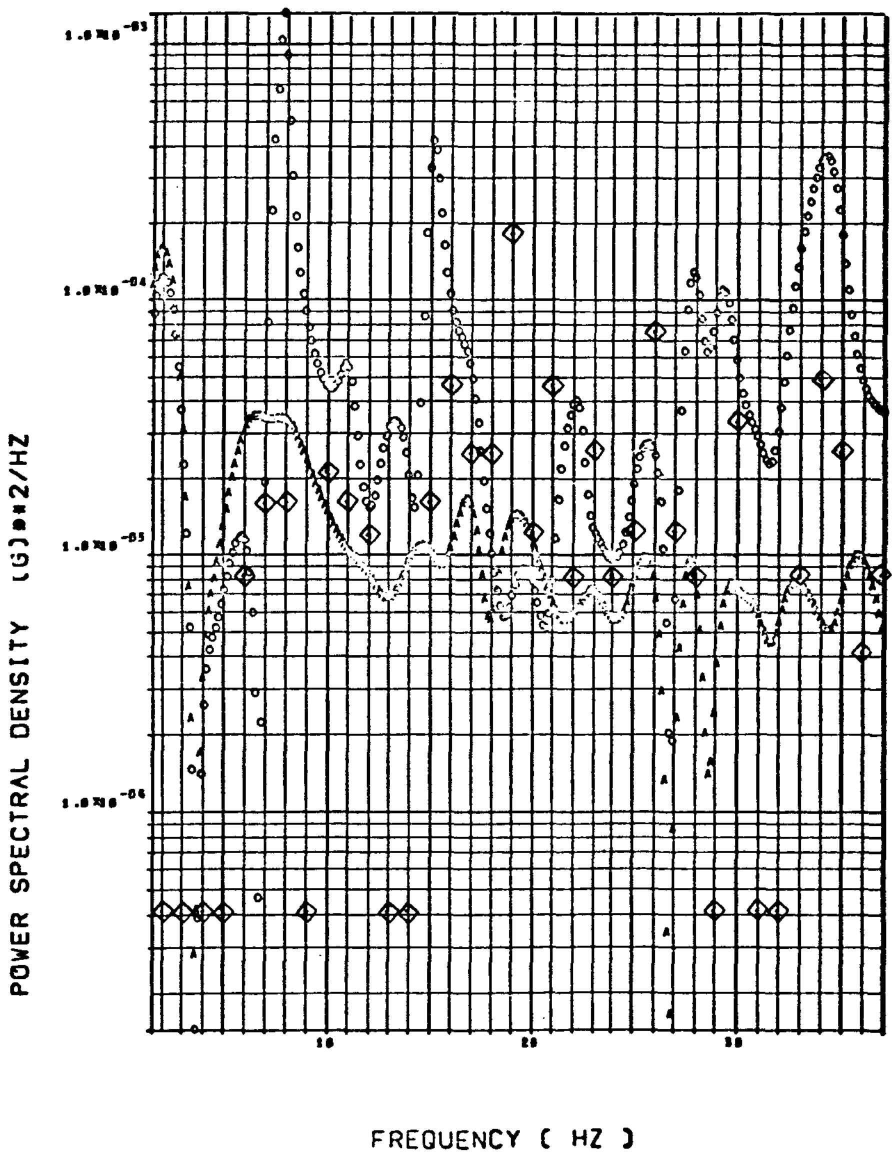

Figure 4.-(d) C.G. lateral accelerometer (continued)

◇ AF010 $\alpha_{FLT} = 8.9^{\circ}$

ANTI F-111A WING BUFFET RESPONSE, FLT 61, RUN R227
SWEEP= 50 DEG, MACH=.85, ALT=3382(M), ALPHA=8.9
PILOT STATION LATERAL ACCELEROMETER, FS = 255
SQUARE = 1 DOF A = 3 DOF CIRCLE = 18 DOF

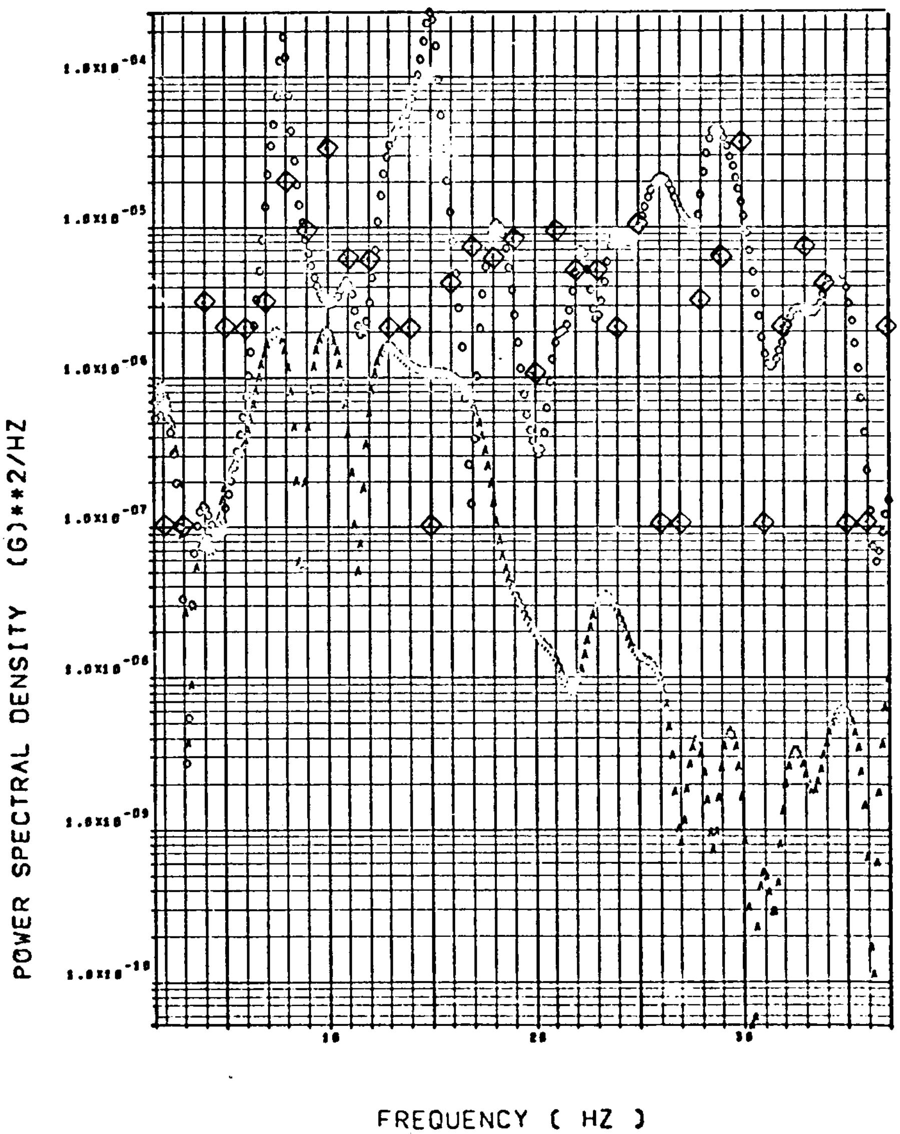

Figure 4.-(e) Pilot seat lateral accelerometer

◇ AF010 $\alpha_{FLT} = 11.1^{\circ}$

ANTI F-111A WING BUFFET RESPONSE. FLT 61. RUN R227
SWEEP= 50 DEG. MACH=.85. ALT=8382(M). ALPHA= 11.1
PILOT STATION LATERAL ACCELEROMETER. FS = 255
SQUARE = 1 DOF A = 3 DOF CIRCLE = 18 DOF

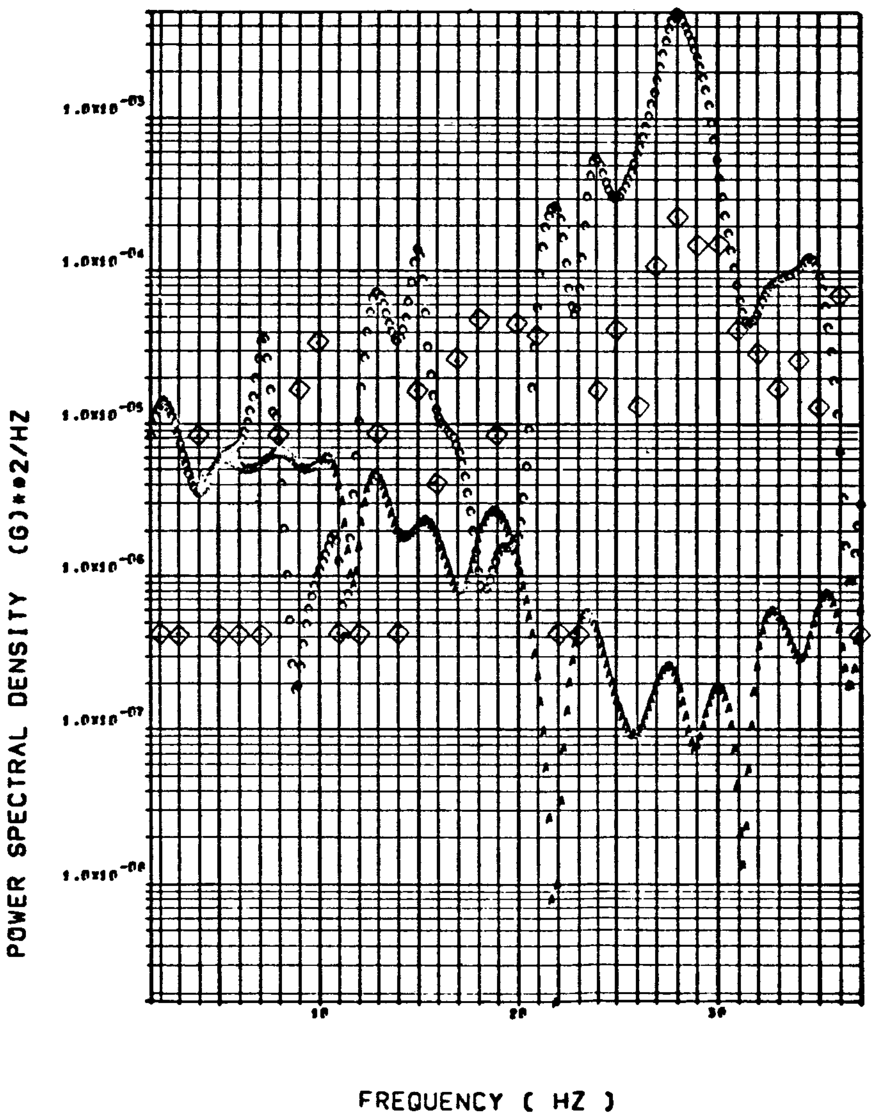

Figure 4.-(e) Pilot seat lateral accelerometer (continued)

◇ AF010 $\alpha_{FLT} = 13.1^{\circ}$

ANTI F-111A WING BUFFET RESPONSE. FLT 61. RUN R227
SWEEP= 50 DEG. MACH=.85. ALT=8382(M). ALPHA=14.4
PILOT STATION LATERAL ACCELEROMETER. FS = 255
SQUARE = 1 DOF A = 3 DOF CIRCLE = 18 DOF

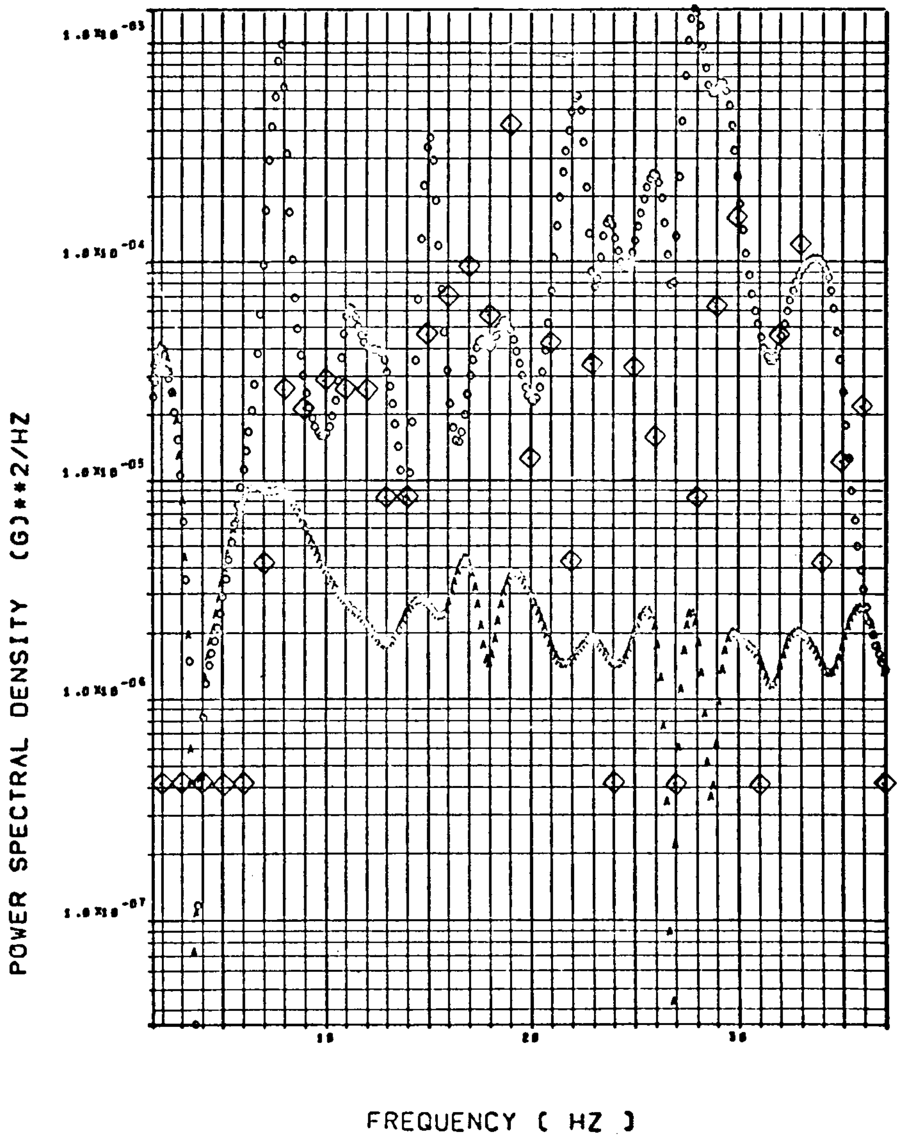

Figure 4.-(e) Pilot seat lateral accelerometer (continued)

△ SW123 $\alpha_{FLT} = 8.9^{\circ}$

F-111A WING BUFFET RESPONSE, FLT 61, RUN R227
SWEEP= 50 DEG, MACH=.85, ALT=8382(M), ALPHA= 8.9
WING SHEAR (N) AT SPAN STATION 75
CIRCLE = UPPER BOUNDS SQUARE = LOWER BOUNDS

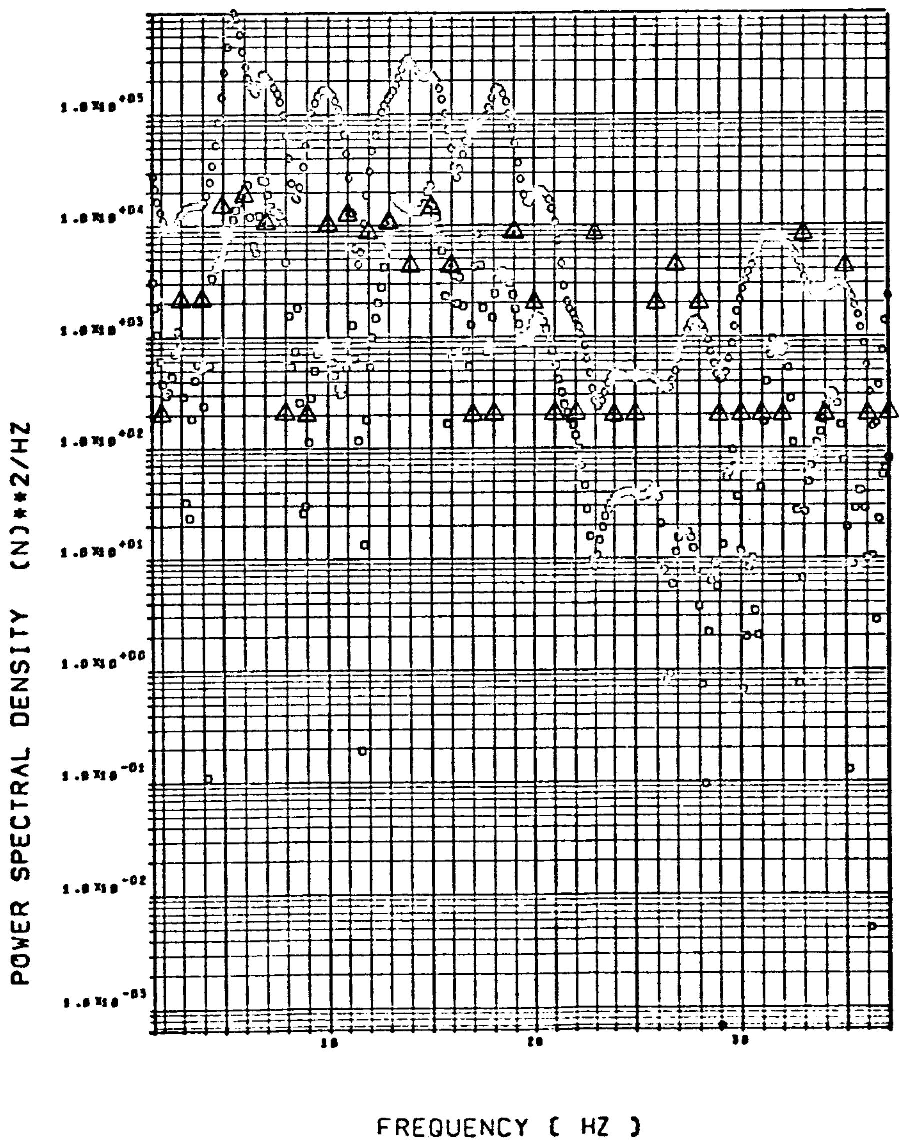

Figure 4.-(f) Wing shear

Δ SW123 $\alpha_{FLT} = 11.1^{o}$

F-111A WING BUFFET RESPONSE, FLT 61, RUN R227
SWEEP= 50 DEG, MACH=.85, ALT=8382(M), ALPHA= 11.1
WING SHEAR (N) AT SPAN STATION 75
CIRCLE = UPPER BOUNDS SQUARE = LOWER BOUNDS

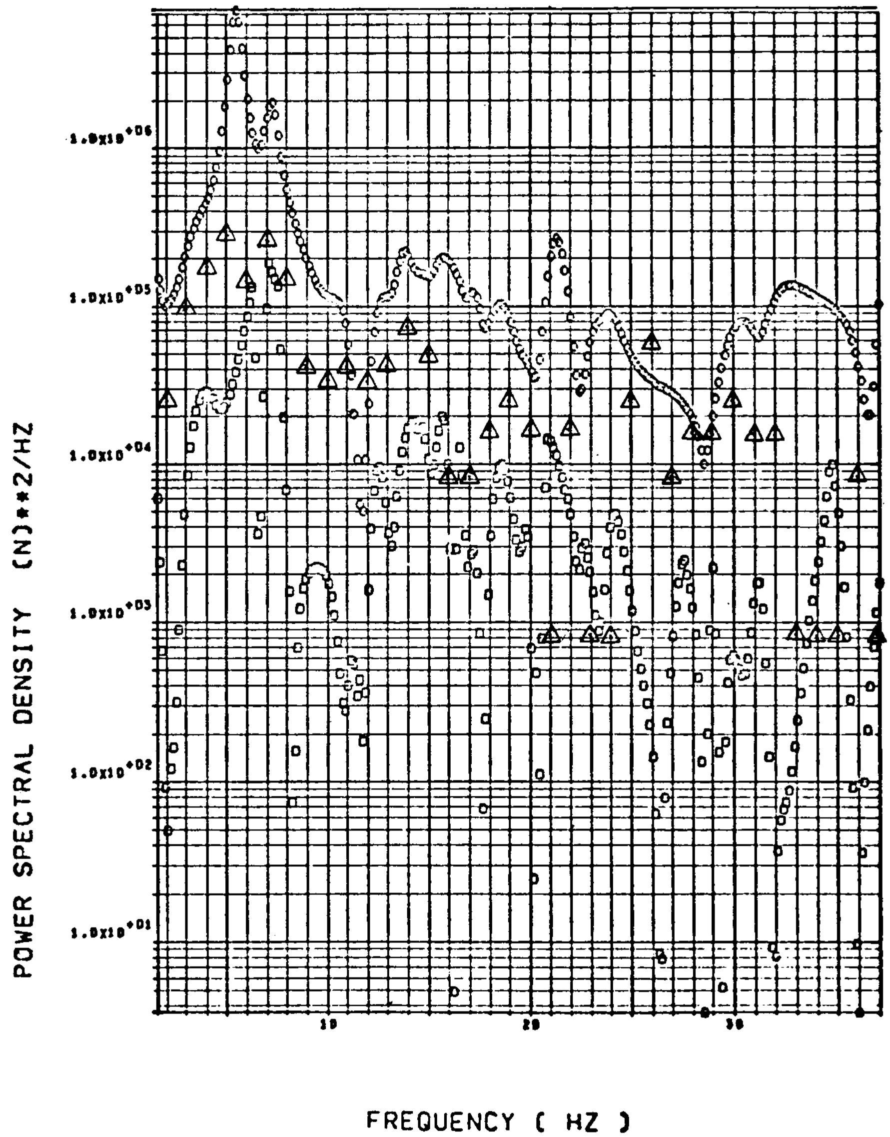

Figure 4.-(f) Wing shear (continued)

△ SW123 $\alpha_{FLT} = 13.1^{\circ}$

F-111A WING BUFFET RESPONSE, FLT 61, RUN R227
SWEEP= 50 DEG, MACH=.85, ALT=8382(M), ALPHA= 14.4
WING SHEAR (N) AT SPAN STATION 75
CIRCLE = UPPER BOUNDS SQUARE = LOWER BOUNDS

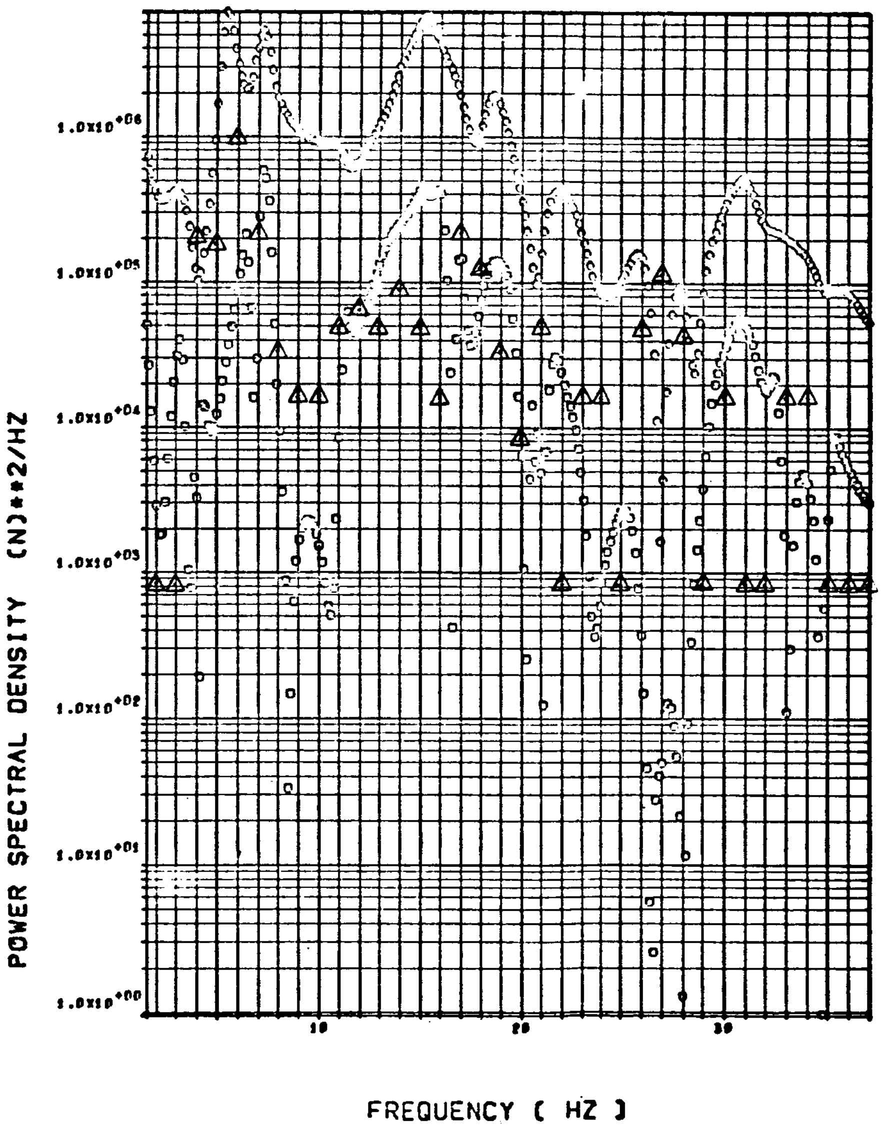

Figure 4.-(f) Wing shear (continued)

△ SW124 $\alpha_{FLT} = 8.9^{o}$

F-111A WING BUFFET RESPONSE. FLT 61. RUN R227
SWEEP= 50 DEG. MACH=.85. ALT=8382(M). ALPHA= 8.9
WING BENDING MOMENT (M-N) AT SPAN STATION 75
CIRCLE = UPPER BOUNDS SQUARE = LOWER BOUNDS

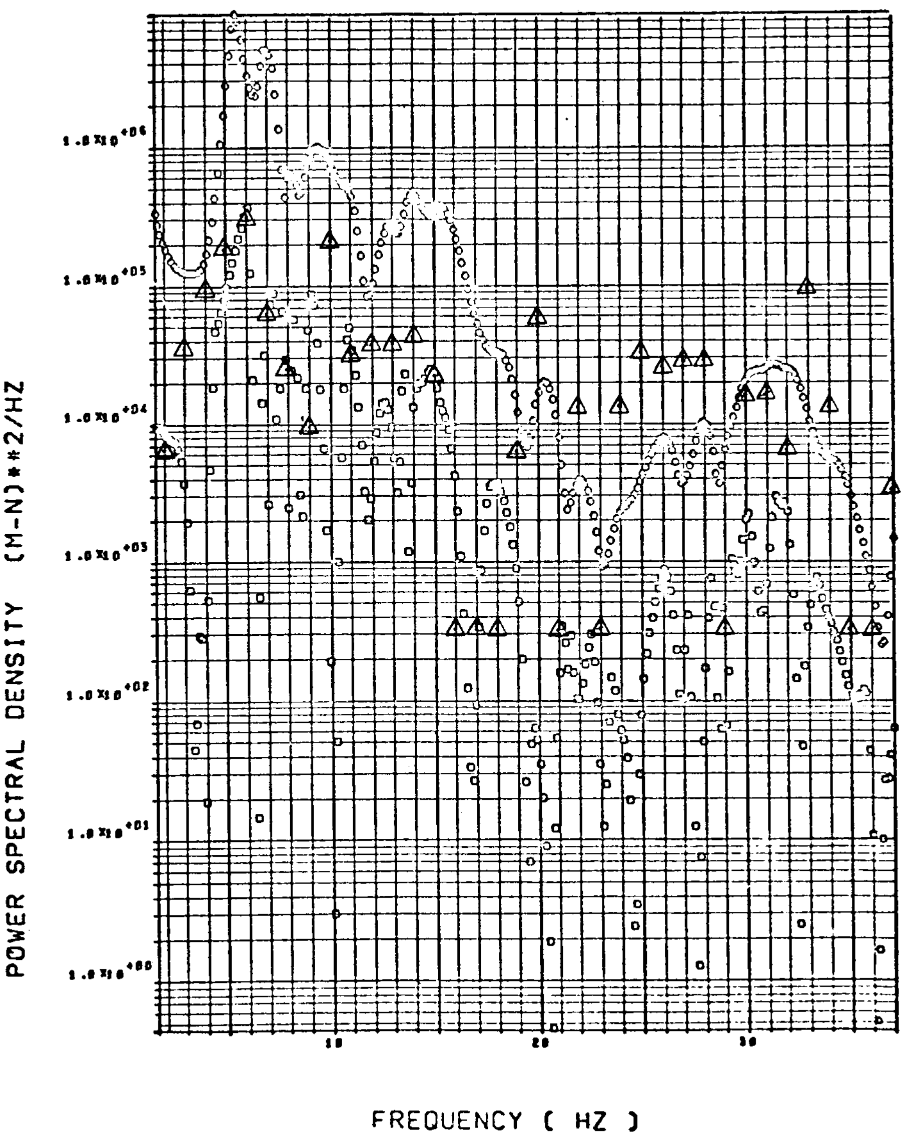

Figure 4.-(g) Wing bending moment

△ SW124 $\alpha_{FLT} = 11.1^{o}$

F-111A WING BUFFET RESPONSE, FLT 61, RUN R227
SWEEP= 50 DEG. MACH=.85. ALT=8382(M). ALPHA= 11.1
WING BENDING MOMENT (M-N) AT SPAN STATION 75
CIRCLE = UPPER BOUNDS SQUARE = LOWER BOUNDS

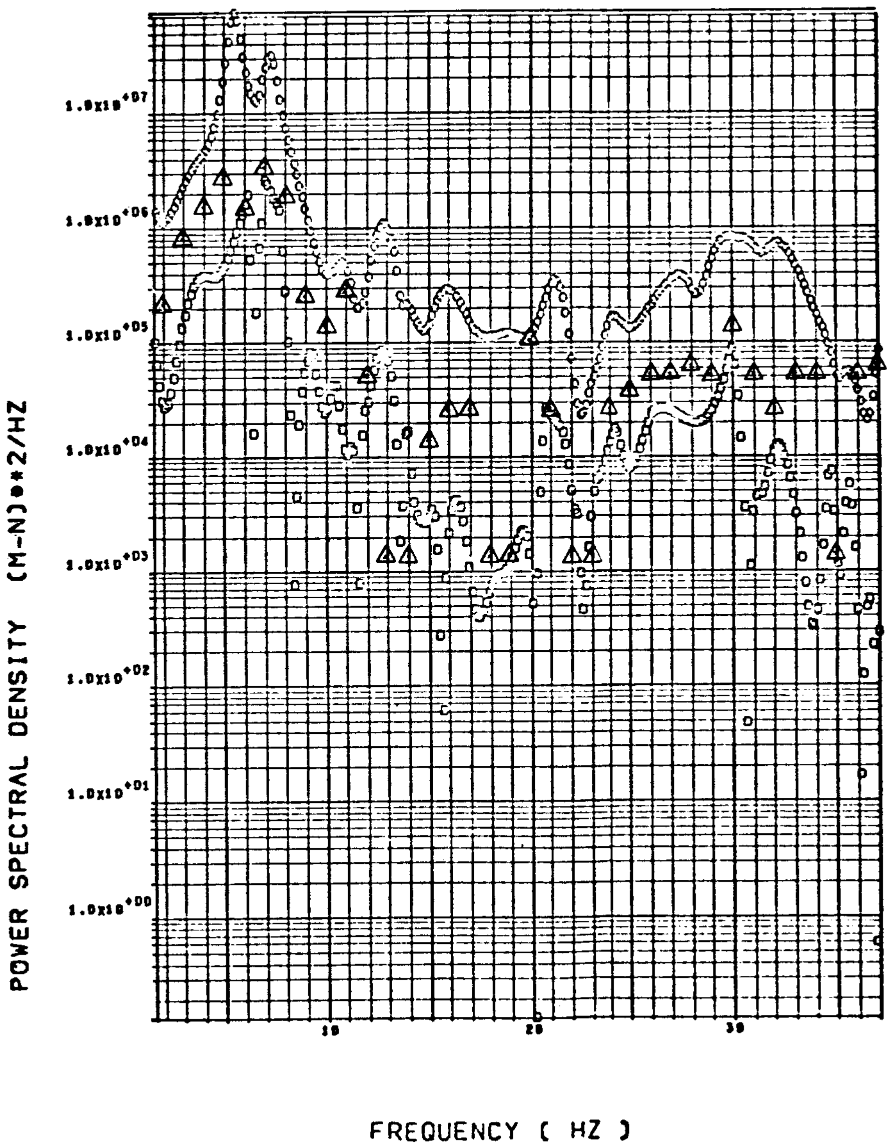

Figure 4.-(g) Wing bending moment (continued)

△ SW124 $\alpha_{FLT} = 13.1^{\circ}$

F-111A WING BUFFET RESPONSE. FLT 61. RUN R227
SWEEP= 50 DEG. MACH=.85. ALT=8302(M). ALPHA= 14.4
WING BENDING MOMENT (M-N) AT SPAN STATION 75
CIRCLE = UPPER BOUNDS SQUARE = LOWER BOUNDS

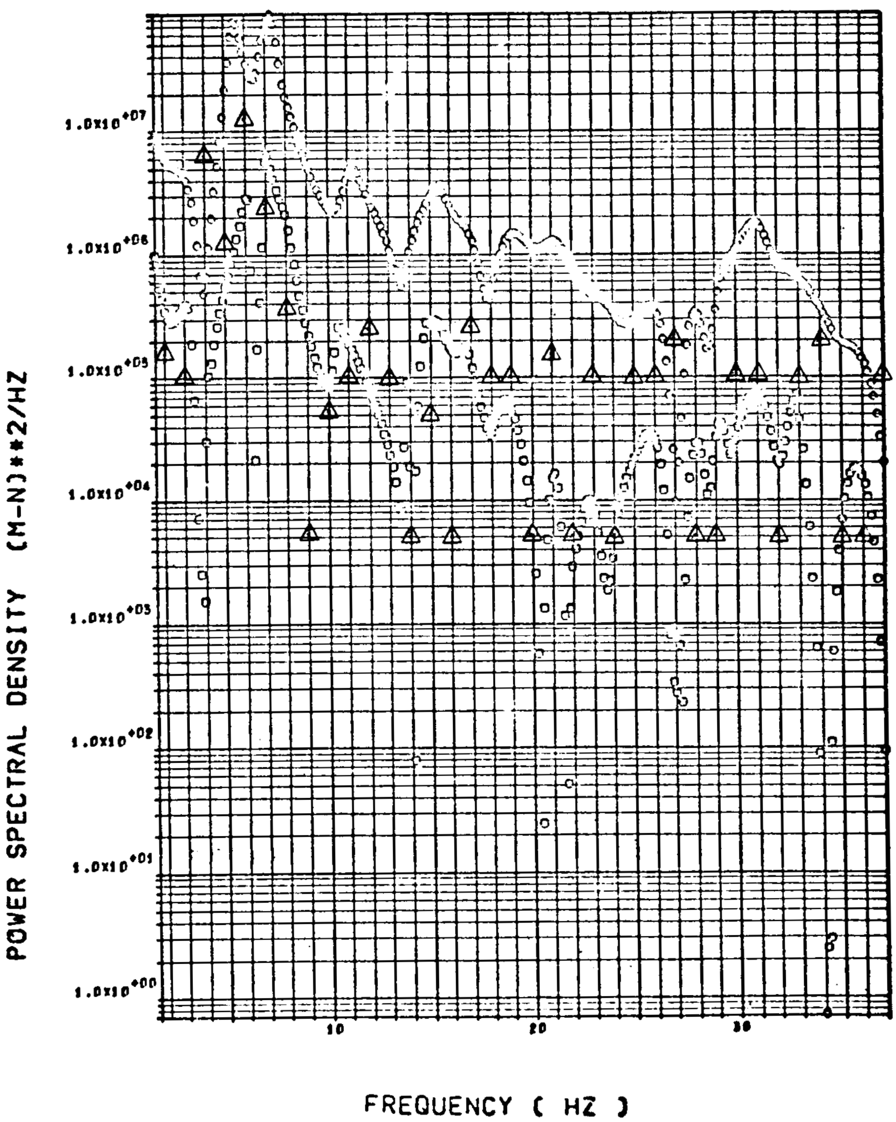

Figure 4.-(g) Wing bending moment (continued)

△ SW125 $\alpha_{FLT} = 8.9^{o}$

F-111A WING BUFFET RESPONSE. FLT 61. RUN R227
SWEEP= 50 DEG. MACH=.85. ALT=8382(M). ALPHA=8.9
WING TORQUE (M-N) AT SPAN STATION 75
CIRCLE = UPPER BOUNDS SQUARE = LOWER BOUNDS

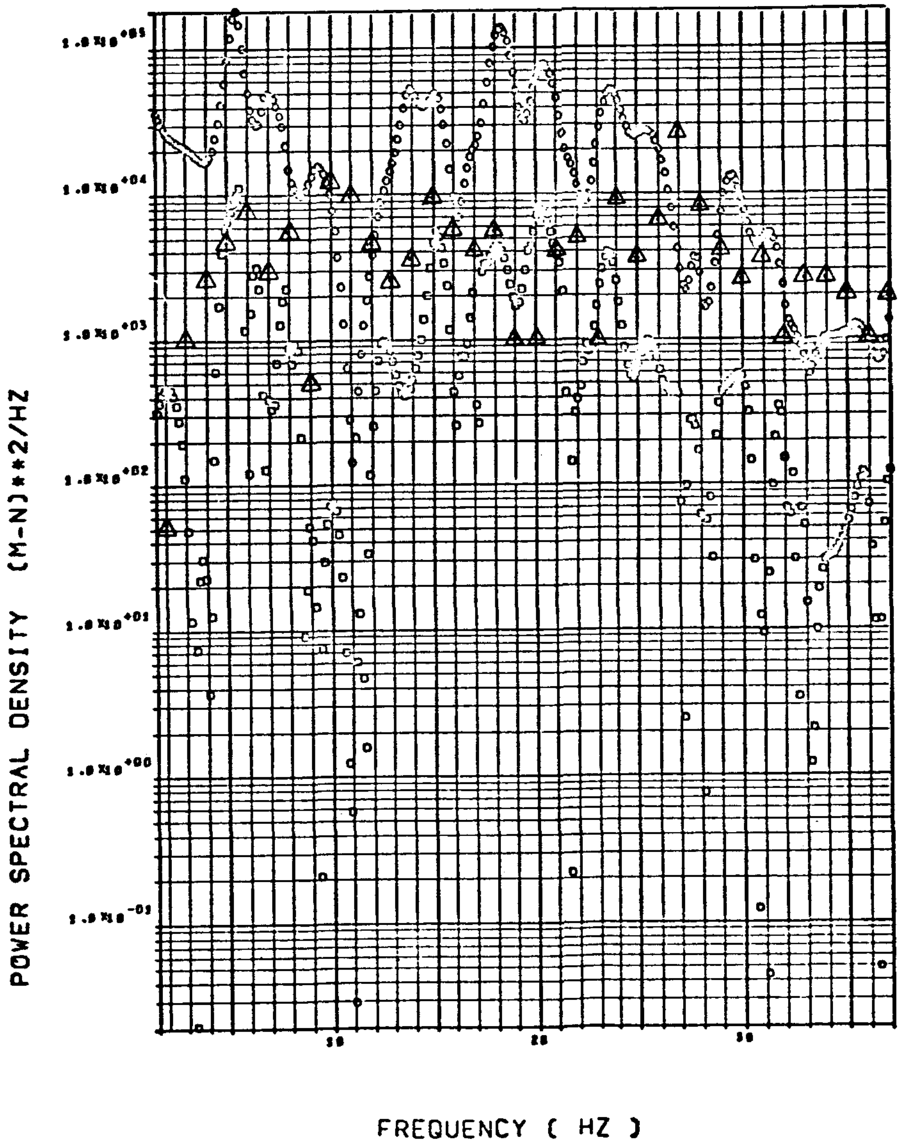

Figure 4.-(h) Wing torsion

Δ SW125

$\alpha_{FLT} = 11.1^{\circ}$

F-111A WING BUFFET RESPONSE. FLT 61. RUN R227
SWEEP= 50 DEG. MACH=.85. ALT=8382(M). ALPHA= 11.1
WING TORQUE (M-N) AT SPAN STATION 75
CIRCLE = UPPER BOUNDS   SQUARE = LOWER BOUNDS

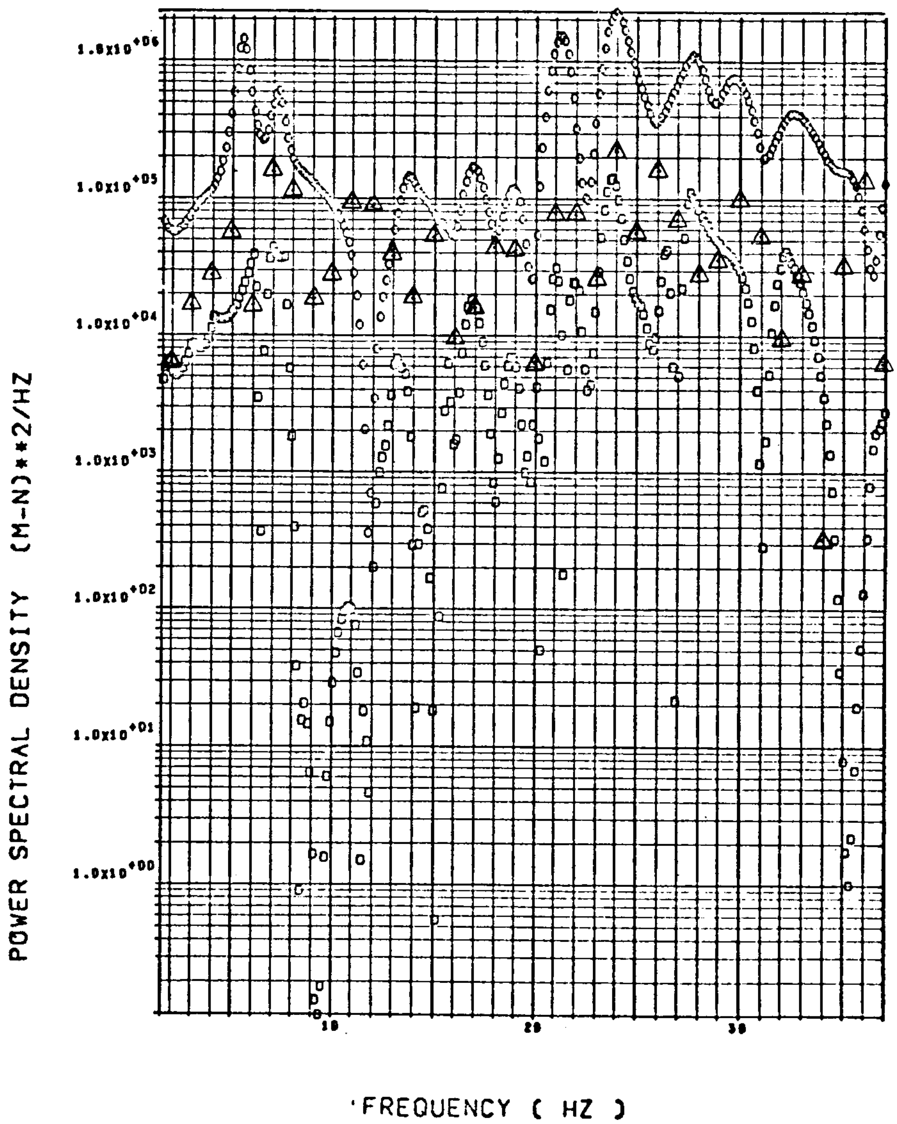

Figure 4.-(h) Wing torsion (continued)

△ SW125 $\alpha_{FLT} = 13.1^{o}$

F-111A WING BUFFET RESPONSE. FLT 61. RUN R227
SWEEP= 50 DEG. MACH=.85. ALT=8302(M). ALPHA= 14.4
WING TORQUE (M-N) AT SPAN STATION 75
CIRCLE = UPPER BOUNDS SQUARE = LOWER BOUNDS

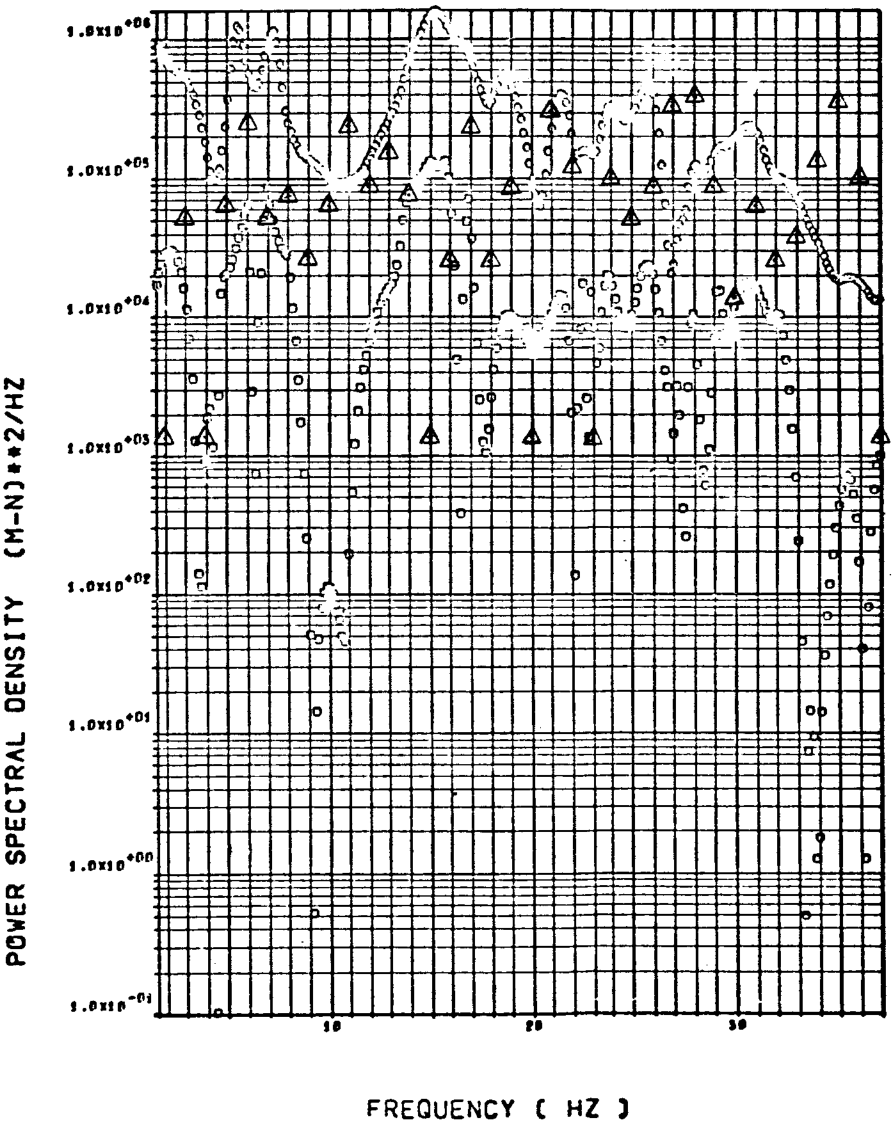

Figure 4.-(h) Wing torsion (continued)

△ ST077 ◇ ST072 $\alpha_{FLT} = 8.9^{o}$

F-111A WING BUFFET RESPONSE, FLT 61, RUN R227
SWEEP= 50 DEG, MACH=.85, ALT=8382(M), ALPHA= 8.9
H.T. PIVOT SHEAR (N)
CIRCLE = UPPER BOUNDS SQUARE = LOWER BOUNDS

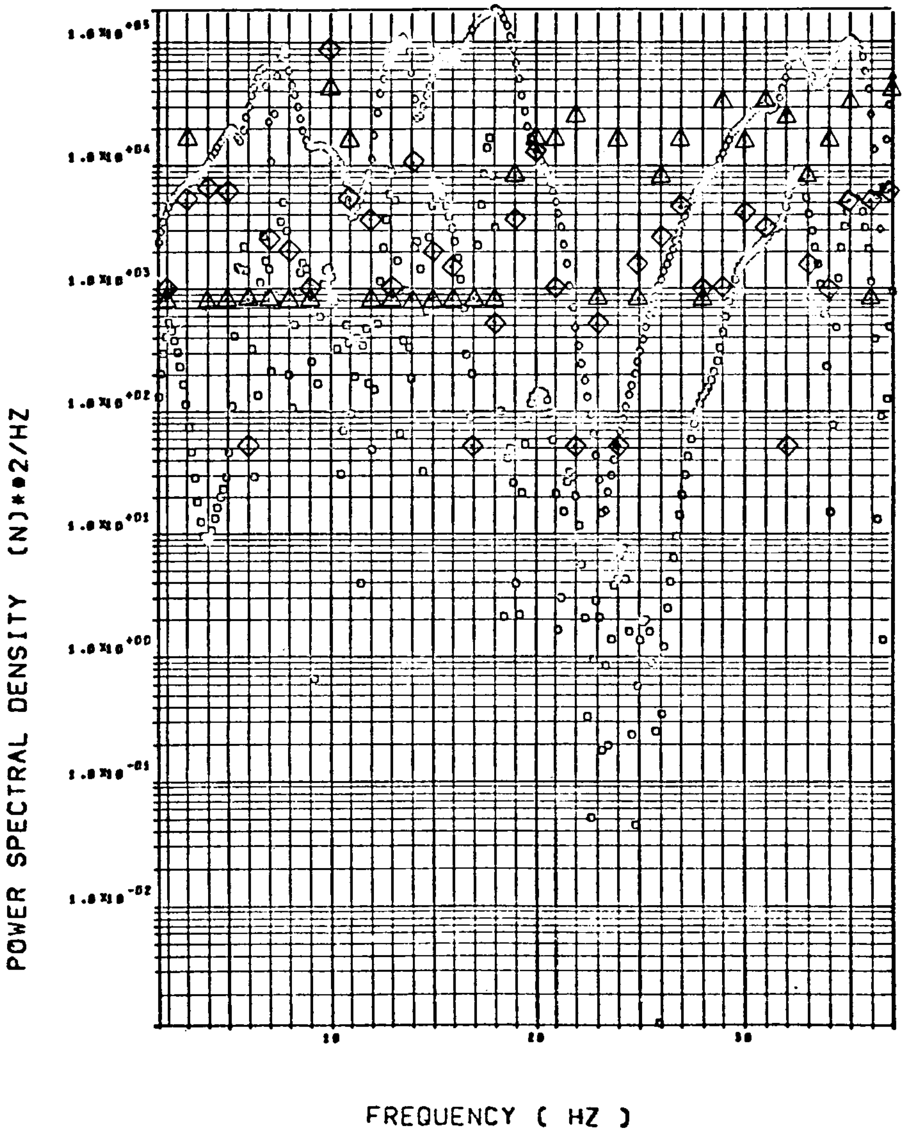

Figure 4.-(i) Horizontal tail shear

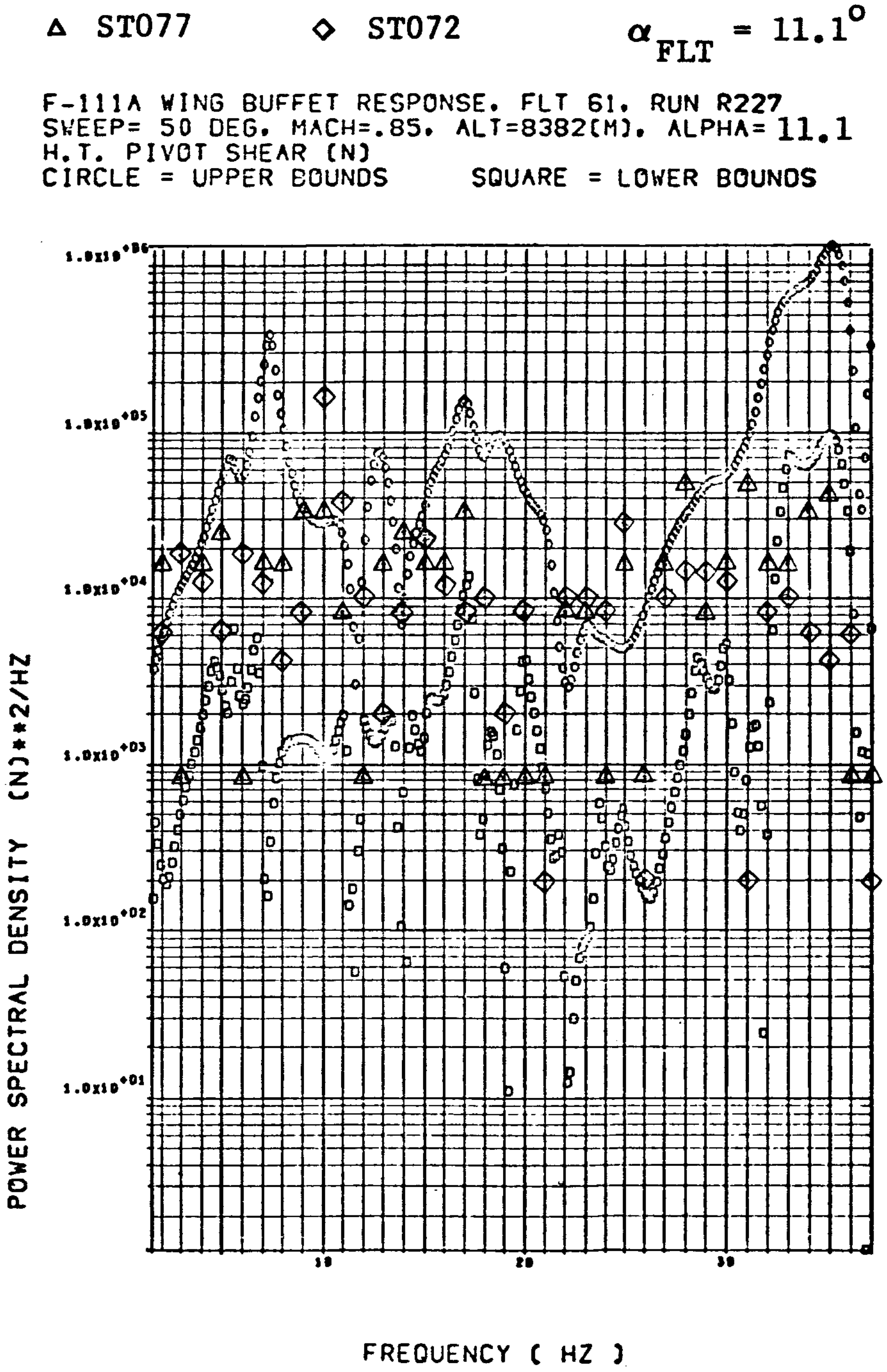

Figure 4.-(i) Horizontal tail shear (continued)

△ ST077　　◇ ST072　　α_{FLT} = 13.1°

F-111A WING BUFFET RESPONSE, FLT 61, RUN R227
SWEEP= 50 DEG, MACH=.85, ALT=8302(M), ALPHA= 14.4
H.T. PIVOT SHEAR (N)
CIRCLE = UPPER BOUNDS　　SQUARE = LOWER BOUNDS

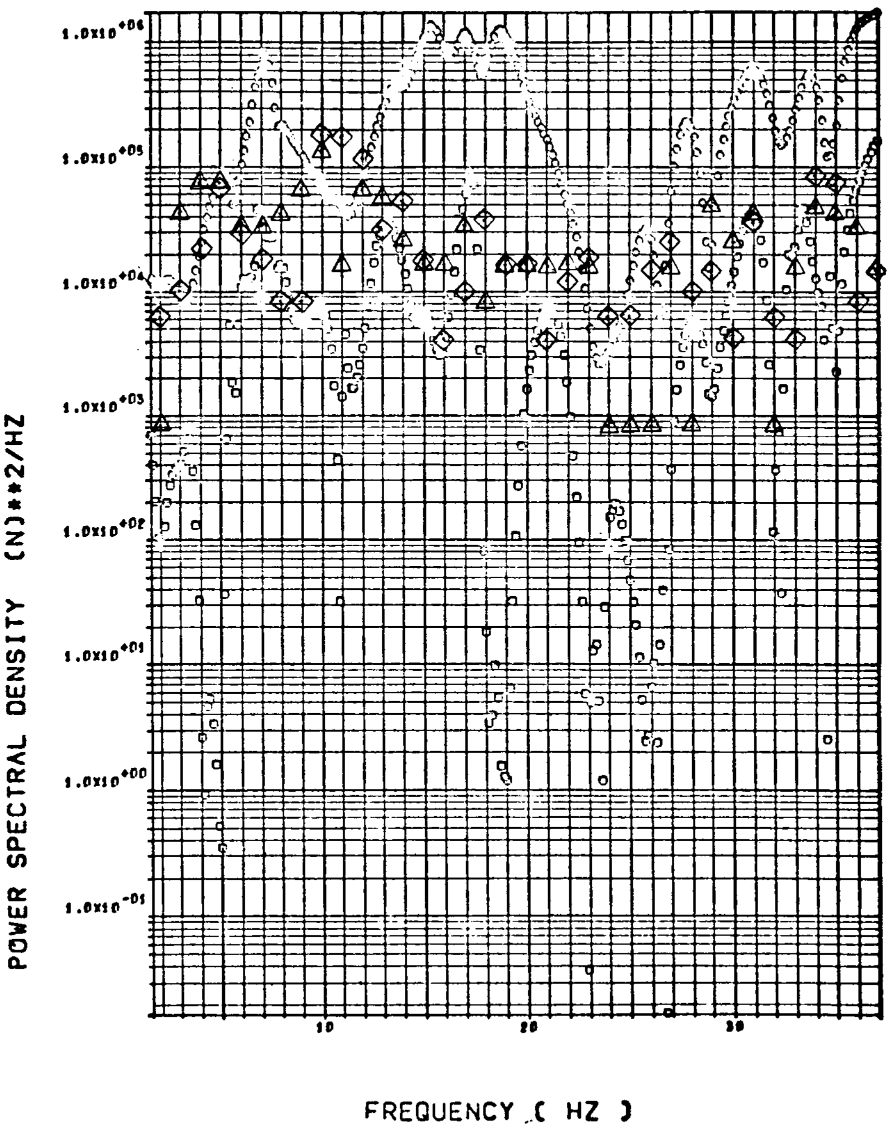

Figure 4.-(i) Horizontal tail shear (continued)

△ ST078 ◇ ST073 $\alpha_{FLT} = 8.9^{o}$

F-111A WING BUFFET RESPONSE. FLT 61. RUN R227
SWEEP= 50 DEG. MACH=.85. ALT=8382(M). ALPHA= 8.9
H.T. PIVOT BENDING MOMENT (M-N)
CIRCLE = UPPER BOUNDS SQUARE = LOWER BOUNDS

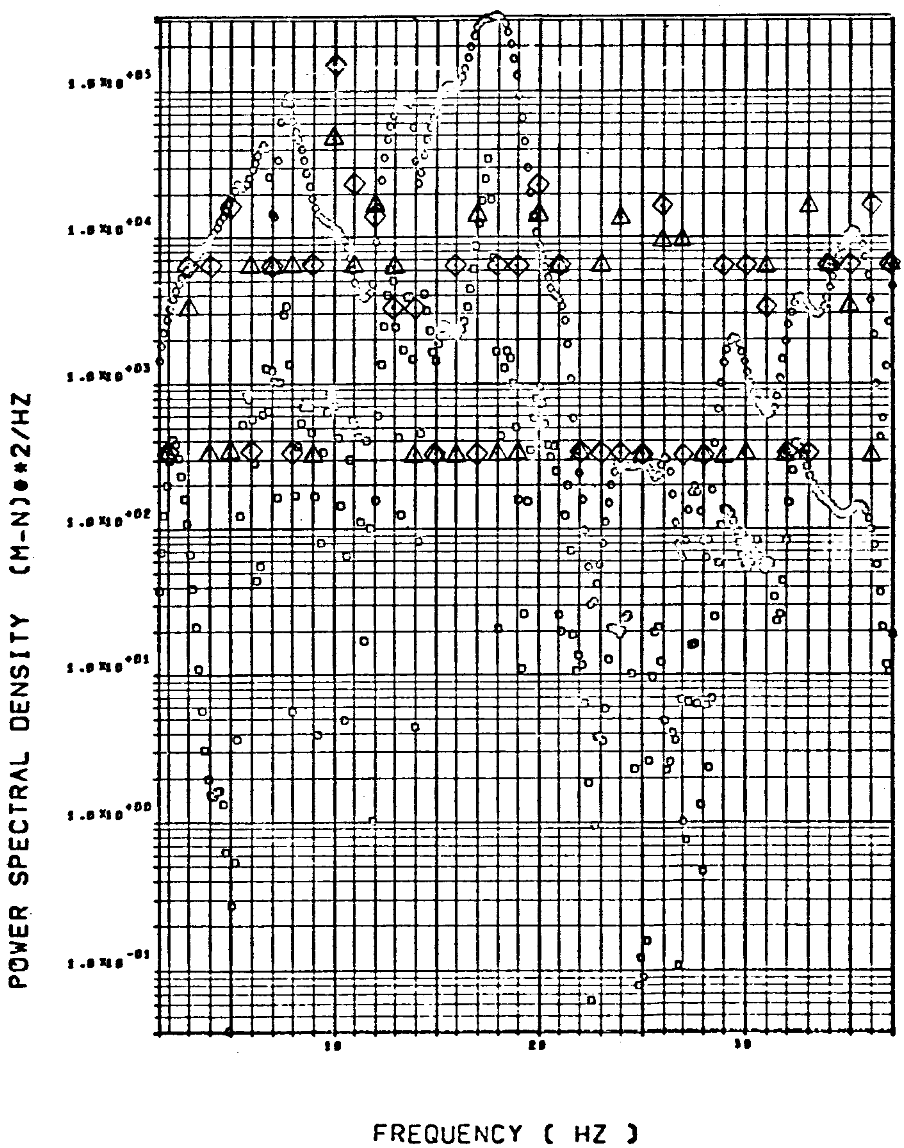

Figure 4.-(j) Horizontal tail bending moment

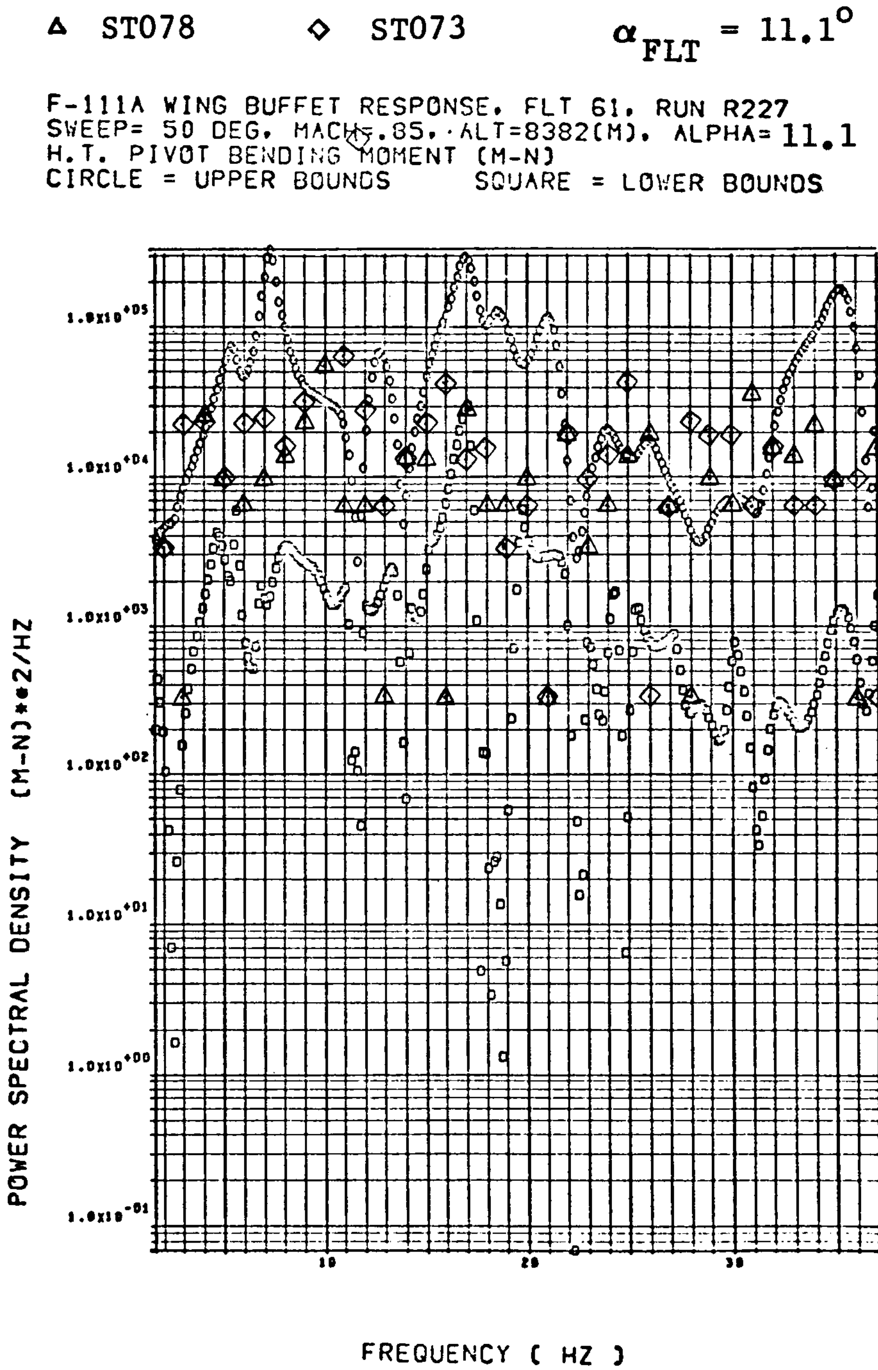

Figure 4.-(j) Horizontal tail bending moment (continued)

△ ST078 ◇ ST073 $\alpha_{FLT} = 13.1^{\circ}$

F-111A WING BUFFET RESPONSE, FLT 61, RUN R227
SWEEP= 50 DEG, MACH=.85, ALT=8332(M), ALPHA= 14.4
H.T. PIVOT BENDING MOMENT (M-N)
CIRCLE = UPPER BOUNDS SQUARE = LOWER BOUNDS

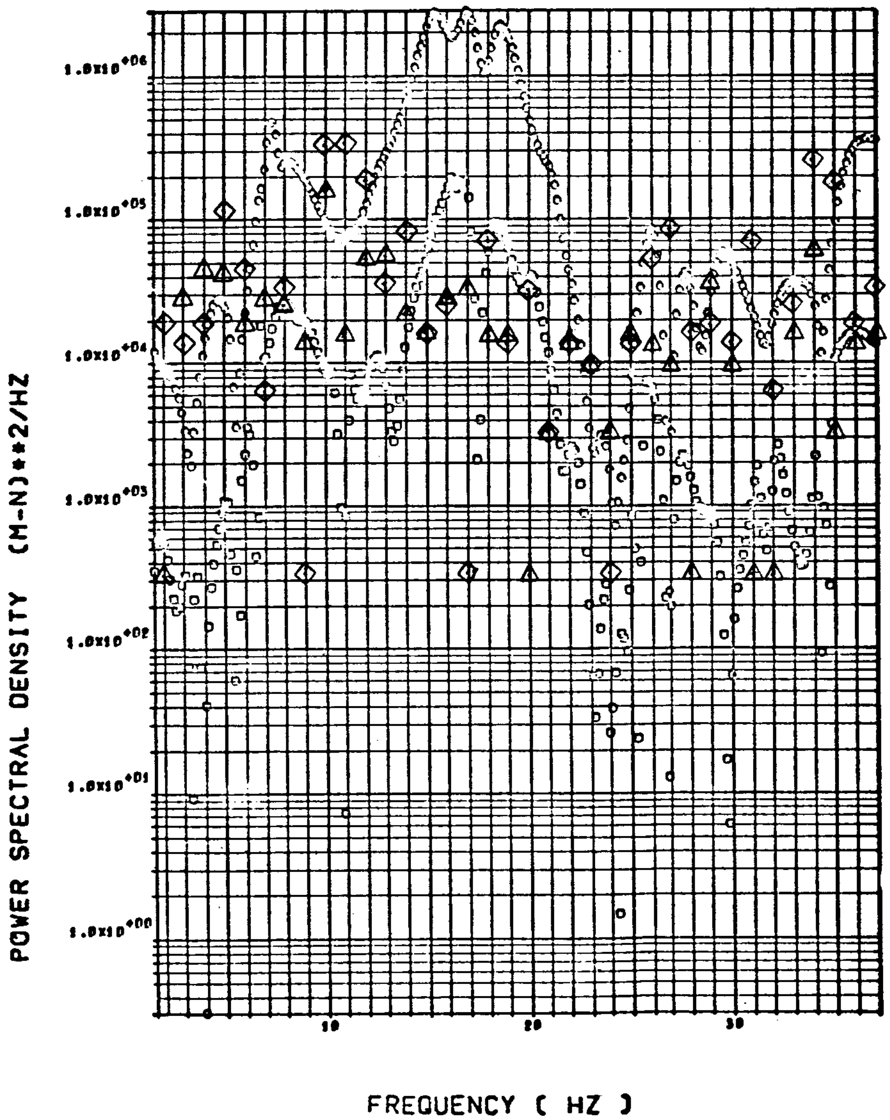

Figure 4.-(j) Horizontal tail bending moment (continued)

△ ST135   ◇ ST118 $\alpha_{FLT} = 8.9^{\circ}$

F-111A WING BUFFET RESPONSE, FLT 61, RUN R227
SWEEP= 50 DEG, MACH=.85, ALT=8382(M), ALPHA=8.9
H.T. PIVOT TORQUE (M-N)
CIRCLE = UPPER BOUNDS   SQUARE = LOWER BOUNDS

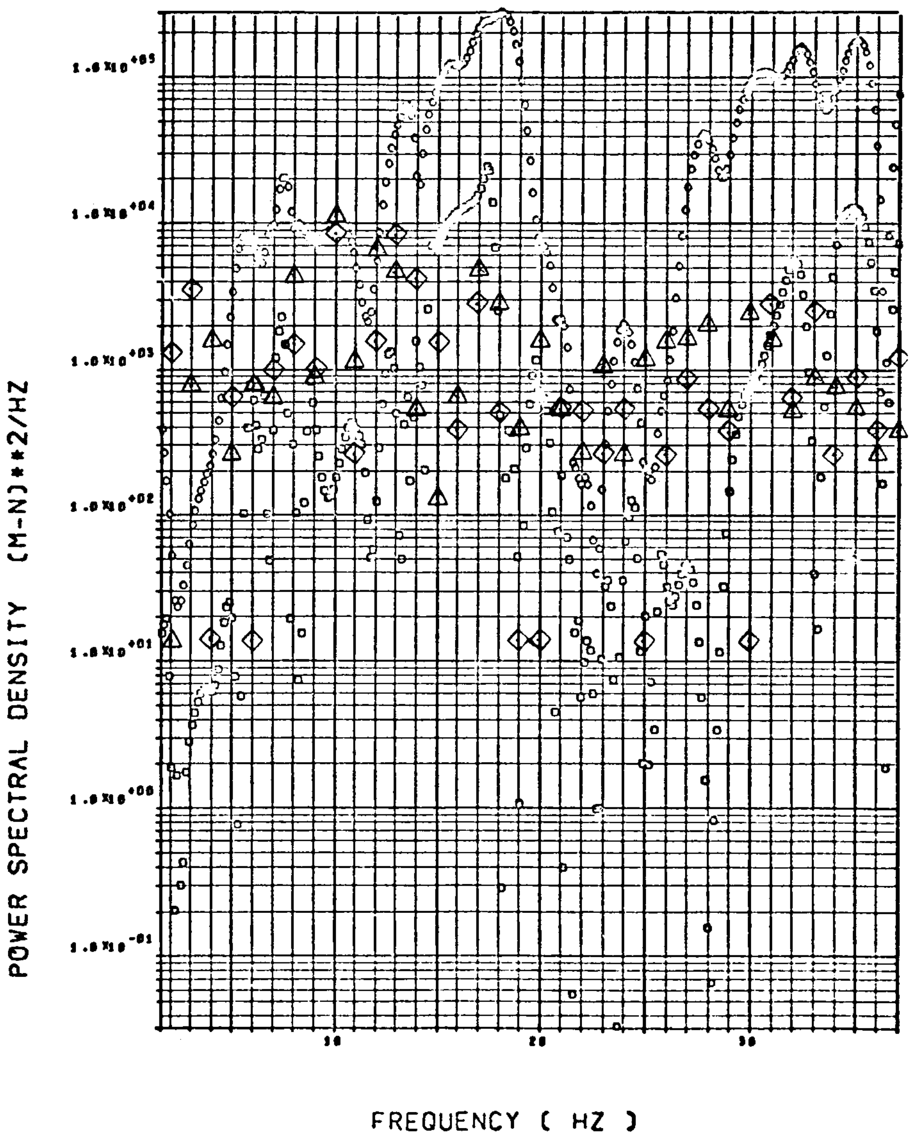

Figure 4.-(k) Horizontal tail torsion

△ ST135 ◇ ST118 $\alpha_{FLT} = 11.1^{\circ}$

F-111A WING BUFFET RESPONSE. FLT 61. RUN R227
SWEEP= 50 DEG. MACH=.85. ALT=8382(M). ALPHA= 11.1
H.T. PIVOT TORQUE (M-N)
CIRCLE = UPPER BOUNDS SQUARE = LOWER BOUNDS

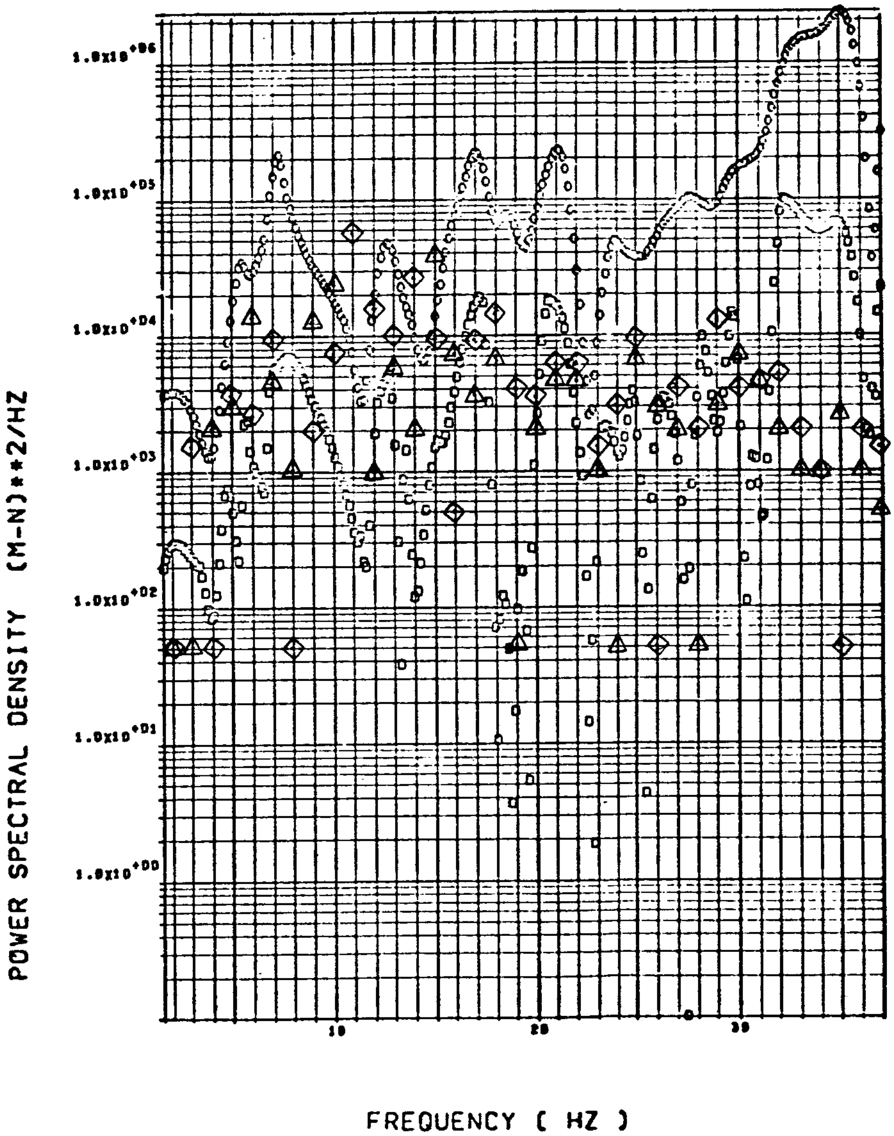

Figure 4.-(k) Horizontal tail torsion (continued)

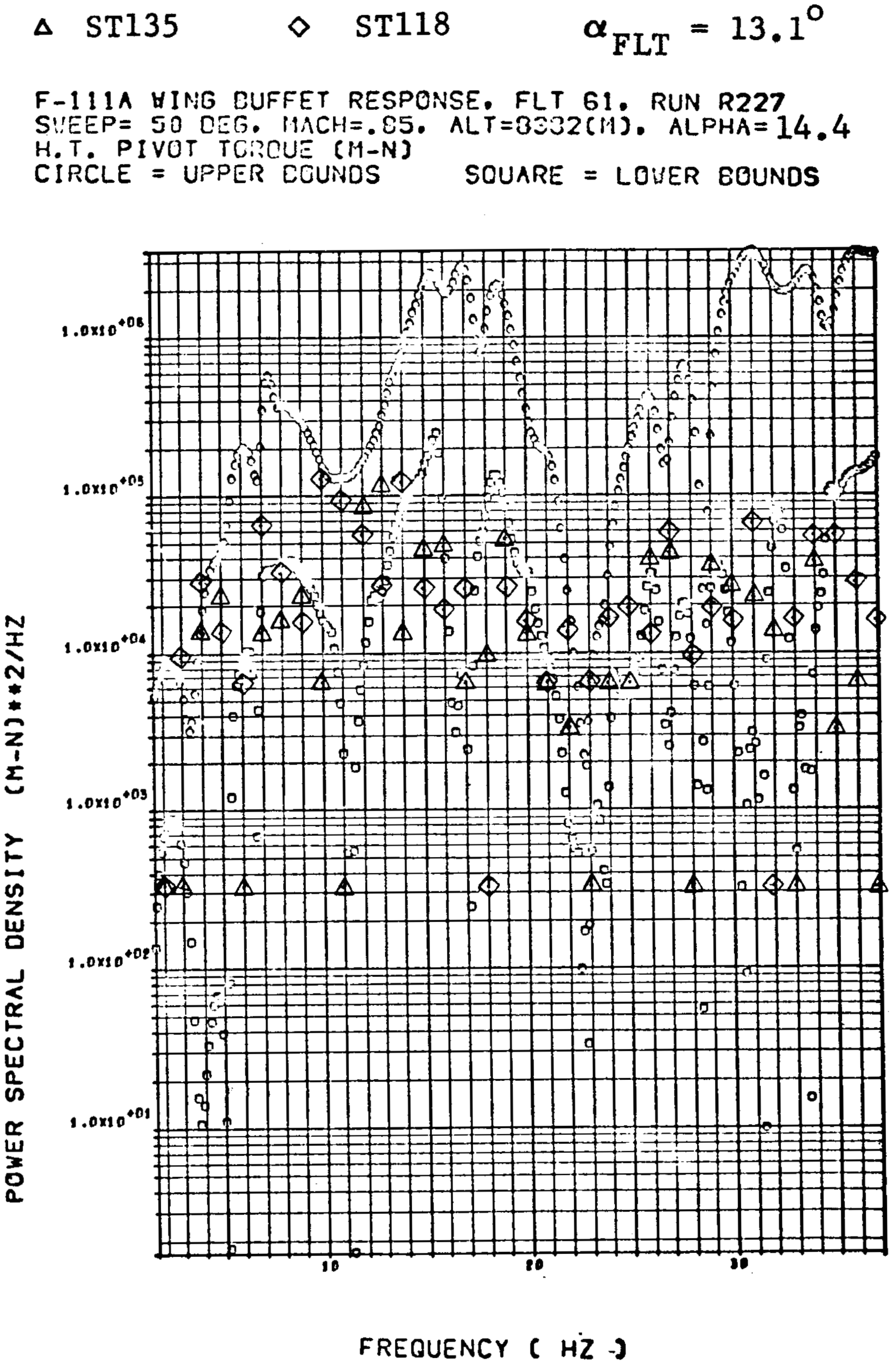

Figure 4.-(k) Horizontal tail torsion (continued)

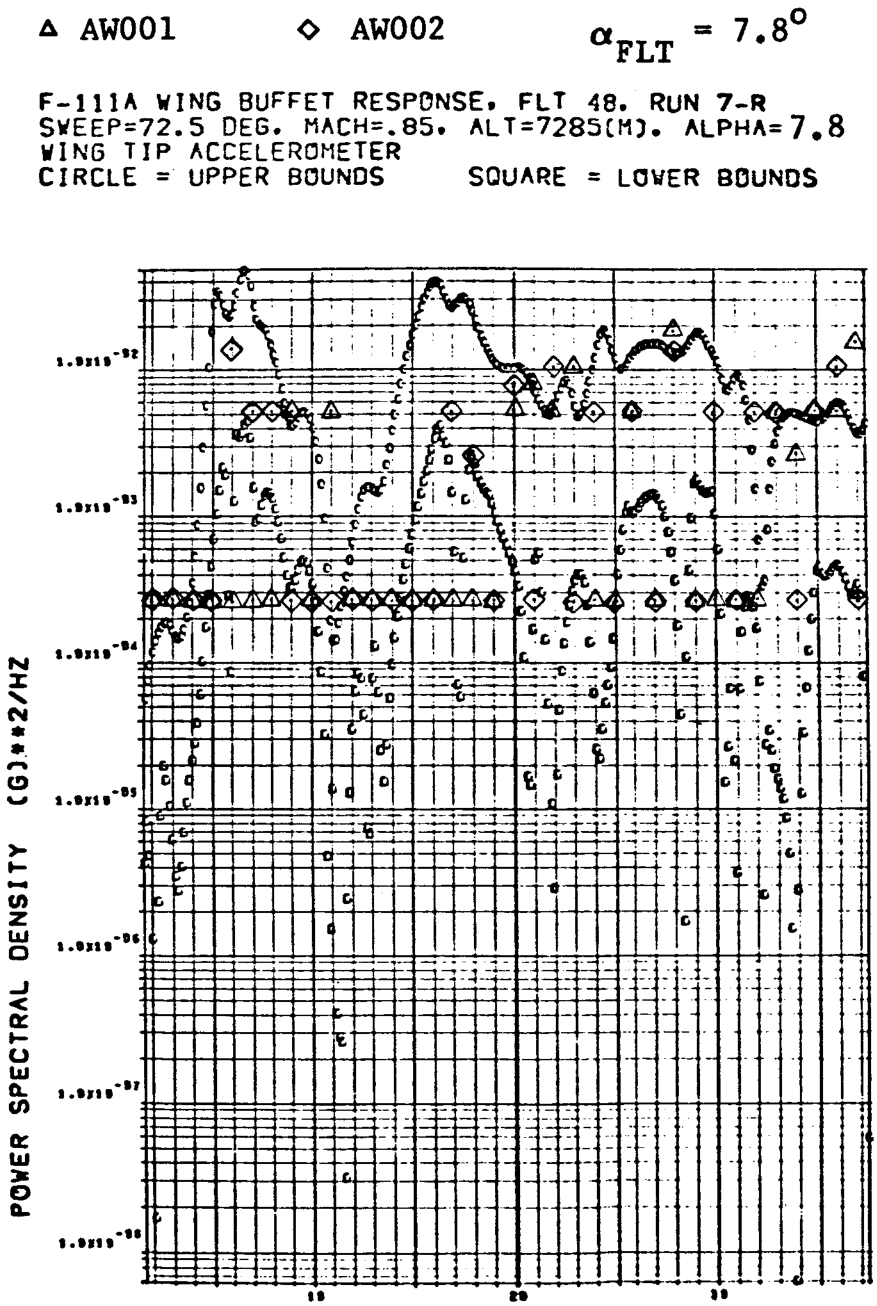

Figure 5.- Power spectra for
Case 5, total airplane (final method),
Λ=72.5°, M=0.85, alt.=7285m (23,900 ft)
(a) wing tip accelerometer

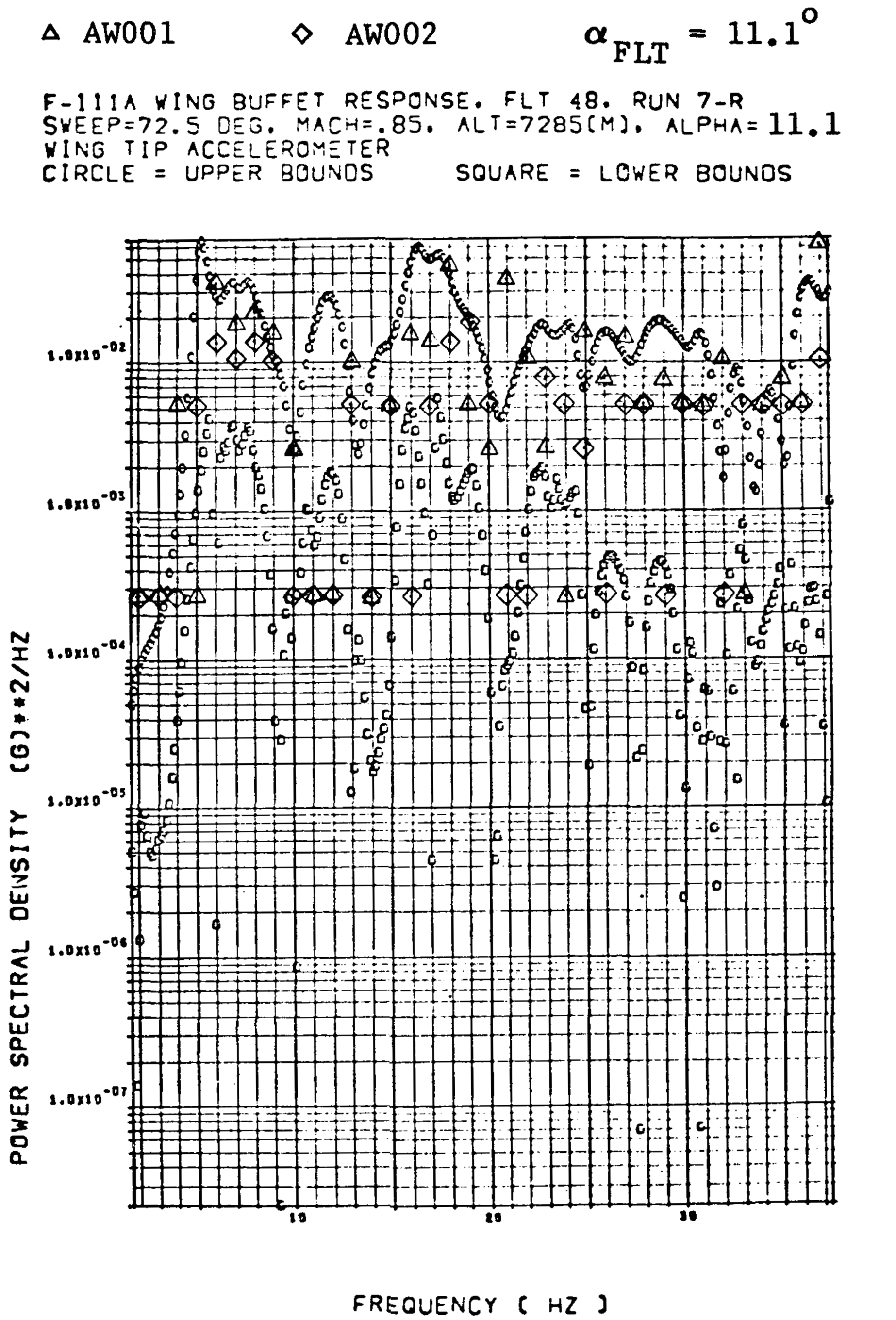

Figure 5.-(a) Wing tip accelerometer (continued)

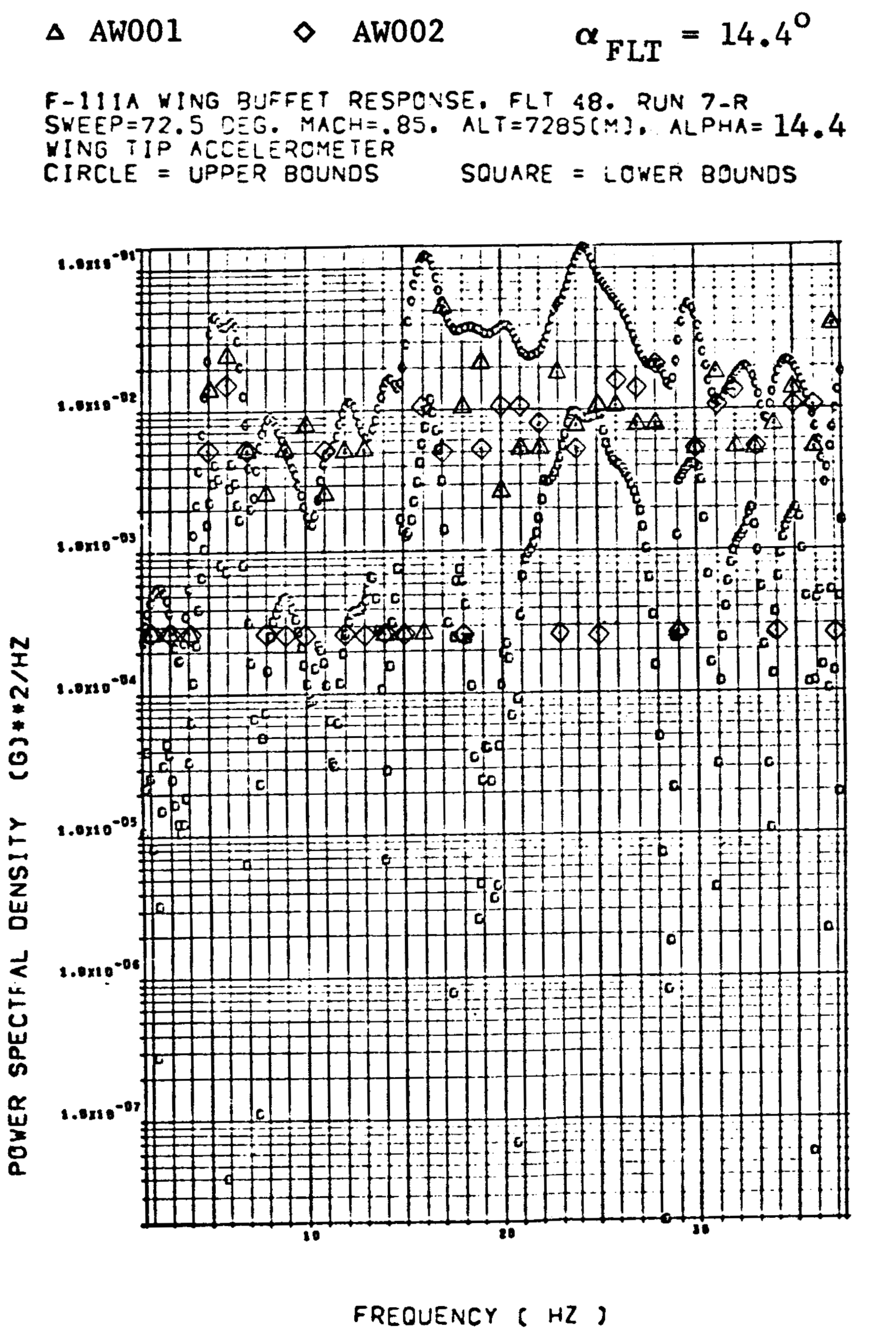

Figure 5.-(a) Wing tip accelerometer (continued)

◇ AB018 $\alpha_{FLT} = 7.8^{\circ}$

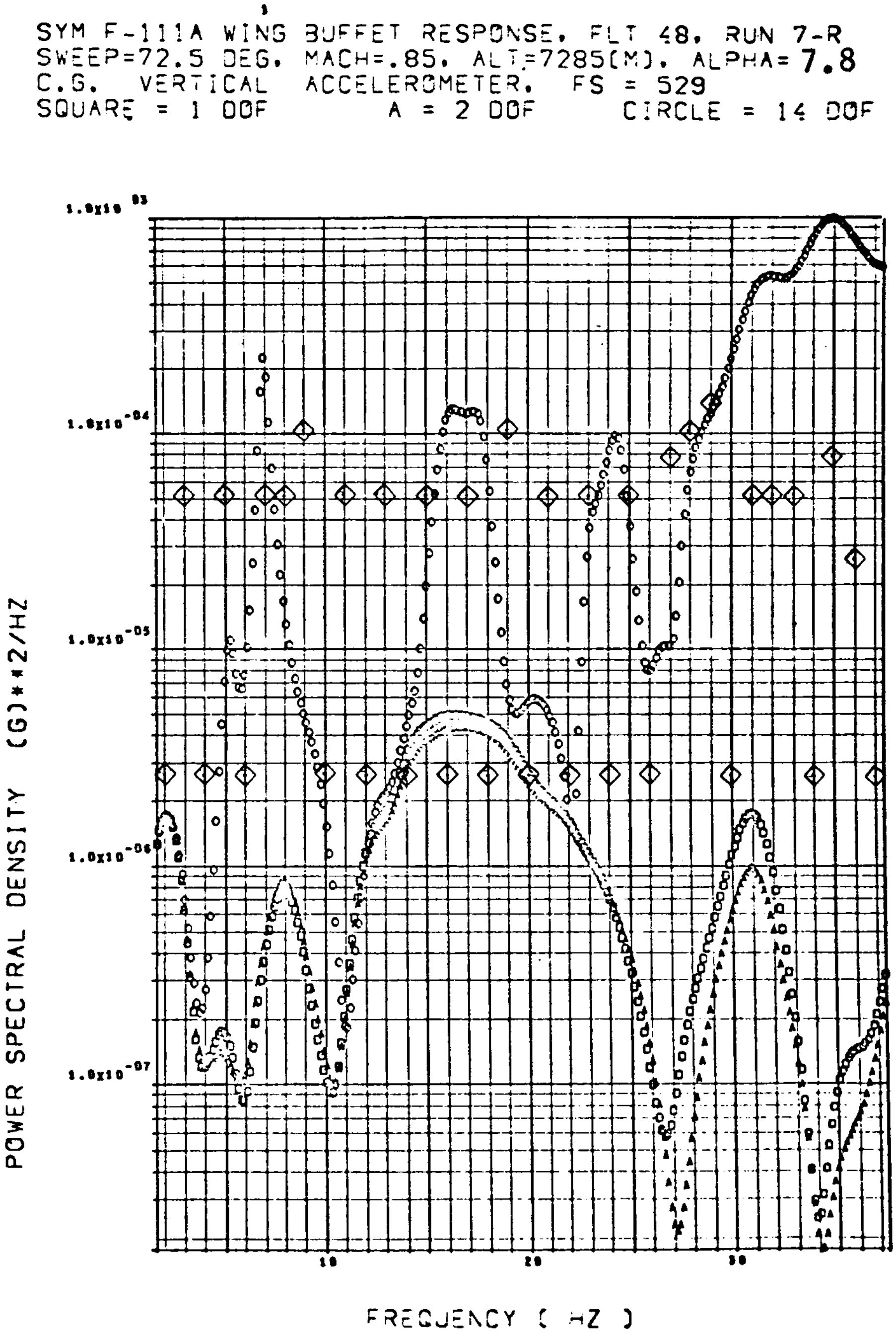

Figure 5.-(b) C.G. vertical accelerometer

◇ AB018 $\alpha_{FLT} = 11.1^{\circ}$

SYM F-111A WING BUFFET RESPONSE. FLT 40. RUN 7-R
SWEEP=72.5 DEG. MACH=.85. ALT=7225(M). ALPHA= 11.1
C.G. VERTICAL ACCELEROMETER. FS = 529
SQUARE = 1 DOF A = 2 DOF CIRCLE = 14 DOF

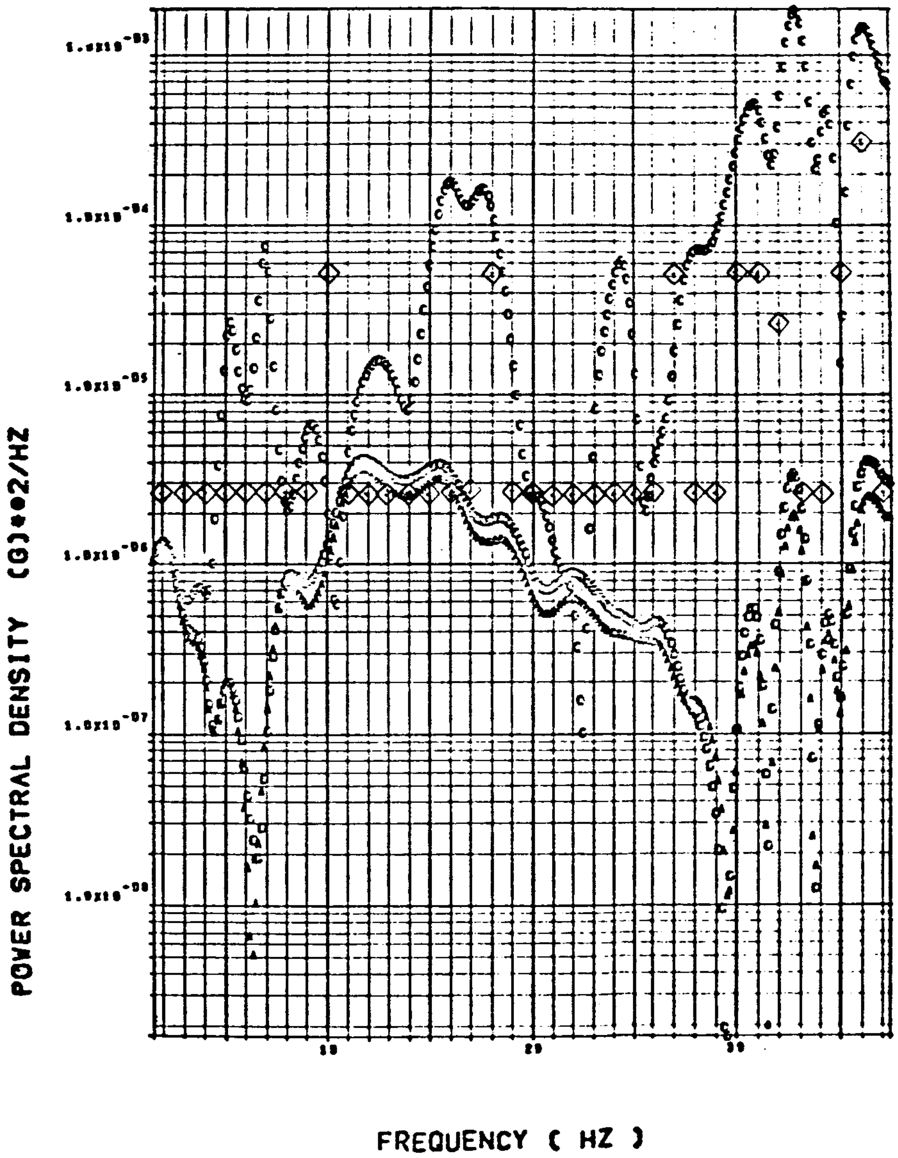

Figure 5.-(b) C.G. vertical accelerometer (continued)

◇ AB018 $\alpha_{FLT} = 14.4^{o}$

SYM F-111A WING BUFFET RESPONSE, FLT 43, RUN 7-R
SWEEP=72.5 DEG, MACH=.65, ALT=7205(M), ALPHA=14.4
C.G. VERTICAL ACCELEROMETER, FS = 529
SQUARE = 1 DOF A = 2 DOF CIRCLE = 14 DOF

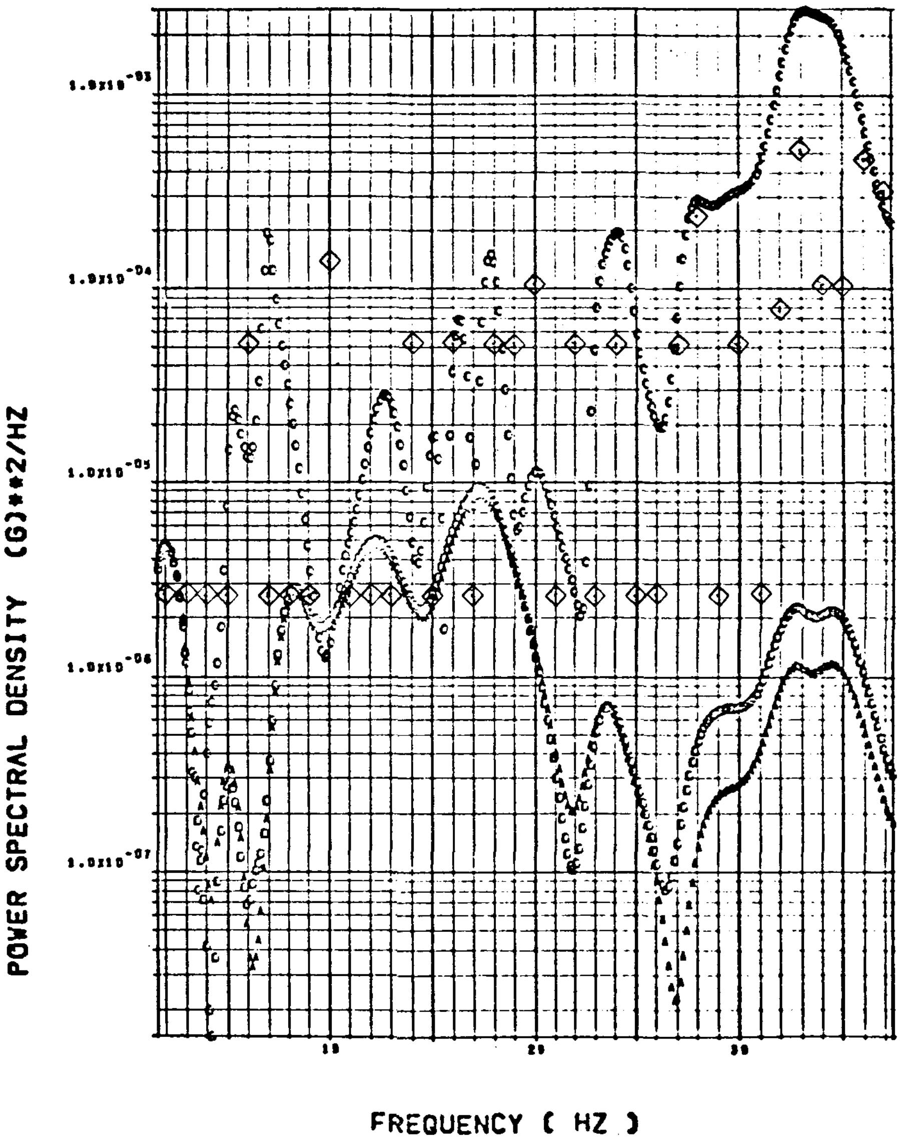

Figure 5.-(b) C.G. vertical accelerometer (continued)

◇ AF009 $\alpha_{FLT} = 7.8^{o}$

SYM F-111A WING BUFFET RESPONSE, FLT 48, RUN 7-R
SWEEP=72.5 DEG, MACH=.85, ALT=7285(M), ALPHA= 7.8
PILOT STATION VERTICAL ACCELEROMETER, FS = 255
SQUARE = 1 DOF A = 2 DOF CIRCLE = 14 DOF

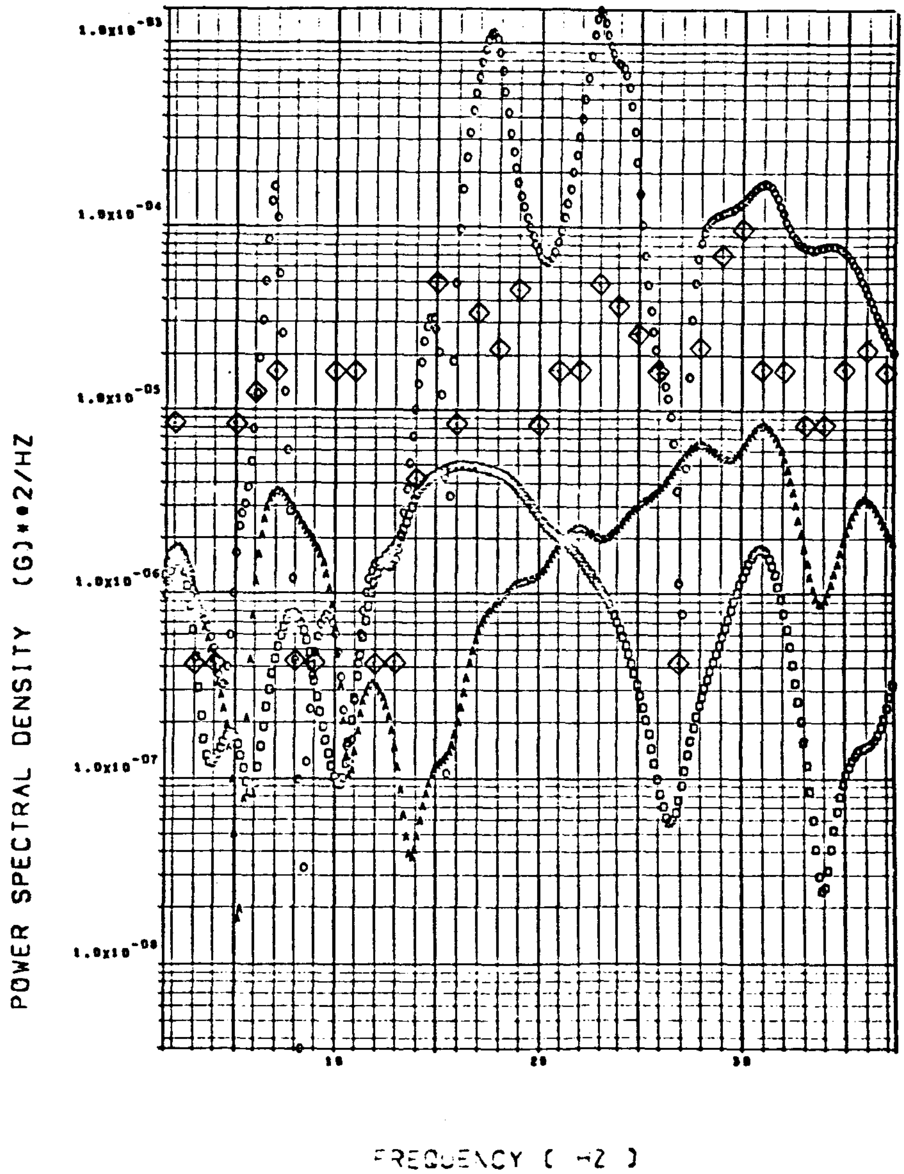

Figure 5.-(c) Pilot seat vertical accelerometer

◇ AF009 $\alpha_{FLT} = 11.1^{\circ}$

SYM F-111A WING BUFFET RESPONSE, FLT 40, RUN 7-R
SWEEP=72.5 DEG, MACH=.85, ALT=7200(M), ALPHA= 11.1
PILOT STATION VERTICAL ACCELEROMETER, FS = 255
SQUARE = 1 DOF A = 2 DOF CIRCLE = 14 DOF

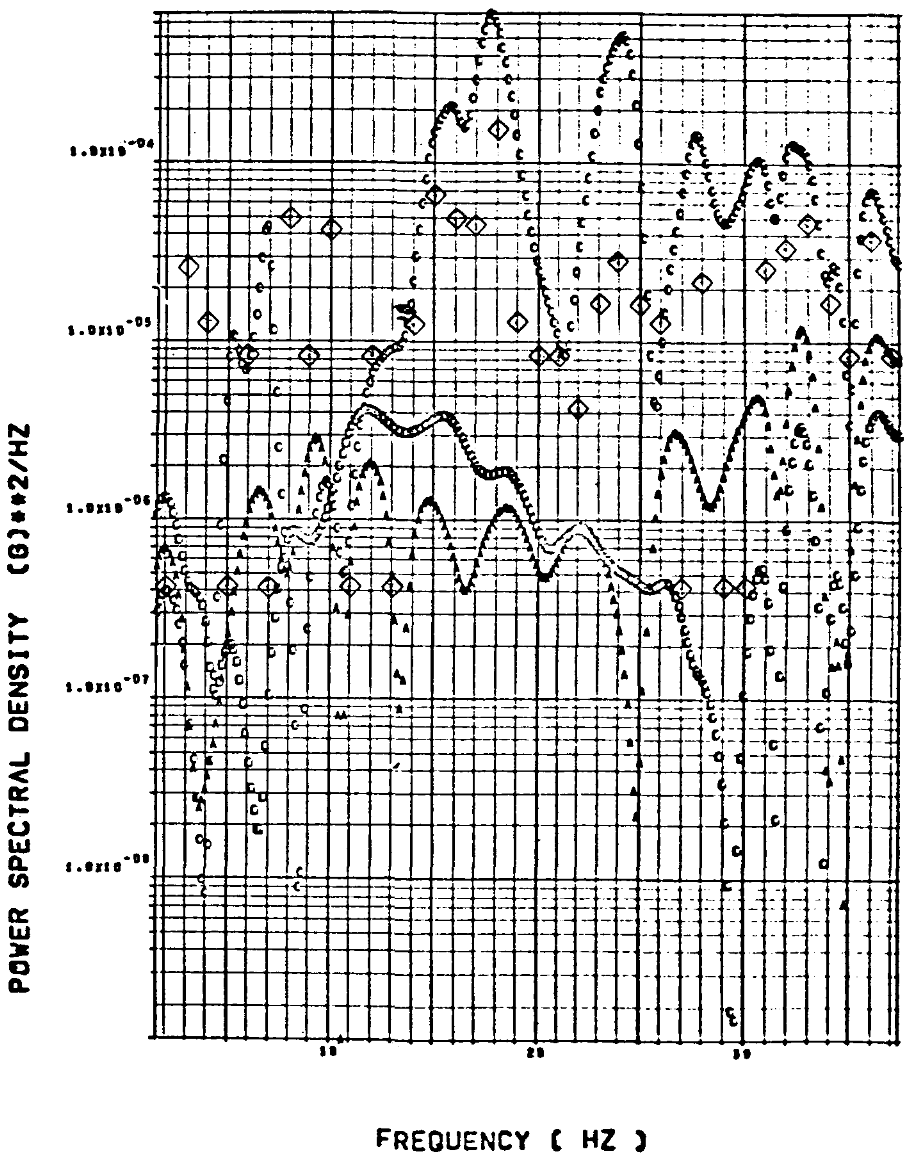

Figure 5.-(c) Pilot seat vertical accelerometer (continued)

◇ AF009 $\alpha_{FLT} = 14.4^{o}$

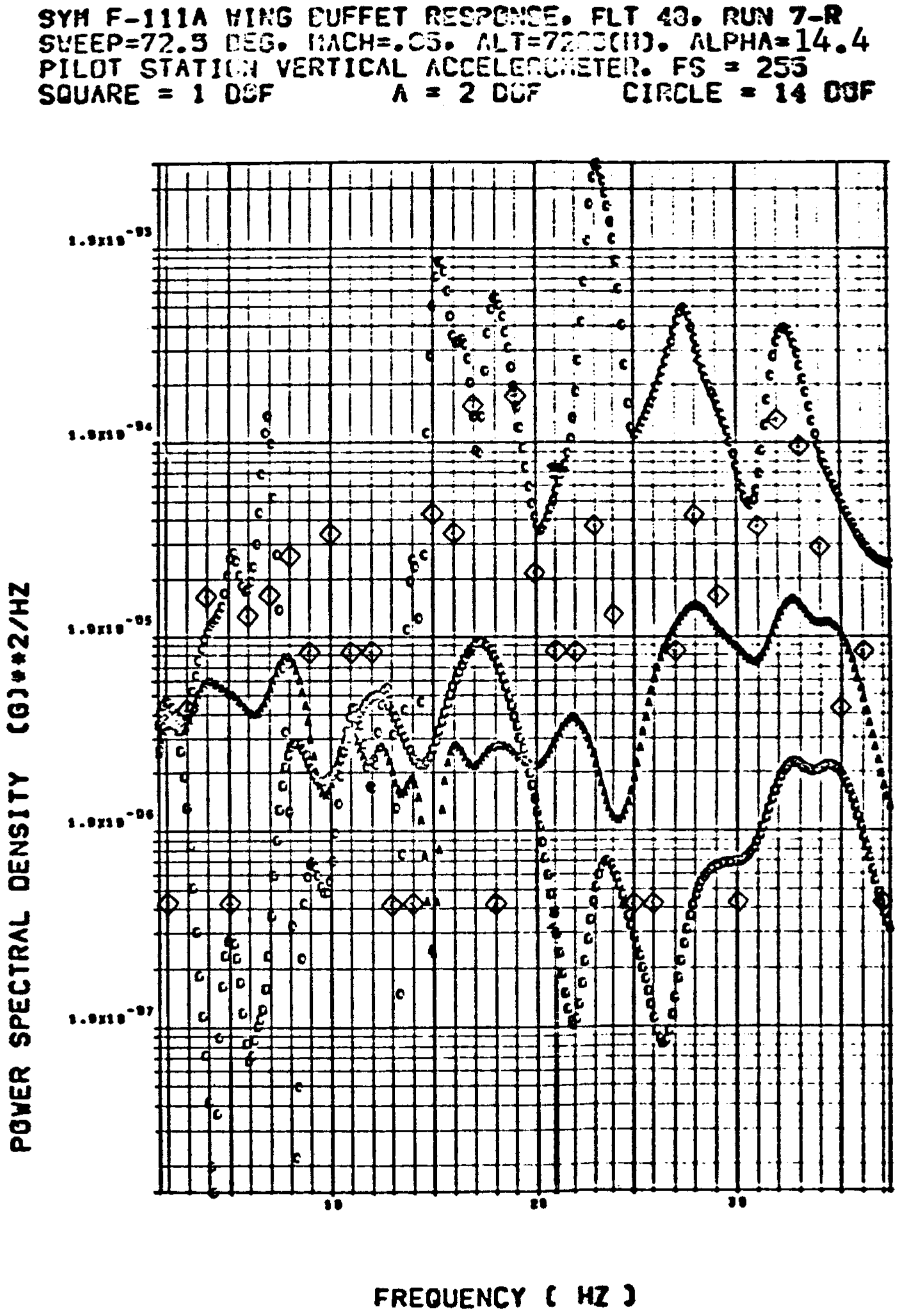

Figure 5.-(c) Pilot seat vertical accelerometer (continued)

◇ AB020 $\alpha_{FLT} = 7.8^{\circ}$

ANTI F-111A WING BUFFET RESPONSE. FLT 48. RUN 7-R
SWEEP=72.5 DEG. MACH=.85. ALT=7285(M). ALPHA=7.8
C.G. LATERAL ACCELEROMETER. FS = 529
SQUARE = 1 DOF A = 3 DOF CIRCLE = 18 DOF

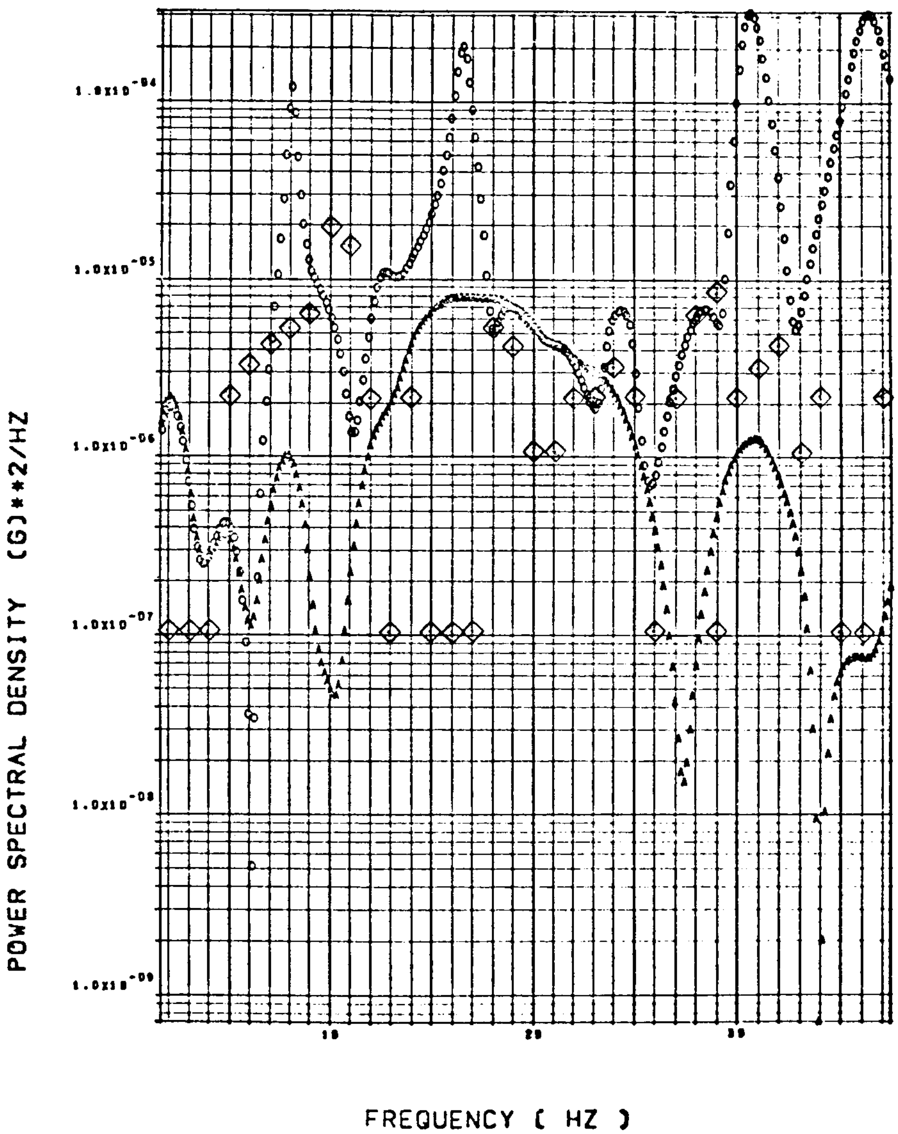

Figure 5.-(d) C.G. lateral accelerometer

◇ AB020 $\alpha_{FLT} = 11.1^{o}$

ANTI F-111A WING BUFFET RESPONSE, FLT 40, RUN 7-R
SWEEP=72.5 DEG, MACH=.65, ALT=7200(M), ALPHA= 11.1
C.G. LATERAL ACCELEROMETER, FS = 523
SQUARE = 1 DOF A = 3 DOF CIRCLE = 10 DOF

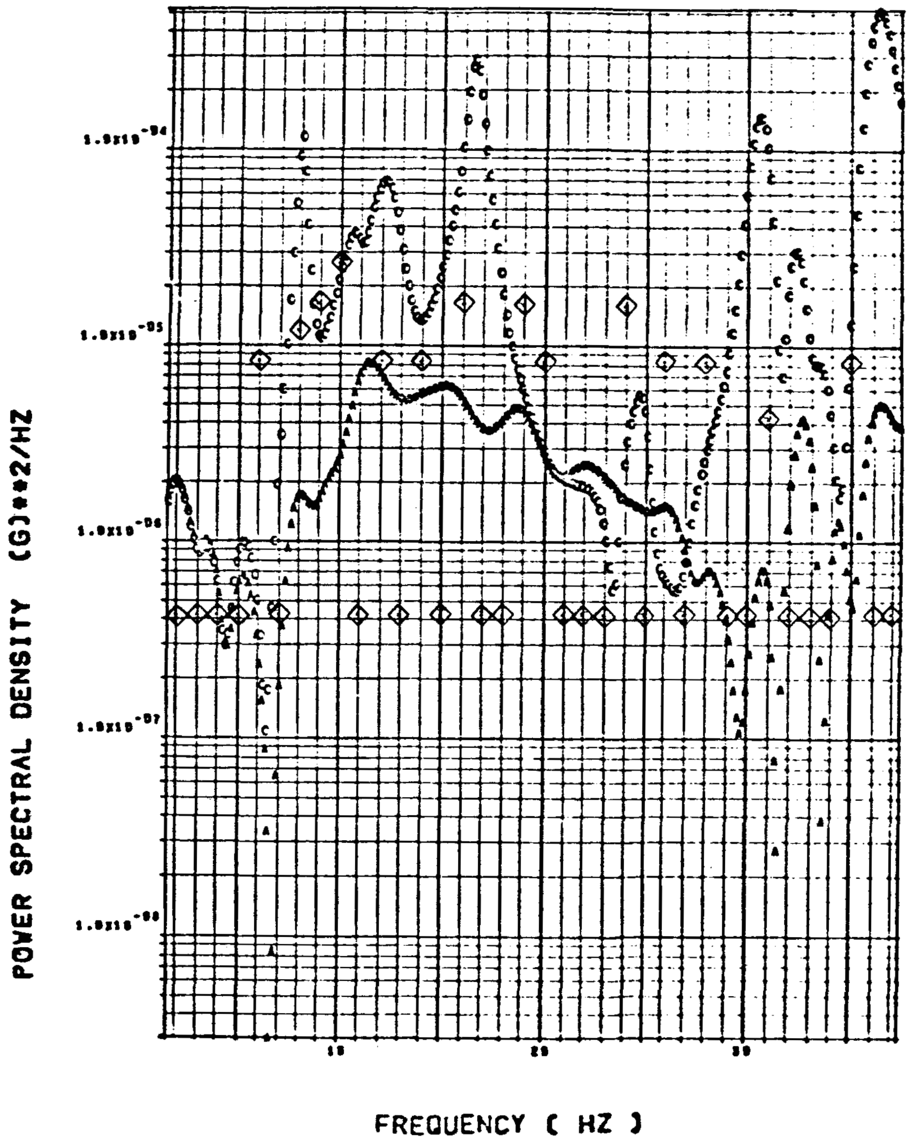

Figure 5.-(d) C.G. lateral accelerometer (continued)

◇ AB020

$\alpha_{FLT} = 14.4^{o}$

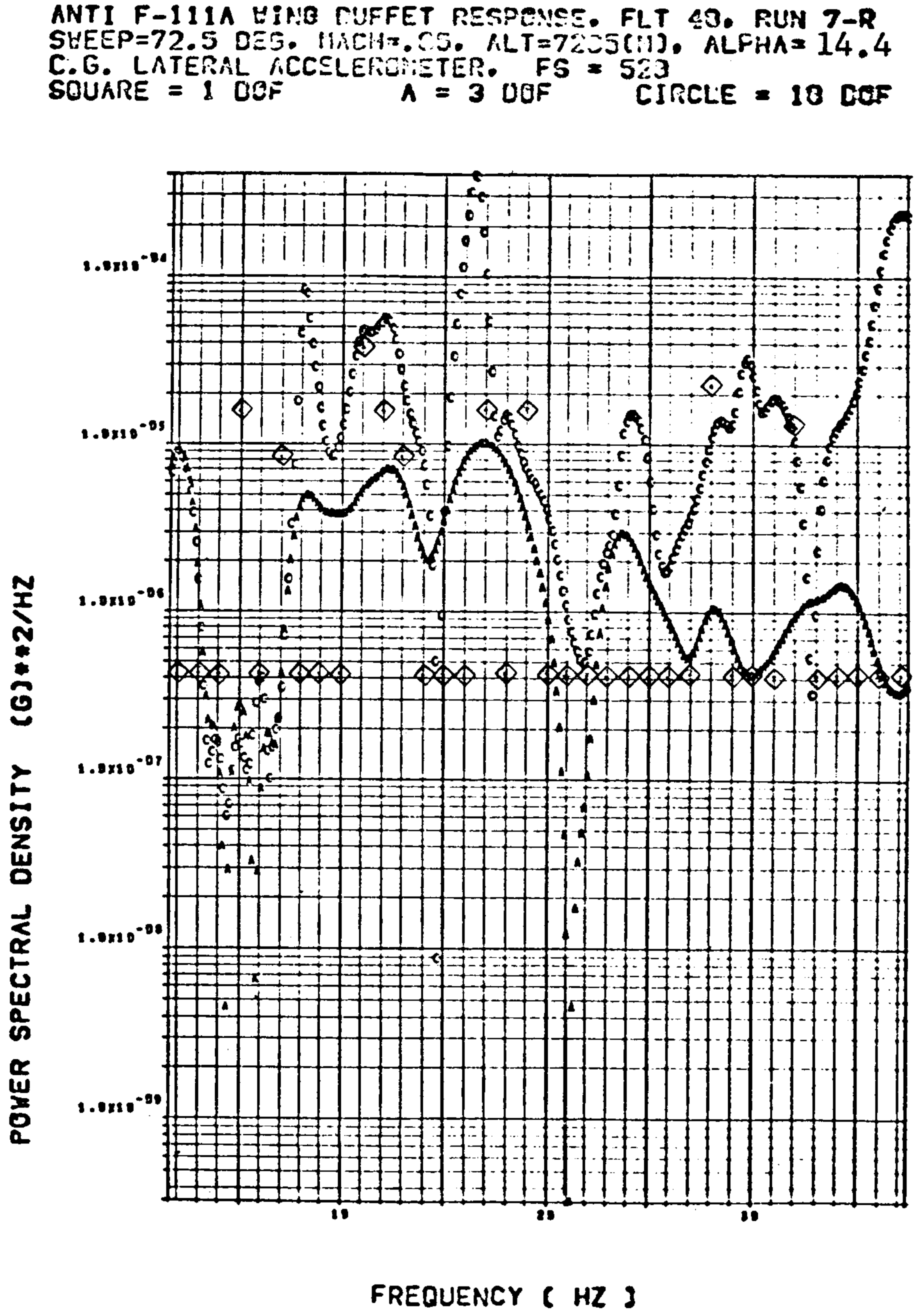

Figure 5.-(d) C.G. lateral accelerometer (continued)

◇ AF010 $\alpha_{FLT} = 7.8^{o}$

ANTI F-111A WING BUFFET RESPONSE. FLT 48. RUN 7-R
SWEEP=72.5 DEG. MACH=.85. ALT=7285(M). ALPHA= 7.8
PILOT STATION LATERAL ACCELEROMETER. FS = 255
SQUARE = 1 DOF A = 3 DOF CIRCLE = 18 DOF

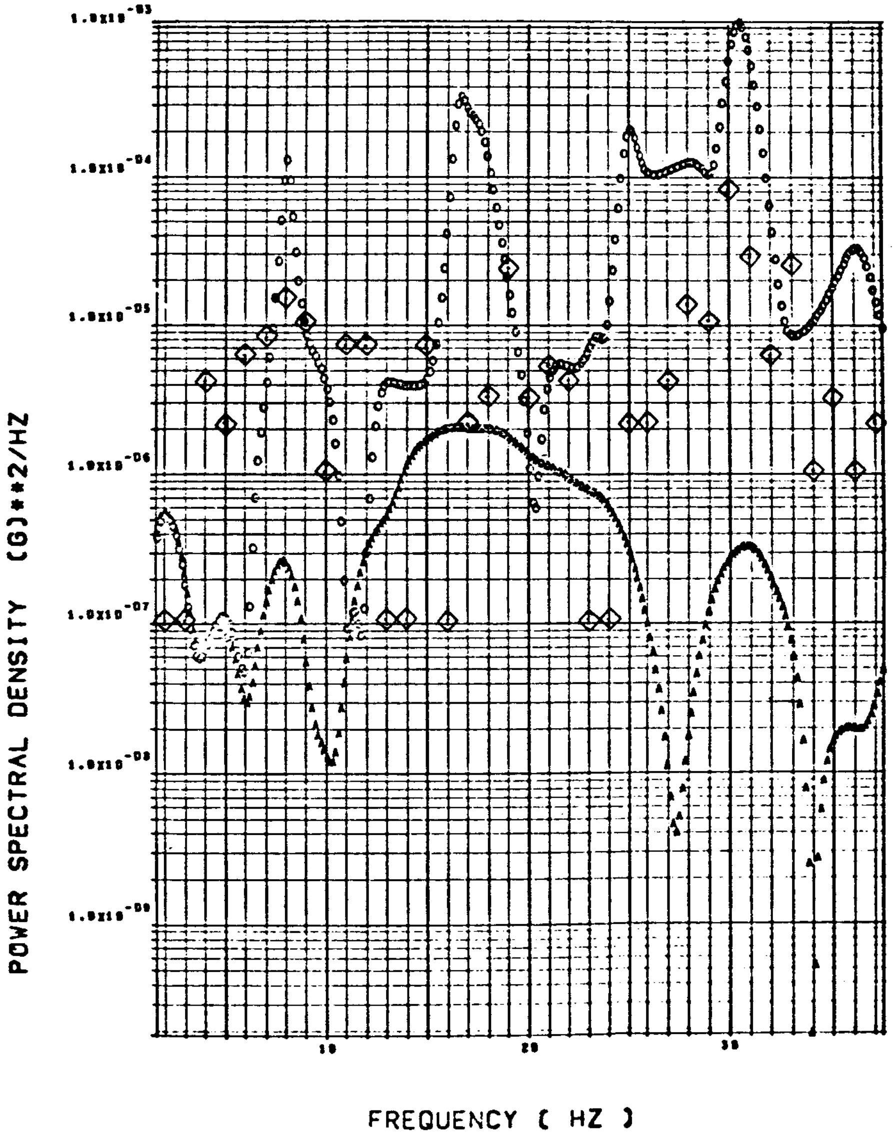

Figure 5.-(e) Pilot seat lateral accelerometer

◇ AF010 $\alpha_{FLT} = 11.1^{o}$

ANTI F-111A WING BUFFET RESPONSE. FLT 43. RUN 7-R
SWEEP=72.5 DEG. MACH=.[illegible]. ALT=7[illegible](M). ALPHA= 11.1
PILOT STATION LATERAL ACCELEROMETER. FS = 255
SQUARE = 1 DOF Λ = 3 DOF CIRCLE = 10 DOF

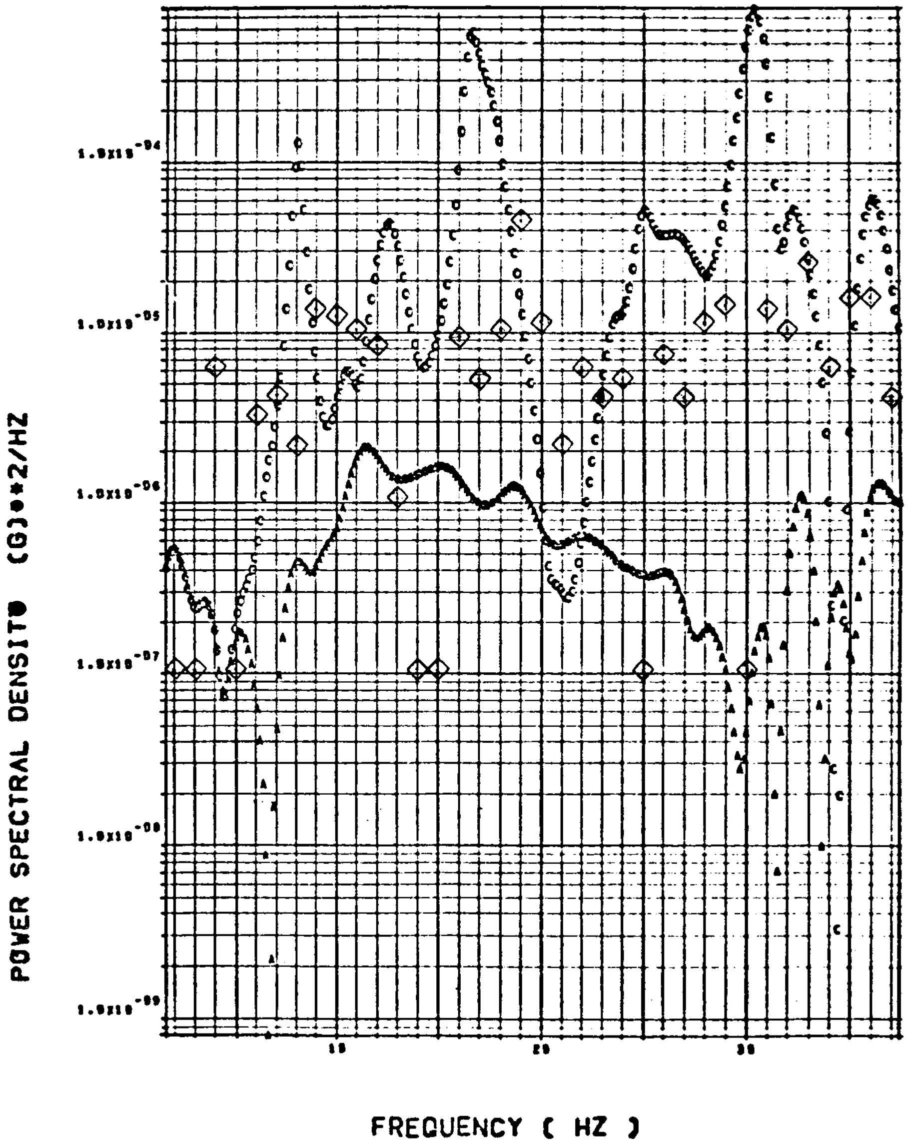

Figure 5.-(e) Pilot seat lateral accelerometer (continued)

◇ AF010 $\alpha_{FLT} = 14.4^{o}$

ANTI F-111A WING BUFFET RESPONSE. FLT 40. RUN 7-R
SWEEP=72.5 DEG. MACH=.05. ALT=7000(M). ALPHA=14.4
PILOT STATION LATERAL ACCELEROMETER. FS = 235
SQUARE = 1 DOF A = 3 DOF CIRCLE = 10 DOF

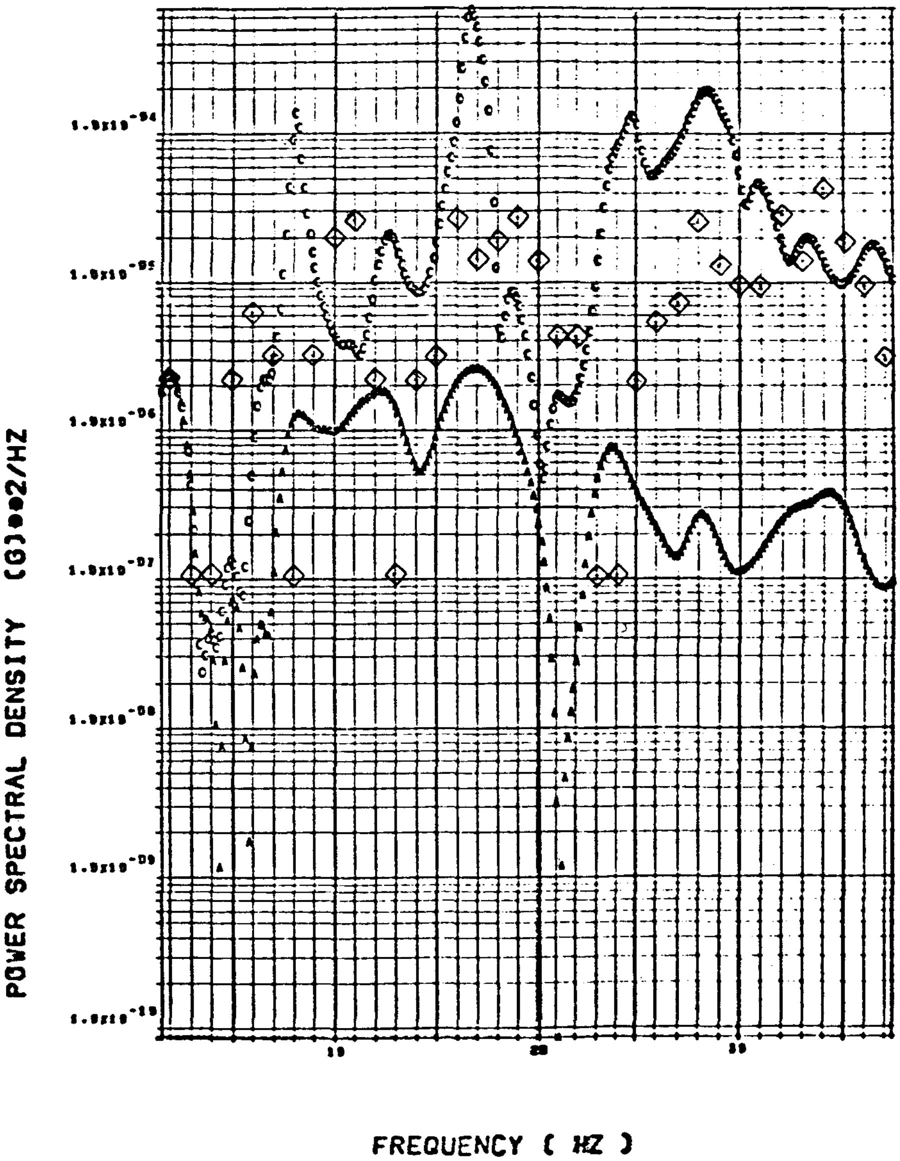

Figure 5.-(e) Pilot seat lateral accelerometer (continued)

△ SW123 $\alpha_{FLT} = 7.8^{\circ}$

F-111A WING BUFFET RESPONSE, FLT 48, RUN 7-R
SWEEP=72.5 DEG, MACH=.85, ALT=7285(M), ALPHA= 7.8
WING SHEAR (N) AT SPAN STATION 75
CIRCLE = UPPER BOUNDS SQUARE = LOWER BOUNDS

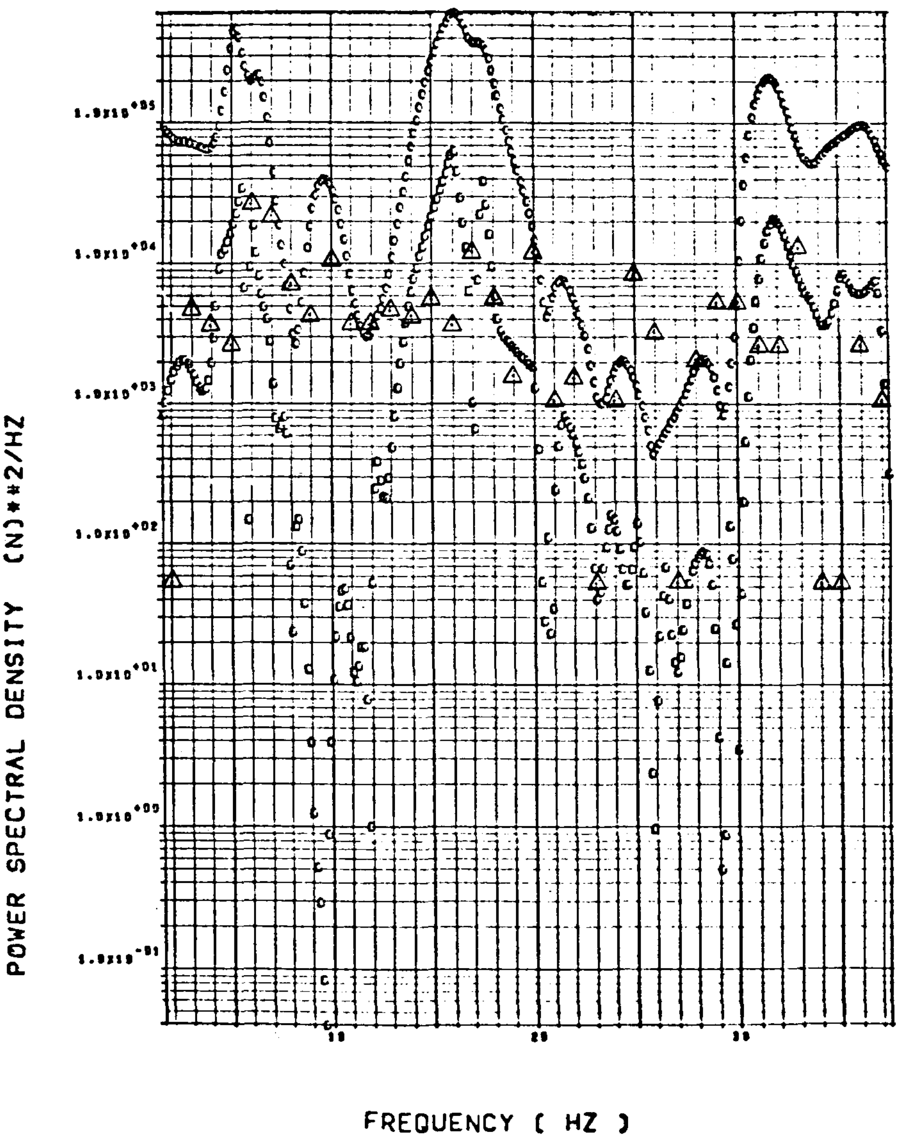

Figure 5.-(f) Wing shear

△ SW123 $\alpha_{FLT} = 11.1^{o}$

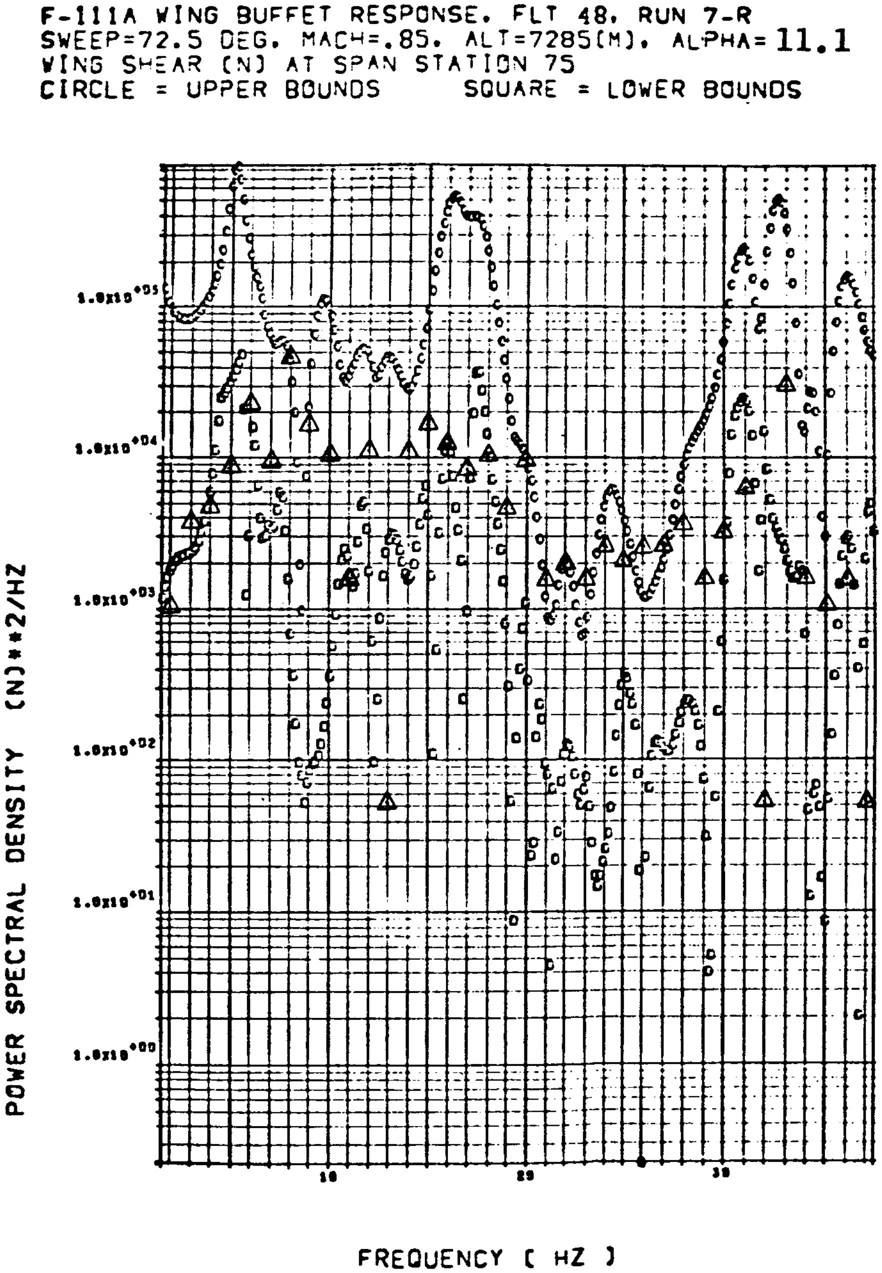

Figure 5.-(f) Wing shear (continued)

△ SW123 $\alpha_{FLT} = 14.4^{o}$

F-111A WING BUFFET RESPONSE, FLT 48, RUN 7-R
SWEEP=72.5 DEG, MACH=.85, ALT=7285(M), ALPHA=14.4
WING SHEAR (N) AT SPAN STATION 75
CIRCLE = UPPER BOUNDS SQUARE = LOWER BOUNDS

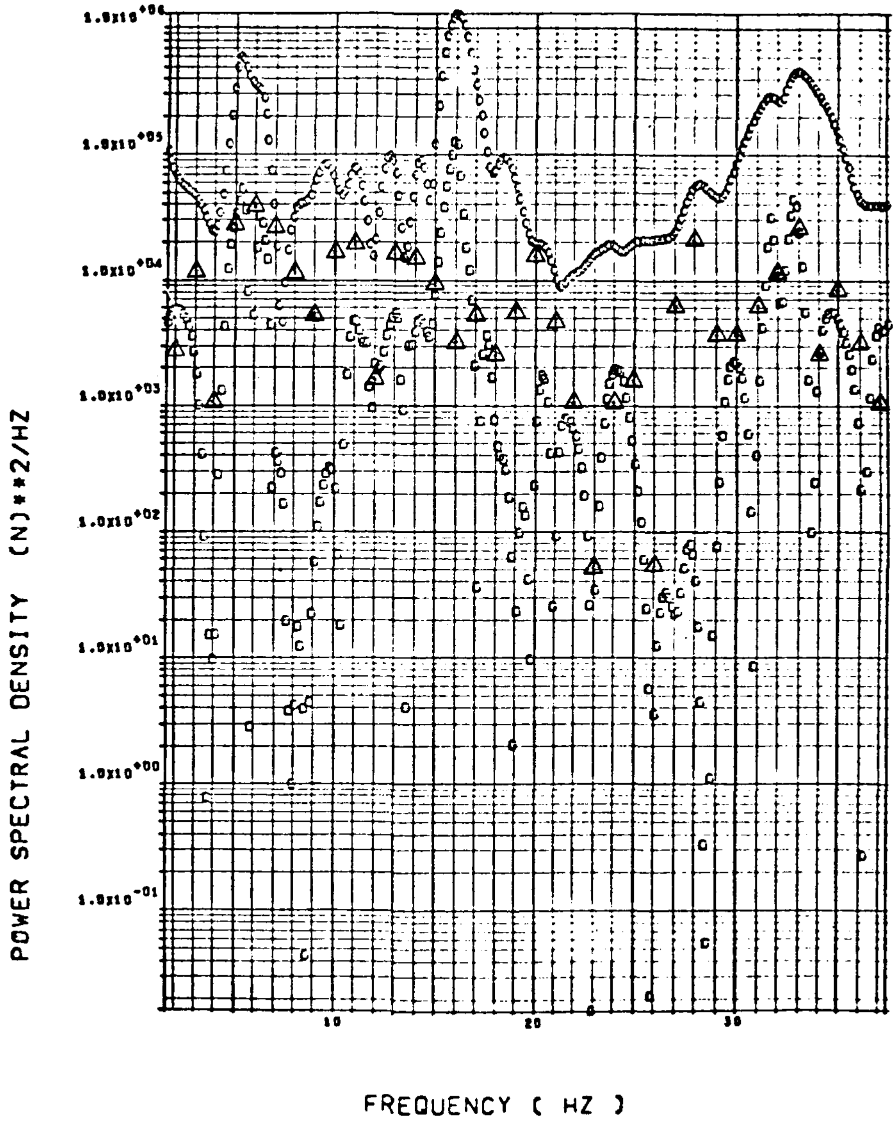

Figure 5.-(f) Wing shear (continued)

△ SW124 $\alpha_{FLT} = 7.8^{o}$

F-111A WING BUFFET RESPONSE. FLT 48. RUN 7-R
SWEEP=72.5 DEG. MACH=.85. ALT=7285(M). ALPHA=7.8
WING BENDING MOMENT (M-N) AT SPAN STATION 75
CIRCLE = UPPER BOUNDS SQUARE = LOWER BOUNDS

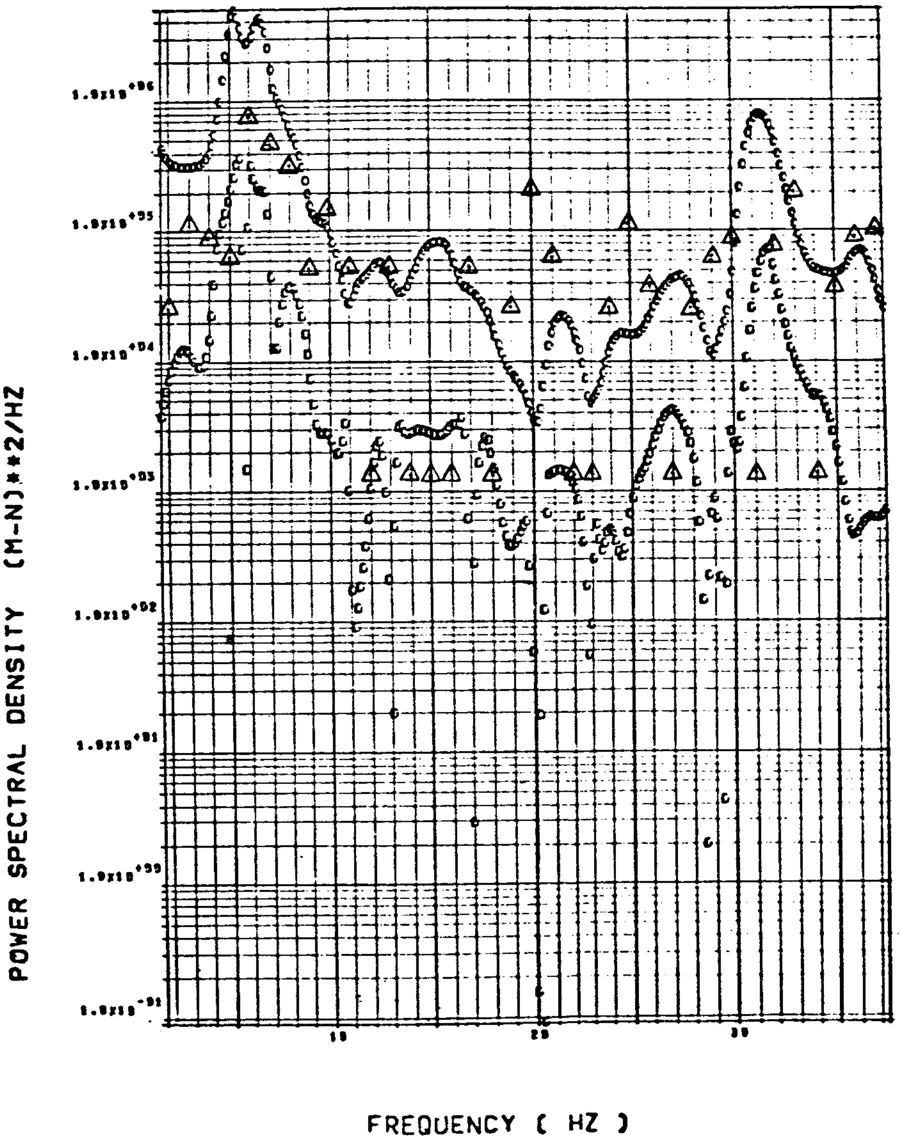

Figure 5.-(g) Wing bending moment

Δ SW124 $\alpha_{FLT} = 11.1^{o}$

F-111A WING BUFFET RESPONSE. FLT 48, RUN 7-R
SWEEP=72.5 DEG. MACH=.85, ALT=7285(M). ALPHA= 11.1
WING BENDING MOMENT (M-N) AT SPAN STATION 75
CIRCLE = UPPER BOUNDS SQUARE = LOWER BOUNDS

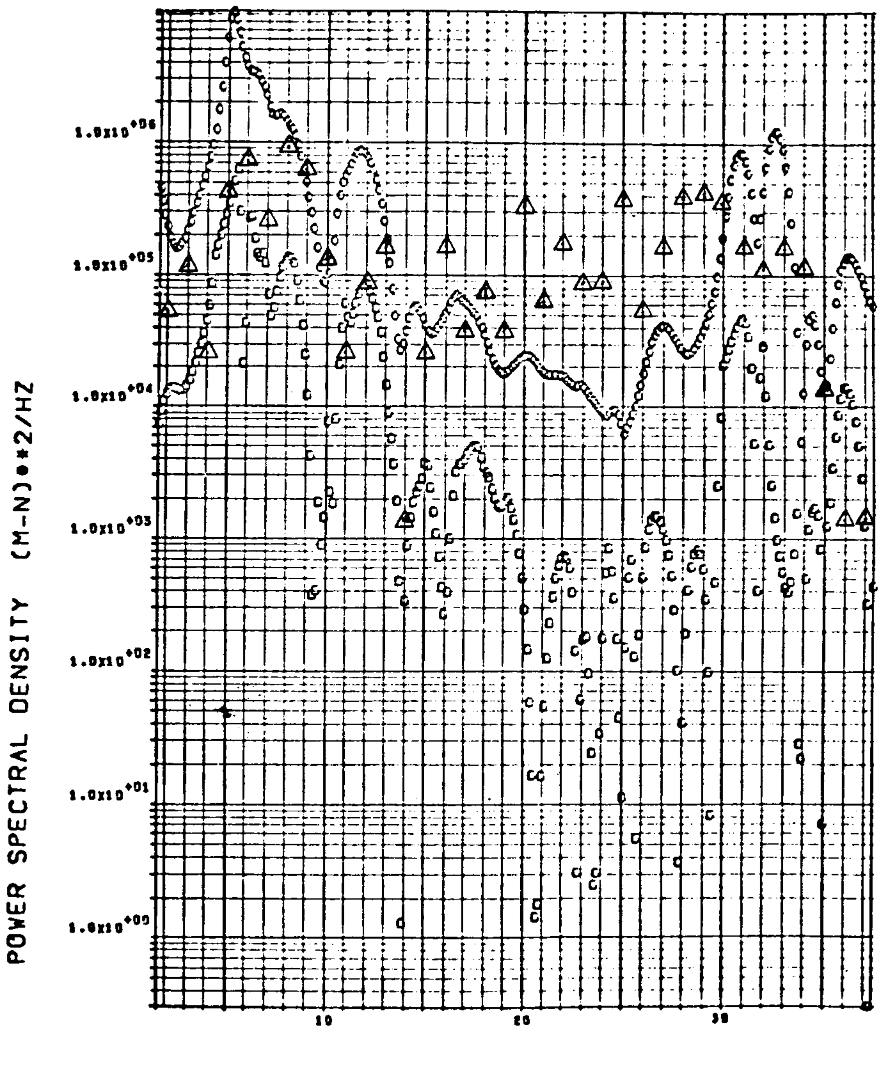

Figure 5.-(g) Wing bending moment (continued)

Δ SW124 $\alpha_{FLT} = 14.4^{o}$

F-111A WING BUFFET RESPONSE. FLT 48. RUN 7-R
SWEEP=72.5 DEG. MACH=.85. ALT=7285(M). ALPHA= 14.4
WING BENDING MOMENT (M-N) AT SPAN STATION 75
CIRCLE = UPPER BOUNDS SQUARE = LOWER BOUNDS

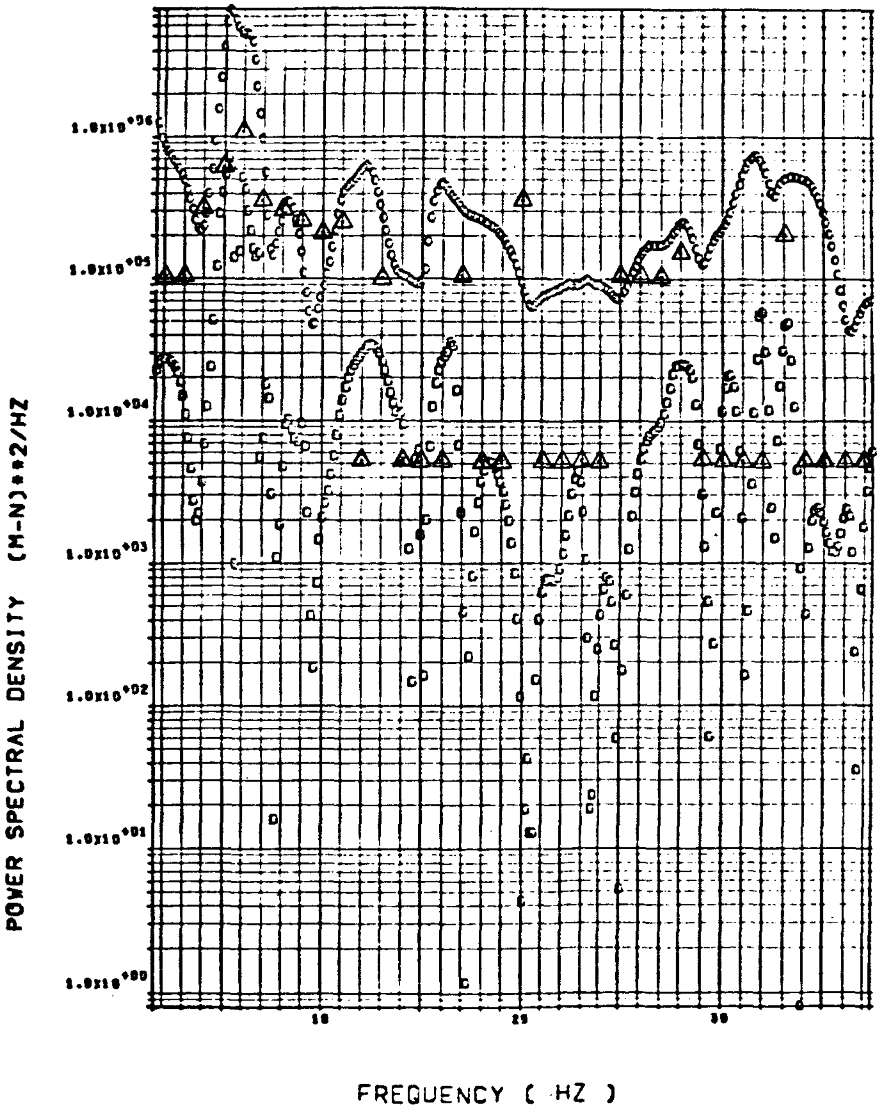

Figure 5.-(g) Wing bending moment (continued)

△ SW125 $\alpha_{FLT} = 7.8^{o}$

F-111A WING BUFFET RESPONSE. FLT 48. RUN 7-R
SWEEP=72.5 DEG. MACH=.85. ALT=7285(M). ALPHA= 7.8
WING TORQUE (M-N) AT SPAN STATION 75
CIRCLE = UPPER BOUNDS SQUARE = LOWER BOUNDS

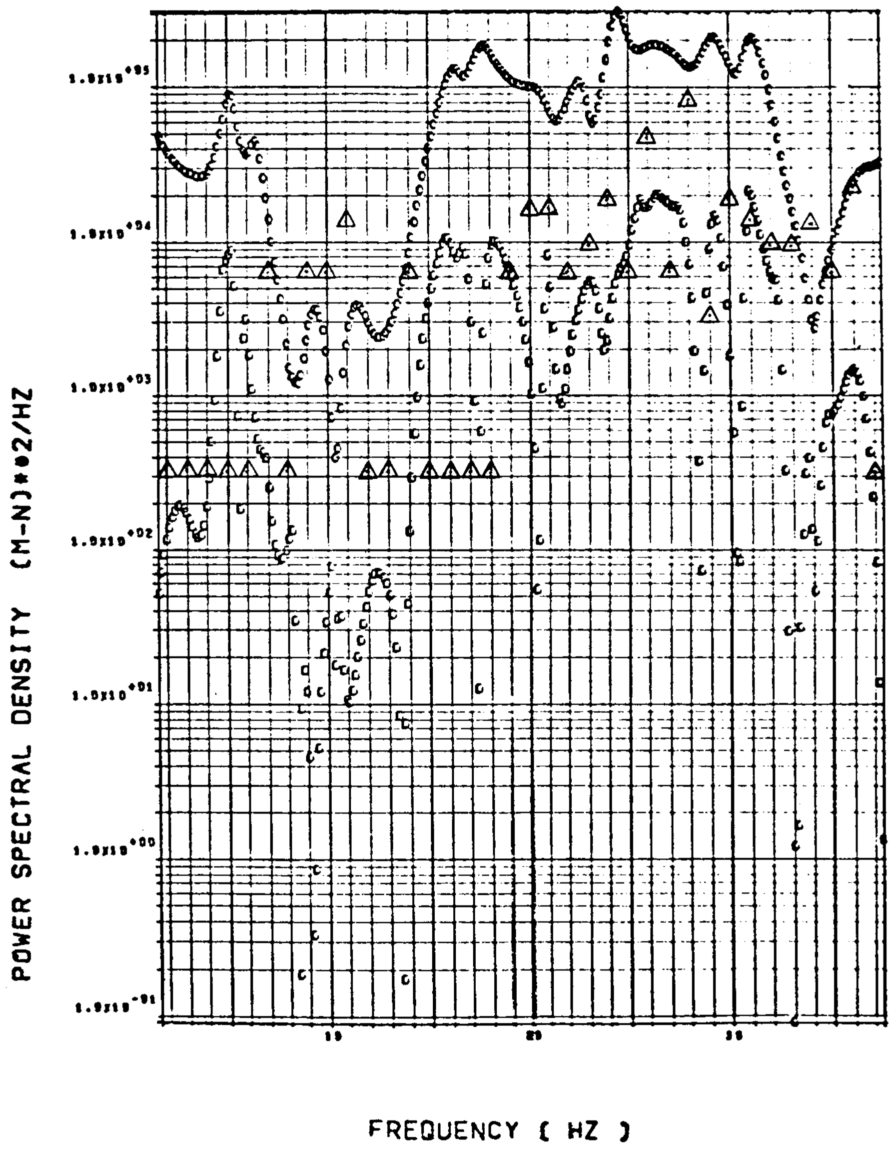

Figure 5.-(h) Wing torsion

△ SW125 $\alpha_{FLT} = 11.1^{o}$

F-111A WING BUFFET RESPONSE, FLT 48, RUN 7-R
SWEEP=72.5 DEG. MACH=.85. ALT=7285(M). ALPHA= 11.1
WING TORQUE (M-N) AT SPAN STATION 75
CIRCLE = UPPER BOUNDS SQUARE = LOWER BOUNDS

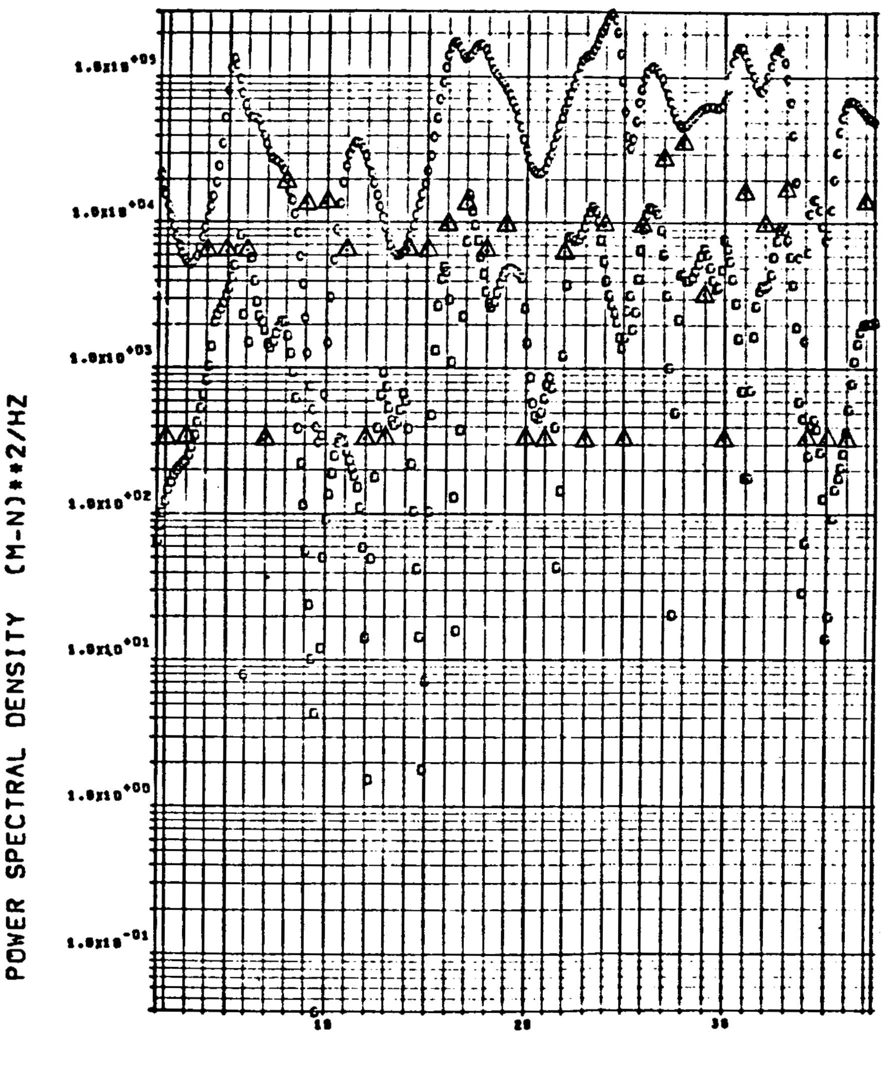

Figure 5.-(h) Wing torsion (continued)

△ SW125 $\alpha_{FLT} = 14.4^{\circ}$

F-111A WING BUFFET RESPONSE. FLT 48. RUN 7-R
SWEEP=72.5 DEG. MACH=.85. ALT=7285(M). ALPHA= 14.4
WING TORQUE (M-N) AT SPAN STATION 75
CIRCLE = UPPER BOUNDS SQUARE = LOWER BOUNDS

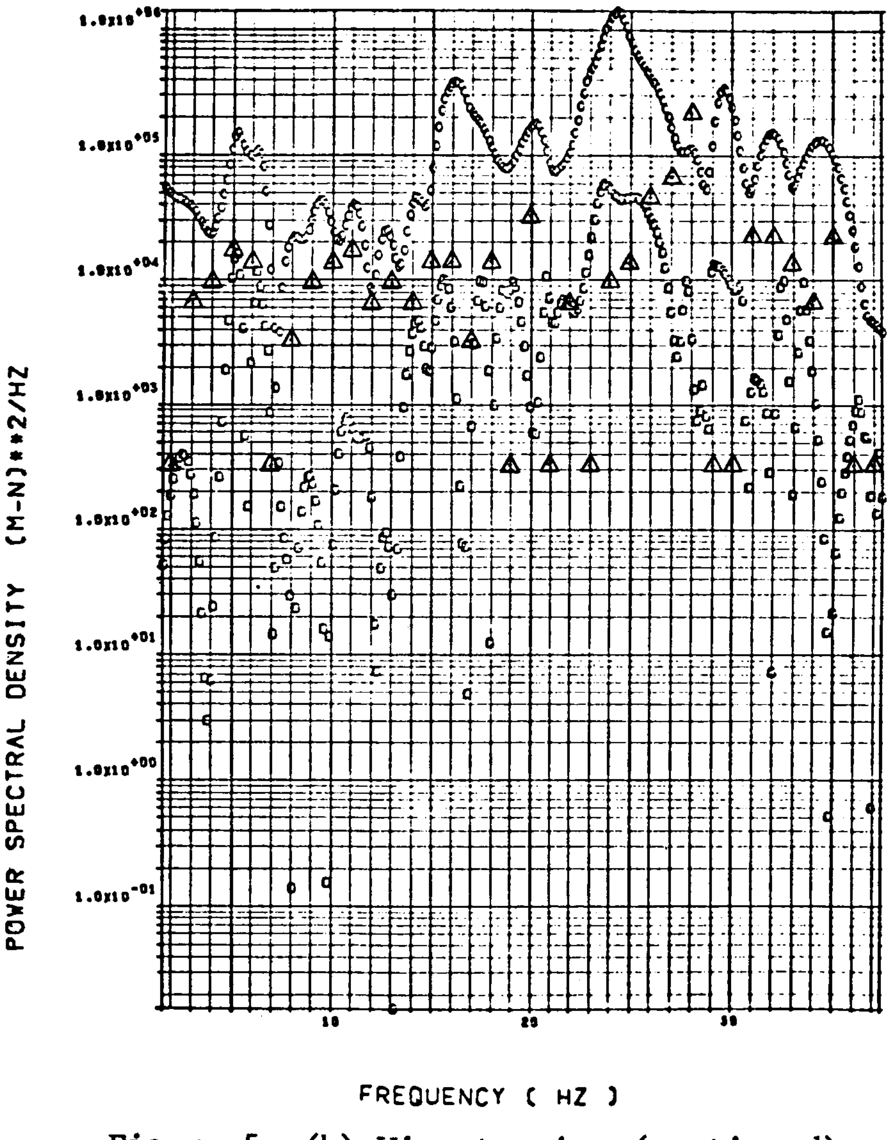

Figure 5.-(h) Wing torsion (continued)

△ ST077 ◇ ST072 $\alpha_{FLT} = 7.8^{o}$

F-111A WING BUFFET RESPONSE, FLT 48, RUN 7-R
SWEEP=72.5 DEG, MACH=.85, ALT=7285(M), ALPHA= 7.8
H.T. PIVOT SHEAR (N)
CIRCLE = UPPER BOUNDS SQUARE = LOWER BOUNDS

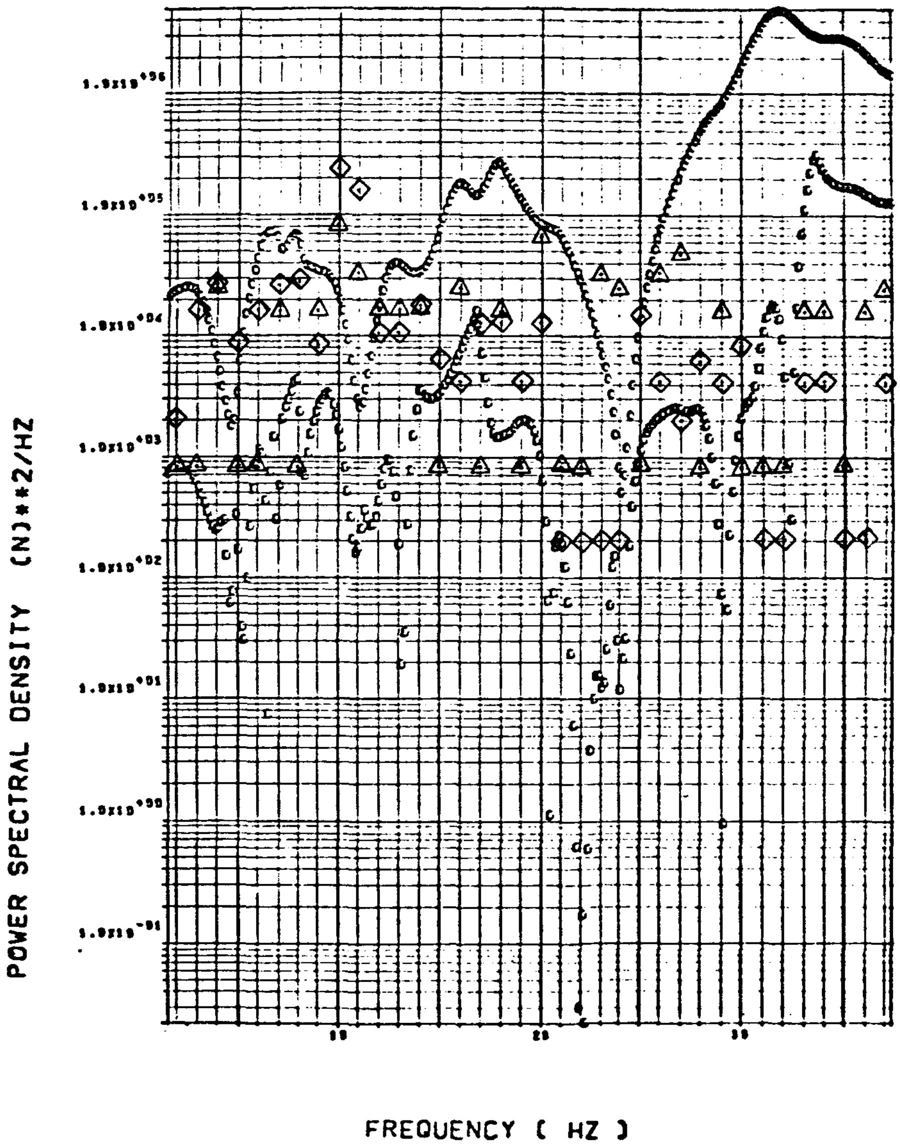

Figure 5.-(i) Horizontal tail shear

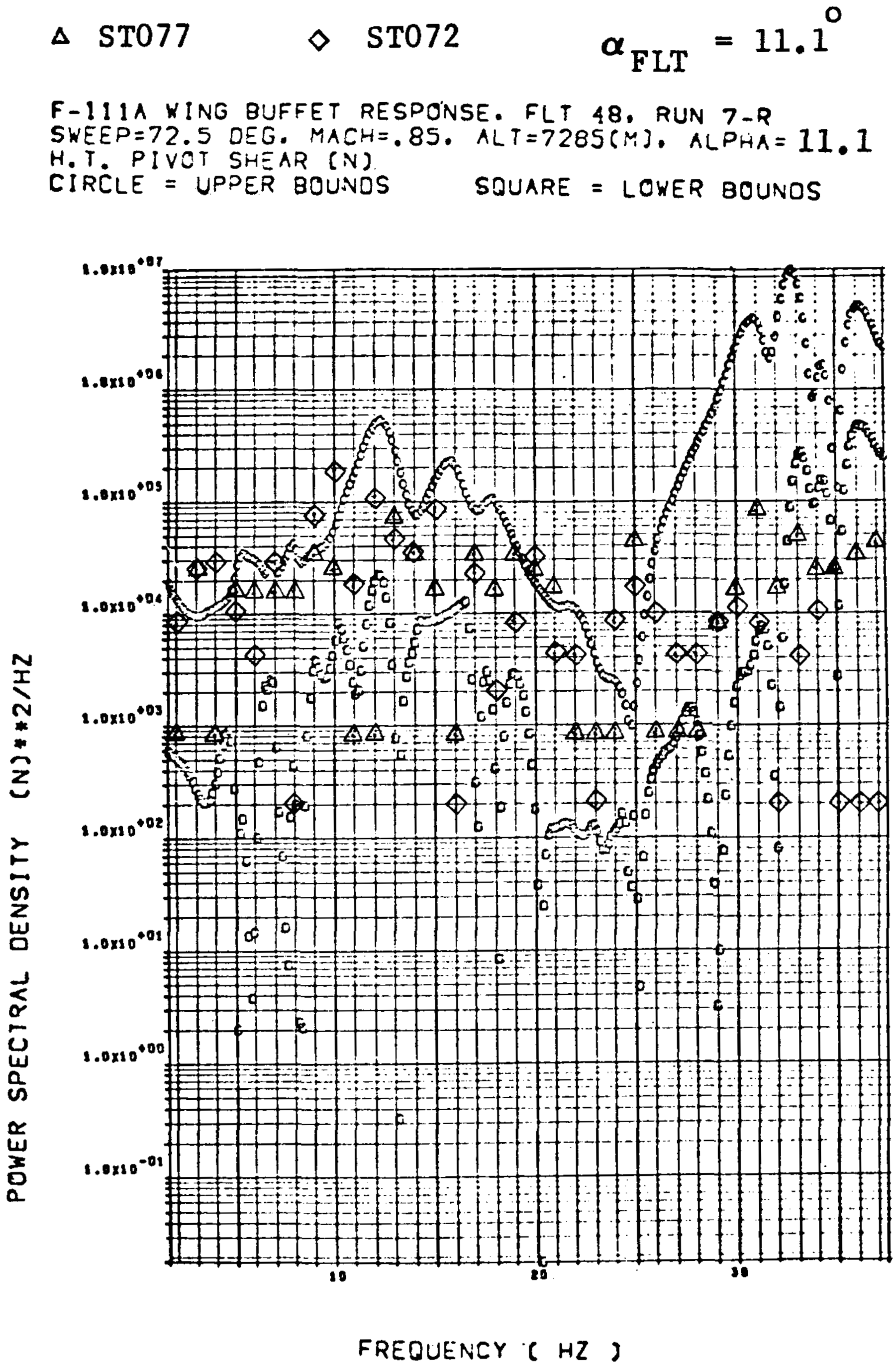

Figure 5.-(i) Horizontal tail shear (continued)

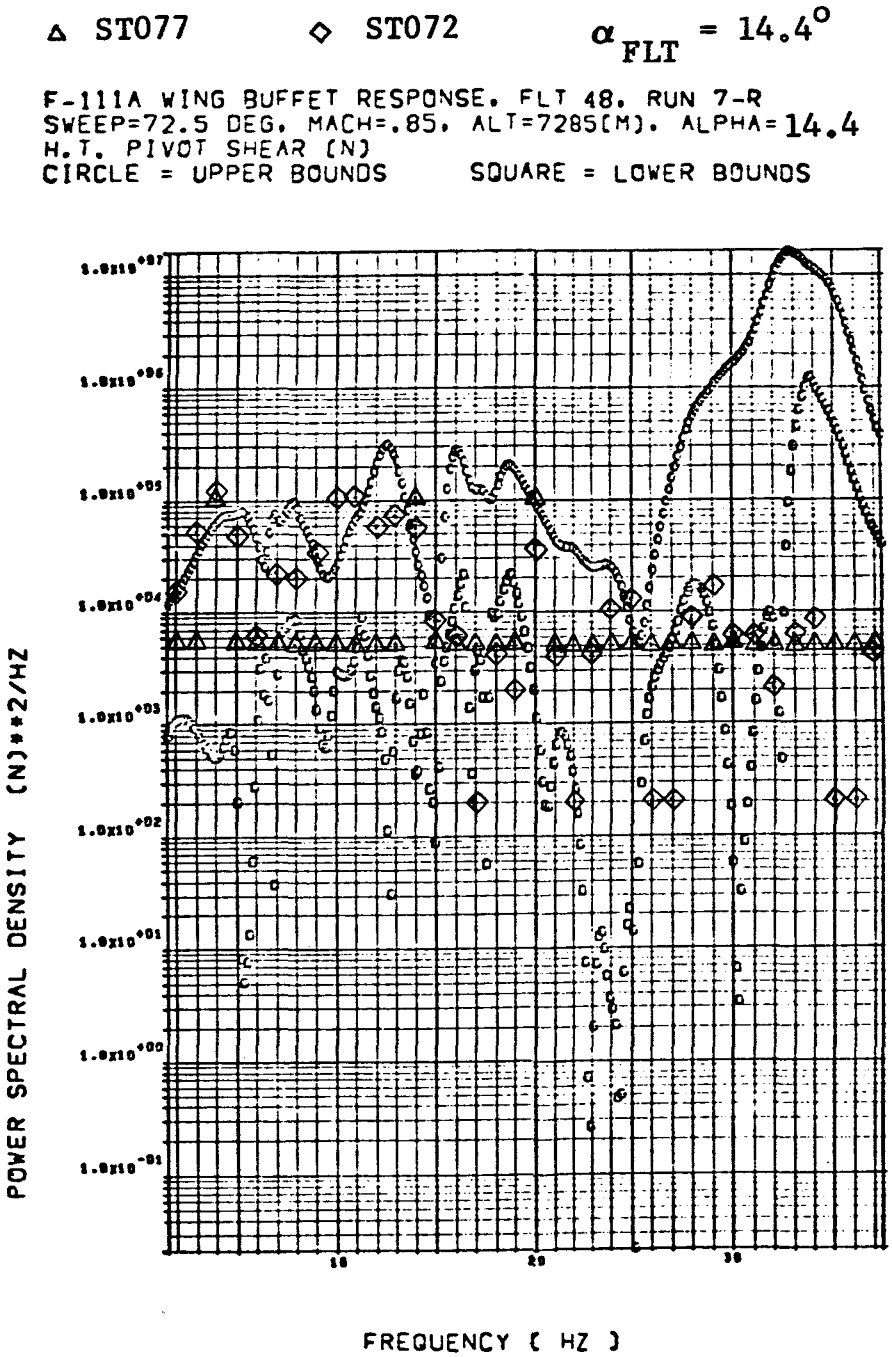

Figure 5.-(i) Horizontal tail shear (continued)

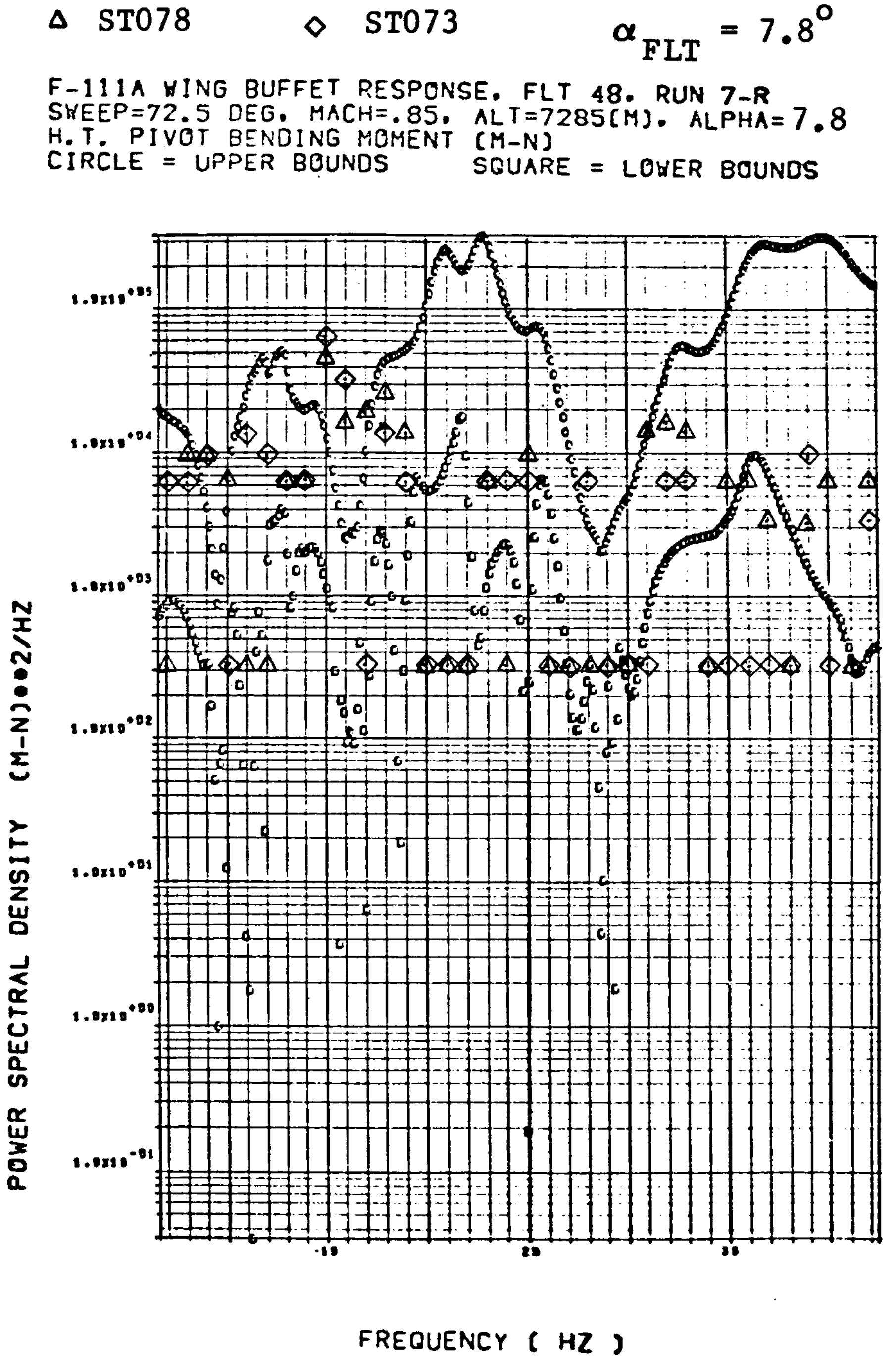

Figure 5.-(j) Horizontal tail bending moment

△ ST078 ◇ ST073 $\alpha_{FLT} = 11.1^{o}$

F-111A WING BUFFET RESPONSE. FLT 48. RUN 7-R
SWEEP=72.5 DEG. MACH=.85. ALT=7285(M). ALPHA= 11.1
H.T. PIVOT BENDING MOMENT (M-N)
CIRCLE = UPPER BOUNDS SQUARE = LOWER BOUNDS

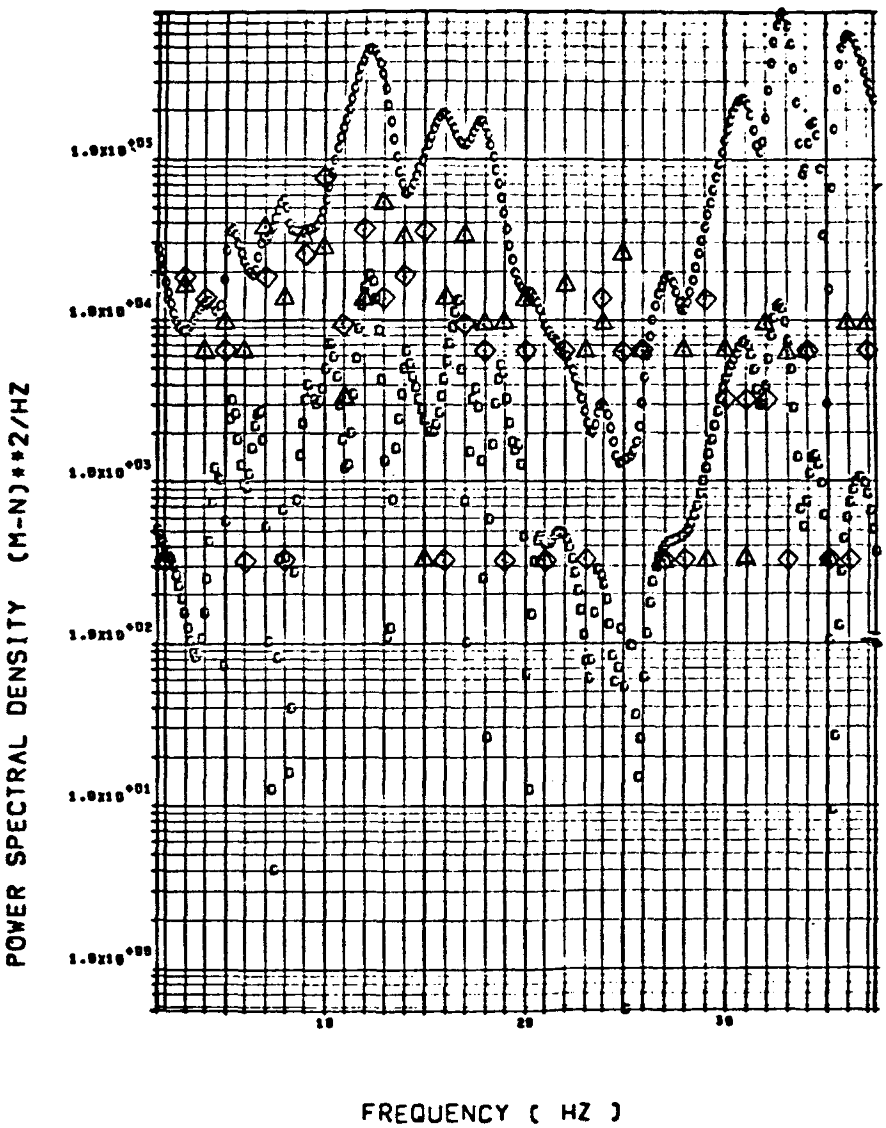

Figure 5.-(j) Horizontal tail bending moment (continued)

△ ST078 ◇ ST073 $\alpha_{FLT} = 14.4^{o}$

F-111A WING BUFFET RESPONSE, FLT 48, RUN 7-R
SWEEP=72.5 DEG, MACH=.85, ALT=7285(M), ALPHA= 14.4
H.T. PIVOT BENDING MOMENT (M-N)
CIRCLE = UPPER BOUNDS SQUARE = LOWER BOUNDS

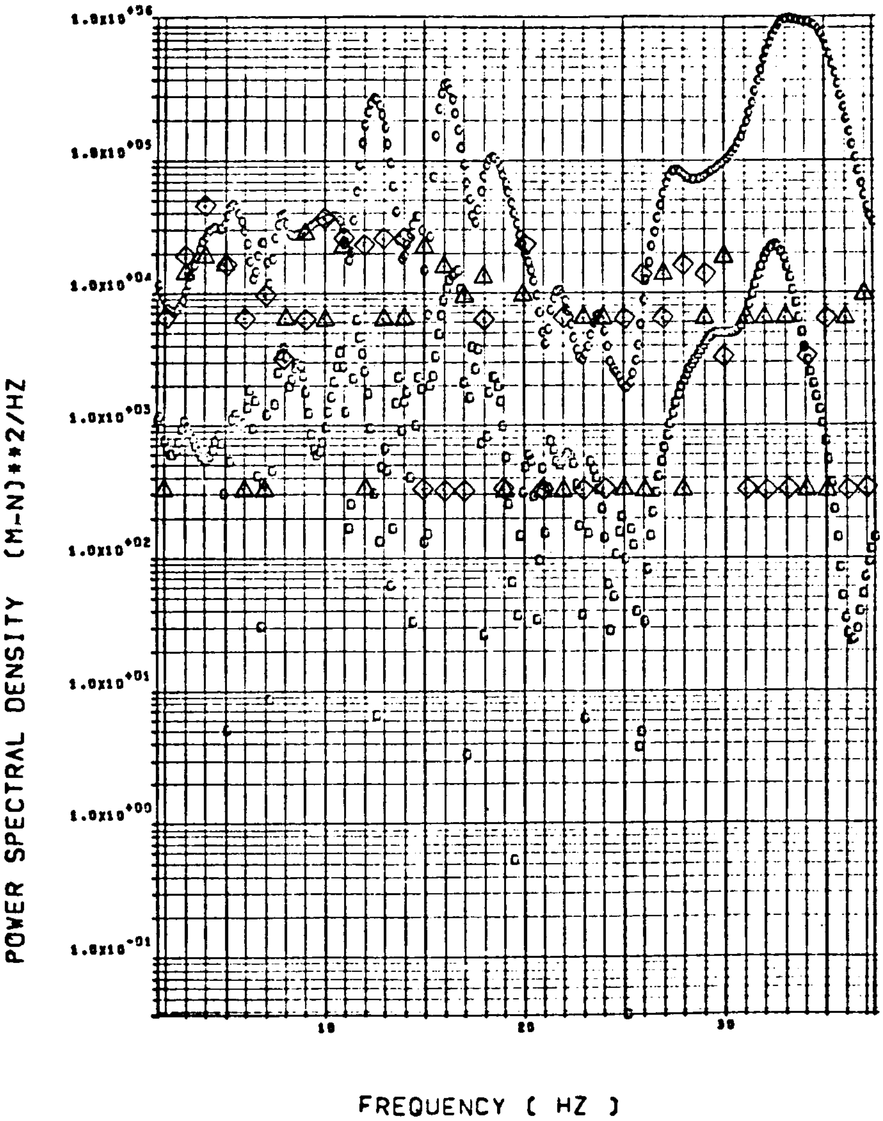

Figure 5.-(j) Horizontal tail bending moment (continued)

△ ST135 ◇ ST118 $\alpha_{FLT} = 7.8^{o}$

F-111A WING BUFFET RESPONSE. FLT 48. RUN 7-R
SWEEP=72.5 DEG. MACH=.85. ALT=7285(M). ALPHA= 7.8
H.T. PIVOT TORQUE (M-N)
CIRCLE = UPPER BOUNDS SQUARE = LOWER BOUNDS

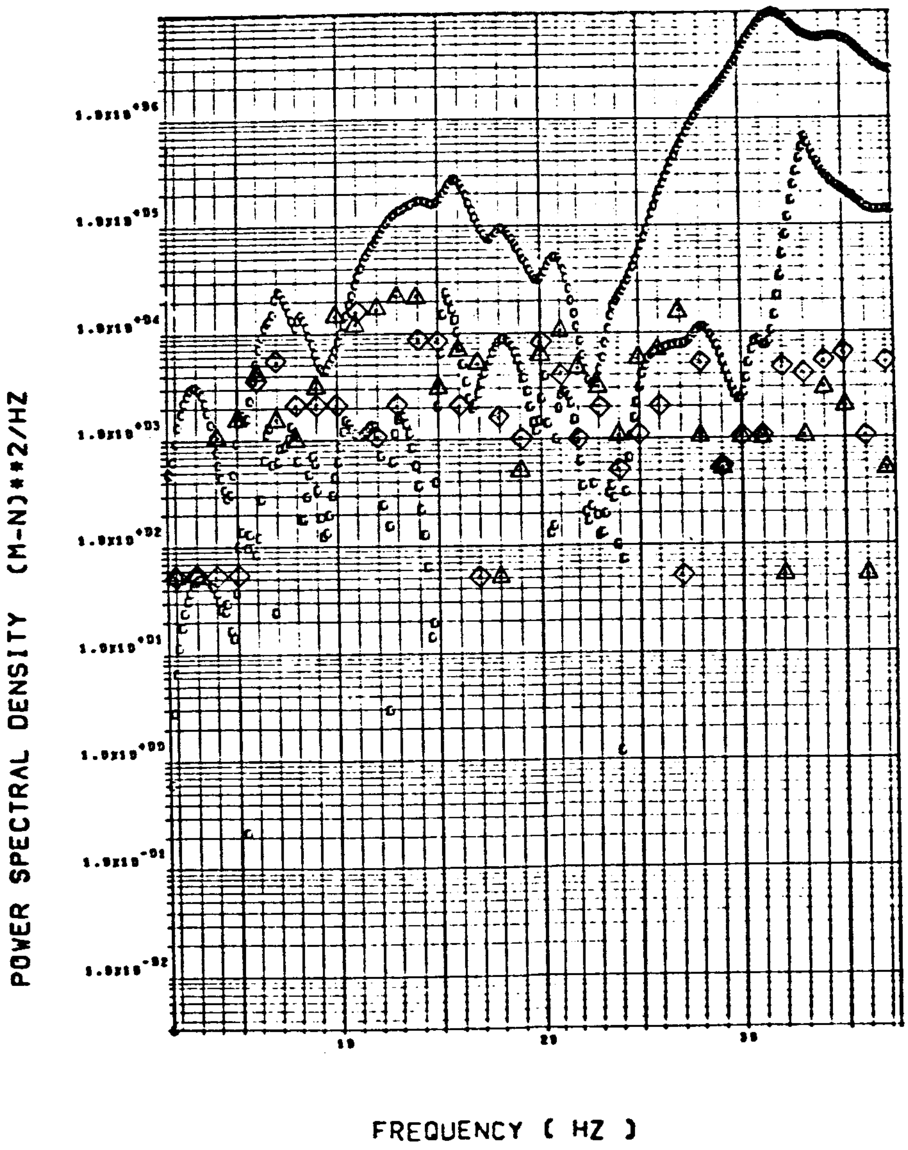

Figure 5.-(k) Horizontal tail torsion

△ ST135 ◇ ST118 $\alpha_{FLT} = 11.1^{o}$

F-111A WING BUFFET RESPONSE. FLT 48. RUN 7-R
SWEEP=72.5 DEG. MACH=.85. ALT=7285(M). ALPHA= 11.1
H.T. PIVOT TORQUE (M-N)
CIRCLE = UPPER BOUNDS SQUARE = LOWER BOUNDS

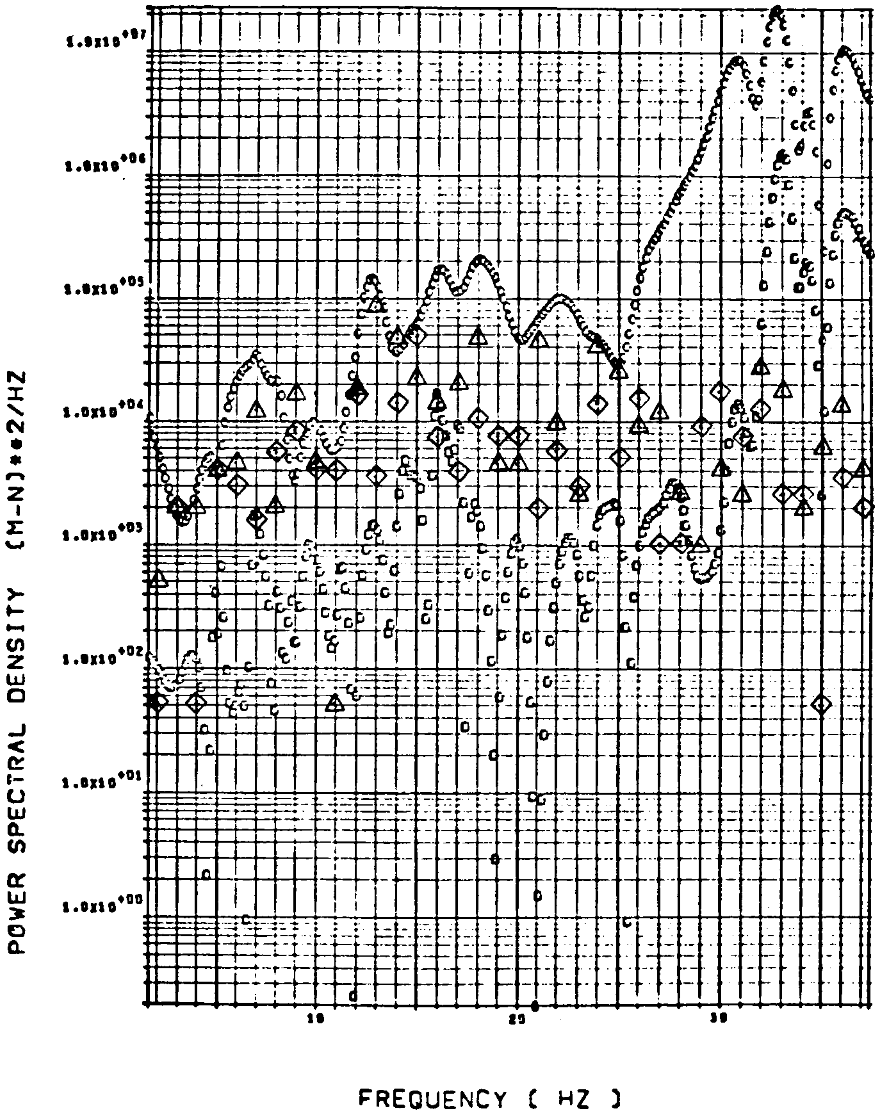

Figure 5.-(k) Horizontal tail torsion (continued)

△ ST135 ◇ ST118 $\alpha_{FLT} = 14.4^{o}$

F-111A WING BUFFET RESPONSE. FLT 48. RUN 7-R
SWEEP=72.5 DEG. MACH=.85. ALT=7285(M). ALPHA= 14.4
H.T. PIVOT TORQUE (M-N)
CIRCLE = UPPER BOUNDS SQUARE = LOWER BOUNDS

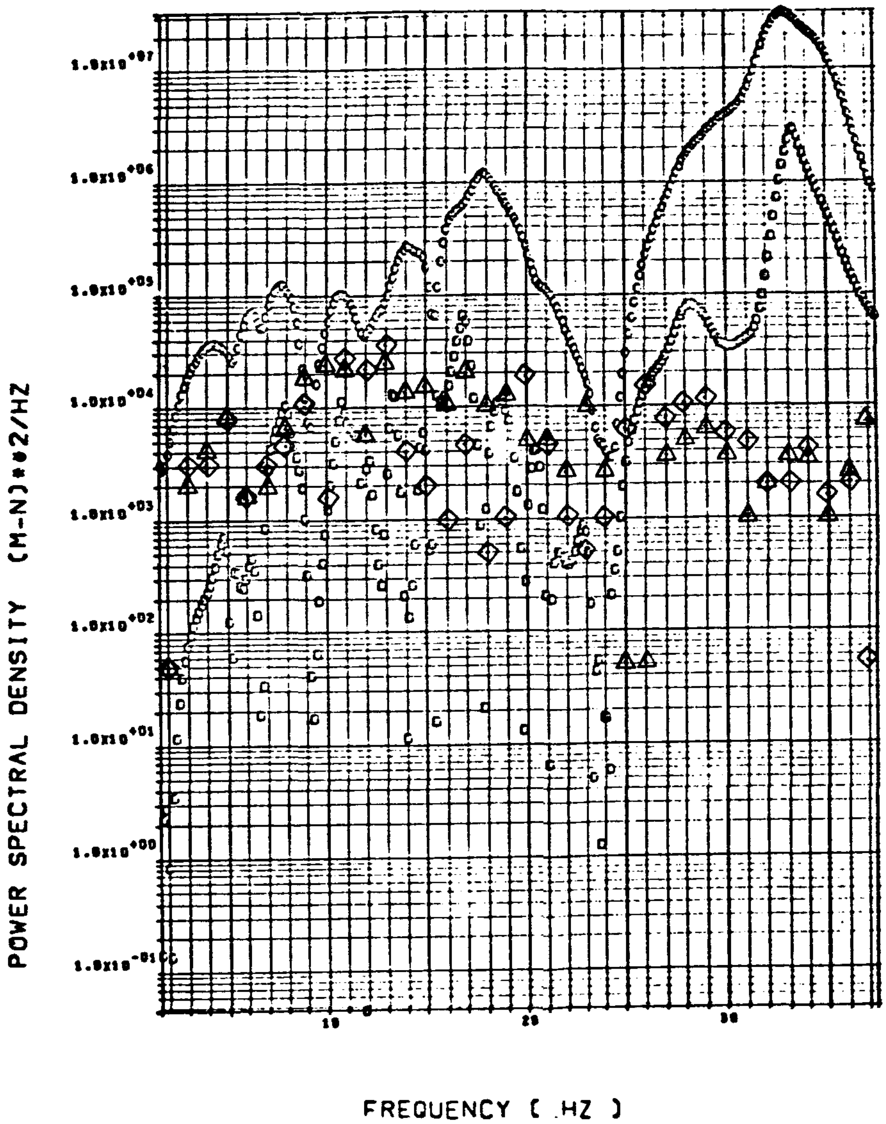

Figure 5.-(k) Horizontal tail torsion (continued)

△ AW001 ◇ AW002 $\alpha_{FLT} = 12.4^{o}$

F-111A WING ALONE BUFFET RESPONSE. FLT 48. RUN 4
SWEEP= 50 DEG. MACH=1.2. ALT=9053(M). ALPHA= 12.4
WING TIP ACCELEROMETER
CIRCLE = UPPER BOUNDS SQUARE = LOWER BOUNDS

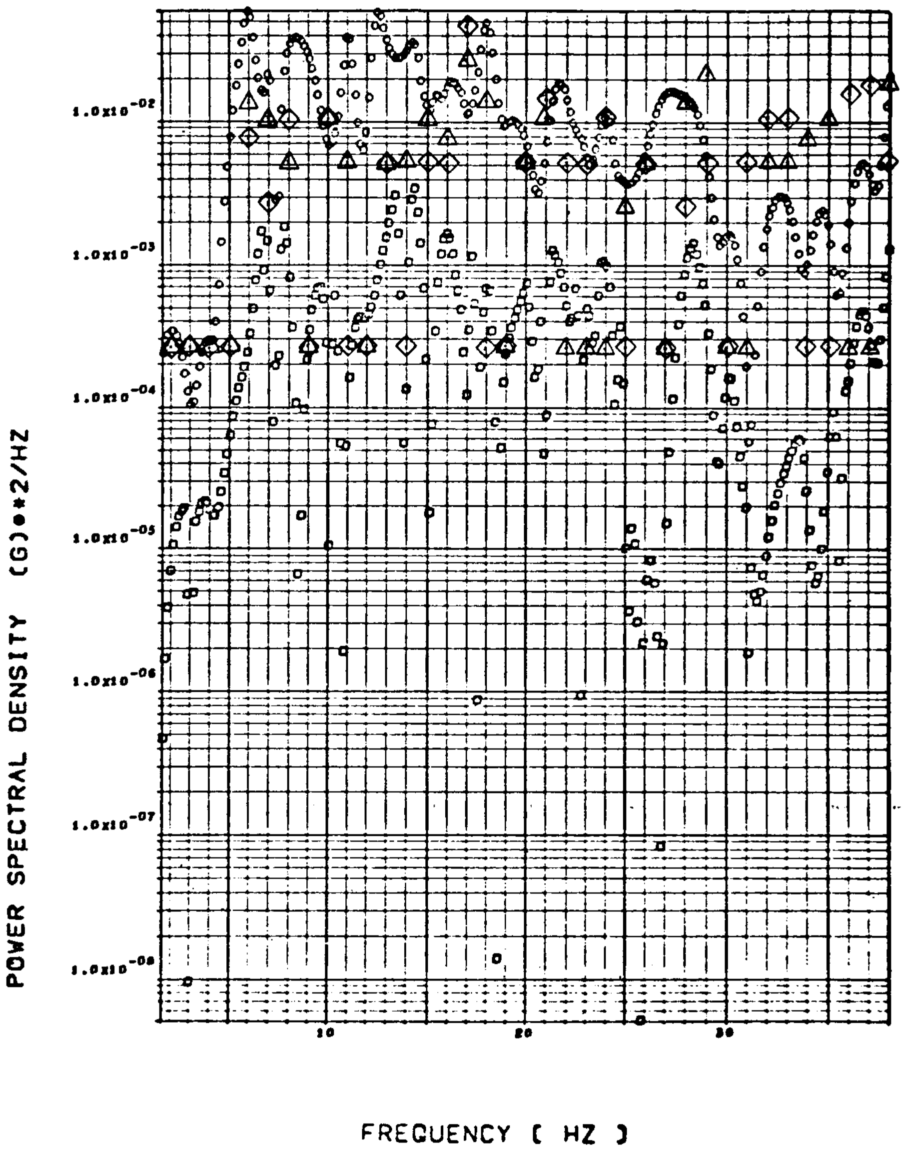

Figure 6.- Power spectra for
Case 6, wing alone (final method),
$\Lambda=50^{o}$, M=1.20, alt.=9053m (29,700 ft)
(a) wing tip accelerometer

△ AW001 ◇ AW002 $\alpha_{FLT} = 13.65^{o}$

F-111A WING ALONE BUFFET RESPONSE. FLT 48. RUN 4
SWEEP= 50 DEG. MACH=1.2. ALT=9053(M). ALPHA= 16.1
WING TIP ACCELEROMETER
CIRCLE = UPPER BOUNDS SQUARE = LOWER BOUNDS

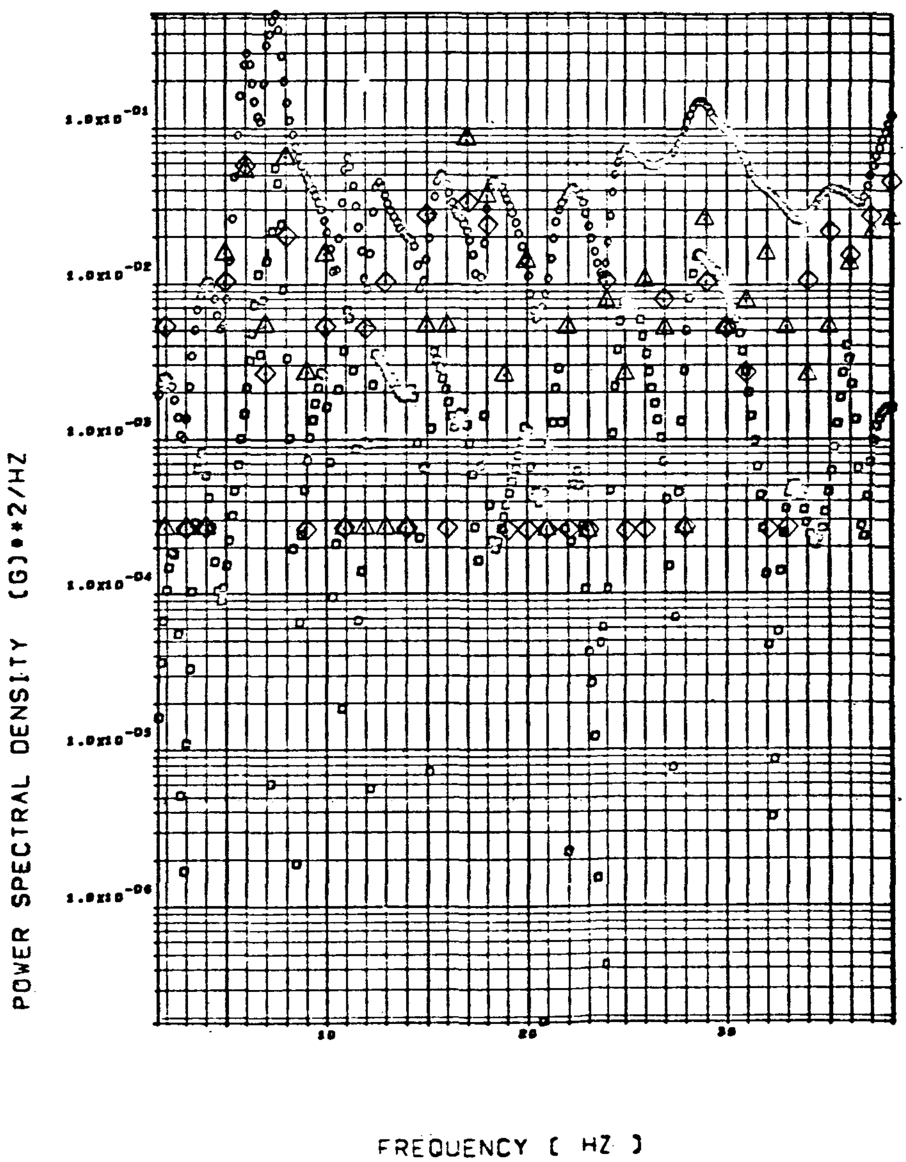

Figure 6.-(a) Wing tip accelerometer (continued)

◇ AB018 α_{FLT} = 12.4°

F-111A WING ALONE BUFFET RESPONSE, FLT 48, RUN 4
SWEEP= 50 DEG, MACH=1.2, ALT=9053(M), ALPHA= 12.4
C.G. VERTICAL ACCELEROMETER, FS = 529
SQUARE = 1 DOF A = 2 DOF CIRCLE = 11 DOF

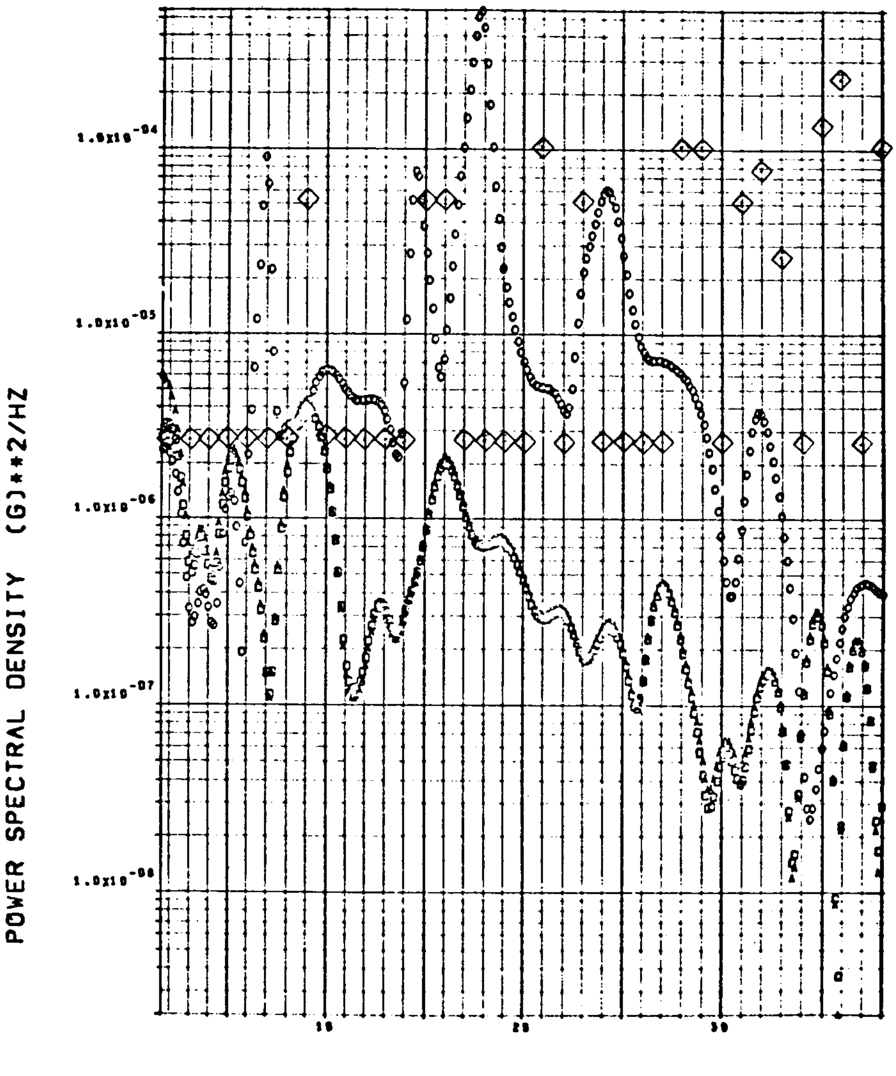

Figure 6.-(b) C.G. vertical accelerometer

◇ AB018 $\alpha_{FLT} = 13.65^{o}$

F-111A WING ALONE BUFFET RESPONSE, FLT 48, RUN 4
SWEEP= 50 DEG, MACH=1.2, ALT=9053(M), ALPHA= 16.1
C.G. VERTICAL ACCELEROMETER, FS = 529
SQUARE = 1 DOF A = 2 DOF CIRCLE = 11 DOF

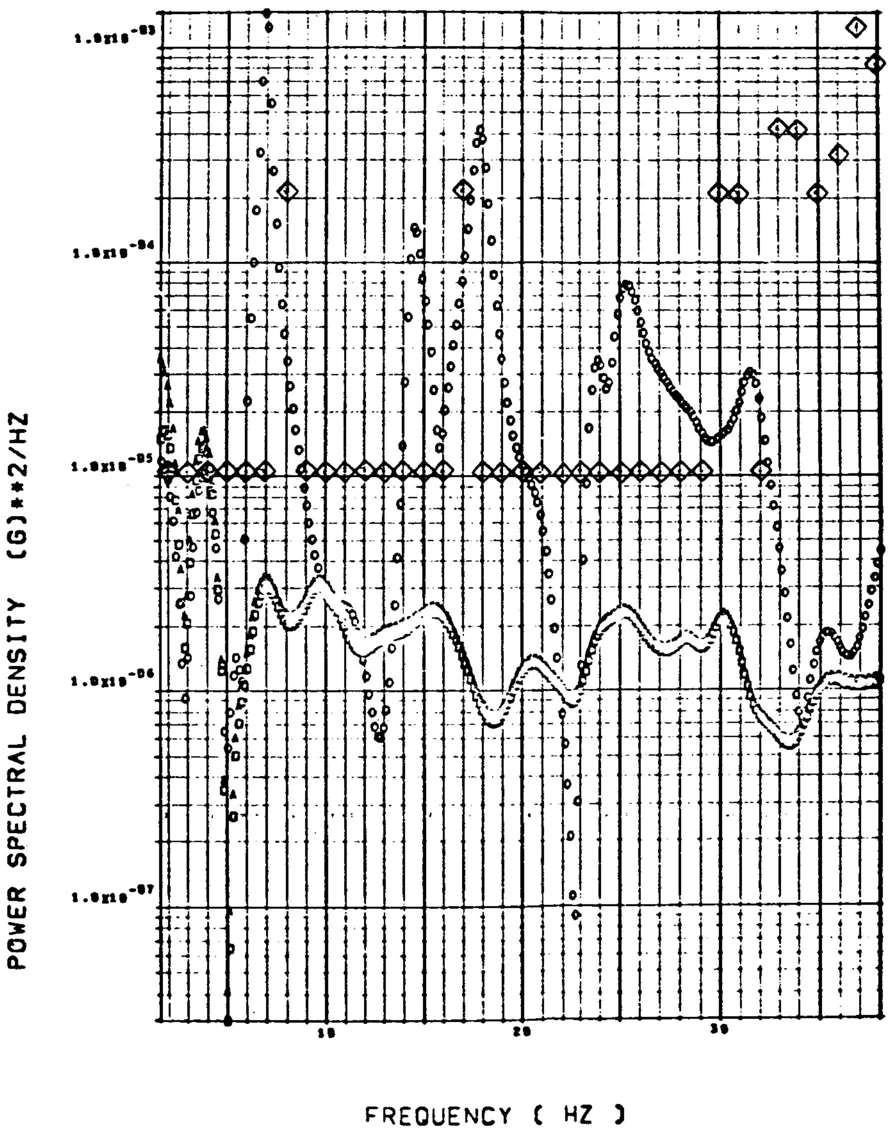

Figure 6.-(b) C.G. vertical accelerometer (continued)

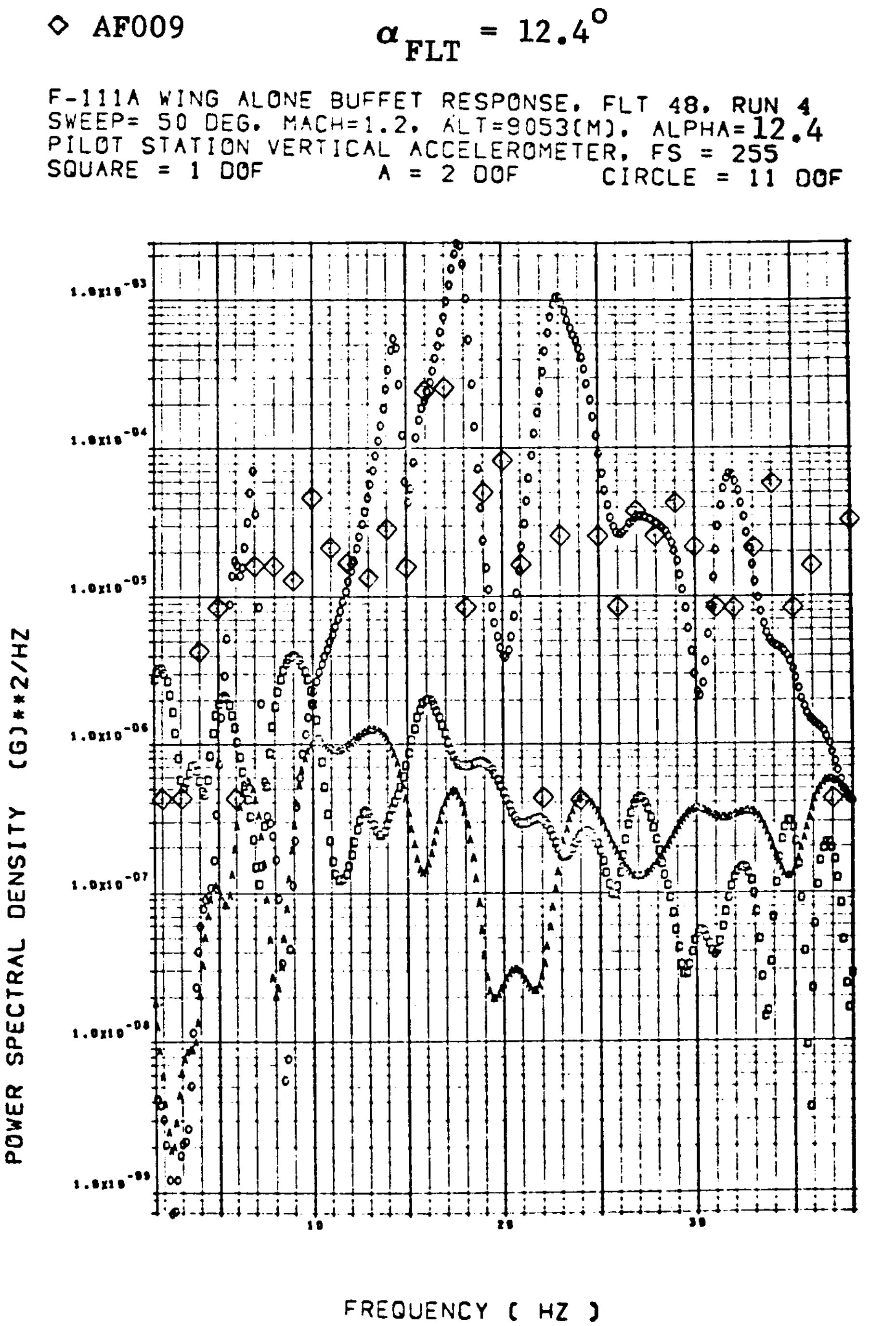

Figure 6.-(c) Pilot seat vertical accelerometer

◇ AF009 $\alpha_{FLT} = 13.65^{\circ}$

F-111A WING ALONE BUFFET RESPONSE, FLT 48, RUN 4
SWEEP= 50 DEG, MACH=1.2, ALT=9053(M), ALPHA=16.1
PILOT STATION VERTICAL ACCELEROMETER, FS = 255
SQUARE = 1 DOF A = 2 DOF CIRCLE = 11 DOF

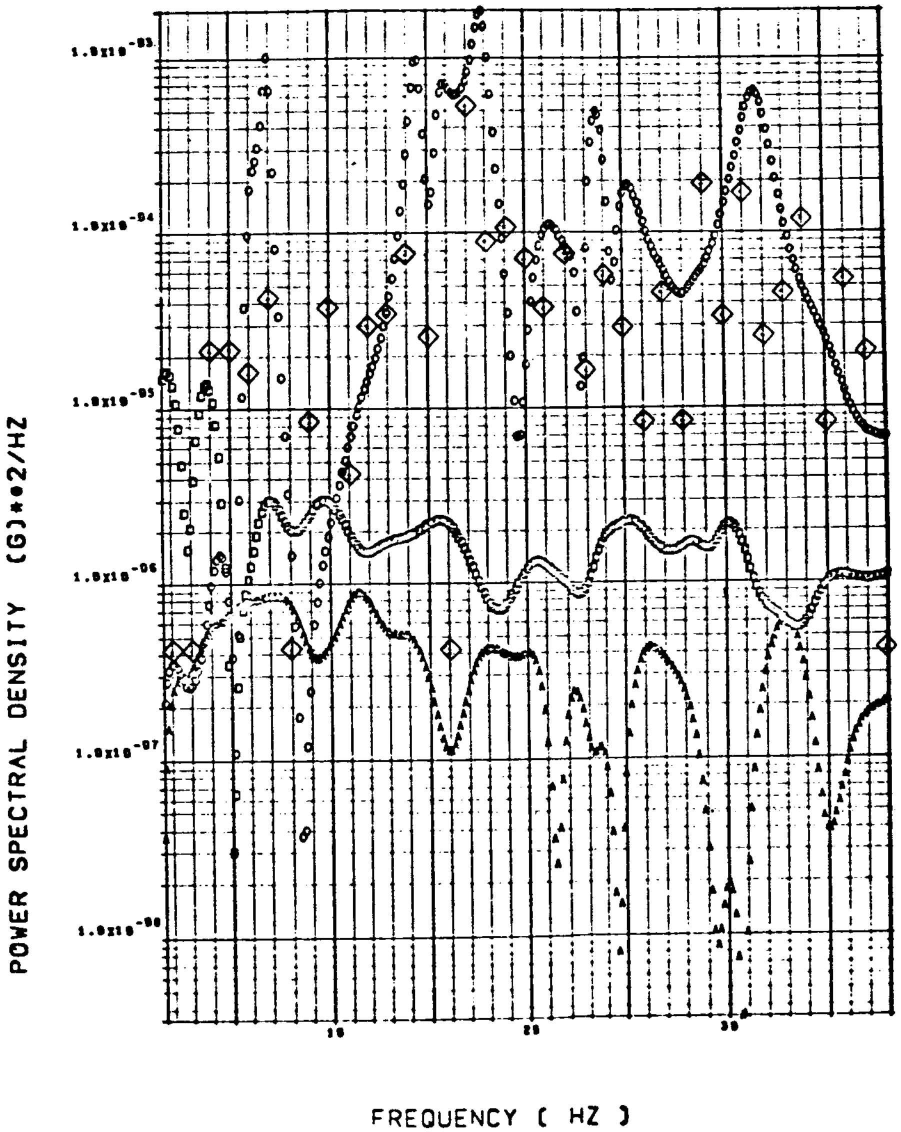

Figure 6.-(c) Pilot seat vertical accelerometer (continued)

◇ AB020 $\alpha_{FLT} = 12.4^{o}$

F-111A WING ALONE BUFFET RESPONSE, FLT 48, RUN 4
SWEEP= 50 DEG, MACH=1.2, ALT=9053(M), ALPHA=12.4
C.G. LATERAL ACCELEROMETER, FS = 529
SQUARE = 1 DOF CIRCLE = 12 DOF

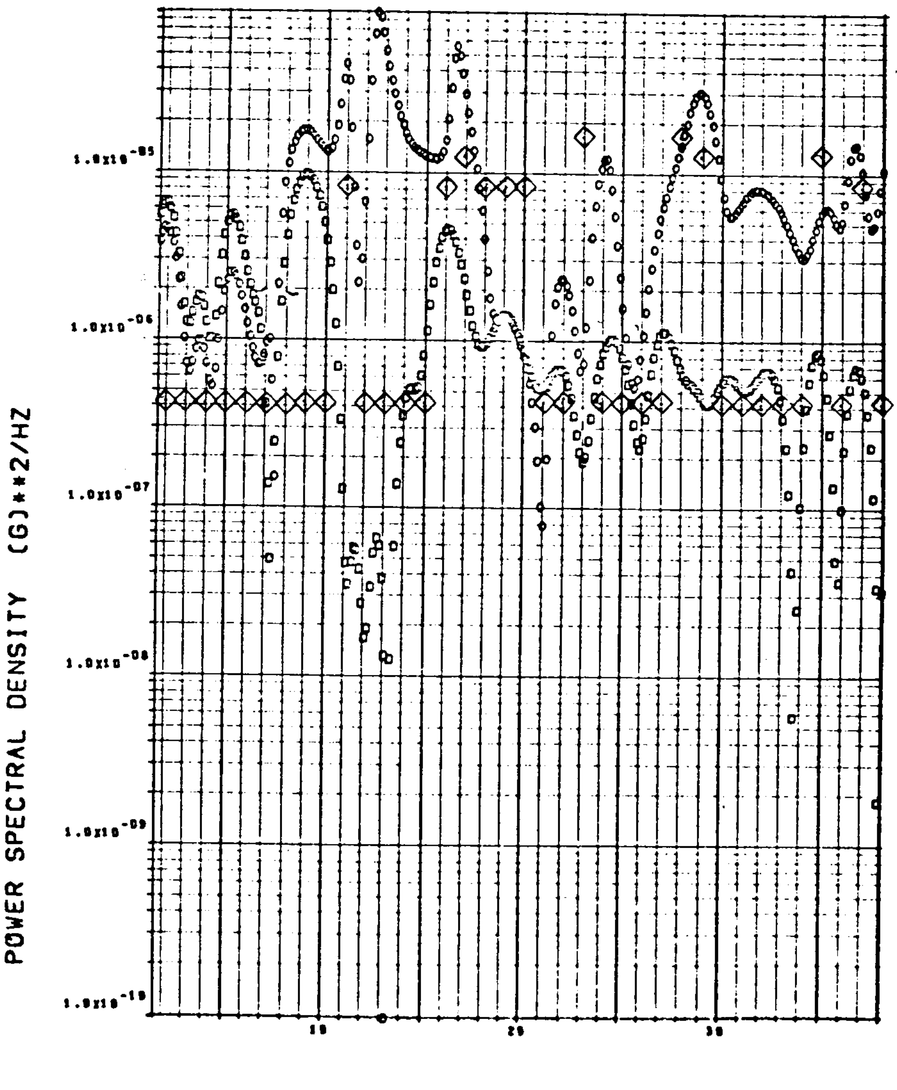

Figure 6.-(d) C.G. lateral accelerometer

◇ AB020 $\alpha_{FLT} = 13.65^{\circ}$

F-111A WING ALONE BUFFET RESPONSE. FLT 48. RUN 4
SWEEP= 50 DEG. MACH=1.2. ALT=9053(M). ALPHA= 16.1
C.G. LATERAL ACCELEROMETER. FS = 529
SQUARE = 1 DOF CIRCLE = 12 DOF

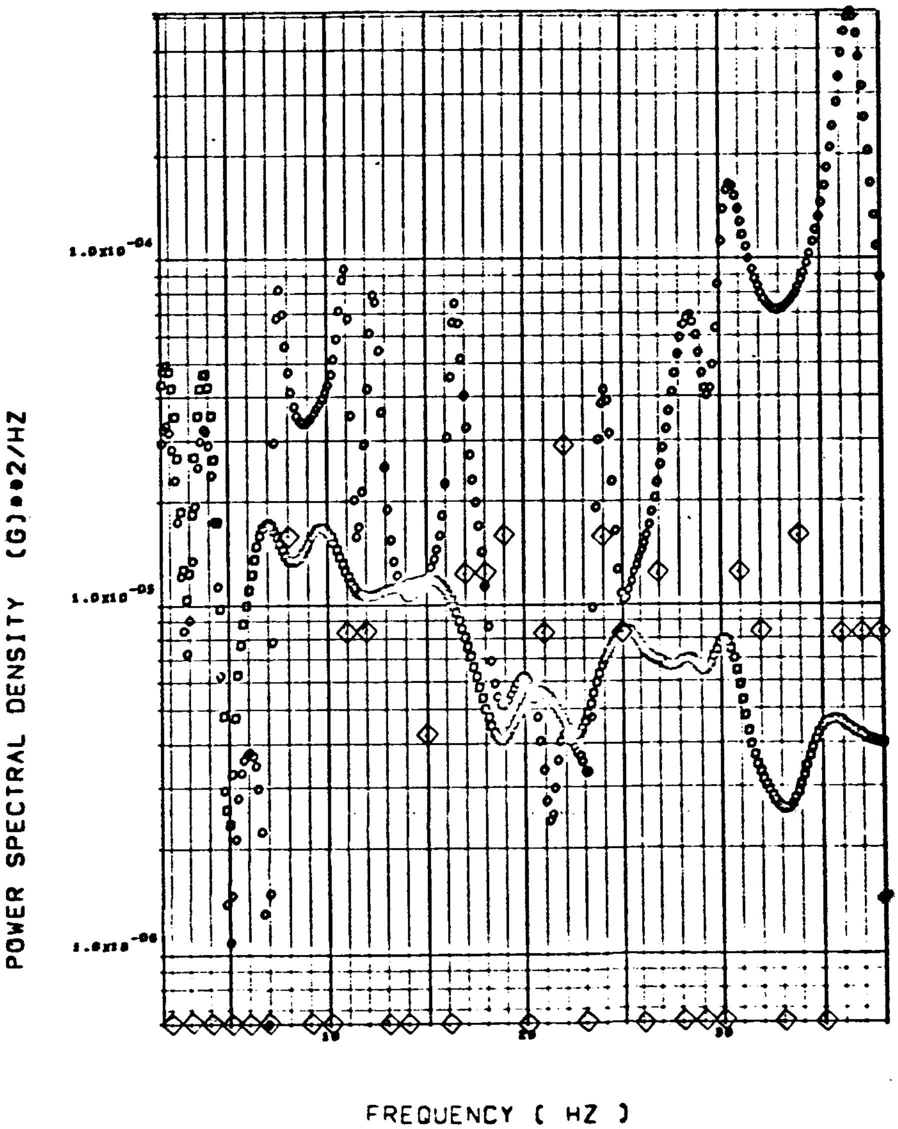

Figure 6.-(d) C.G. lateral accelerometer (continued)

◇ AF010 $\alpha_{FLT} = 12.4^{\circ}$

F-111A WING ALONE BUFFET RESPONSE, FLT 48, RUN 4
SWEEP= 50 DEG, MACH=1.2, ALT=9053(M), ALPHA= 12.4
PILOT STATION LATERAL ACCELEROMETER, FS = 255
SQUARE = 1 DOF CIRCLE = 12 DOF

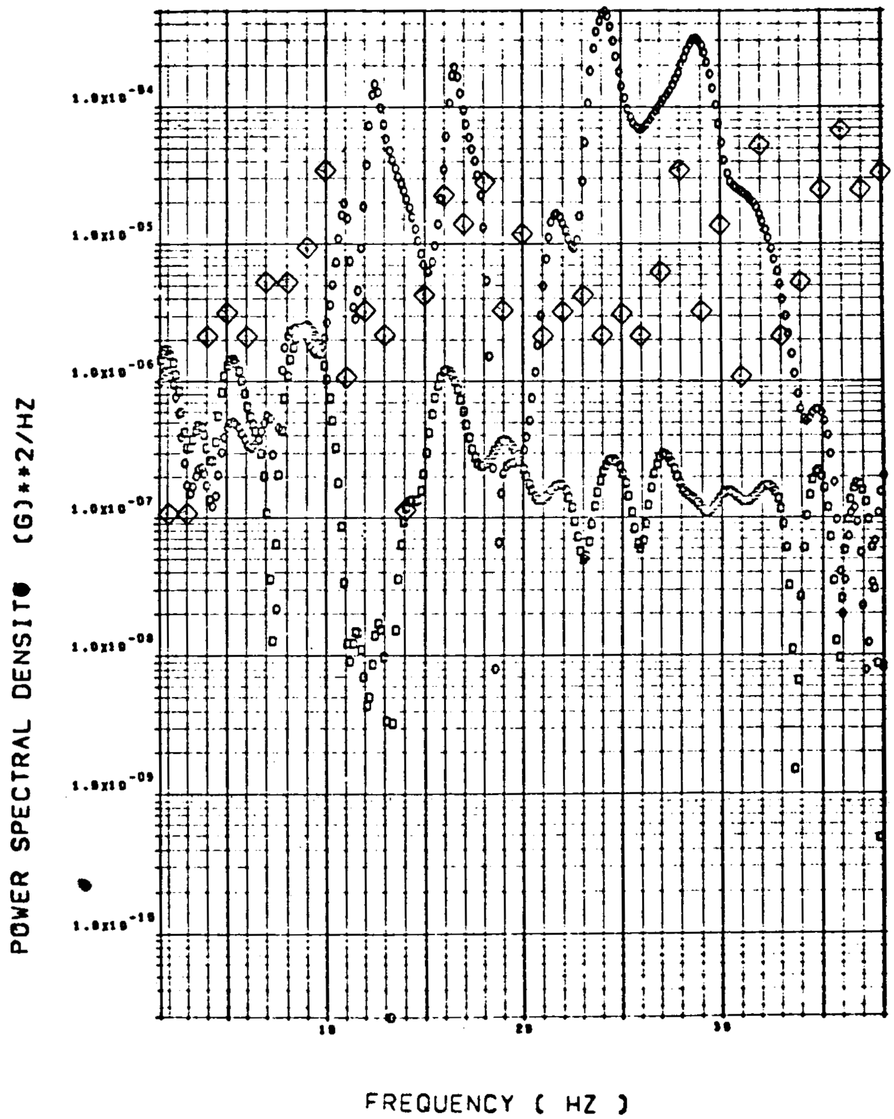

Figure 6.-(e) Pilot seat lateral accelerometer

◇ AF010 $\alpha_{FLT} = 13.65^{\circ}$

F-111A WING ALONE BUFFET RESPONSE. FLT 48. RUN 4
SWEEP= 50 DEG. MACH=1.2. ALT=9053(M). ALPHA=16.1
PILOT STATION LATERAL ACCELEROMETER. FS = 255
SQUARE = 1 DOF CIRCLE = 12 DOF

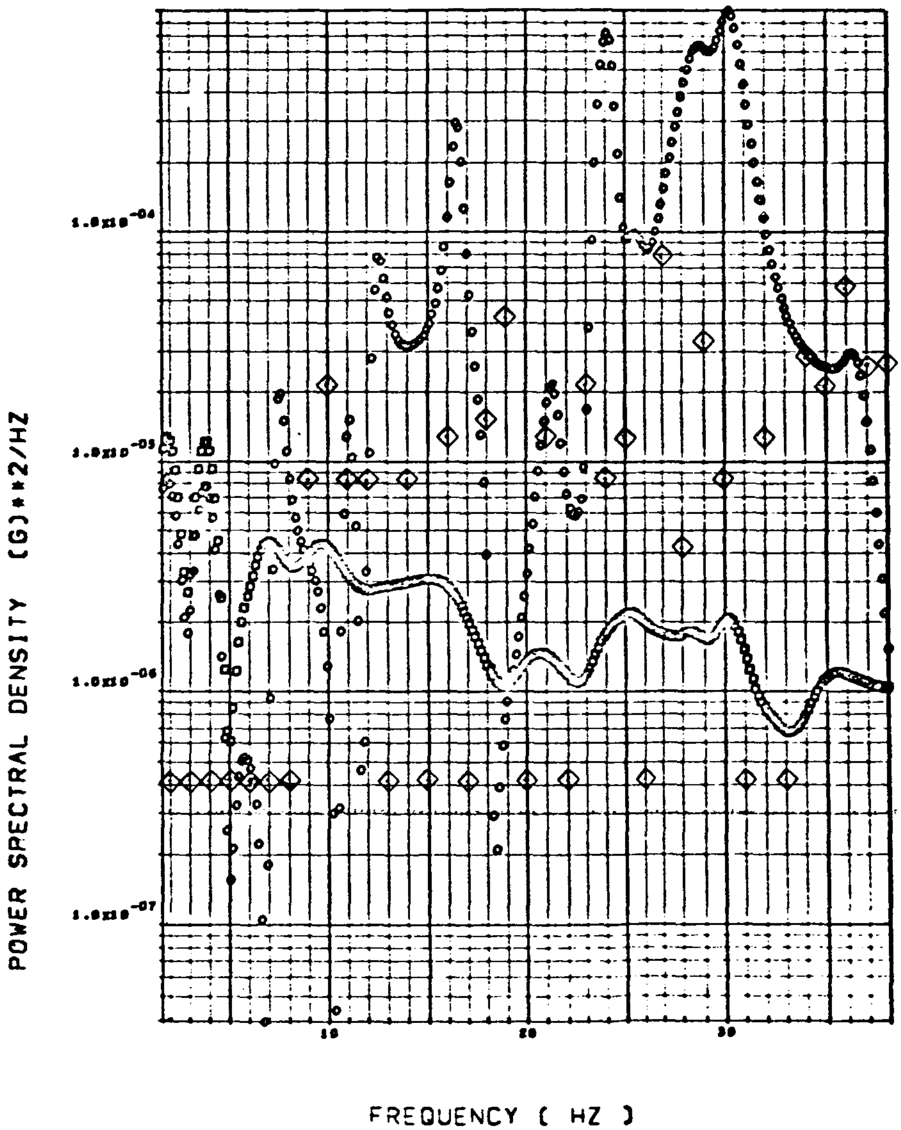

Figure 6.-(e) Pilot seat lateral accelerometer (continued)

Δ SW123

$\alpha_{FLT} = 12.4^{o}$

F-111A WING ALONE BUFFET RESPONSE, FLT 48, RUN 4
SWEEP= 50 DEG, MACH=1.2, ALT=9053(M), ALPHA= 12.4
WING SHEAR (N) AT SPAN STATION 75
CIRCLE = UPPER BOUNDS SQUARE = LOWER BOUNDS

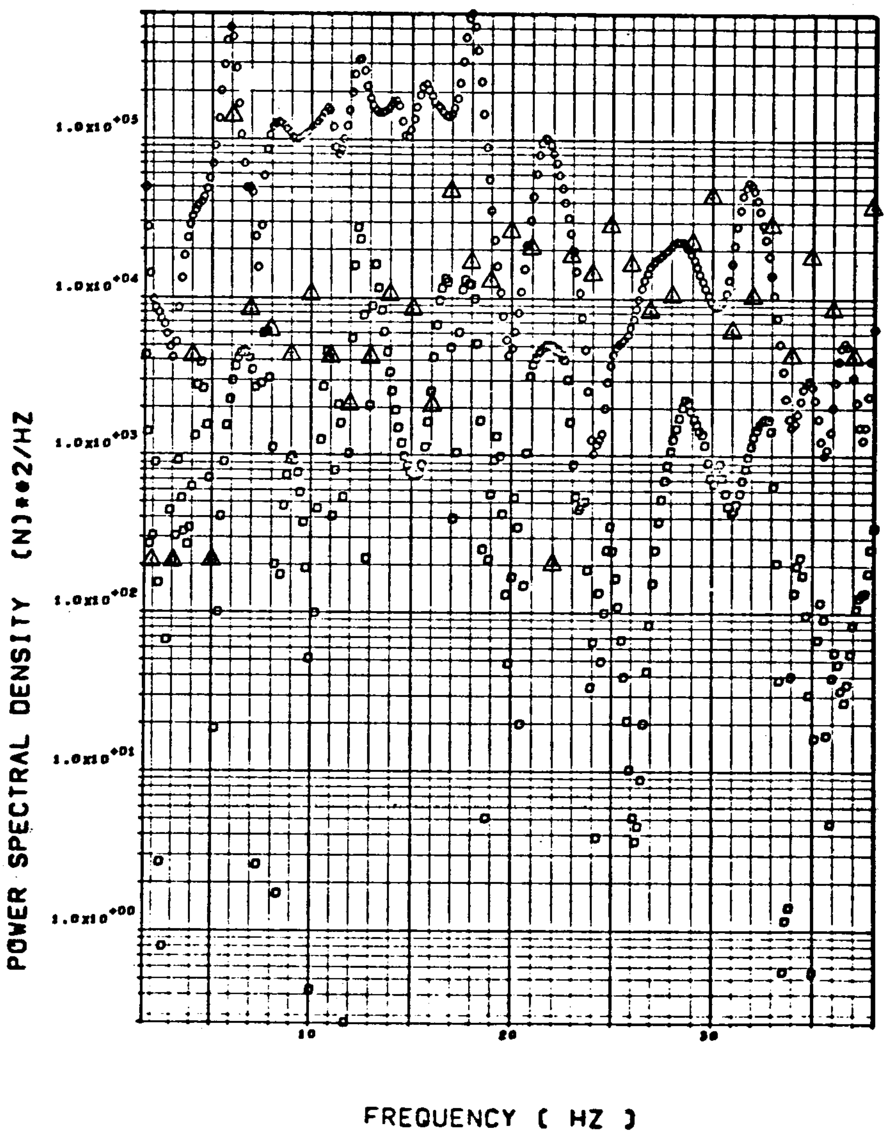

Figure 6.-(f) Wing shear

△ SW123 $\alpha_{FLT} = 13.65^{\circ}$

F-111A WING ALONE BUFFET RESPONSE. FLT 48. RUN 4
SWEEP= 50 DEG. MACH=1.2. ALT=9053(M). ALPHA=16.1
WING SHEAR (N) AT SPAN STATION 75
CIRCLE = UPPER BOUNDS SQUARE = LOWER BOUNDS

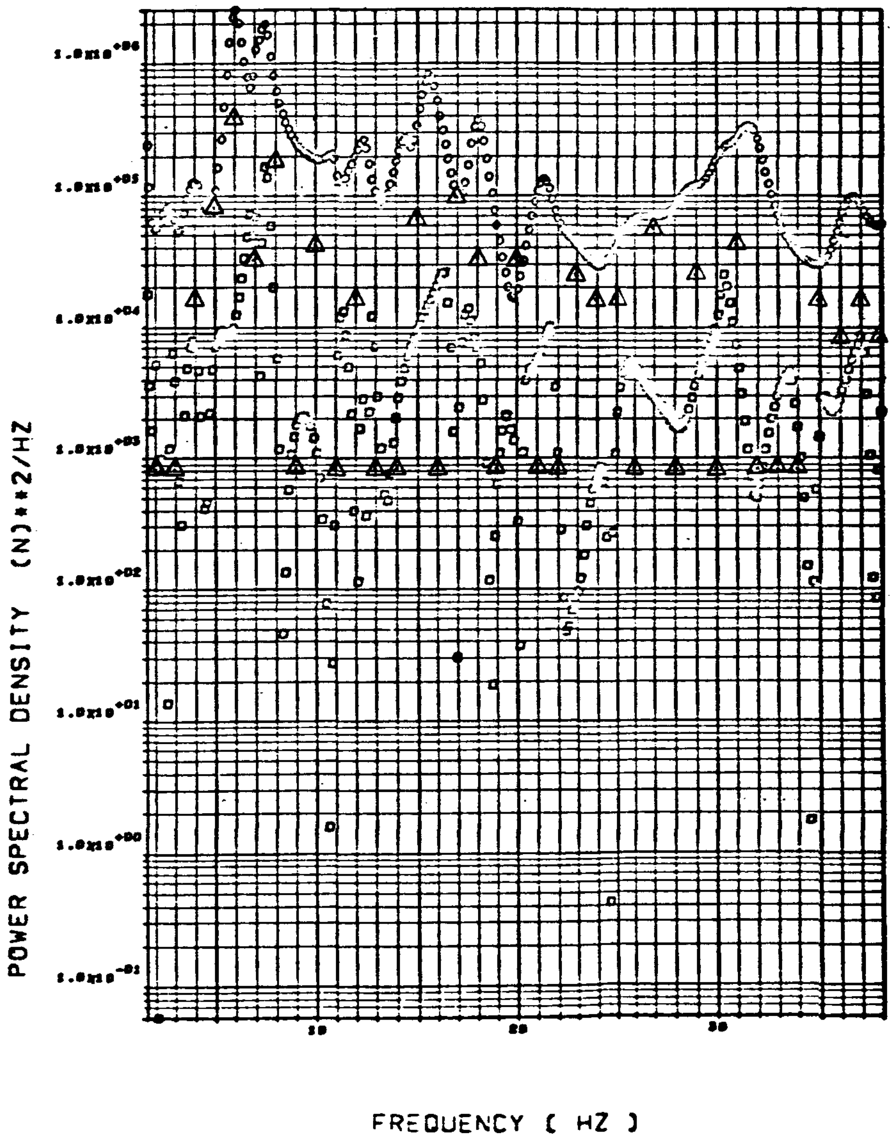

Figure 6.-(f) Wing shear (continued)

△ SW124 $\alpha_{FLT} = 12.4^{o}$

F-111A WING ALONE BUFFET RESPONSE. FLT 48. RUN 4
SWEEP= 50 DEG. MACH=1.2. ALT=9053(M). ALPHA= 12.4
WING BENDING MOMENT (M-N) AT SPAN STATION 75
CIRCLE = UPPER BOUNDS SQUARE = LOWER BOUNDS

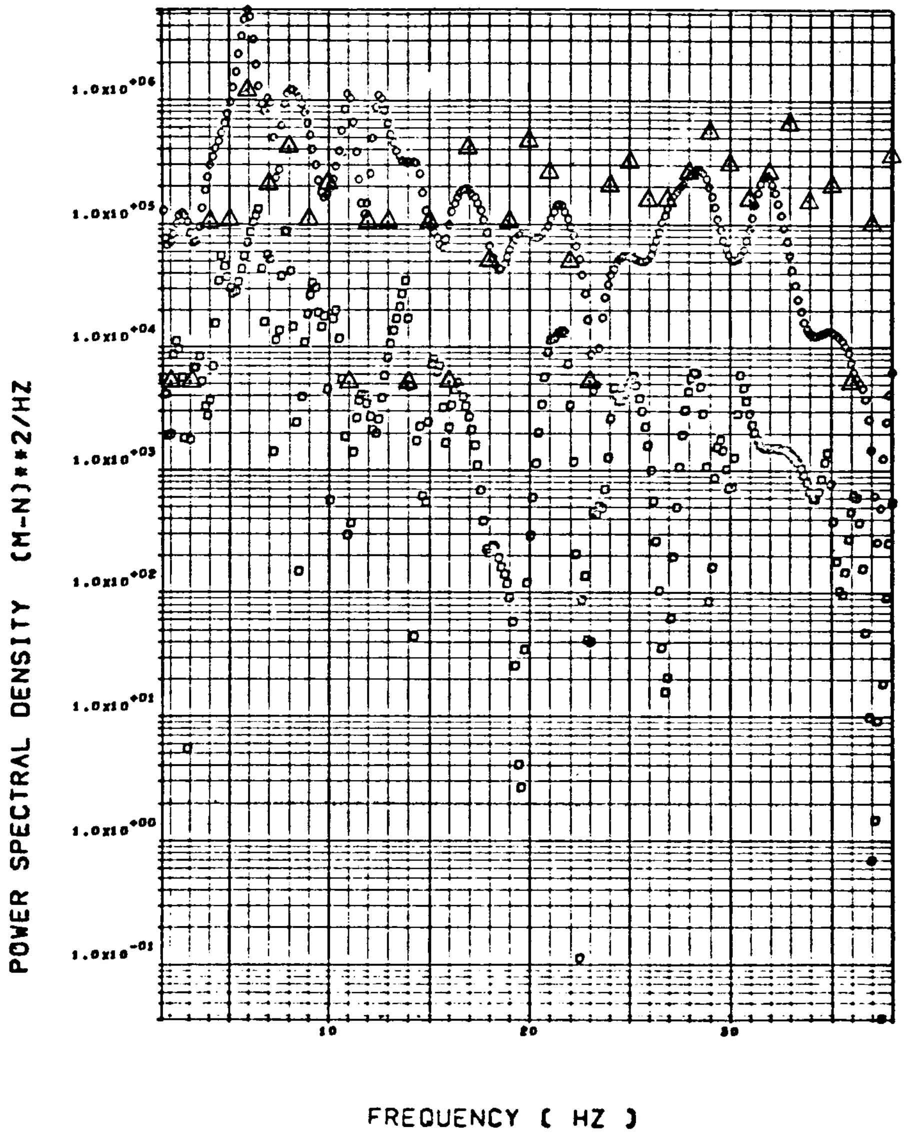

Figure 6.-(g) Wing bending moment

△ SW124 $\alpha_{FLT} = 13.65^{o}$

F-111A WING ALONE BUFFET RESPONSE. FLT 48. RUN 4
SWEEP= 50 DEG. MACH=1.2. ALT=9053(M). ALPHA= 16.1
WING BENDING MOMENT (M-N) AT SPAN STATION 75
CIRCLE = UPPER BOUNDS SQUARE = LOWER BOUNDS

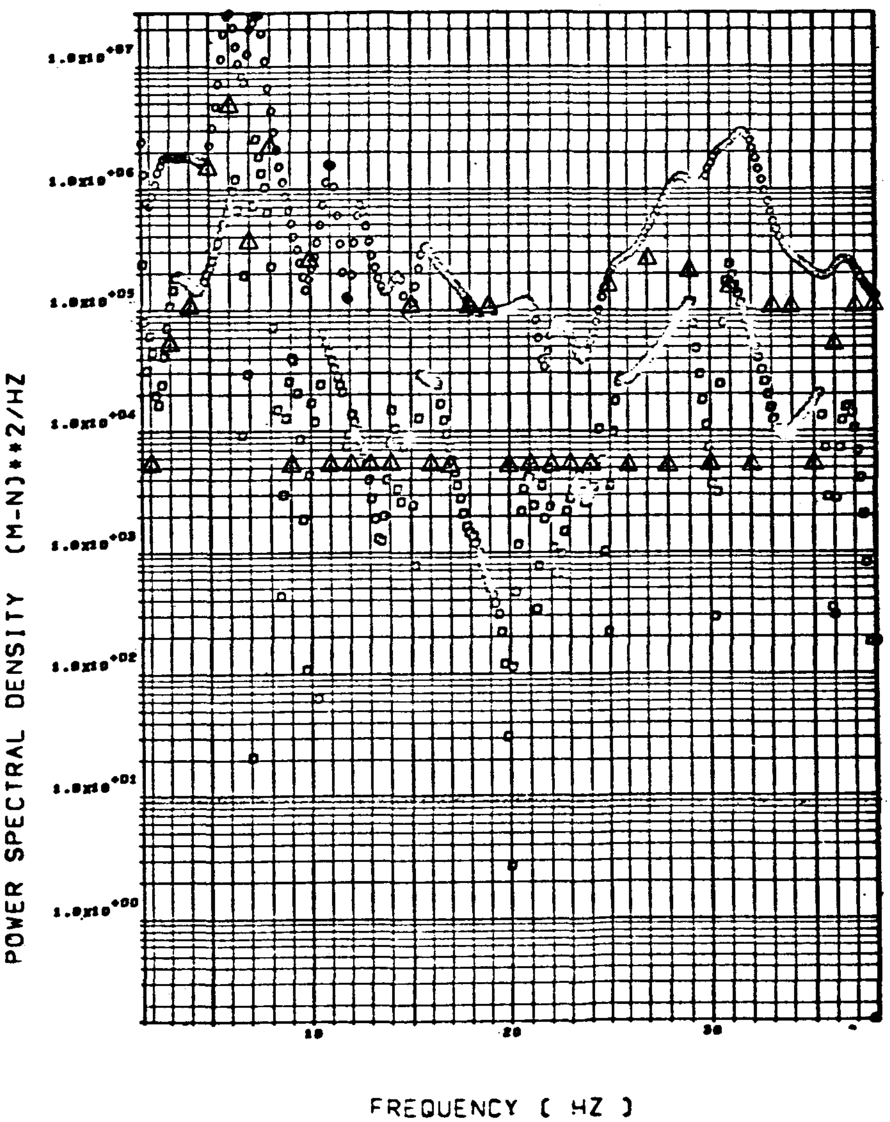

Figure 6.-(g) Wing bending moment (continued)

△ SW125

$\alpha_{FLT} = 12.4^{o}$

F-111A WING ALONE BUFFET RESPONSE, FLT 48, RUN 4
SWEEP= 50 DEG, MACH=1.2, ALT=9053(M), ALPHA= 12.4
WING TORQUE (M-N) AT SPAN STATION 75
CIRCLE = UPPER BOUNDS SQUARE = LOWER BOUNDS

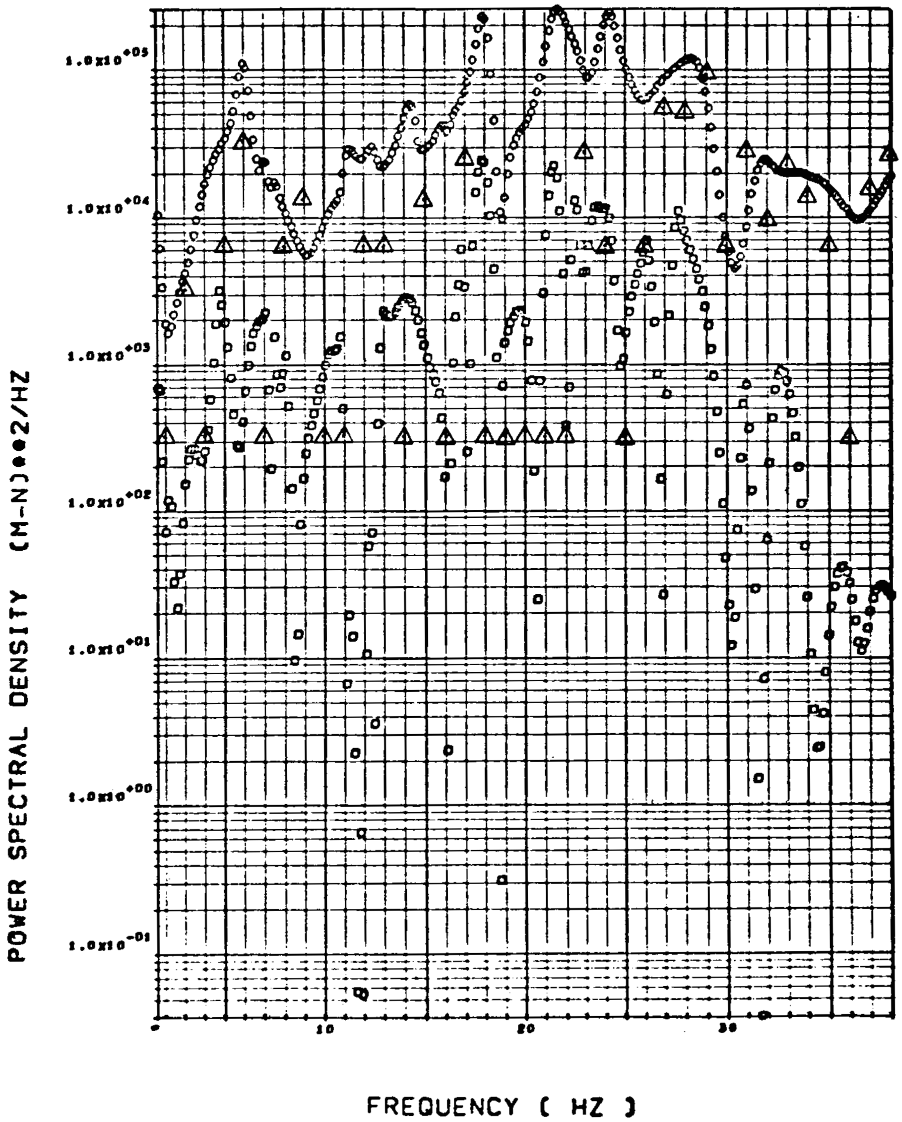

Figure 6.-(h) Wing torsion

△ SW125 $\alpha_{FLT} = 13.65^{o}$

F-111A WING ALONE BUFFET RESPONSE. FLT 48. RUN 4
SWEEP= 50 DEG. MACH=1.2. ALT=9053(M). ALPHA=16.1
WING TORQUE (M-N) AT SPAN STATION 75
CIRCLE = UPPER BOUNDS SQUARE = LOWER BOUNDS

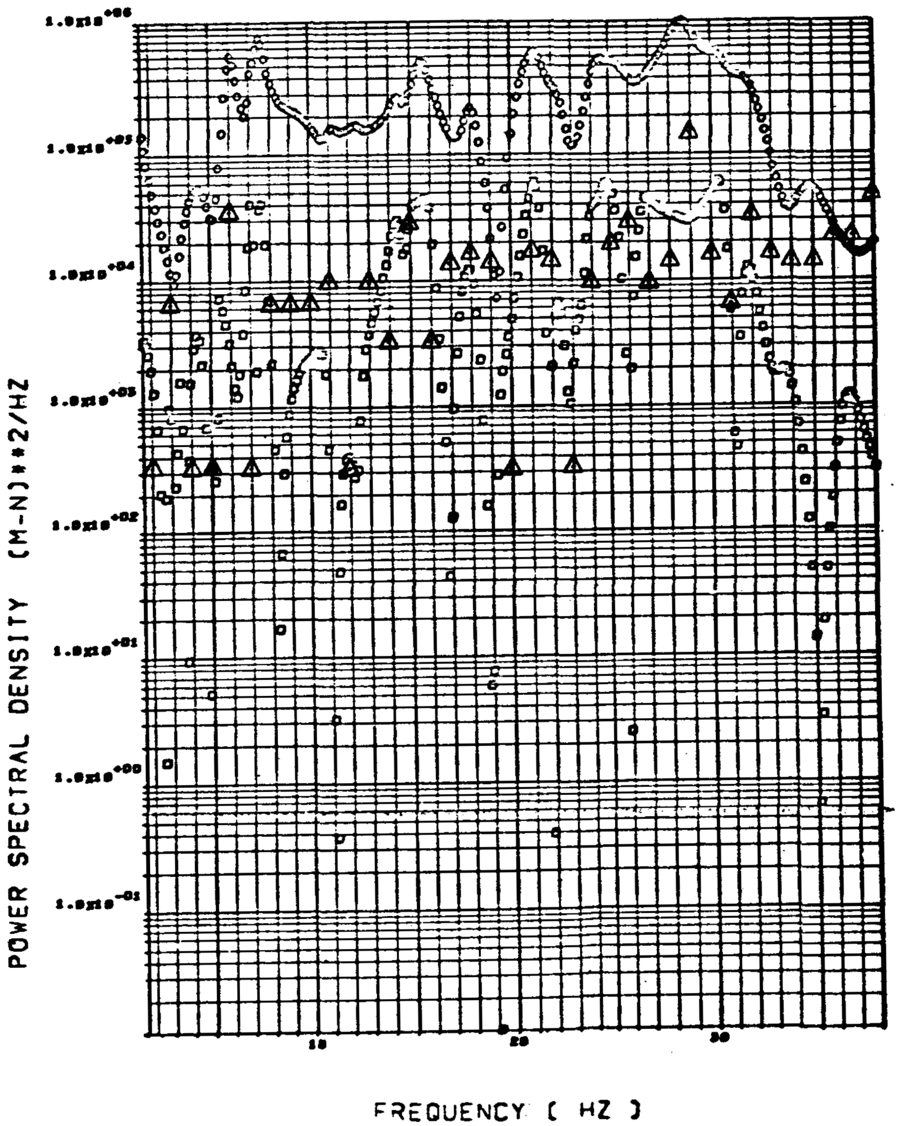

Figure 6.-(h) Wing torsion (continued)

△ AW001 ◇ AW002 $\alpha_{FLT} = 8.1^o$

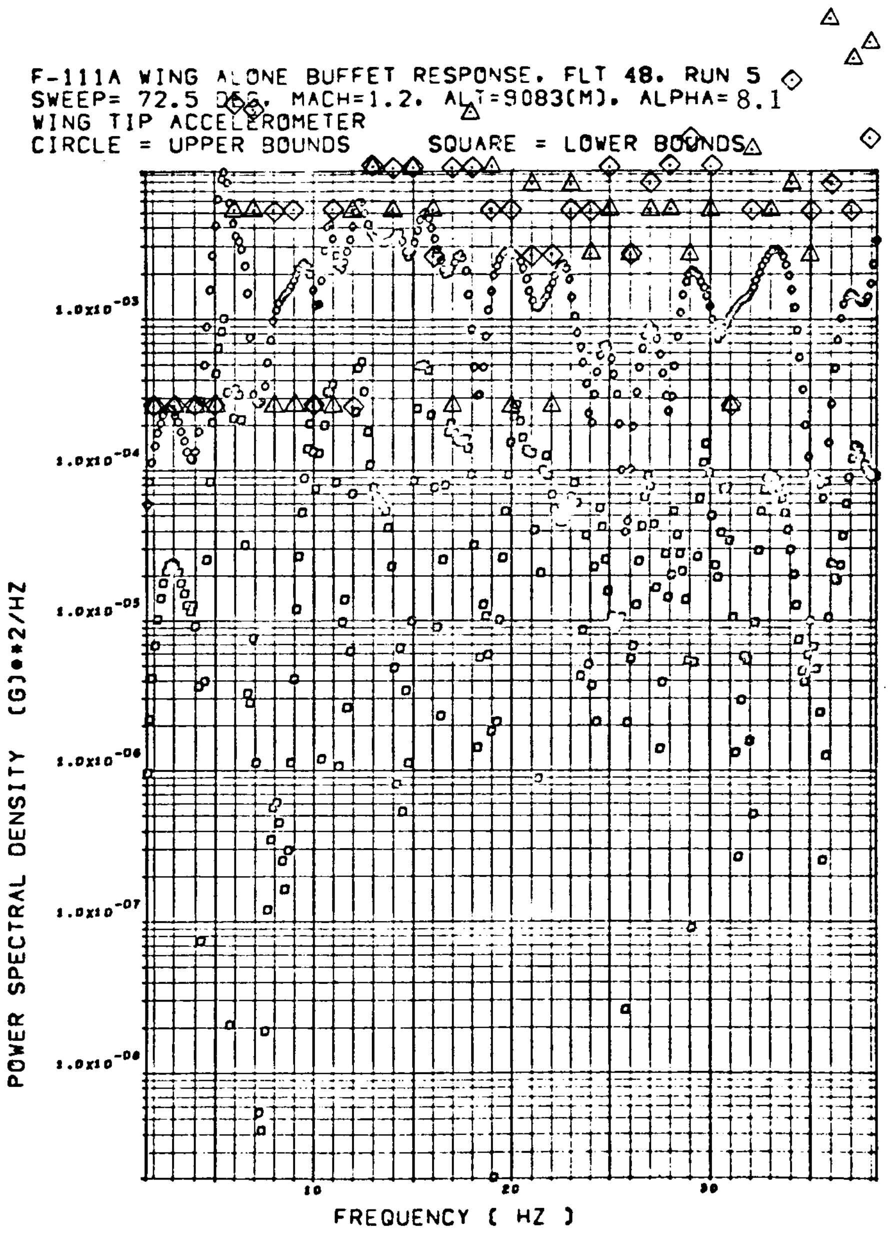

Figure 7.- Power spectra for
Case 7, wing alone (final method),
$\Lambda=72.5^o$, M=1.20, alt.=9083m (29,800 ft)
(a) wing tip accelerometer

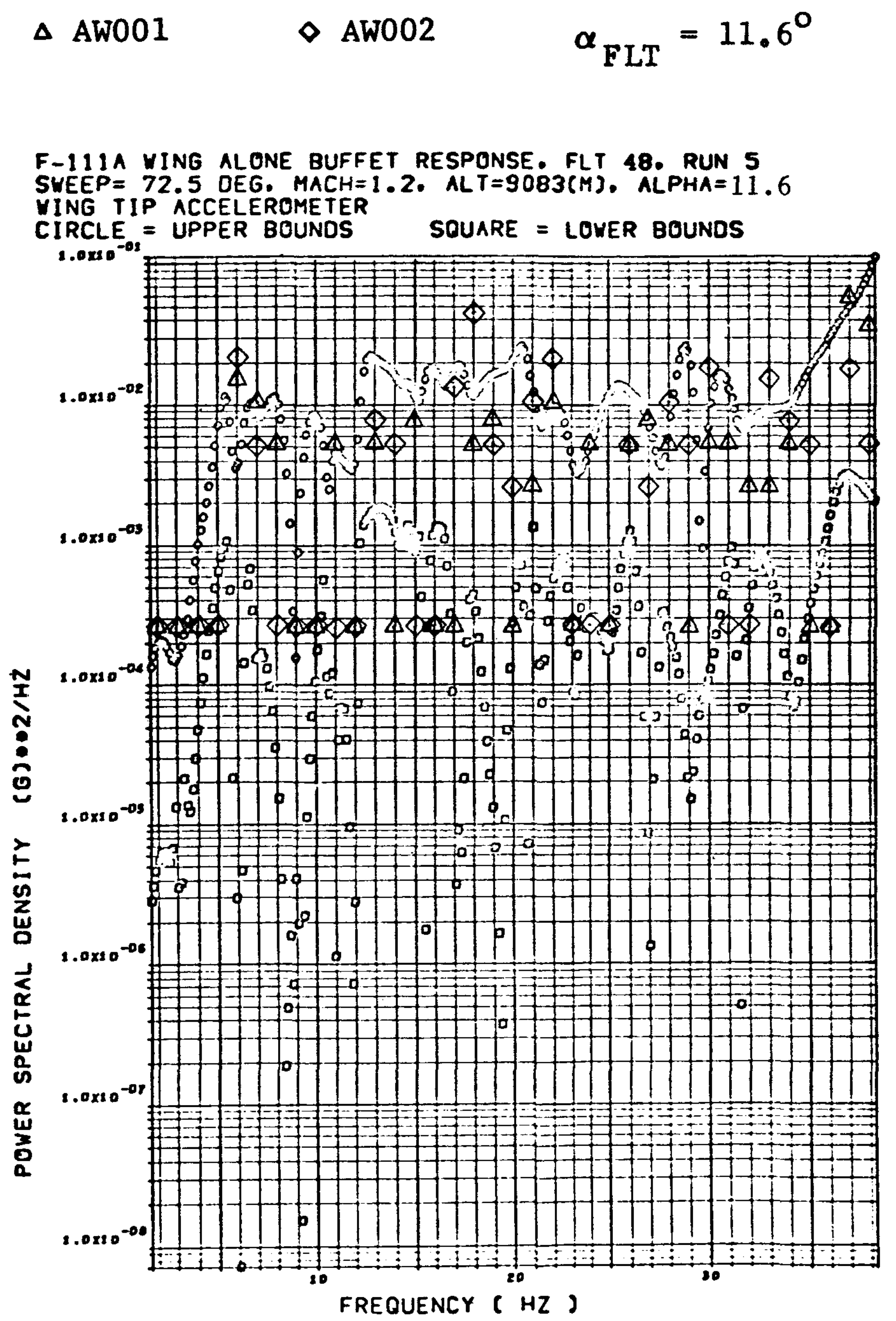

Figure 7.-(a) Wing tip accelerometer (continued)

△ AW001 ◇ AW002 $\alpha_{FLT} = 15.1^{\circ}$

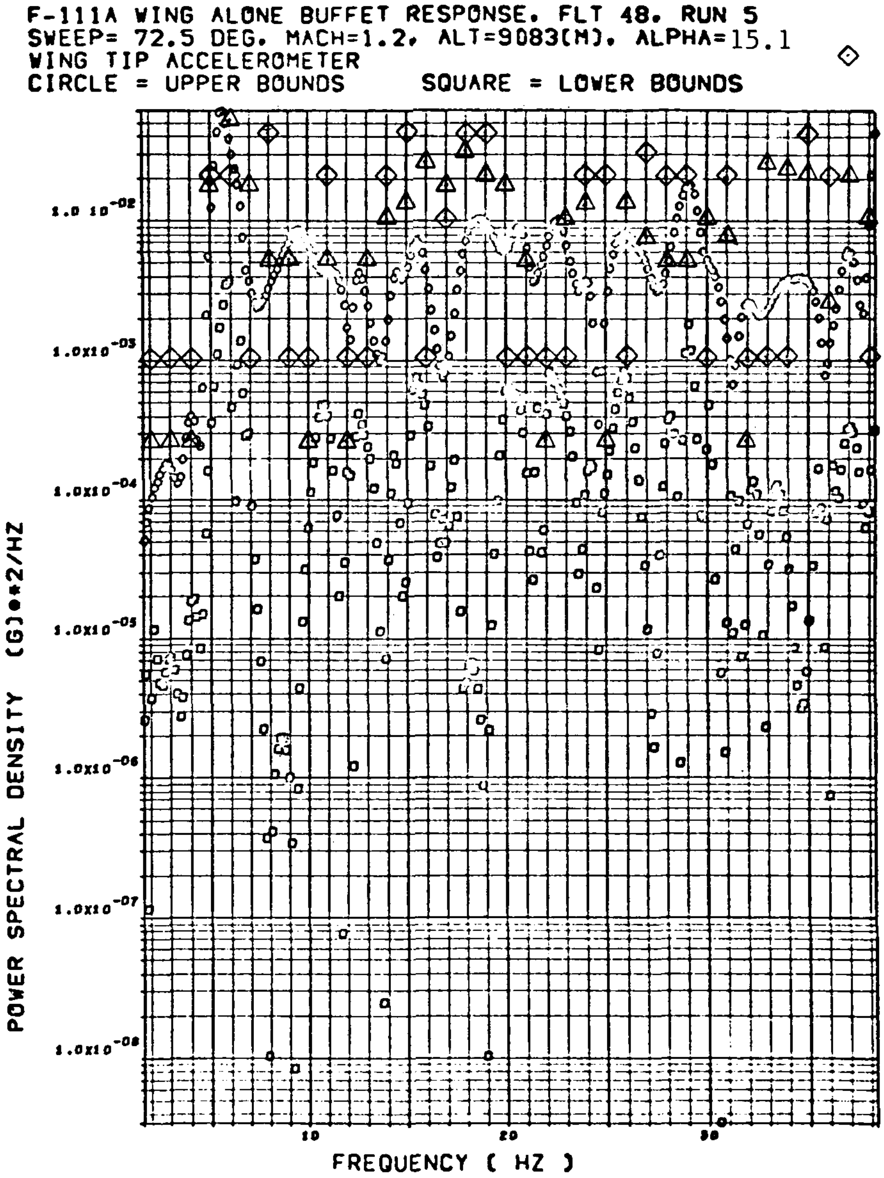

Figure 7.-(a) Wing tip accelerometer (continued)

◇ AB018 $\alpha_{FLT} = 8.1^{o}$

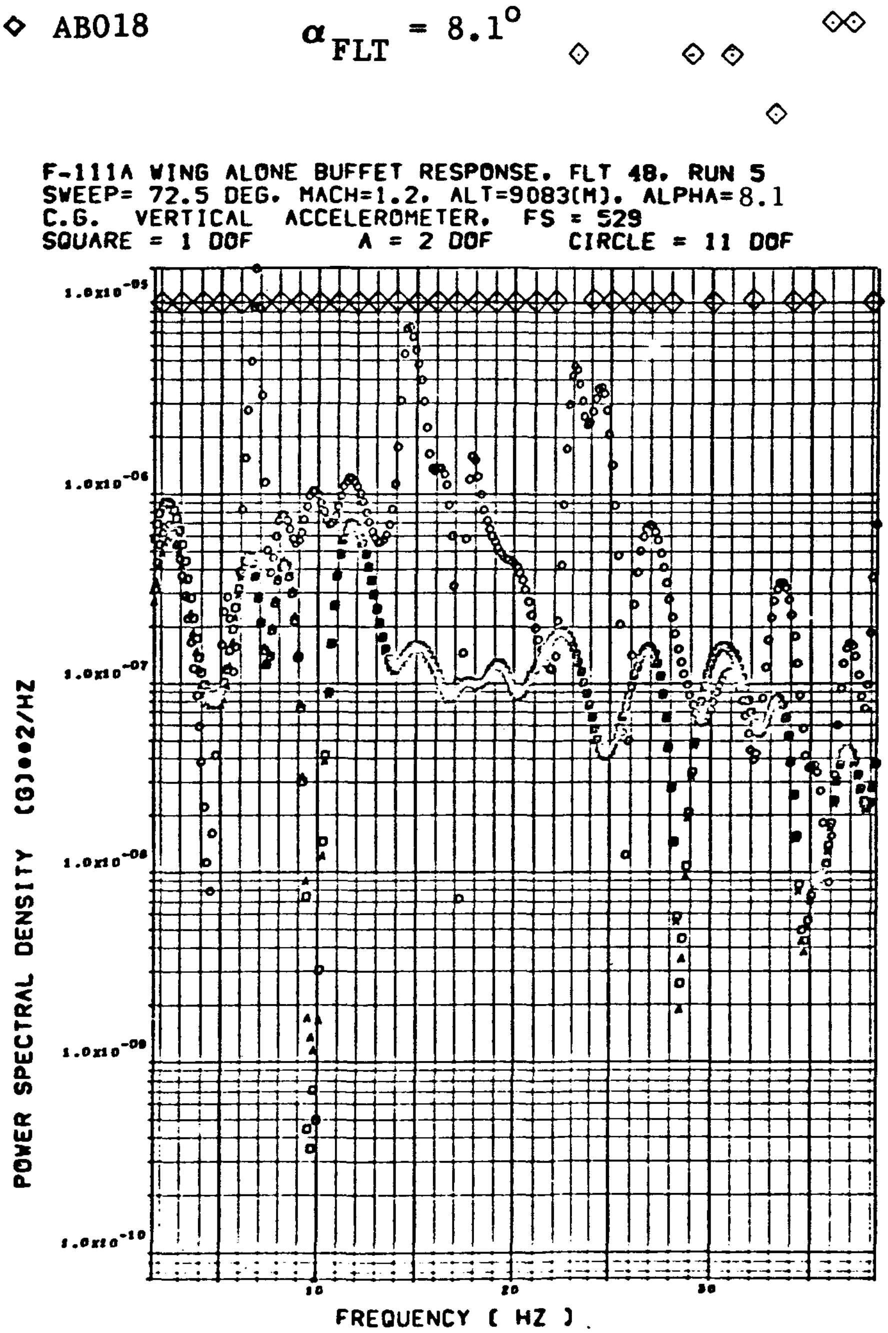

Figure 7.-(b) C.G. vertical accelerometer

◇ AB018 $\alpha_{FLT} = 11.6^{o}$

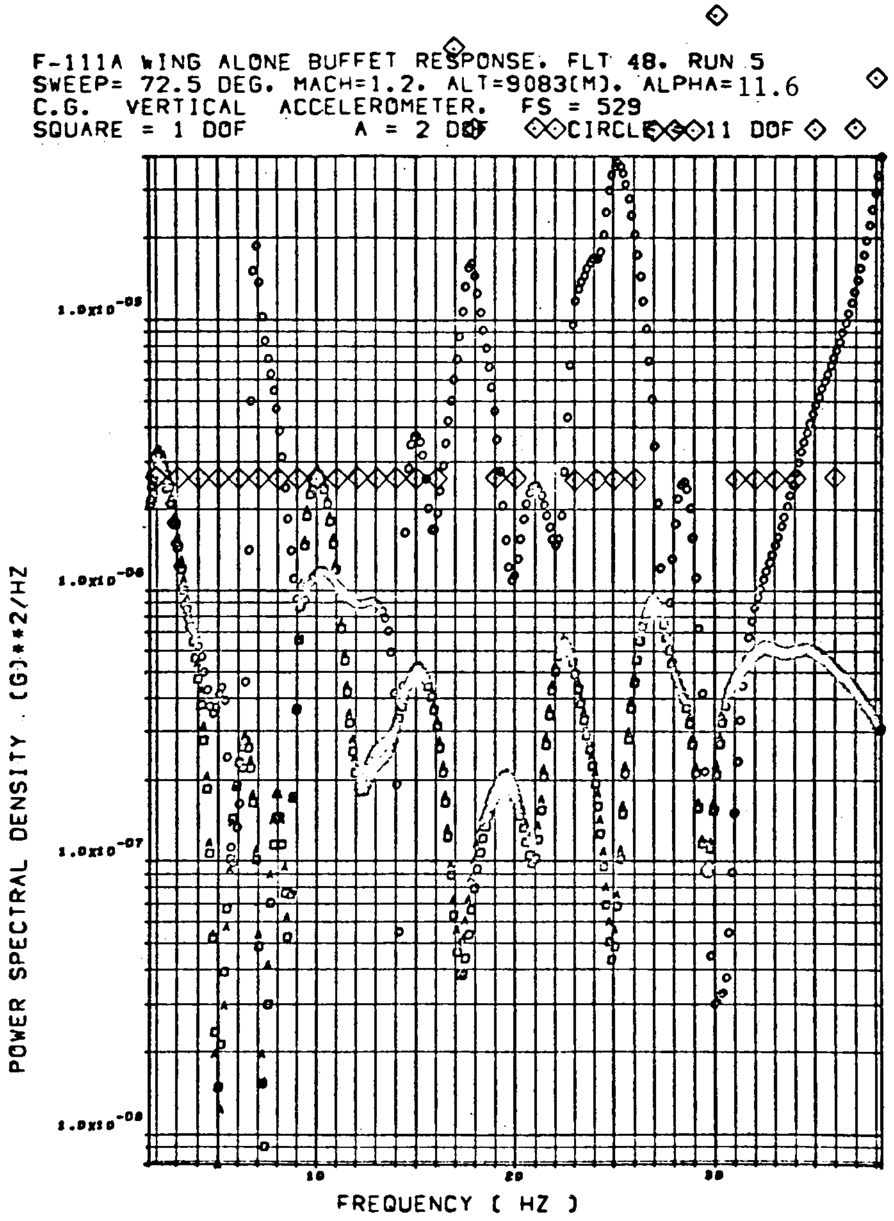

Figure 7.-(b) C.G. vertical accelerometer (continued)

◇ AB018 $\alpha_{FLT} = 15.1^{\circ}$

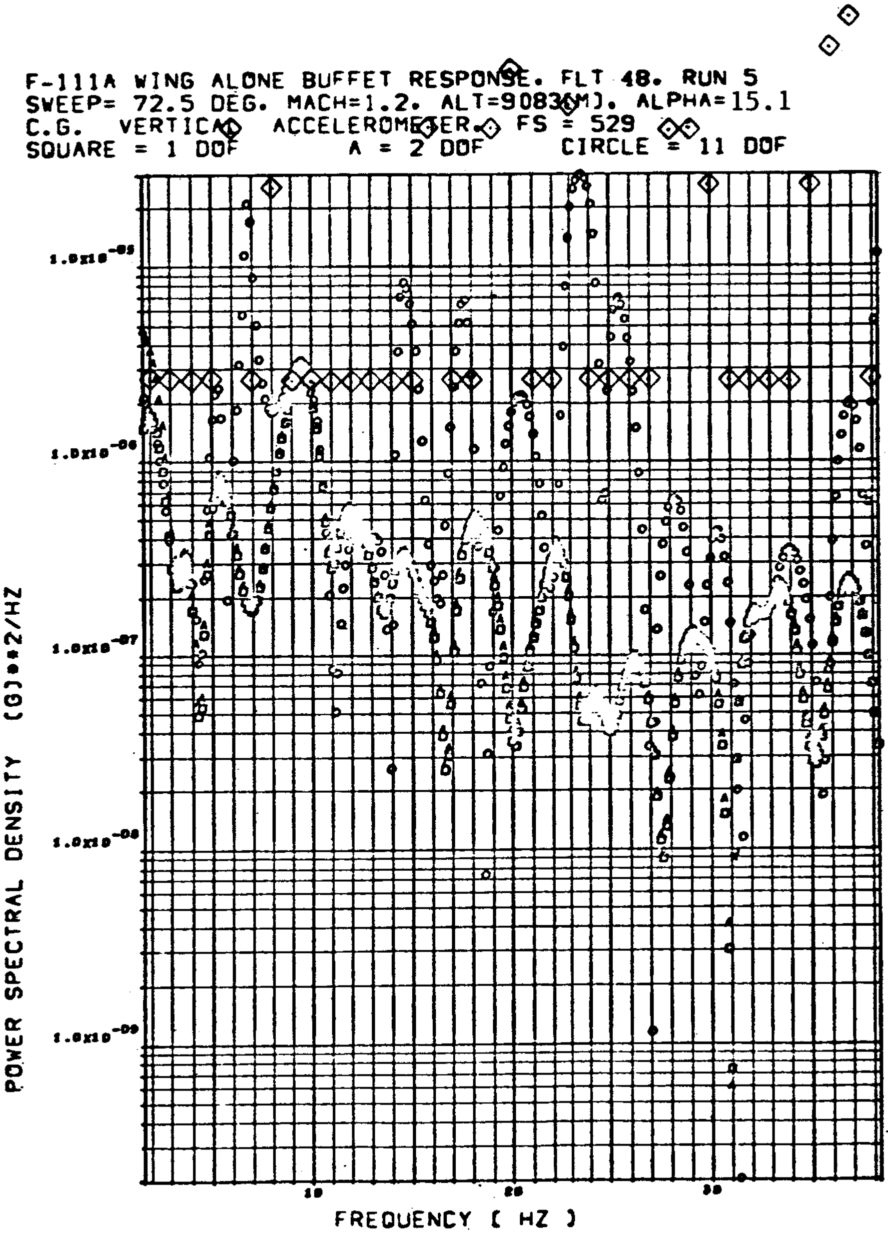

Figure 7.-(b) C.G. vertical accelerometer (continued)

◇ AF009 $\alpha_{FLT} = 8.1^{o}$

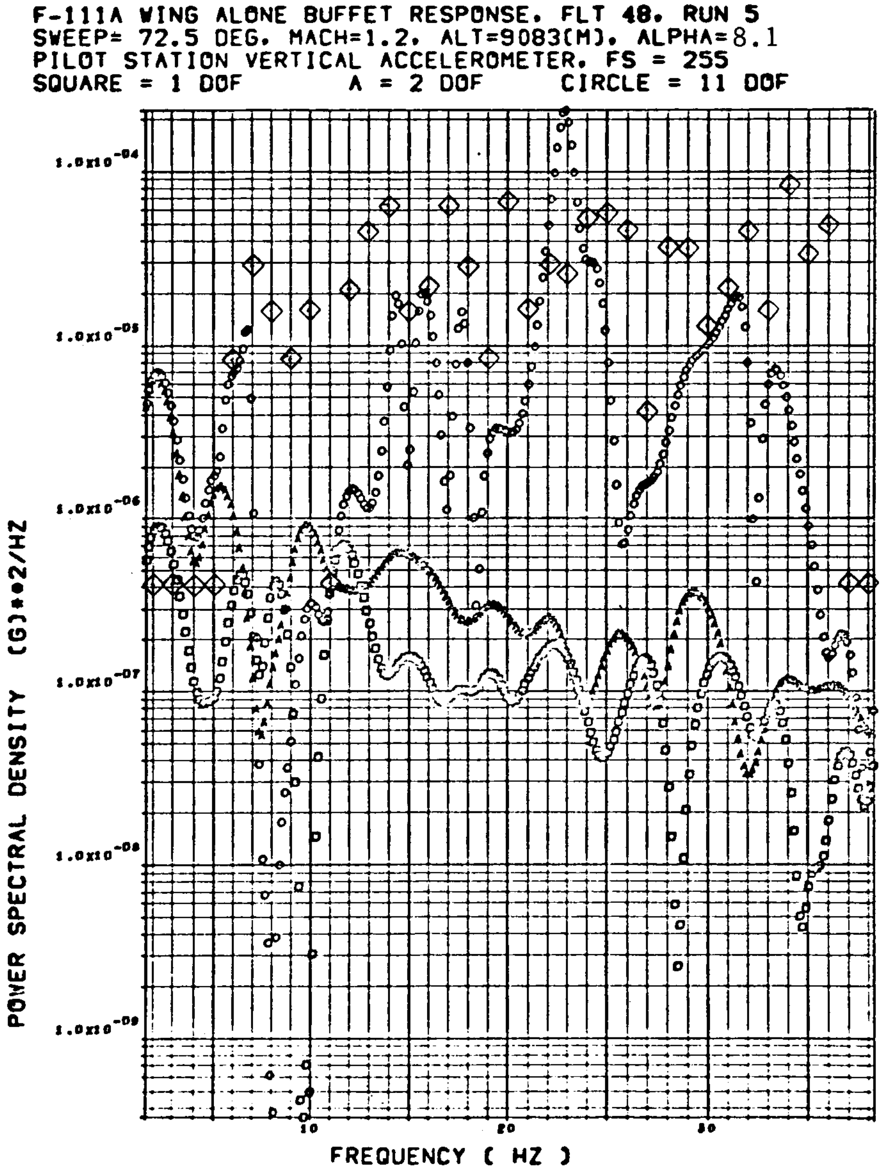

Figure 7.-(c) Pilot seat vertical accelerometer

◇ AF009 $\alpha_{FLT} = 11.6^{o}$

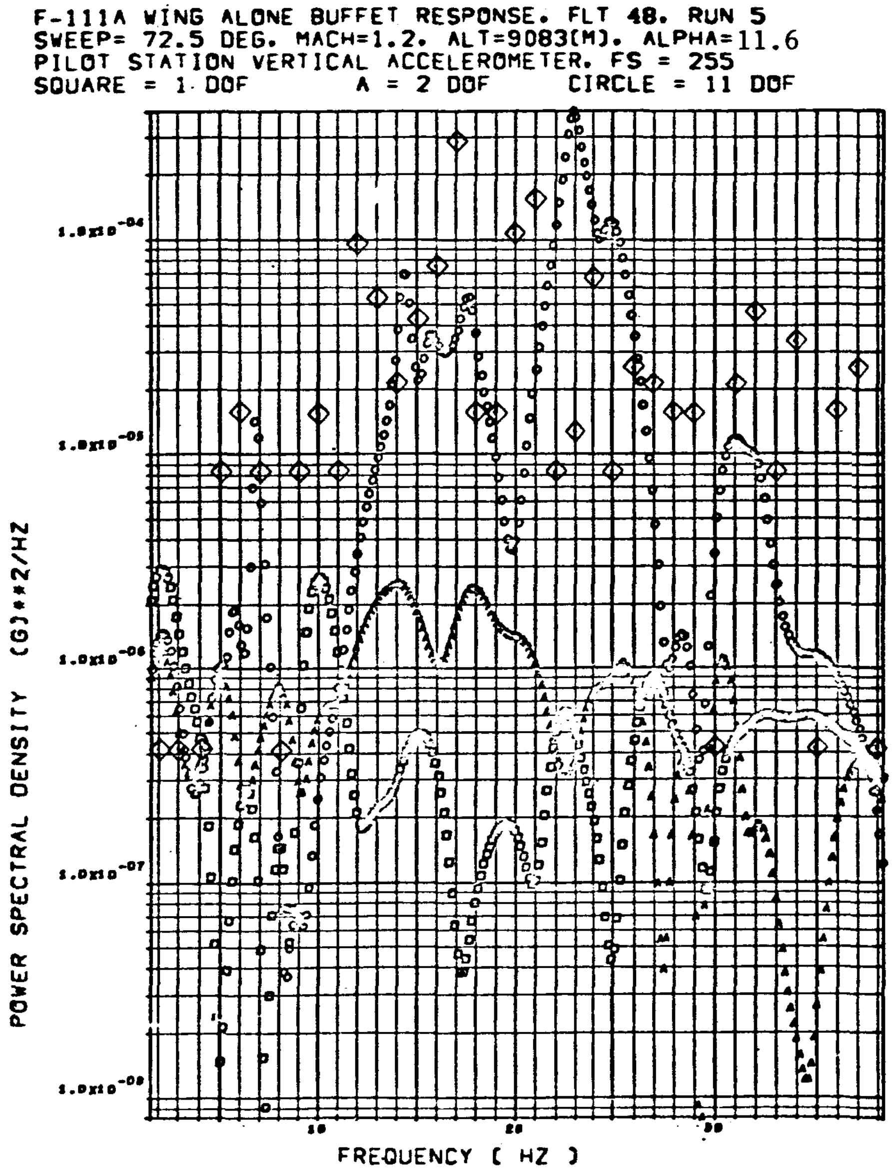

Figure 7.-(c) Pilot seat vertical accelerometer (continued)

◇ AF009 $\alpha_{FLT} = 15.1^{o}$

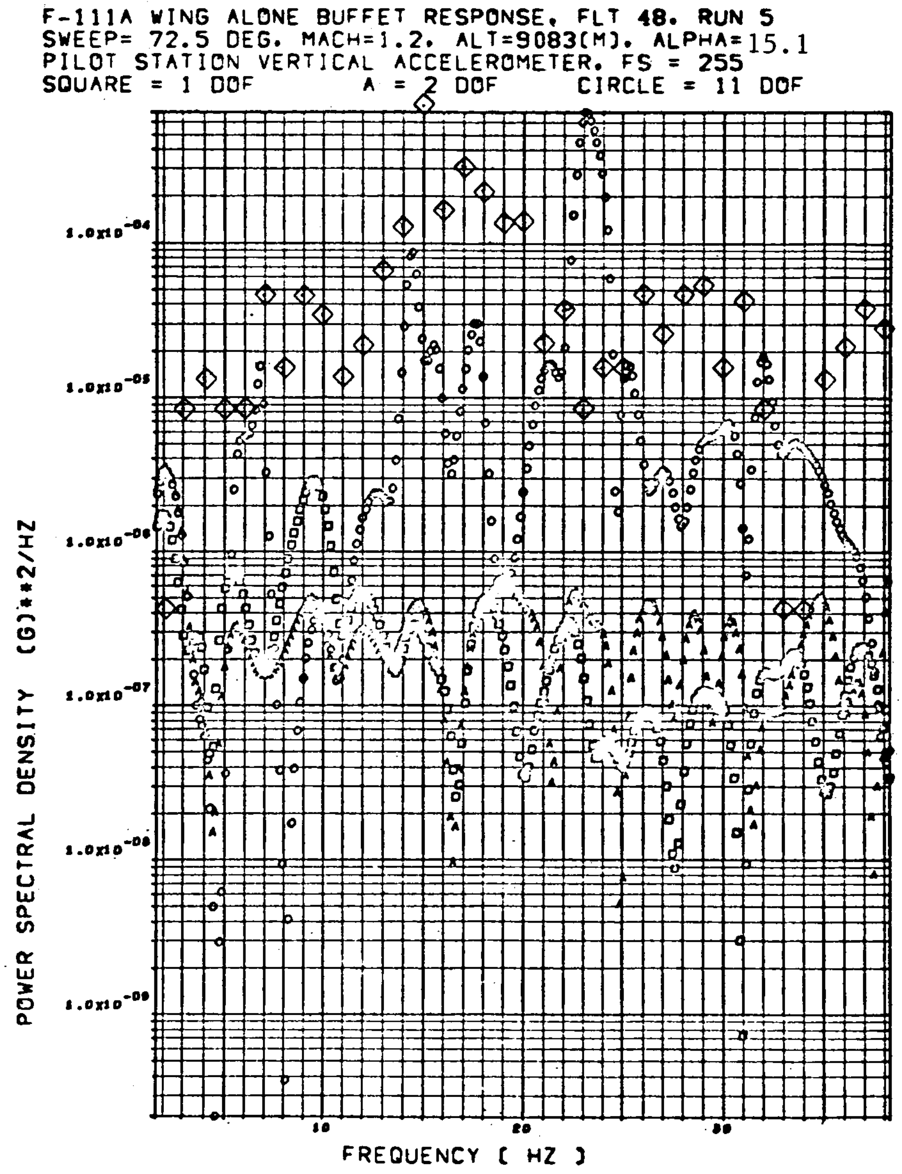

Figure 7.-(c) Pilot seat vertical accelerometer (continued)

◇ AB020 $\alpha_{FLT} = 8.1^{o}$

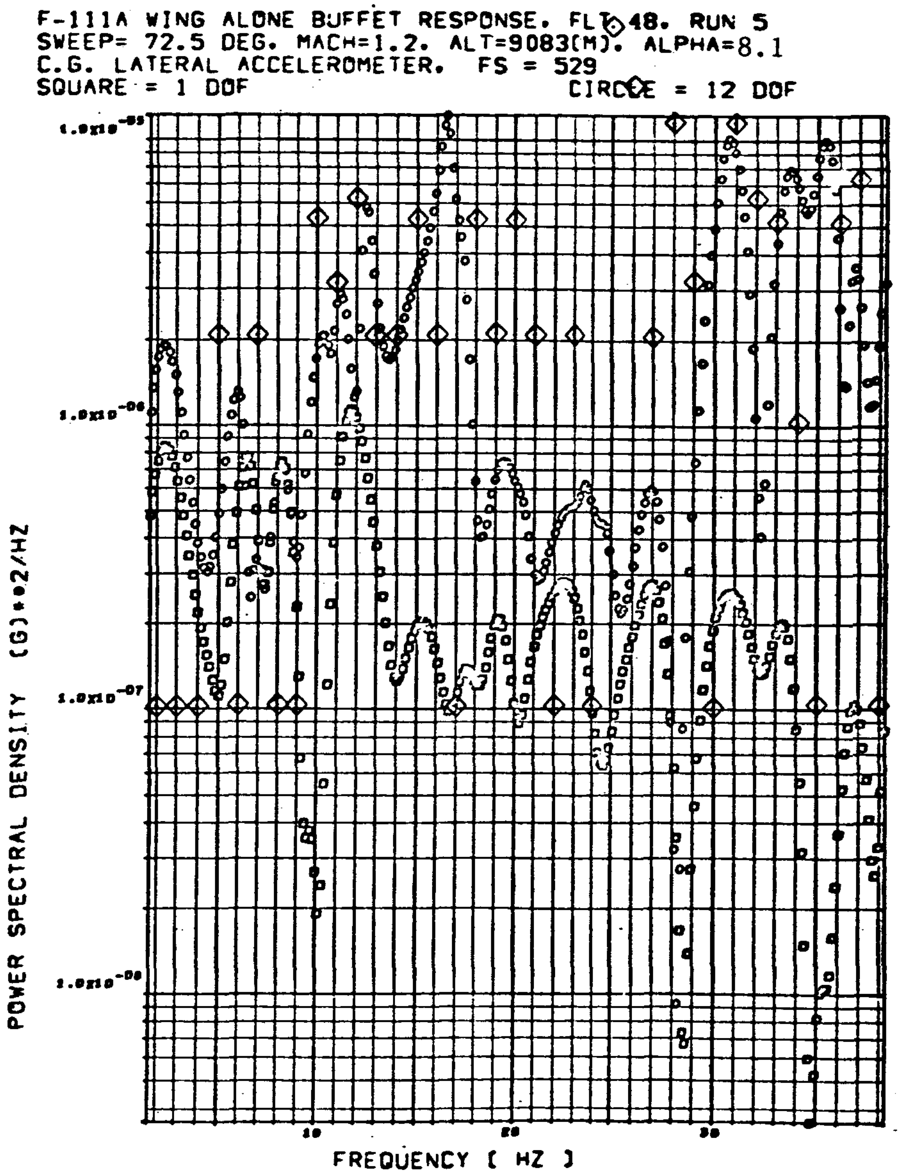

Figure 7.-(d) C.G. lateral accelerometer

◇ AB020 $\alpha_{FLT} = 11.6^{o}$

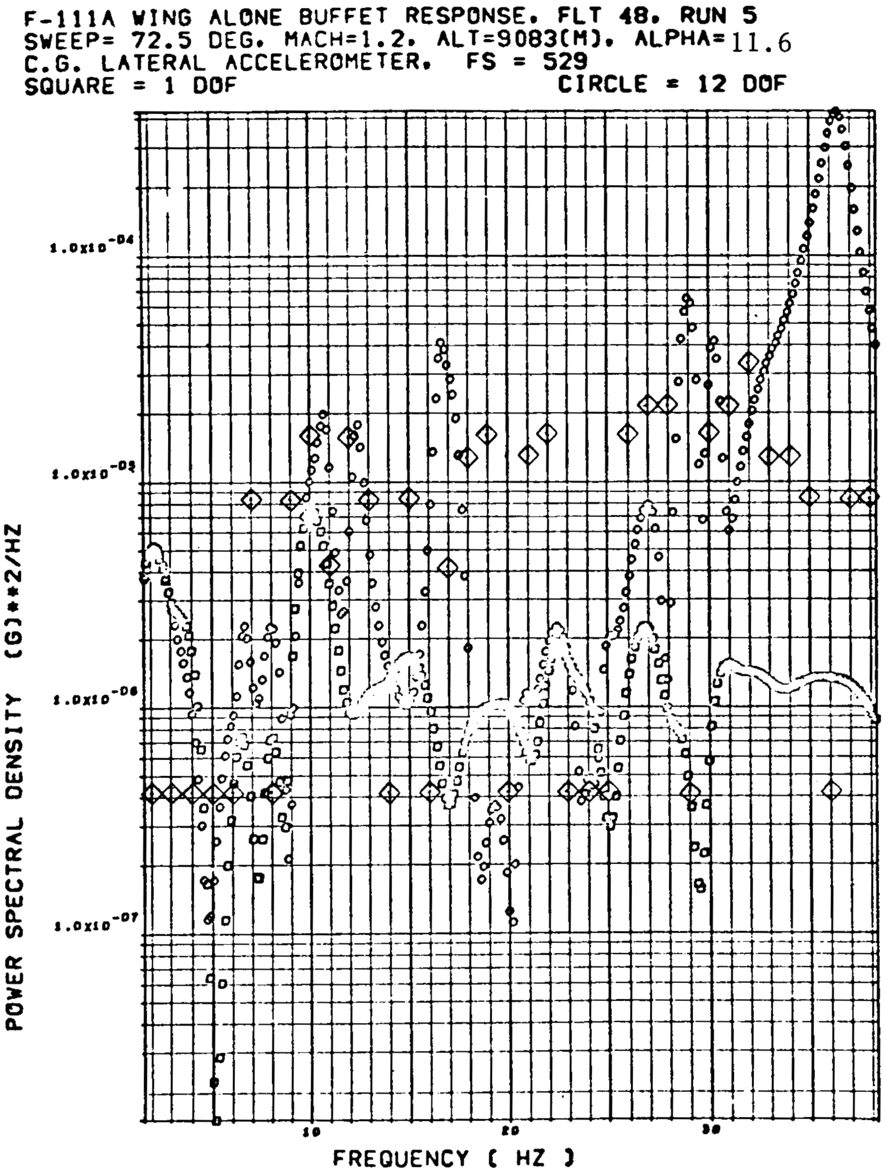

Figure 7.-(d) C.G. lateral accelerometer (continued)

◇ AB020

$\alpha_{FLT} = 15.1^{\circ}$

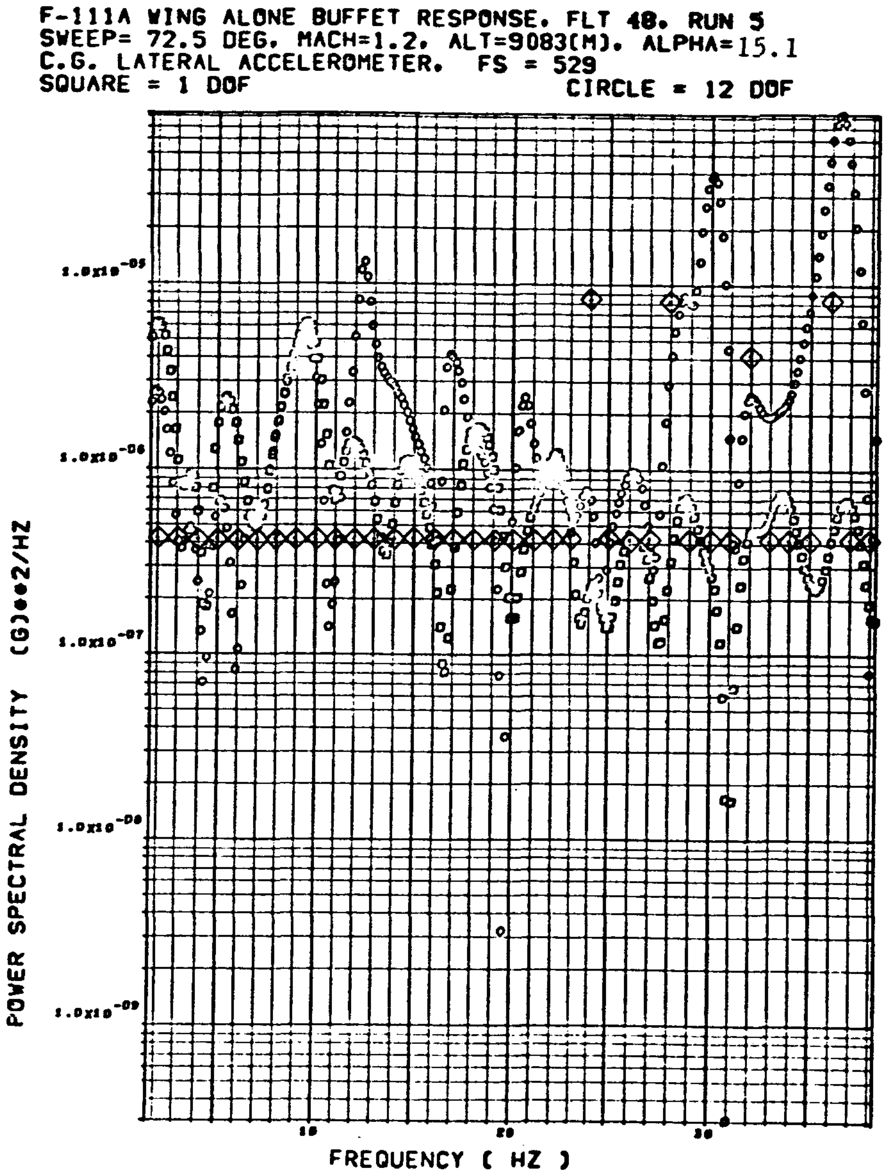

Figure 7.-(d) C.G. lateral accelerometer (continued)

◇ AF010 $\alpha_{FLT} = 8.1^{o}$

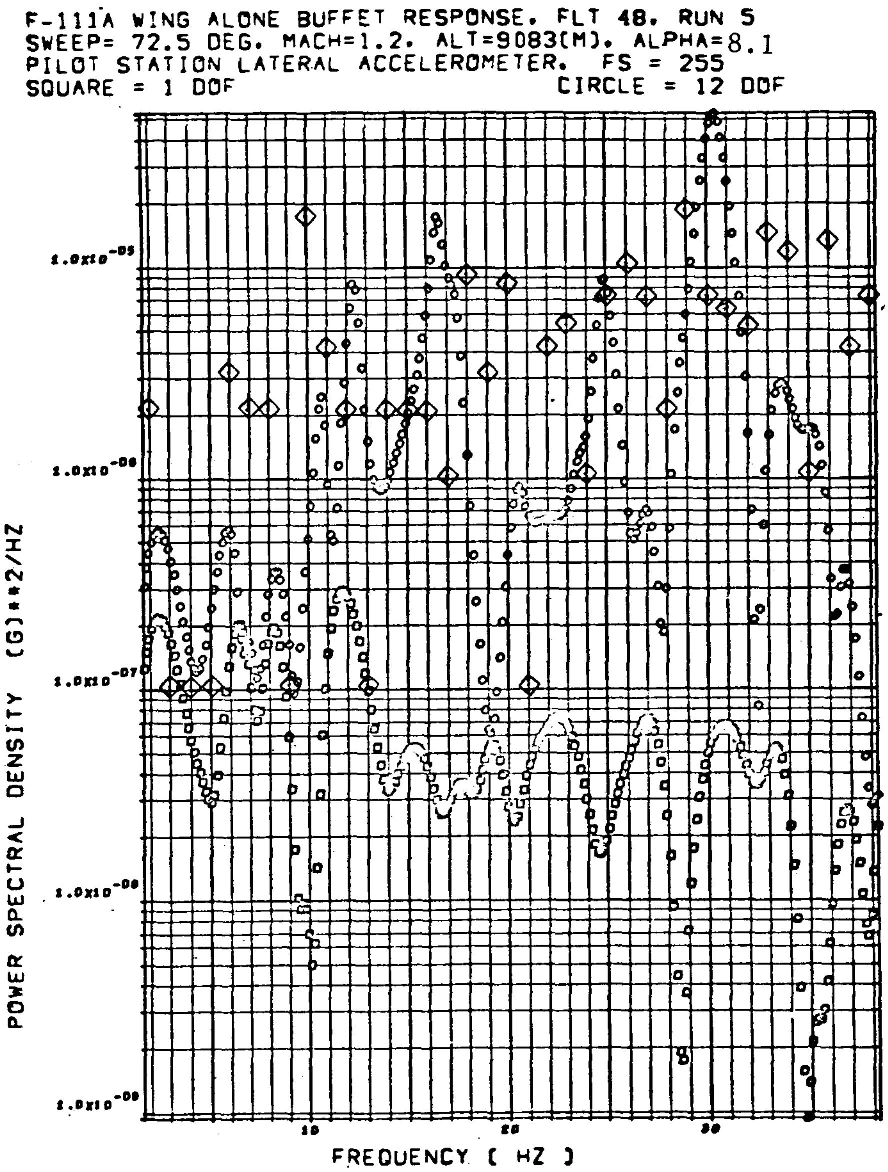

Figure 7.-(e) Pilot seat lateral accelerometer

◇ AF010 $\alpha_{FLT} = 11.6^{\circ}$

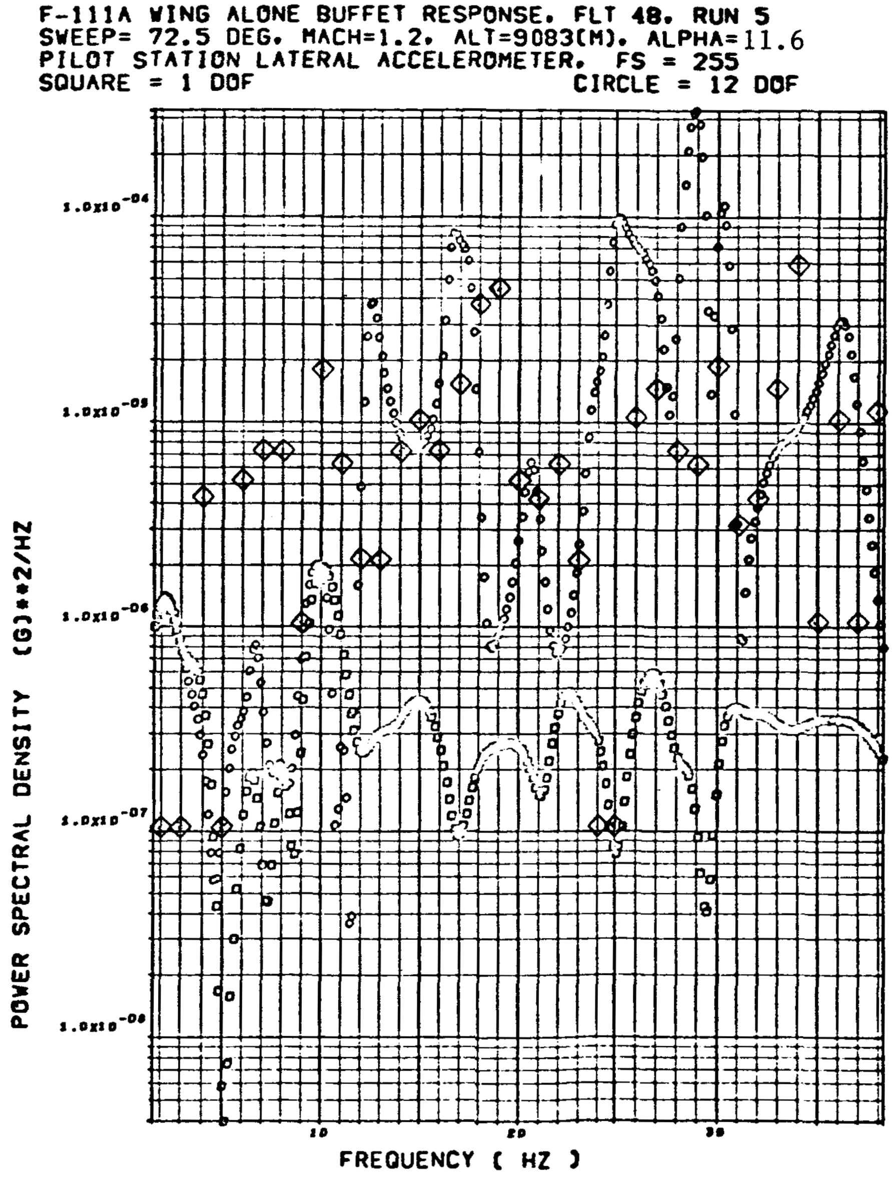

Figure 7.-(e) Pilot seat lateral accelerometer (continued)

◇ AF010 $\alpha_{FLT} = 15.1^{o}$

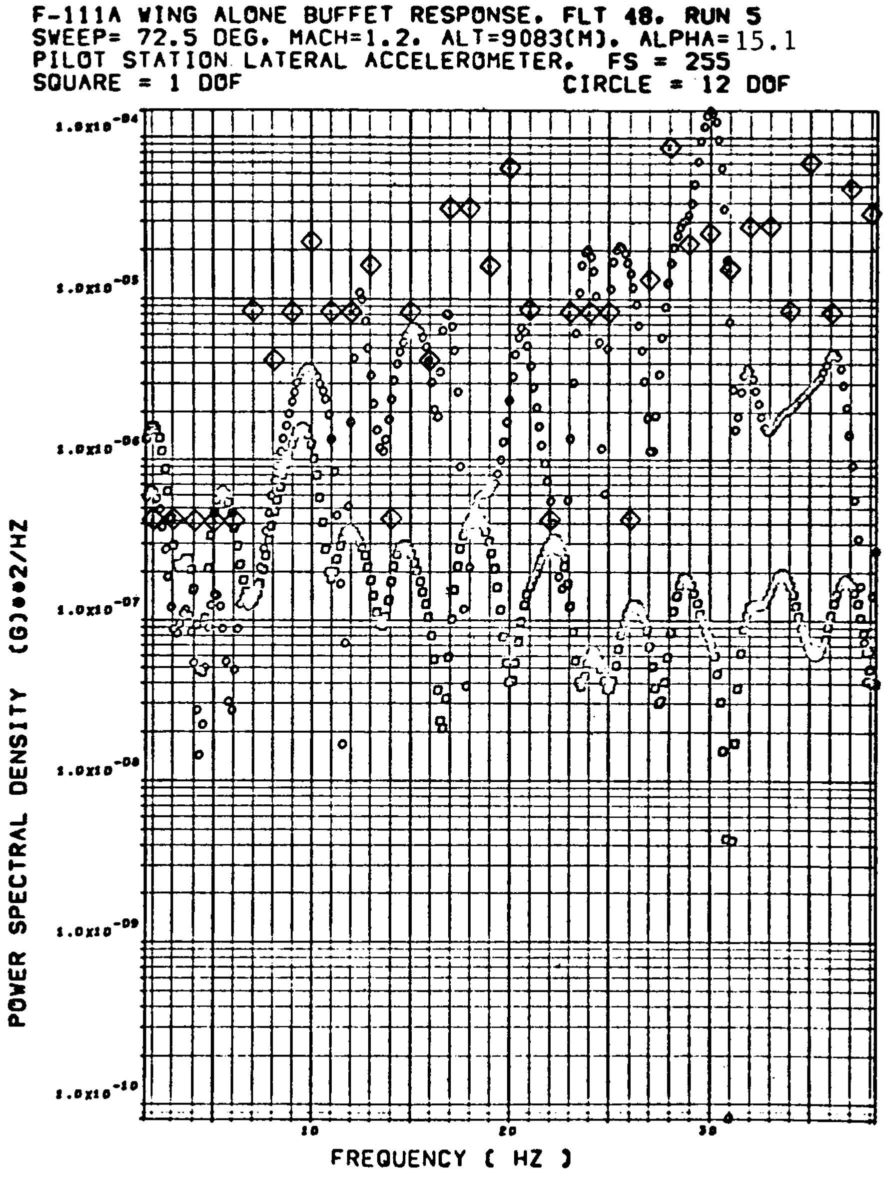

Figure 7.-(e) Pilot seat lateral accelerometer (continued)

△ SW123 $\alpha_{FLT} = 8.1^{\circ}$

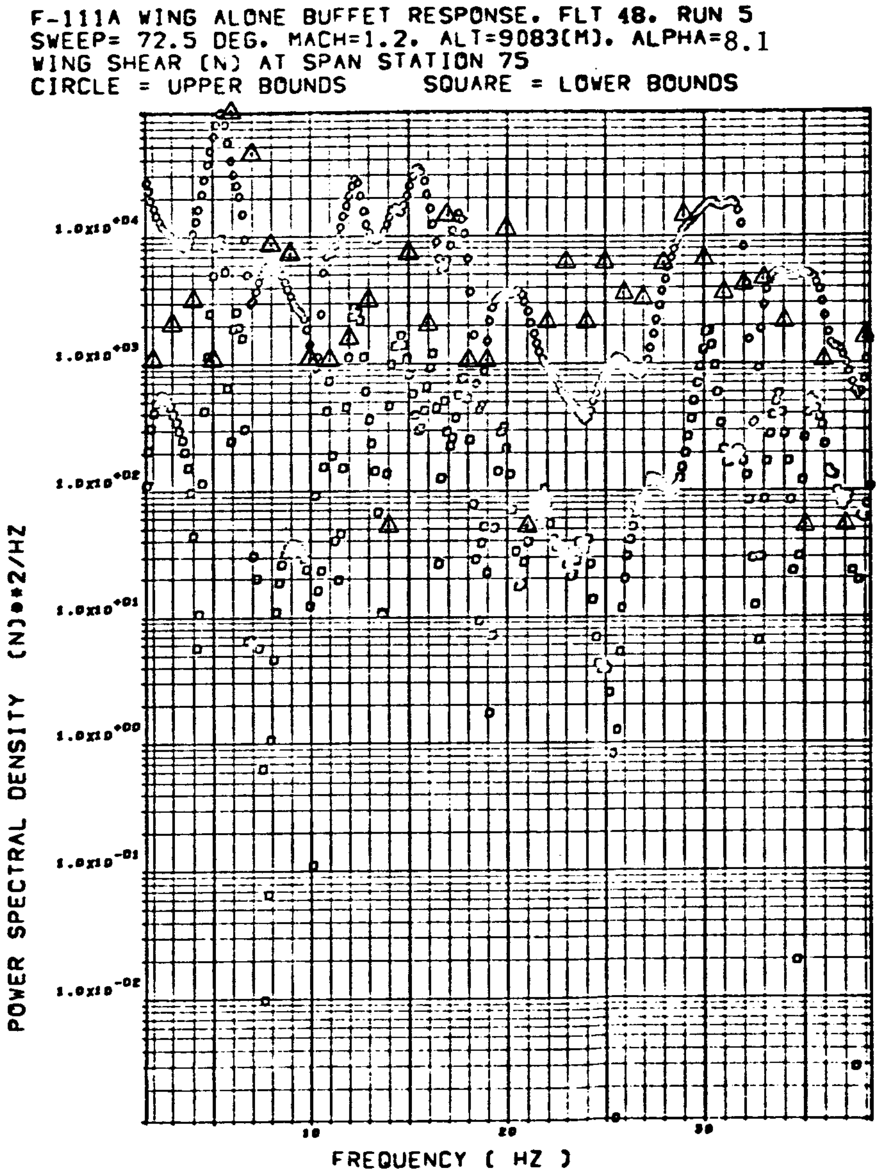

Figure 7.-(f) Wing shear

△ SW123 $\alpha_{FLT} = 11.6^{\circ}$

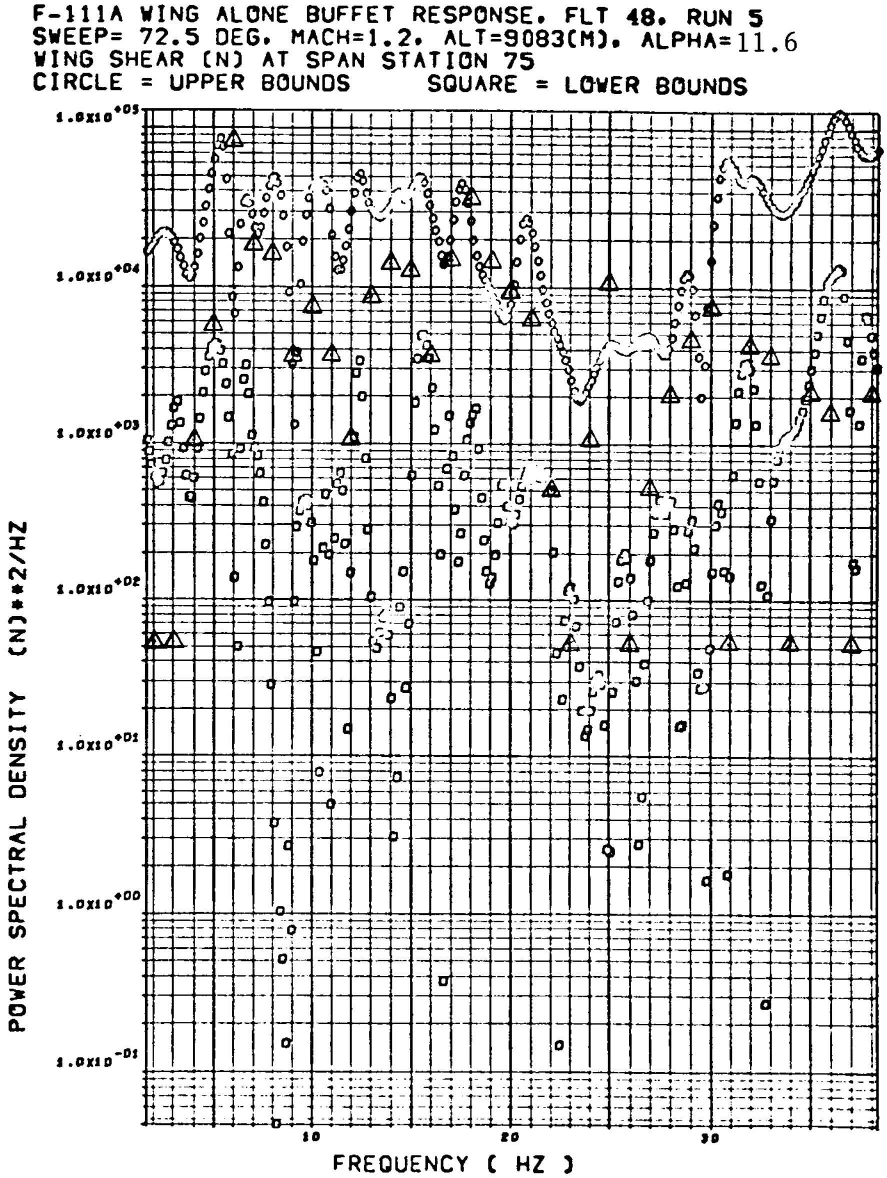

Figure 7.-(f) Wing shear (continued)

△ SW123 $\alpha_{FLT} = 15.1^{\circ}$

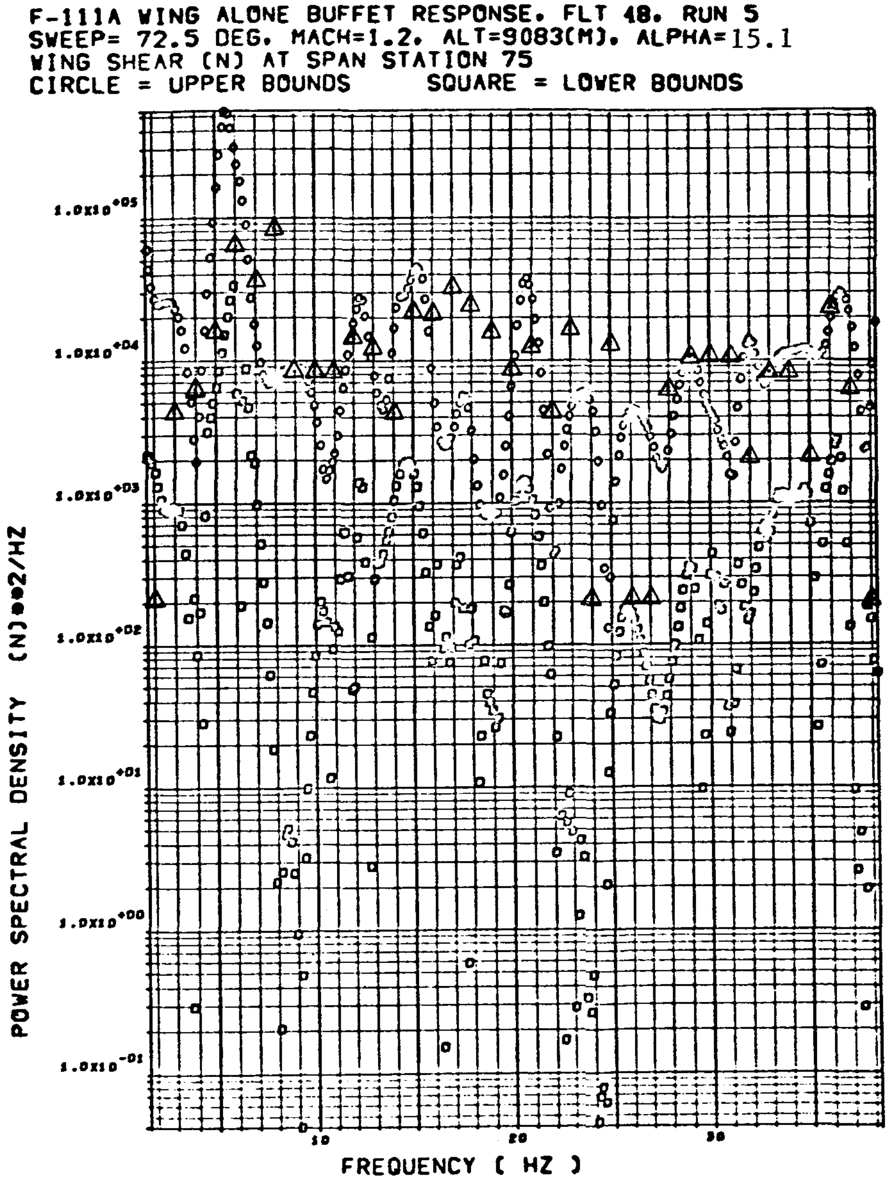

Figure 7.-(f) Wing shear (continued)

△ SW124 $\alpha_{FLT} = 8.1^{o}$

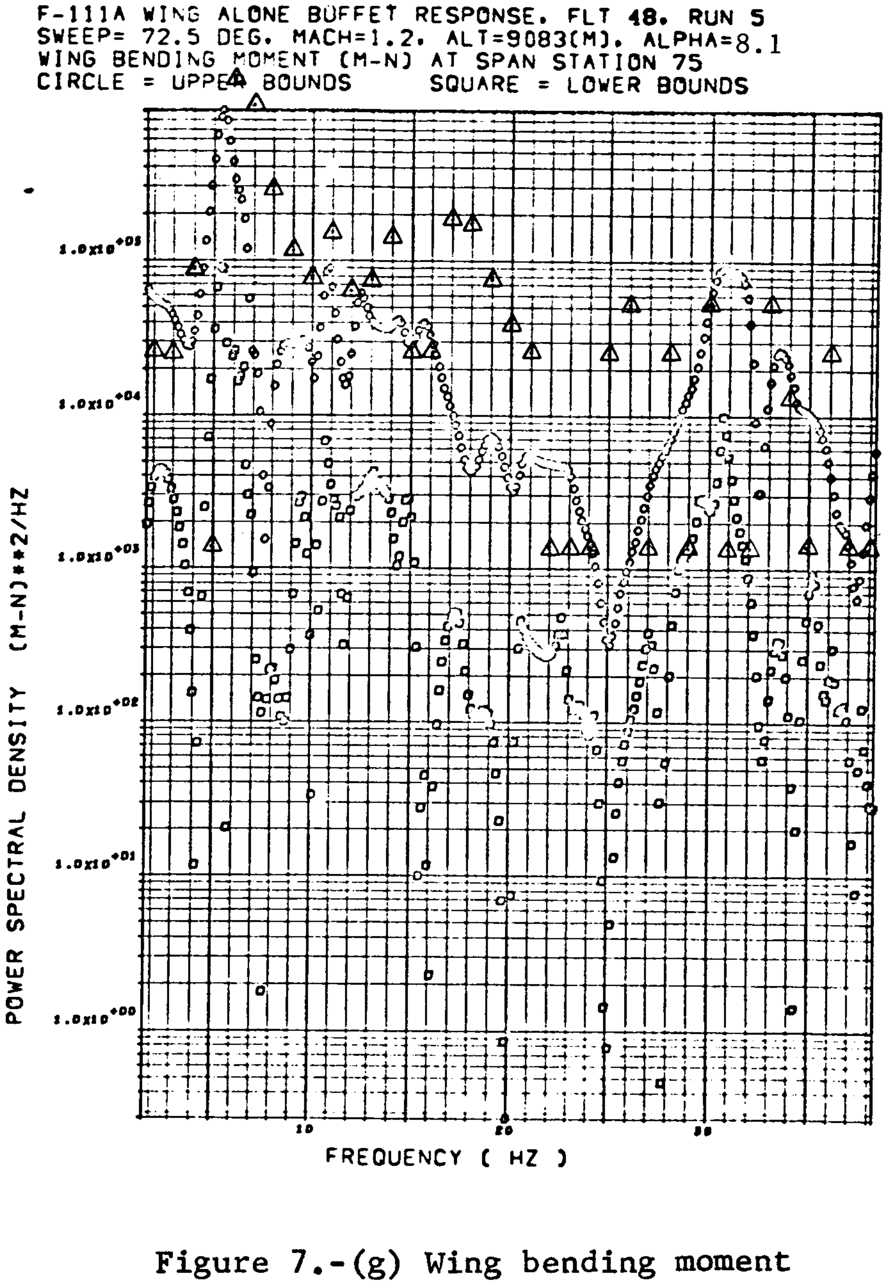

Figure 7.-(g) Wing bending moment

△ SW124 $\alpha_{FLT} = 11.6^{o}$

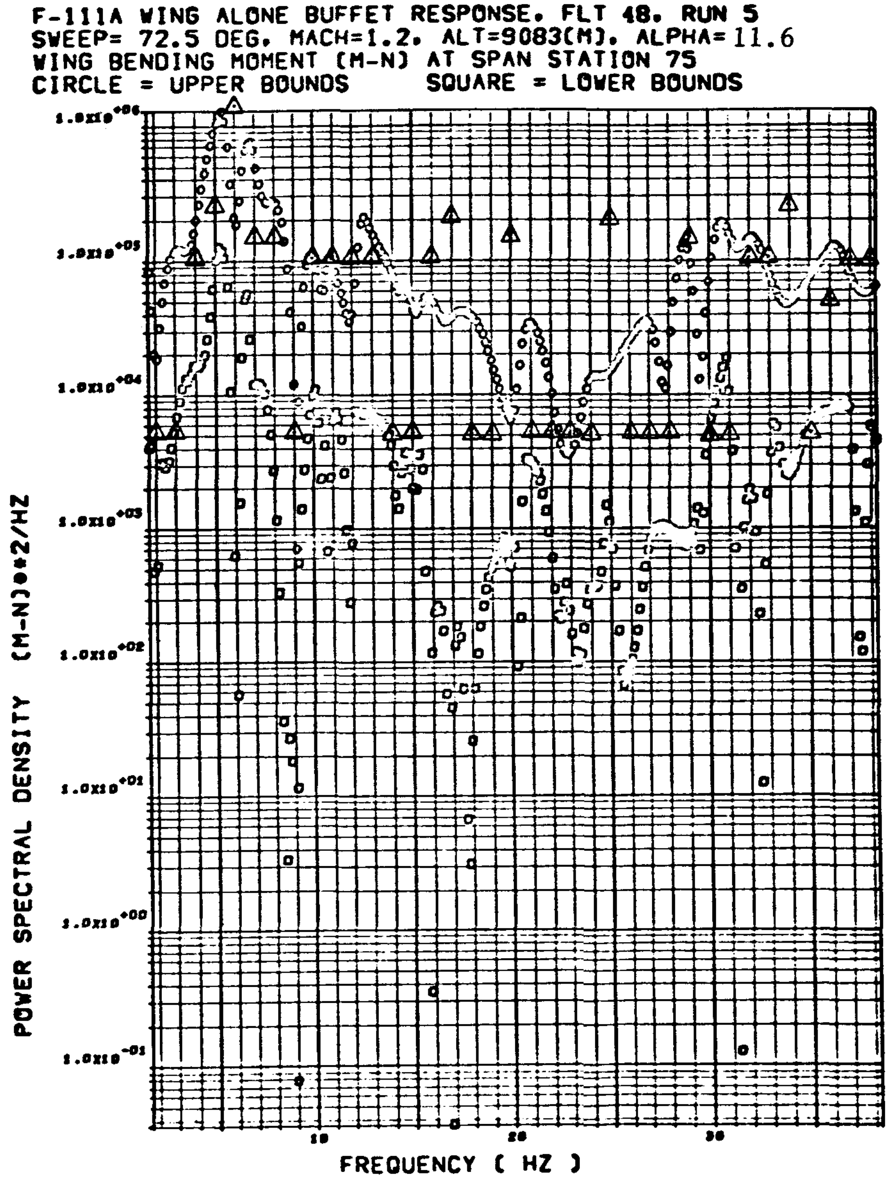

Figure 7.-(g) Wing bending moment (continued)

△ SW124 $\alpha_{FLT} = 15.1^{\circ}$

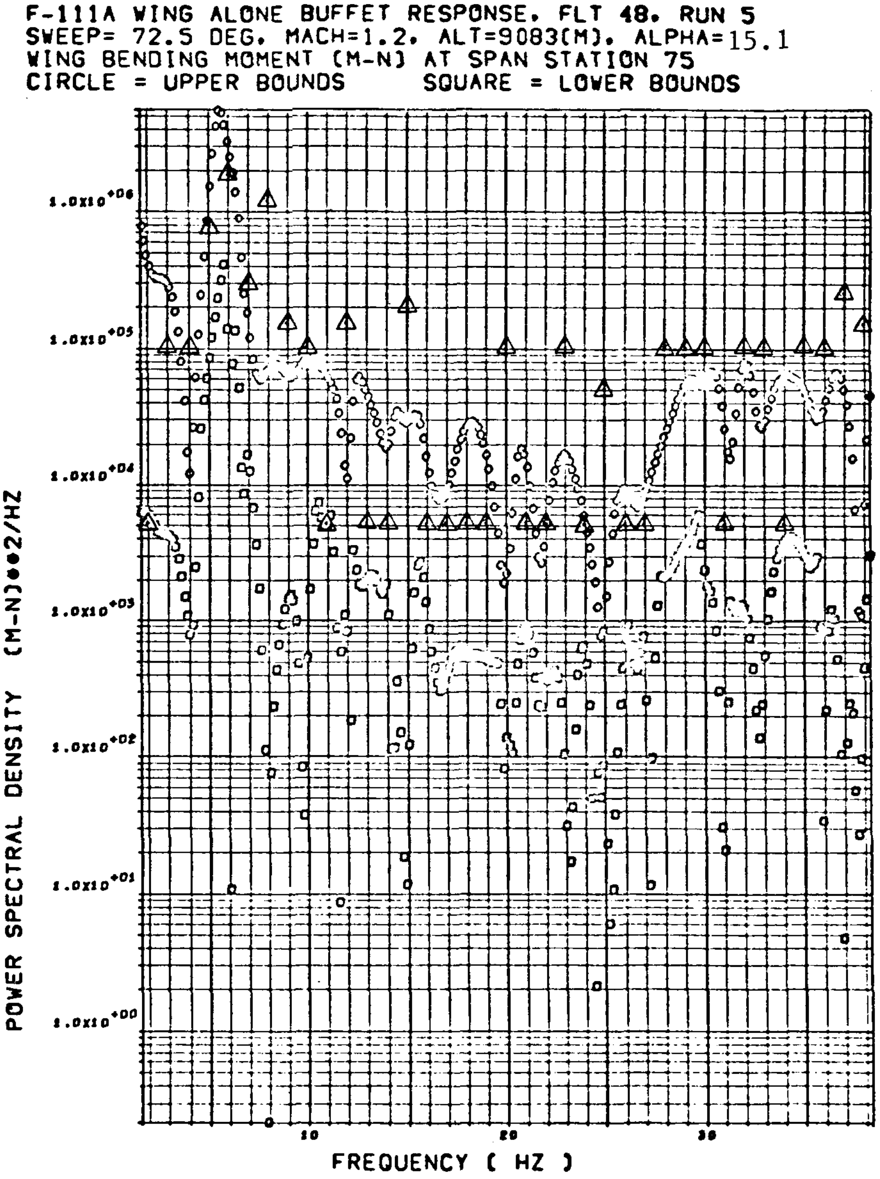

Figure 7.-(g) Wing bending moment (continued)

Δ SW125 $\alpha_{FLT} = 8.1^{o}$

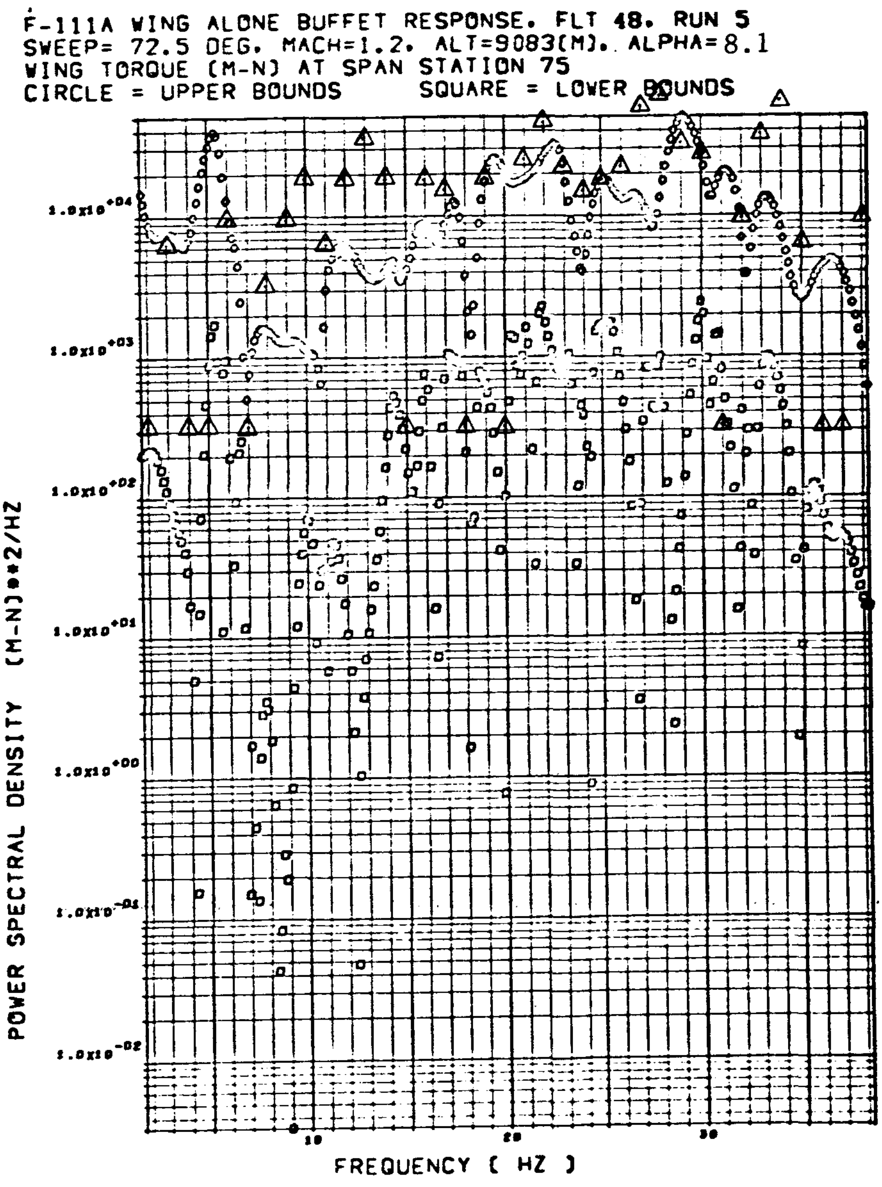

Figure 7.-(h) Wing torsion

△ SW125 $\alpha_{FLT} = 11.6^{o}$

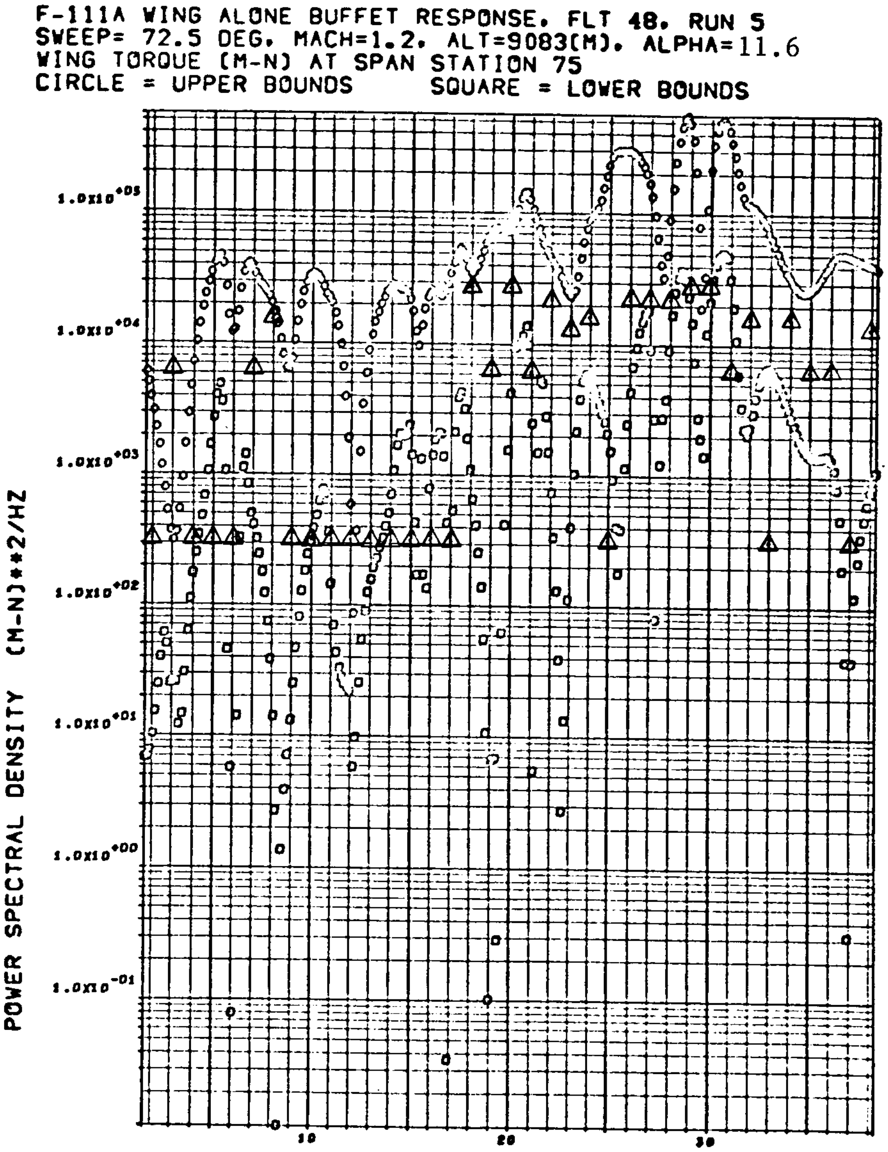

Figure 7.-(h) Wing torsion (continued)

△ SW125 $\alpha_{FLT} = 15.1^{o}$

F-111A WING ALONE BUFFET RESPONSE. FLT 48. RUN 5
SWEEP= 72.5 DEG. MACH=1.2. ALT=9083(M). ALPHA= 15.1
WING TORQUE (M-N) AT SPAN STATION 75
CIRCLE = UPPER BOUNDS SQUARE = LOWER BOUNDS

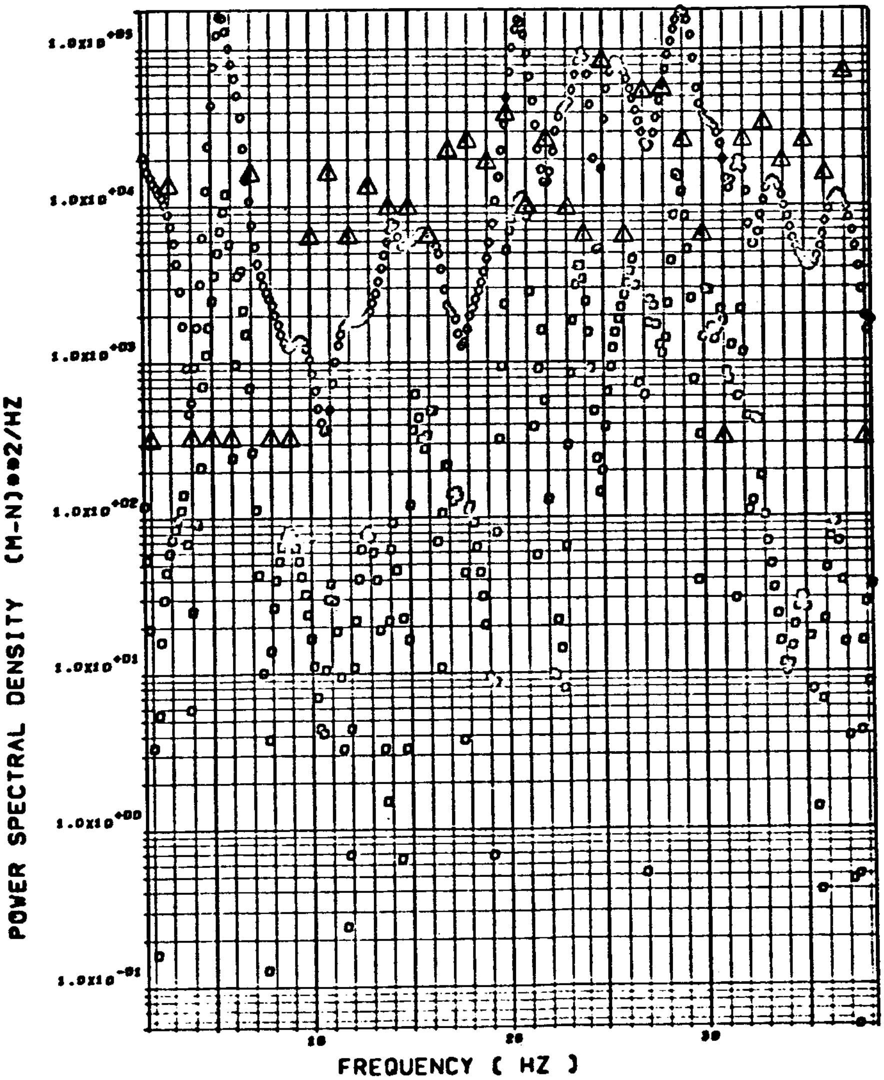

Figure 7.-(h) Wing torsion (continued)

1. Report No.	2. Government Accession No.	3. Recipient's Catalog No.
NASA CR-3036		

4. Title and Subtitle	5. Report Date
"A Method for Predicting Full Scale Buffet Response with Rigid Wind Tunnel Model Fluctuating Pressure Data, Volume II: Power Spectral Densities for Method Assessment"	November 1978
	6. Performing Organization Code
7. Author(s) Atlee M. Cunningham, Jr., David B. Benepe, Darlene Watts, and Paul G. Waner	8. Performing Organization Report No.
	10. Work Unit No.
9. Performing Organization Name and Address General Dynamics Corporation Fort Worth Division Fort Worth, Texas	11. Contract or Grant No. NAS2-7091
	13. Type of Report and Period Covered Contractor Report
12. Sponsoring Agency Name and Address National Aeronautics and Space Administration Washington, D. C. 20546	14. Sponsoring Agency Code

15. Supplementary Notes

16. Abstract

This report documents the development and assessment of a method with which fluctuating pressure data obtained from rigid scaled wind-tunnel models can be used to predict flexible full-scale buffet response. The method requires unsteady aerodynamic forces, natural airplane modes, and the measured pressure data as input. A gust response computer program is used to calculate buffet response due to the forcing function posed by the measured pressure data. By calculating both symmetric and antisymmetric solutions, upper and lower bounds on full-scale buffet response are formed. Final results are given in the form of upper and lower bounds on the power spectral densities and the RMS values for angle of attack variation in maneuvers at several Mach-altitudes. Comparisons of predictions with flight test results are made and the effects of horizontal tail loads and static aeroelasticity are shown. Discussions are also presented on the effects of primary wing torsion modes, chordwise and spanwise phase angles, and altitudes. Volume II presents the predicted upper and lower bounds power spectra for all of the cases and response items given in Volume I.

17. Key Words (Suggested by Author(s))	18. Distribution Statement
Buffeting, Aircraft Maneuverability	Unclassified Star Category - 02

19. Security Classif. (of this report)	20. Security Classif. (of this page)	21. No. of Pages	22. Price*
Unclassified	Unclassified	231	$9.50

*For sale by the National Technical Information Service, Springfield, Virginia 22161

NASA-Langley, 1978